Stefan Huggenberger

# FUNCTIONAL MORPHOLOGY, DEVELOPMENT, AND EVOLUTION OF THE UPPER RESPIRATORY TRACT IN TOOTHED WHALES (ODONTOCETI)

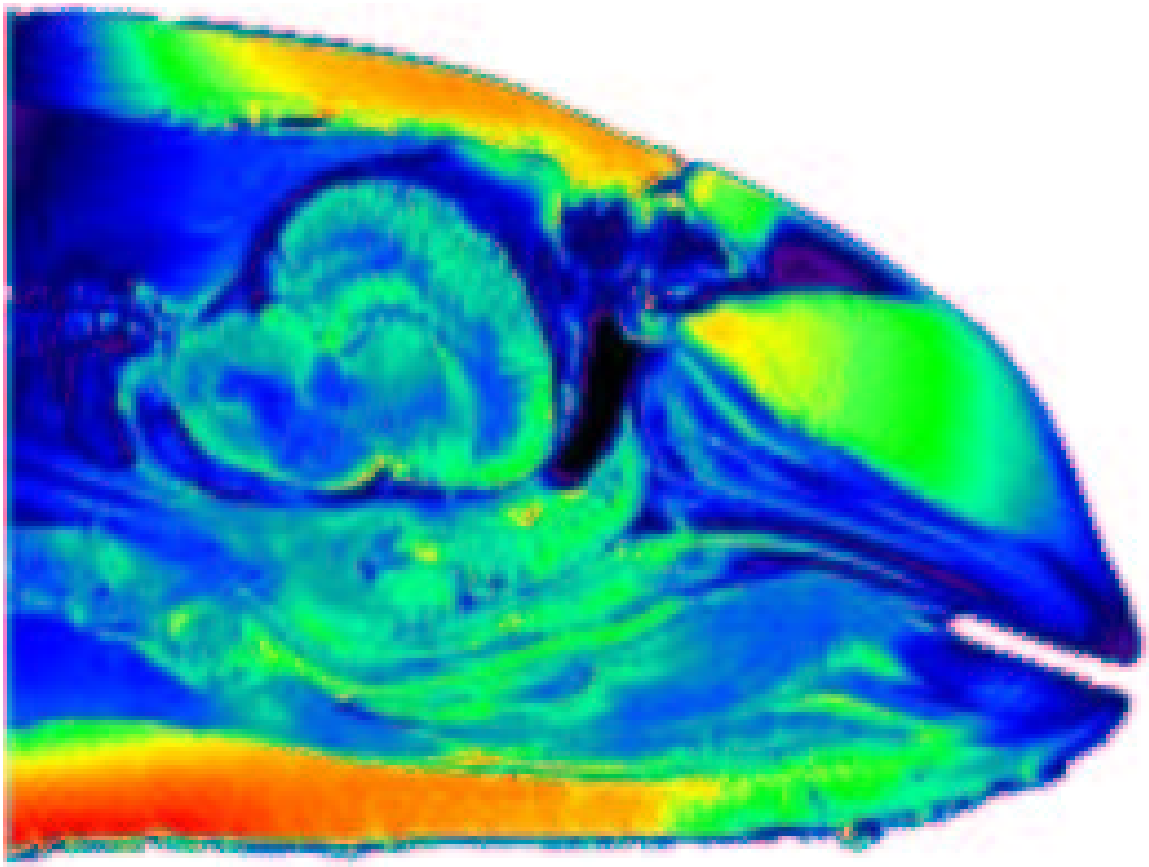

Frankfurt am Main 2003

Front page: Color-coded mid-sagittal MRI scan of a harbor porpoise head

# FUNCTIONAL MORPHOLOGY, DEVELOPMENT, AND EVOLUTION OF THE UPPER RESPIRATORY TRACT IN TOOTHED WHALES (ODONTOCETI)

# FUNKTIONELLE MORPHOLOGIE, ENTWICKLUNG UND EVOLUTION DES OBEREN RESPIRATIONSTRAKTES BEI ZAHNWALEN (ODONTOCETI)

DISSERTATION

zur Erlangung des Doktorgrades der Naturwissenschaften

vorgelegt beim Fachbereich Biologie

der Johann Wolfgang Goethe-Universität

in Frankfurt am Main

von

Stefan Huggenberger

aus

Dormagen

Frankfurt 2003

Dekan: Prof. Dr. Bruno Streit

1. Gutachter: Prof. Dr. Dr. h.c. Christian Winter

2. Gutachter: Prof. Dr. Helmut A. Oelschläger

Ich widme diese Dissertation meinen Eltern, die mich mein gesamtes Studium beispiellos unterstützt haben und meinem kleinen Sohn Leander Epicur, der mir zeigt, wo die Prioritäten im Leben sind.

Ich danke Susanne für ihre selbstlose Unterstützung meiner Forschungen, ihre Rücksicht und ihren Blick für das Wesentliche.

"At the Wednesday morning session, Dr. John Lilly had no sooner completed his lecture on sea mammal intelligence, ending with the idea that "a continuing dialogue with cetaceans could transform our view of all living species and the planet we share", than he was challenged by a segment of the audience that considered it a waste of time and money to try to communicate with animals when we couldn't communicate with each other. … Tunnel vision."

by Tom Robbins "Still Life with Woodpecker"

CONTENTS

## 1. SUMMARY

Despite our restricted knowledge on the biosonar of mammals, there is currently very little research being conducted on this important aspect of mammalian biology. This study is dedicated to a better understanding of the mechanisms of sound generation and emission in toothed whales. It is based on morphological documentation and bio-acoustic interpretation and focuses on the physical conditions of biosonar in the aquatic environment. Toothed whales (Odontoceti, Cetacea) are the only aquatic mammals known to use an active sonar system for orientation. Probably all toothed whales are able to produce (ultra) sonic click sounds and to synthesize the echoes into a three-dimensional "acoustic picture". In contrast to other mammals, toothed whales generate these vocalizations by a pneumatically-driven process in their nasal complex. But also the larynx may play an important role in sound production by generating the air pressure needed. Studies on the mechanisms of sound production in whales were rather rare during the last decades. Most of the fundamental investigations on the anatomy of the toothed whale head were carried out a long time ago, when the principle of sonar in mammals was still unknown. In recent years only single papers on the functional morphology of the head in whales have been published. The central question is how toothed whales produce sound for echolocation and how they can use their sonar system for hunting in murky, deep waters or at night. The results of this study may have consequences for further physiological experiments and bio-physical research as well as behavioral tests.

This project deals with the anatomy (macroscopical dissection, cryo-sectioning), histology, and modern imaging techniques (CT, and MRI, including 3-d computer reconstruction) of the sound generator and transmitter in the head of toothed whales. The harbor porpoise (*Phocoena phocoena*) and the giant sperm whale

(*Physeter macrocephalus*) were examined in some detail. In comparison, fetal and postnatal specimens of other toothed whale species were analyzed including delphinids (*Tursiops truncatus*, *Stenella attenuata*, *Delphinus delphis*), river dolphins (*Pontoporia blainvillei*, *Inia geoffrensis*), and the pygmy sperm whale (*Kogia breviceps*).

In general, the morphological data presented in this study could substantiate and enlarge the unified "phonic lips" hypothesis of sound generation in toothed whales mentioned by Cranford, Amundin, and Norris [J. Morphol. 228 (1996): 223-285]. Their hypothesis describes a valve-like structure (phonic lips) in the nasal passage(s), the so-called "monkey lips/dorsal bursae complex" (MLDB complex), as the sound generator. The mechanism involved is a pneumatically-driven clapping of the lips which creates the initial tissue-borne sound vibration. This vibration is guided and focused by the melon, a hypertrophied fat body in the toothed whale forehead, and transmitted into the water. Nasal air sacs and specific structures of the skull and the connective tissue may contribute to focus the sound to the front.

Whereas the signals of **harbor porpoises** (*Phocoena phocoena*) are rather specialized and differ from those of other toothed whales, their sound generating system reaches the same degree of complexity as in dolphins. The similarities of nasal structures in porpoises and dolphins as to the topography and shape point to the same general functional properties in both groups regarding echolocation sound generation and emission. But there are some morphological peculiarities in the porpoise nasal complex that might explain the unique structure of the clicks used by the animal. Thus, the nearly symmetrical nasal complex of the harbor porpoise could be responsible for the narrow-band clicks: symmetry in both (left and right) MLDB complexes and potential acoustic pathways should produce rather similar frequency components. Furthermore, the strong high-frequency component of the

clicks may depend on the sheet of tough connective tissue ("porpoise capsule") which circle the sound generation site with the specialized structure of the air sac system. In conclusion, it can be hypothesized that the structural specializations in the nasal morphology of the harbor porpoises are adaptations of the sonar system to their coastal habitats.

The two "river" dolphin species, the **La Plata dolphin** (*Pontoporia blainvillei*) and the **Amazon river dolphin** (*Inia geoffrensis*), are similar to delphinids regarding nasal morphology. Although the anatomical studies presented here for these species are not as detailed as those on the harbor porpoise, the results imply that the functional properties of the nasal region are, in principle, equivalent in all of these toothed whales. But it is likely that some unique features of the nasal complex in *Pontoporia* and *Inia* may correlate with specific types of biosonar characteristic for their individual habitats. Since *Pontoporia* and *Phocoena*, on the one hand, belong to different systematic groups but, on the other hand, live in coastal habitats both, they could be an interesting example of parallel evolution regarding their sonar system.

The most striking difference in nasal morphology between the **giant** and the **pygmy sperm whales** and non-physeterid toothed whales is the high degree of asymmetry. In sperm whales, the right nasal passage carries a valve-like structure (monkey lips, phonic lips) that is probably the site of click sound generation. The left nasal passage lacks this structure and, therefore, is not involved in sound generation but mainly serves respiration. According to the morphological studies in the giant sperm whale presented here it is likely that in this animal the hypertrophied epicranial complex may have evolved in order to maximize directionality and loudness (source levels) of echolocation clicks. The topography and shape of the huge fat bodies (spermaceti organ, junk), reminiscent of a bent acoustic horn, and

their air sac system in the nasal complex are good candidates for this proposed specialized function. The adaptation to long-range echolocation may have been the main factor in sperm whale evolution leading to this unique big "sound cannon". In contrast to the mechanism described for dolphins, sperm whales may drive the initial pulse generation process with air pressurized by structures associated with the right nasal passage (and not by laryngeal structures). Contraction of the longitudinal muscles that cover the nasal complex should result in the "squeezing out" of air in the right nasal passage from rear to front through the monkey lips. This mechanism can be taken as an adaptation to deep-diving when shrinking air volumes may restrict sonar sound production. Additionally, the right nasal passage and axilliary structures may control the transmission of sound from one acoustic fat body (spermaceti organ) to the other (junk) and thus the emission of signals into the environment by manipulating the volume and position of air within the passage. In this theoretical scenario the right nasal passage serves as an "acoustic valve" which may switch between two modes of click production: one for coda (communication) click production while the passage is air-filled and a second for the generation of echolocation clicks with the nasal tract nearly collapsed. Thus it seems that the central position and the sub-horizontal orientation of the right nasal passage within the sperm whale head as an interface between the two gigantic fat bodies are prerequisites for sound production with changing volumes of air. In comparison, the nasal structures of the pygmy sperm whale point to a sound generation mechanism at the monkey lips analogous to the procedure described for *Physeter*. In sperm whales, the two fat bodies in the nose may serve as a device for sound transduction and for the focusing of pulses. The topographical relationships of the two fat bodies in physeterids have led to the hypothesis that they are homologous throughout the odontocete group [Cranford et al., J. Morphol. 228 (1996): 223-285]. Moreover, the morphological evidence presented here suggests that also the nasal air sac system, in principle, is homologous throughout

the suborder. Since all these structures are involved in sound production it is likely, first, that the sonar system arose only once in odontocete evolution and, second, that the toothed whale group is monophyletic; the latter is supported by the fossil record.

Comparison of **fetal and perinatal stages of toothed whales** shows that many structures within the nasal complex (air sacs, fat bodies) start their development and/or differentiation in late fetal stages, obviously later than many structures of the ear complex, the second functional unit of the active sonar system. This fact may demonstrate some parallels in the sequence of ontogenetic and phylogenetic events. According to paleontological evidence, the ear complex of the cetacean ancestors was already largely adapted since some time to aquatic hearing when the first osteological sign for echolocation arose. On the other hand, the epicranial complex and the head, in general, of perinatal dolphins are rather similar morphologically to that of the adult animals and this precocial situation is reflected in the behavior of newborn dolphins.

The typical directional asymmetry of the nose of toothed whales, often accompanied with **asymmetry of the facial skull**, is probably related to the generation and/or emission of click sounds. In this study, the two-dimensional shape of facial skulls in various toothed whale species from different systematic groups (Delphinidae, Phocoenidae, Inioidea, Physeteroidea) was analyzed morphometrically with respect to their sonar beam structure. The statistical results reveal a classification of taxa examined into three discrete groups: one group is formed by delphinid species (*Delphinus delphis, Stenella attenuata* and *Tursiops truncatus*) and a second by porpoises (*Phocoena phocoena, Phocoenoides dalli*), river dolphins (*Inia geoffrensis, Pontoporia blainvillei*) and the delphinid *Cephalorhynchus commersonii.* A third group comprises only one member, the dwarf

sperm whale (*Kogia sima*), which differs markedly from other species analyzed. Closer inspection of the statistical results shows that this grouping may be caused by asymmetric representation of characters in the facial skull. Therefore, these results suggest that the pattern of asymmetry is not related to systematic and phylogenetic relationship but to the type of sonar system, which, in turn, seems to be an ecological adaptation.

As stated before, it was shown that echolocation sound generation in the nasal complex of toothed whales is pneumatically-driven. Whereas the muscles of the epicranial complex are probably important for the regulation of air flow along the potential sound-generating structures in the odontocete nose, most of the modern hypotheses consider the **larynx** and its surrounding musculature to produce the initial air pressure. In toothed whales, the larynx is situated in the medioventral vault immediately below the skull base. It is characterized by an elongation of the epiglottic and cuneiform cartilages which form a goose beak-like spout at its rostral end. The tip of the epiglottis forms a neck and lip which is surrounded and held in position by a strong sphincter. By this muscle the epiglottic spout is suspended from the bony nasal passages and the skull base, respectively. Nevertheless, other muscle groups of the gular region and the skull base associated with the larynx as well as the hyoid apparatus may help force the larynx into the choanae. The biological significance of the larynx and the surrounding structures is hard to determine since this complex is a multi-functional system which serves respiration, feeding, and sound production. But from an anatomical point of view it is likely that, in odontocetes, sound production is initiated by piston-like movements of the larynx in the direction of the choanae in order to create the air flow in the nasal complex needed for sound generation. Contraction of the strong pipe-like sphincter muscle complex which connects the choanae to the epiglottic spout of the larynx, may provide most of the power for this process.

But in addition, muscles that connect the larynx/hyoid complex with the skull base and the mandibles may support these laryngeal movements. Furthermore, nearly all these laryngeal muscles may work together in a relatively complicated way to secure the intranarial (water-proof) connection of the respiratory tract during feeding.

Future research on the mechanisms involved in the toothed whale sonar system will have to create and apply functional models to test existing hypotheses and to explain the functional principles of the system in general. The outcome of such scientific approaches may help to find new strategies in nature conservation and applied technology. Small cetaceans are often victims of fishery activities and the entanglement in fishing gear is a major factor in the mortality of even large whales. In order to reduce by-catch it is necessary to understand the mechanism of the sonar system. Insights into the sound generation and emission process can thus support the development and use of adequate precautions. Whale strandings are also believed to be caused by failures of the echolocation system. A better understanding of the principles in whale orientation might help to explain and prevent mass strandings and thus rescue animals. Furthermore, insights into biosonar function offer the opportunity for new technical applications, because the principle of ultrasound generation and emission in whales differs basically from our modern technologies.

## 2. ZUSAMMENFASSUNG

Trotz unseres begrenzten Wissens über das Bio-Sonar der Säugetiere (Zahnwale und Fledermäuse) wird aktuell nur wenig über diesen wichtigen Aspekt der Säugetierforschung gearbeitet. Die vorliegende Studie ist dem Verständnis des Mechanismus der Schallerzeugung und -emission bei Zahnwalen (Odontoceti, Cetacea) gewidmet und basiert auf morphologischen Untersuchungen und bio-akustischen Interpretationen. Die Ergebnisse beinhalten Anregungen für weitere physiologische Experimente und verhaltensbiologische Tests. Zahnwale sind die einzige Säugetiergruppe, die umfassend an ein Leben im Wasser angepasst ist und dabei ein aktives Sonarsystem zur Orientierung nutzt. Wahrscheinlich produzieren alle Zahnwalarten sonische oder ultrasonische Klicklaute, deren Echos die Tiere zu einem drei-dimensionalen „akustischen Bild" zusammensetzen. Im Gegensatz zu den meisten anderen Säugetieren produzieren Zahnwale diese Laute im Nasen-Komplex durch einen pneumatisch betriebenen Mechanismus. Jedoch spielt auch der Kehlkopf dabei eine wichtige Rolle, indem er den nötigen Luftdruck in der Nase erzeugt. Untersuchungen des Mechanismus der Schallproduktion waren in den letzten Jahrzehnten relativ selten. Die meisten grundlegenden anatomischen Studien des Zahnwalkopfes wurden schon vor langer Zeit durchgeführt, als das Prinzip eines Sonarsystems noch unbekannt war. In den letzten zehn Jahren sind nur wenige Beiträge zur funktionellen Morphologie des Kopfes von Walen erschienen. Die zentrale Frage dieser Dissertation ist, wie Zahnwale ihre Echolotlaute produzieren und wie sie ihr Sonarsystem in trüben, tiefen Gewässern oder bei Nacht nutzen. Dazu werden anatomische und histologische Methoden sowie moderne bildgebende Verfahren genutzt, um den Schallgenerator und Transmitter im Zahnwalkopf zu untersuchen. Die Ergebnisse werden in Bezug auf die physikalischen Voraussetzungen eines Bio-Sonars in einer aquatischen Umwelt interpretiert.

Um die morphologischen Eigenschaften (Struktur, Form, Topographie) der Organe im Kopf verschiedener Zahnwalarten vollständig zu erfassen, wurden diese mittels Computertomographie (CT) und Magnetresonanztomographie (MRT) gescannt. Daraufhin wurden die Köpfe makroskopisch präpariert und histologische Schnitte von Gewebeproben angefertigt. Schließlich wurden die Ergebnisse durch digitale dreidimensionale Rekonstruktionen vervollständigt. Diese Studie basiert zum größten Teil auf der Untersuchung von Schweinswalen (*Phocoena phocoena*) und Pottwalen (*Physeter macrocephalus*). Zum Vergleich wurden fetale und postnatale Individuen anderer Zahnwalarten herangezogen wie Delphinartige (*Delphinus delphis*, *Stenella attenuata*, *Tursiops truncatus*), Flussdelphinartige (*Pontoporia blainvillei*, *Inia geoffrensis*) und der Zwergpottwal (*Kogia breviceps*).

Im Allgemeinen konnte durch die morphologischen Daten dieser Studie die einheitliche „phonic lips"-Hypothese der Schallproduktion bei Zahnwalen, wie sie von Cranford, Amundin und Norris [J. Morphol. 228 (1996): 223-285] aufgestellt wurde, bestätigt werden. Diese Hypothese beschreibt eine ventilartige Struktur in der Nasenpassage, den sogenannten „monkey lips/dorsal bursae complex" (MLDB Komplex) als Schallgenerator. Der pneumatische Mechanismus lässt die beiden Hälften des MLDB Komplexes aufeinanderschlagen und erzeugt damit die initiale Schallschwingung im Gewebe („phonic lips"). Diese Vibration wird über die Melone, einen großen Fettkörper in der vorderen Nasenregion der Zahnwale, fokussiert und in das umgebende Wasser übertragen. Die akzessorischen Nasensäcke und spezielle Schädel- und Bindegewebestrukturen können zu der Fokussierung beitragen.

Obwohl die Echolotsignale der Schweinswale sehr spezialisiert zu sein scheinen und sich von denen anderer Zahnwalarten deutlich unterscheiden, erreicht der schallerzeugende Apparat hier die gleiche Komplexität wie bei Delphinen. Die

Übereinstimmungen in der Topographie und in der Form der Nasenstrukturen bei beiden Gruppen weisen dabei auf eine ganz ähnliche Funktion der Nase bezüglich der Produktion und Emission von Echolotschall hin. Allerdings gibt es einige anatomische Besonderheiten im Nasenkomplex des Schweinswals, welche die besondere Pulsstruktur der Sonarsignale erklären könnte. Die beinahe perfekte Symmetrie des Nasenkomplexes ist wahrscheinlich für das schmale Frequenzband der Klicks verantwortlich, weil die vergleichbaren Dimensionen des linken und rechten MLDB Komplexes und der beiden potentiellen akustischen Wege ganz ähnliche Frequenzen produzieren sollten. Desweiteren sind die Kapseln aus hartem Bindegewebe um die MLDB Komplexe („porpoise capsules") und die spezielle Nasensackstruktur wahrscheinlich für die Hochfrequenzanteile der Klicks verantwortlich. Auf Grund dieser Befunde können die Spezialisierungen der Nasenmorphologie der Schweinswale als Anpassungen des Sonarsystems an ein küstennahes Habitat angesehen werden.

Die Nasenanatomie der „Flussdelphinarten" *Pontoporia* und *Inia* ist der von Delphinen ähnlich. Obwohl die anatomischen Untersuchungen der Flussdelphine in dieser Studie nicht so detailreich waren wie für Schweinswale und Delphine, lassen die Übereinstimmungen der Nasenorgane prinzipiell darauf schließen, dass die funktionellen Eigenschaften der Nase in diesen Gruppen weitgehend ähnlich sind. Jedoch ist wahrscheinlich, dass einige Besonderheiten der Nase von *Pontoporia* und *Inia* mit einem spezialisierten Typ des Sonarsystems korreliert sind und eine Anpassung an das jeweilige Habitat darstellen; an den küstennahen Lebensraum von *Pontoporia* und das Flusshabitat von *Inia*. Da *Pontoporia* und *Phocoena* zu verschiedenen systematischen Gruppen gehören aber beide Arten in küstennahen Gebieten leben, könnte dies ein interessantes Beispiel für eine parallele Evolution sein.

## ZUSAMMENFASSUNG

Bei einem Vergleich der Nasenmorphologie der Pottwale und Zwergpottwale einerseits und der nicht-pottwalartigen Zahnwale andererseits fällt vor allem der Grad der Asymmetrie ins Auge. Der rechte Nasengang der Pottwalartigen weist eine ventilartige Struktur („monkey lips") auf, welche wahrscheinlich den Ort der Produktion der Klicks darstellt. Beim linken Nasengang ist diese Struktur nicht vorhanden. Daher dient diese Nasenpassage wahrscheinlich vorrangig der Respiration. Nach den hier vorgestellten anatomischen Studien am Pottwal zu urteilen hat sich ihr hypertrophierter epicranialer Komplex wahrscheinlich als Anpassung im Sinne einer maximalen Direktionalität und Lautstärke der Echolotklicks entwickelt. Die Topographie und die Form der beiden riesigen Fettkörper („spermaceti organ" und „junk"), die an ein gekrümmtes akustisches Horn erinnern, und die bemerkenswerte Struktur des Nasensacksystems sprechen ebenfalls dafür. Diese Anpassung als „Weitsicht-Echolot" könnte der bedeutenste Faktor in der Evolution der Pottwale gewesen sein, diese ultimative „Schallkanone" zu entwickeln. Im Gegensatz zu dem oben für Delphine beschrieben Mechanismus betreiben Pottwale die Schallproduktion an den „monkey lips" mit Luft, die im rechten Nasengang unter Druck gesetzt wird (und nicht im nasopharyngealen Raum). Die Kontraktion des longitudinalen Muskels, der den Nasenkomplex umgibt (M. maxillonasolabialis), sollte zu einem „Auspressen" des rechten Nasenganges von hinten nach vorn in Richtung der „monkey lips" führen. Dieser Mechanismus kann als eine Anpassung an das Tieftauchen angesehen werden, da schrumpfende Luftvolumina die Lautproduktion einschränken. Zudem könnte durch Änderung des Luftvolumens im rechten Nasengang die Schalltransmission zwischen den Fettkörpern, und somit die Schallemission, kontrolliert werden. In diesem theoretischen Szenario fungiert der breite rechte Nasengang als eine Art „akustische Schranke", welche zwischen zwei verschiedenen Modi der Klickproduktion wechselt: Der erste Modus mit luftgefülltem Nasengang führt zur Produktion der Kommunikationsklicks („coda clicks") und der zweite Modus zur

Aussendung von Echolotklicks, wenn der Nasengang kollabiert ist. Somit scheinen die zentrale Position und die nahezu horizontale Orientierung des rechten Nasengangs im Kopf der Pottwale als Schnittstelle (Schranke) zwischen den beiden großen Fettkörpern mit dem Mechanismus der Schallproduktion bei veränderten Luftvolumina korreliert zu sein. Die Nasenstrukturen beim Zwergpottwal weisen im Vergleich auf einen potentiellen Mechanismus der Schallproduktion hin, welcher der Situation beim Pottwal sehr ähnelt. Die Fettkörper in der Nase stellen wahrscheinlich einen Emissionsapparat dar, der die Fokussierung der Echolotlaute unterstützt. Die charakteristischen topographischen Beziehungen dieser Fettkörper bei allen Pottwalartigen und anderen Zahnwalen führten zu der Hypothese, dass diese innerhalb der gesamten Zahnwalgruppe (Odontoceti) homolog sind [Cranford et al., J. Morphol. 228 (1996): 223-285]. Darüber hinaus legt der interspezifische morphologische Vergleich in der vorliegenden Arbeit nahe, dass auch das Luftsacksystem innerhalb der Odontoceti homolog ist. Da alle diese Strukturen an der Schallproduktion beteiligt sind, ist es wahrscheinlich, dass ein Sonarsystem nur einmal während der Evolution der Zahnwale entwickelt wurde und dass folglich die Zahnwale monophyletisch sind, was auch Fossilfunde belegen.

Untersuchungen an fetalen und perinatalen Stadien von Delphinen zeigen, dass sich der Nasenkomplex im Vergleich zum Ohr, dem zweiten funktionellen Komplex des Sonarsystems, in Teilen erst relativ spät entwickelt. Diese Tatsache deutet auf eine gewisse Parallelität von ontogenetischen und phylogenetischen Prozessen hin. Nach den Fossilfunden von Urwalen und Zahnwalen zu urteilen war der Ohrkomplex schon eine ganze Zeit an eine aquatische Lebensweise angepasst als die ersten osteologischen Anzeichen für die Produktion von Echolotlauten auftraten. Im Übrigen ist die Morphologie sowohl des Nasenkomplexes als auch des gesamten Kopfes von perinatalen Delphinen der von adulten Tieren sehr ähnlich. Diese

Tatsache spiegelt sich auch in dem komplexen Verhalten neugeborener Delphine wider, die wie alle Wale extreme Nestflüchter sind.

Die typische direktionale Asymmetrie des Nasenkomplexes der Zahnwale, oftmals mit einer Asymmetrie des Gesichtschädels korreliert, hängt wahrscheinlich mit dem Mechanismus der Lautproduktion und/oder –emission zusammen. In einem morphometrischen Kapitel dieser Studie wurde die zweidimensionale Gestalt des Gesichtschädels (in Aufsicht) von verschiedenen Zahnwalarten aus vier systematischen Gruppen (Delphinidae, Phocoenidae, Inioidea und Physeteroidea) analysiert. Die statistischen Resultate ergaben eine Klassifikation der Arten in drei Gruppen: Eine erste Gruppe besteht aus Mitgliedern der Delphinfamilie (*Delphinus delphis, Stenella attenuata* and *Tursiops truncatus*) und eine zweite aus Schweinswalen (*Phocoena phocoena, Phocoenoides dalli*), „Flussdelphinen" (*Inia geoffrensis, Pontoporia blainvillei*) und der Delphinart *Cephalorhynchus commersonii.* Die dritte Gruppe wurde nur durch den Zwergpottwal *Kogia sima* gebildet, der sich von allen anderen Arten stark unterscheidet. Eine genauere Analyse der statistischen Ergebnisse zeigte, dass die Klassifikation wahrscheinlich durch asymmetrische Charakteren der Gesichtschädel hervorgerufen werden. Diese Ergebnisse legen nahe, dass die Gestalt und das Ausmaß der Nasenasymmetrie nicht mit der systematischen Zugehörigkeit der jeweiligen Art korrelieren, sondern durch den jeweiligen Typus des Sonarsystems als Ausdruck einer bestimmten ökologischen Anpassung bedingt sind.

Wie oben beschrieben wird die Generation der Echolotklicks im Nasenbereich der Zahnwale pneumatisch betrieben. Während die Muskeln des epicranialen Bereiches wahrscheinlich den Luftstrom durch den Schallgenerator (MLDB) regulieren, beschreiben die meisten modernen Hypothesen den Kehlkopf und seine umgebende Muskulatur als den Produzenten des dafür benötigten Luftdrucks. Bei Zahnwalen

sitzt der Kehlkopf in einem medioventralen Gewölbe unter der Schädelbasis. Er ist charakterisiert durch eine rostrale Verlängerung des Kehldeckels und der beiden Stellknorpel, die ein gänseschnabelartiges Rohr bilden. Die Spitze des Kehldeckels formt einen Hals und eine Lippe, die von einem starken Sphinktermuskel umrundet und dabei in Position gehalten wird. Auf diese Weise ist das Atemrohr zwischen den Choanen und der Schädelbasis einerseits und der Trachea andererseits vollständig vom Digestionstrakt getrennt. Jedoch halten noch weitere Muskelgruppen der Kehlregion und der Schädelbasis, welche jeweils mit dem Kehlkopf und dem Zungenbein assoziiert sind, den Kehlkopf in seiner intranarialen Position. Insgesamt sind die biologische Bedeutung des Kehlkopfes sehr schwer zu erfassen, da er und das Zungenbein ein multifunktionales System bilden, welches der Respiration, der Ernährung und der Schallproduktion dient. Aus anatomischer Sicht ist es wahrscheinlich, dass die Schallerzeugung bei Zahnwalen durch eine Kolbenbewegung des Kehlkopfes in Richtung der Choanen zustande kommt, wodurch der Luftdruck im Nasenbereich erzeugt wird. Die Kontraktion des Sphinktermuskels als einem muskulösen Schlauch, welcher die Choanen mit dem „Kehlkopfrohr" verbindet, erzeugt wahrscheinlich die größte Kraft für diese Kolbenbewegung. Jedoch dürften die Muskelgruppen, die den Kehlkopf und das Zungenbein am Unterkiefer und an der Schädelbasis aufhängen, zur Druckerhöhung beitragen. Darüber hinaus arbeitet wahrscheinlich fast die gesamte Muskulatur um den Kehlkopf in einem relativ komplizierten Ablauf für die Nahrungsaufnahme zusammen, um die intranariale (wasserdichte) Verbindung des Respirationstraktes sicherzustellen.

Die zukünftige Erforschung der Mechanismen des Sonarsystems der Zahnwale sollte die Entwicklung funktioneller Modelle beinhalten, an welchen die bestehenden Hypothesen zur Schallproduktion und Generation getestet und die Funktionsprinzipien dieses Systems vollständig nachvollzogen werden.

Computergestützte Modelle werden auf diesem wichtigen Gebiet wertvolle neue Erkenntnisse im Hinblick auf alternative Methoden und Ansätze im Artenschutz und bei technischen Anwendungen, so u. a. in der Medizin erbringen. Kleinwale sind durch den Einsatz von Fischernetzen sehr gefährdet, in welchen sie sich verfangen können und dann ersticken. Offensichtlich sind die Tiere nicht in der Lage, die Gefahr, die von diesen Netzen ausgeht, mit ihrem Sonarsystem zu erfassen. Um also die Beifangrate der Wale in der Fischerei-Industrie zu reduzieren, ist es demzufolge notwendig, die Prinzipien des Echolotsystems dieser Tiere besser zu verstehen. Detaillierte Einblicke in die Ultraschallerzeugung der Zahnwale sind somit auch die Voraussetzung für die Entwicklung und Anwendung adäquater Schutzmaßnahmen. Auch geht ein Teil der vielen weltweiten Walstrandungen wahrscheinlich auf eine „Schwäche" bzw. eine Fehlfunktion des Sonarsystems zurück. Ein besseres Verständnis der Orientierung der Wale mittels Sonar könnte helfen, Massenstrandungen zu erklären und damit zur Sicherung der Tierbestände beitragen.

## 3. INTRODUCTION

Aristotle stated in 350 BC that the air passage of a whale is situated in the forehead but in a dolphin it goes through its back. He was right with the first half of his remark concerning the location of the nose in these air-breathing animals. But his opinion as to the position of the dolphin's blowhole was obviously not correct. This error may have occurred by assuming that the bulbous epicranial forehead of the dolphin could be the neurocranium. In the ancestors of the whales (Cetacea), generally, the external opening of the respiratory tract (blowhole) has migrated to a more caudal position on top of the head, in front and above the braincase and it is that part of the head to be exposed first during surfacing. Furthermore, the forehead of toothed whales (Odontoceti) is known to produce sounds serving echolocation and/or communication. This implies in turn that, in contrast to most mammals, vocalizations recorded from dolphins and other toothed whales may not have been generated by the larynx but by structures in the nose (Fig. 1; Norris 1968, Cranford et al. 1996) called "epicranial complex".

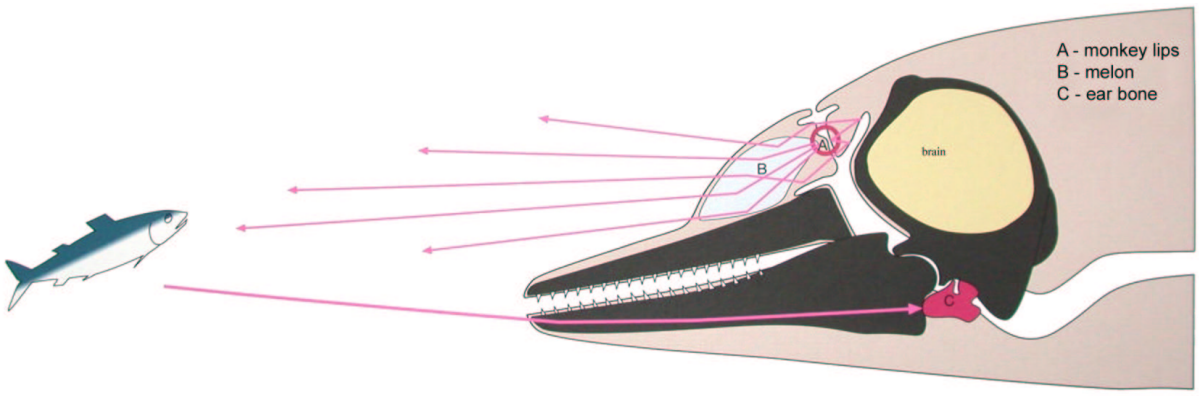


Figure 1: Schematic drawing of sonar function in a dolphin. The arrows represent the sound propagation from and to the dolphin's head. (Courteously: H. Schäfer, Forschungsinstitut und Naturmuseum Senckenberg, Frankfurt a.M., Germany)

The central question of this study is how toothed whales produce sound usually applied in echolocation and how they can use their sonar system for hunting in murky, deep waters or at night. Most of the relevant modern scientific approaches

did not analyze the structure of the ultrasound generator in the head of toothed whales. Instead, they took the dolphin's head as a "black box" and focus on biophysical parameters like the extension of the sound field and the frequency spectrum of the emitted calls as well as audiograms of the animals. Therefore, studies on the mechanisms of sound production were rather rare during the last decades. Most of the fundamental investigations on the anatomy of the toothed whale head were carried out long time ago (e.g., von Baer 1826, Kükenthal 1893, Rawitz 1900, Boenninghaus 1903), when the principle of ultrasound orientation and navigation in mammals was still unknown. In recent years only single papers on functional head morphology in whales have been published (for review see Cranford 2000).

## 3.1. Toothed whale echolocation signals

To outline the functional relevance of the head structures involved in sonar beam generation, the types of echolocation calls need to be characterized first. The echolocation signals emitted by odontocetes tend to fall into at least three broad categories. Dolphins which typically emit whistle signals also emit short broad-band echolocation signals having between four and eight cycles and duration of 40–70 ms (Au 1993, 2000a). Most odontocetes fall into this class. Whether riverine dolphins whistle or not is still an open question since recordings of whistle-like sounds of these animals are rare or even not known (Wartzok and Ketten 1999). So, the Amazon river dolphin (*Inia geoffrensis*) is known to produce whistles and click sounds (Kamminga et al. 1993, Podos et al. 2002). The acoustic abilities of the La Plata dolphin (*Pontoporia blainvillei*), which belongs probably to the river dolphin group (Fordyce and Muizon 2001, Nikaido et al. 2001), are nearly not documented. Only in their nearly 30 year-old paper, Busnel et al. (1974) describe click sounds

for this species. Nevertheless, as far it is known today, river dolphins emit echolocation signals that would fall in this short duration broadband category (Busnel et al. 1974, Kamminga et al. 1993, Wartzok and Ketten 1999).

Odontocetes, which do not emit whistle signals, have narrow-banded echolocation signals with a minimum of about 12 cycles and duration generally longer than 100 ms (Au 1993). Among these odontocetes are the harbor porpoise, *Phocoena phocoena* (Møhl and Andersen 1973, Kamminga and Wiersma 1981, Hatakeyama and Soeda 1990, Goodson and Datta 1995, Goodson et al. 1995, Au et al. 1999), finless porpoise, *Neophocaena phocaenoides* (Kamminga 1988, Goold and Jefferson 2002), Commerson's dolphin, *Cephalorhynchus commersonii* (Kamminga and Wiersma 1982, Evans et al. 1988), Hector's dolphin, *Cephalorhynchus hectori* (Dawson 1988), Dall's porpoise, *Phocoenoides dalli* (Hatakeyama and Soeda 1990), and probably the pygmy sperm whale, *Kogia breviceps* (Wartzok and Ketten 1999).

A third class of echolocators can be predicted for the sperm whale (*Physeter macrocephalus*). Their usual (echolocation) clicks as well as their coda (communication) clicks are broad-banded and consist of 5 to 10 cycles with a peak frequency of approximately 15 kHz (Madsen et al. 2002b). Furthermore, sperm whales are not known to produce whistle-like sounds but so-called slow clicks that are thought to represent communication signals of low frequency around 3 kHz (Madsen et al. 2002b).

Nevertheless, according to Wartzok and Ketten (1999) and Ketten (2000), there are only two different types of odontocete echolocators: type I emits peak frequencies above 100 kHz and type II is characterized by peak frequencies below 80 kHz. Type I echolocators are mainly inshore or riverine species living in a complex environment; e.g. *Phocoena phocoena* or *Inia geoffrensis*. Offshore and

near-shore species, typically belonging to type II and operating in less complex surroundings, are characterized by a more intense social behavior than type I species. Typical examples are *Tursiops truncatus* as well as *Physeter macrocephalus*. Each of these types of echolocators is characterized by peculias cochlea parameters (Wartzok and Ketten 1999, Ketten 2000).

However, to study the morphology of the sound generator and transducer of toothed whales, it is advantageous to distinguish between three classes of echolocators as described above since their epicranial anatomy is significantly different (Mead 1975, Heyning 1989, Cranford et al. 1996, Cranford 1999). Therefore, for this dissertation project, specimens of toothed whales belonging to the three proposed categories of echolocation were compared using macroscopical dissections, routine histological techniques, x-ray computer assisted tomography (CT) as well as magnetic resonance imaging (MRI) and computer-assisted three-dimensional reconstructions. Here, the field of comparative morphology leads to new insights since differences in echolocation signals should be caused, at least in part, by morphological specializations of the sound-generating and emitting structures in the toothed whale head. Therefore, the anatomical results of this study are interpreted with respect to the potential acoustic properties of tissues and macroscopic structures within the aquatic bio-sonar system of toothed whales.

### 3.2. Porpoises (Phocoenidae)

The morphology and function of the nasal (epicranial) complex in most toothed whales (Odontoceti) are still poorly known. A series of structures are unique among the Mammalia and include: an oddly modified skull (Miller 1923), several nasal diverticulae (Mead 1975), and a set of potential acoustic fat bodies (Norris 1968,

Cranford 1996). In historical terms, the harbor porpoise (*Phocoena phocoena*) is one of the few odontocete species that has been studied in some detail. In 1680, Edward Tyson first presented a surprising and fascinating idea about the function of the nasal diverticulae in this species:

"*Near this* (the nasal plug) *there are placed fore Bags or two pairs of them. The first pair which is the largest* (vestibular sacs)*, lyes upon the middle of the Rostrum or snout, … and … at least may serve for the forming the noise they make against storms and bad weather.*"

It was not until 1826 when Karl-Ernst von Baer described and identified the epicranial complex as the true nose of the porpoise and that the blowhole (Spritzloch) does not serve to blow out water. Some years later, in 1848, Francis Sibson considered that the function of the air sacs was to float the blowhole above the water surface during sleep and the act of copulation. But Willy Kükenthal stated in 1893 that the nasal air sacs might help to lock the nasal passage against the incursion of water, since he found no musculature to close it. In contrast, at the turn of the 19th century, Bernhard Rawitz (1900) wrote that the only cause for the anatomy of the porpoise nose is hydrodynamics. According to Georg Boenninghaus (1903), the nasal plug and the epicranial musculature lock the respiratory tract but the nasal diverticulae seem to have no function whereas Kurt Gruhl (1911) stated that the facial muscles can move on the surfaces of the air sacs.

Modern theories imply that sound generation serving the sonar system takes place in the nasal complex of toothed whales. In 1969, Kenneth S. Norris reported observations of trained dolphins with open airways during click production. He saw a sputtering of air and fluid over the lateral edge of the nasal plug concordant with

the emitted signals. Whether such sputtering indicated the pulsation of air deeper within the nasal passage was not clear. Cranford and co-workers (Cranford et al. 1997, Cranford 2000) confirmed and analyzed this sputtering using high-speed video endoscopy during biosonar experiments. They observed a synchronization of vibrations at the monkey lips (valve-like structures in the soft nasal tract at the dorsal end of the nasal plugs) with the emission of sonar signals. No other nasal structure showed vibrations synchronous with sonar pulses. These and other observations (Norris et al. 1961, Norris and Harvey 1974, Dormer 1979, Ridgway et al. 1980, Mackay and Liaw 1981, Amundin and Andersen 1983, Amundin 1991, Cranford et al. 1996, Aroyan et al. 2000) collectively provide very strong evidence for a nasal sound production mechanism. The exact mechanism is unclear but the process probably involves a complex of tissues and structures, including the phonic lips or monkey lips (Pouchet and Beauregard 1885, Norris and Harvey 1972, Cranford 1999), as well as the set of fat bodies and several other associated structures. Cranford et al. (1996) defined this tissue complex and dubbed it the monkey lips/dorsal bursae (MLDB) complex. Their hypothesis characterizes the dorsal bursae, a pair of small elliptical fat bodies associated with each pair of monkey lips in the MLDB complex as the site of sound production (Figs. 1, 2). The proposed mechanism is a pneumatically driven "clapping" process at the monkey lips (Ridgway et al. 1980, Amundin and Andersen 1983, Marten et al. 1988, Cranford 2000) which creates an initial sound vibration at the anterior dorsal bursae. This vibration is guided via the melon, a large fat body comprising most of the forehead region in dolphins and porpoises (Figs. 1, 2), into the water. Nasal air sacs and specific features of the skull and connective tissue may help to guide and focus the sound to the front (Fleischer 1975, 1976, 1982, Oelschläger 1990, Cranford et al. 1996, Aroyan et al. 2000). For detailed reviews on odontocete forehead anatomy and function the reader is referred to Schenkkan (1973), Mead (1975), Heyning (1989), and Cranford et al. (1996).

Dolphins, in general, are able to produce a wide variety of sounds (Au 1993, Wartzok and Ketten 1999) and some species can vary amplitude, frequency, and click interval of their sonar sounds (Au 1993, Au and Benoit-Birrd 2003). Most approaches to analyze the sound generation process have relied on experiments with the bottlenose dolphin (*Tursiops truncatus*; Au 1993, Cranford 2000). Within the genuine dolphins (Delphinidae), there are many similarities but only a few differences in vocalization pattern and in MLDB complex morphology suggesting that these animals all use the same fundamental (unified) sound generation mechanism (Cranford et al. 1996). When compared to the few well-studied dolphin species, the sound repertoire of harbor porpoises seems to be somewhat restricted (Wartzok and Ketten 1999) and the sonar signals of harbor porpoises differ in some way from those of most delphinid species. Whereas echolocation clicks of dolphins are broad-band signals with three to seven pressure cycles in the time domain (peak frequency smaller or arround 80 kHz), harbor porpoises have narrow-band signals with a peak frequency of 130 to 140 kHz and eight to twenty pressure cycles (Kastelein et al. 1999, Au et al. 1999). According to Cranford (1999, 2000) the porpoise click pattern should be termed polycyclic whereas the clicks of most dolphin species are oligocyclic. Apart from the intense high frequencies in the signals of *P. phocoena*, a low-frequency component of lower intensity can be found. Amundin (1991) demonstrated that this low-frequency component is an air-borne effect, probably a by-product of the pneumatically-driven process generating the tissue-borne high frequencies (Cranford et al. 1996). Whistle-like sounds of porpoises were reported only a few times in the literature (Verboom and Kastelein 1995, 1997).

Toothed whales are peculiar in that they have no facial expression. The facial musculature is instead concentrated around the blowhole as part of the nasal or epicranial complex. The latter also includes the upper respiratory tract with a

system of air sacs (Mead 1975) and (acoustic) fat bodies (Cranford et al. 1996) which apparently have no counterparts in terrestrial mammals. All odontocetes, in contrast to the baleen whales (mysticetes), show at least some degree of asymmetry in the skull roof and the overlying epicranial complex.

Differences between the acoustic characteristics of echolocation sounds of harbor porpoises and delphinids point to group-related adaptations in the click production and/or emission mechanisms. In turn, these differences in mechanism should be linked to morphological specializations of the sound generator and/or emitter. The forehead anatomy of harbor porpoises was described in some detail by Curry (1992). In general, she states that sound production occurs at the same level as in dolphins, i.e. about the nasal plug lips, at the lips of the blowhole ligament (free lip between the nasal passage and the posterior nasofrontal sac), and at the "elliptical bodies" (dorsal bursae). Curry (1992) suggests that differences in sound production between dolphins and porpoises can be attributed to differences in the size of the nasal sacs, in the control of air flow through the nasal passage, and in the mode of sound transmission. In this paper (Curry 1992), a functional model of sonar click production in the harbor porpoise is presented in comparison with recent data on delphinids.

### 3.3. "River dolphins" (*Pontoporia blainvillei* and *Inia geoffrensis*)

At least three living groups of "river dolphins", represented by 1) the La Plata dolphin (*Pontoporia blainvillei*), 2) the Amazon river dolphin (*Inia geoffrensis*), and 3) the baiji (*Lipotes vexillifer*), seem to be more closely related to the delphinids than to the Platanistidae, the other "river dolphin" group with 4) the Ganges and Indus river dolphins (*Platanista gangetica*). But there are indications that at least

the pontoporiids have long been distinct from other toothed whales (Fordyce and Muizon 2001). In general, the extant so-called river dolphins are characterized by a long and narrow (tweezers-like) rostrum, a small melon (Mead 1975), and a relatively symmetric facial skull (except *Platanista gangetica.;* Ness 1967); all of these characteristics are thought to be plesiomorphic features (Barnes 1985, Oelschläger 1990).

As to the nasal anatomy of the La Plata dolphin not much is known. Schenkkan (1972) published a comprehensive overview on its gross morphology, Mead (1975) a short note, and Cranford et al. (1996) a short description including morphometric measurements of potential acoustic structures based on CT data. Vocalizations were documented only once by Busnel et al. (1974) but this relatively old study must be interpreted with precaution since modern acoustic equipment brought some new insights into the sound repertoire of toothed whales.

There is only a small amount of information on the nasal anatomy of the Amazon river dolphin. Whereas Mead (1975) published a preliminary note, Schenkkan (1977) gave the first detailed description on the epicranial complex of this species. In comparison, the documentation of the acoustic behavior of this species is poor but not as unreliable as for *Pontoporia*. Click sounds are reported to have a peak frequency around 100 kHz (Kamminga et al. 1993, Wartzok and Ketten 1999).

In this study the nasal morphology of the La Plata dolphin and the Amazon river dolphin is compared with the situation found in dolphins and porpoises.

## 3.4. Sperm whales (Superfamily Physeteroidea)

Some of the most asymmetric and specialized foreheads are found in members of the superfamily *Physeteroidea* (Heyning and Mead 1990) which include only three extant species: the giant sperm whale (*Physeter macrocephalus*), the dwarf and the pigmy sperm whales (*Kogia sima* and *K. breviceps*). Male giant sperm whales may attain a body length of nearly 20 m but females usually reach only half of this total length. Thus, sexual dimorphism is more pronounced here than in other cetaceans (Berzin 1972). The head of this animal, similar to the bow of a submarine in shape, is extremely large in both absolute and relative terms and, in the adult male, may attain nearly one third of the total body length and its weight may equal more than one third of the total body weight (Nishiwaki et al. 1963). Hypertrophy of the epicranial complex and its structures on the right side as well as the concomitant secondary forward projection of the nasal tract (Klima et al. 1986, Cranford et al. 1996; Cranford 1999) have led to this grotesquely enlarged and asymmetric nose. Accordingly, the world's largest nose degrades the skull, and the neurocranium in particular, to an insignificant small structure (Klima 1990). In these terms the sperm whale can be described as "a nose with outborder" (Møhl 2003). The most recent examination of this immense nasal apparatus interpret it as bio-acoustic machine that is capable of generating the highest biological source level ever recorded of up to 223 dB *re* 1 µPa (Møhl et al. 2000, Møhl 2001). This sound level corresponds to an emitted acoustic power of 167 kW (omnidirectional) or approximately 167 W with a directivity index in the order of 30 dB (Møhl et al. 2000).

The anatomy of this "biggest nose on record" (Raven and Gregory 1933) has received a great deal of attention over time and so various hypotheses regarding the function of this enlarged "organ" came on file. Most proposals fall into two

broad categories: buoyancy regulation and sound generation. In the 1970s Clarke (1970, 1978b) picked up and expanded an earlier notion of Raven and Gregory (1933) that the sperm whale should be able to control its buoyancy by alternately heating and cooling the large lipid structures within the nose. On the other hand, Norris and Harvey (1972) proposed a primarily acoustic function for the sperm whale nose. Norris and Møhl (1983) marshaled evidence suggesting acoustic debilitation of prey by the enlarged nasal apparatus in odontocetes, a function that may have reached its zenith in the giant sperm whale.

Intrepid anatomists have periodically investigated the structure of the sperm whale nose; initial descriptions date back as early as the end of the 19$^{th}$ century (Pouchet and Beauregard 1885). Discussions of functional aspects and of the relationships between nasal structures across the odontocete cetaceans are known from Raven and Gregory (1933), Schenkkan and Purves (1973), Mead (1975), Cranford et al. (1996), and Cranford (1999). Cranford et al. (1996) used anatomic landmarks to propose a parsimonious scheme for these homologous structures. They suggested that the spermaceti organ of the sperm whale, one of the giant nasal fat bodies in the animal, is an extremely hypertrophied homologue of the right posterior dorsal bursa in non-physeterid odontocetes. This hypothesis implies that the spermaceti organ did not develop de novo, as had been suggested previously (Heyning 1989), but evolved with the exceptional hypertrophy of the right side of the forehead and the concomitant reduction in size of structures on the left side, resulting in extreme asymmetry.

These proposed homologies between nasal structures across the odontocete suborder (Cranford et al. 1996), in combination with accumulated evidence from visual inspection (Norris et al. 1971 cited after Norris 1980, Ridgway et al. 1980), manual palpation (Amundin and Andersen 1983, Ridgway and Carder 2001),

observations using high-speed video endoscopy in dolphins (Cranford 2000), examinations of artificial sound in dead animals (Møhl 2001, Møhl et al. 2002), and the analysis of acoustic behavior (Wahlberg 2002) strongly suggest that the odontocete nose generates the impulse sounds used mainly in echolocation. This implies that homologous structures in the epicranial complex of toothed whales may have a similar function during sonar sound generation and emission. Therefore, Cranford (1999) concluded that the sperm whale nose functions similarly as in other toothed whales but may have reached its immense size in response to a combination of selective pressures, most notably those associated with feeding ecology and sexual selection. The author interpreted the sex-related size dimorphism of the sperm whale nose in terms of sexual selection of adult males via this acoustic display.

Due to the hypertrophied size of the right nasal structures, some nasal components of the left side seem to be degenerated. This, however, does not hold for the left nasal passage which, in contrast to the acoustic function of the right nasal tract, mainly serves respiration (Norris and Harvey 1972). According to this asymmetry, the remnants of the nasal septum and tectum, the so-called nasal roof cartilage (Klima 1999), appear to be shifted to the left. The nasal roof cartilage of the sperm whale was described first by Behrmann and Klima (1985). Histological investigations of early fetuses and adult whales revealed differences of these cartilaginous tissues regarding fiber characteristics (Klima 1990). The histogenetic process, however, leading to tissue differentiation could not be studied so far since the intermediate stages of development were lacking. Therefore, this study of neonate sperm whales offers the unique chance to reconstruct the histogenesis of the nasal roof cartilage and to explain the developmental process of this tissue, in general. Furthermore, the results obtained may give insights into the functional implications of this unique cetacean structure.

According to the development of the cartilaginous nasal skull, the cetacean order can be divided into at least three groups: baleen whales, sperm whales, and toothed whales (except sperm whales). In this context, sperm whales show a pattern similar to the situation in baleen whales and both these groups are different from the non-physeterid toothed whales (Klima 1995, 1999). These findings have been interpreted in favor of a presumed closer relationship of sperm whales with baleen whales than with the remaining odontocetes (Klima 1999) in accordance with the analysis of Milinkovitch (1995) which was based on genetic studies.

At first sight, the nasal anatomy of the pygmy and dwarf sperm whales (*Kogia breviceps* and *K. sima*) is strikingly different from that of other odontocetes: whereas these small sperm whales have a melon like non-physeterid toothed whales and their blowhole is situated at the vertex of the head in front of the brain case, they have a spermaceti organ and their epicranial complex is characterized by extreme asymmetry. The dorsal accessory air sacs (vestibular sacs, nasofrontal sacs) are very much enlarged on the right and reduced on the left hand side (Schenkkan and Purves 1973). In contrast, the ventralmost air sac, the premaxillary sac, is only present on the left hand side and the nasal plug on the left is several times larger than that on the right as is the case for the accessory bony nostrils in all sperm whales. In *Kogia*, the right nasal passage ends in the vestibular sac by a pair of lips known as the monkey lips (museau du singe; Schenkkan and Purves 1973). However, these lips fit into a connective tissue "cushion" which is situated in the center of the vestibular sac.

*Kogia* has a relatively large melon which abuts to the spermaceti organ caudally. The latter "organ" is strongly curved and projects from the melon to the posterior monkey lip. It has a bent cone shape with the apex in the lip so that it appears to have been rotated clockwise in dorsal view. As stated before, the melon is a

character shared by *Kogia* and the non-physeterid toothed whales. But the existence of the spermaceti organ and the shape of the monkey lips suggest a close relationship between the sperm whale genera (*Physeter* and *Kogia*). As a consequence, Cranford et al. (1996) proposed the following homologies for the extant odontocete families based on identical structural characteristics and topographical relationships within the epicranial complex: (1) the monkey lips (throughout the physeterid and non-physeterid odontocetes), (2) the spermaceti organ (in physeterids) and the right posterior dorsal bursa (in non-physeterid odontocetes) as well as (3) the junk (in *Physeter*) and the melon (in *Kogia* and non-physeterids). Furthermore, the authors postulated similar acoustic implications of these structures regarding sound generation and emission.

## 3.5. Development of the upper respiratory tract in toothed whales

Cetaceans are a unique group of highly derived aquatic mammals. Starting out from fossil terrestrial ancestors among the hoofed animals they have gone through numerous transformations during their evolution. Among the most fascinating trends in the evolution of toothed whales are the fundamental reconstruction of the nose and the size increase of the whole brain as well as allometric growth and the characteristic specialization of its constituents (Oelschläger and Oelschläger 2002). These and other morphological peculiarities among various cetacean organs can be interpreted in the light of their secondary adaptations to the aquatic environment and have been presented in detail in a number of publications (for review see Oelschläger 2000, Fordyce and de Muizon 2001, Williams and Worthy 2002). Interestingly, only a few papers exist on the prenatal anatomy of these animals (for review see Reidenberg and Laitman 2002), and yet it is exactly the developmental aspect which gives most valuable insights into the morphological

details of cetacean evolution (Sedmera 1997a, b, Klima 1999, Kinkel et al. 2001, Richardson and Oelschläger 2002).

In this chapter the morphology of specific organ systems in the heads of late fetal/neonatal spotted dolphins (*Stenella attenuata*) is compared with the situation found in early fetuses and with the adult. For that purpose, three perinatal spotted dolphins were documented using macroscopical dissection, cryo-sectioning, X-ray computer assisted tomography (CT), and magnetic resonance imaging (MRI). These data were compared with microslide series and one magnetic resonance microscopy (MRM) dataset of early fetal dolphins. By this, important ontogenetic changes within the upper respiratory tract become evident at the turn from the embryonal to the fetal period when the cetacean bauplan appears and is gradually accomplished in the various organ systems in order to suffice the requirements of birth in the open sea. In order to compare these findings with the anatomy of adult dolphins and to their life in the open sea we refer in the results chapter (Observations) to existing data in the cetacean literature and then discuss all these observations in the discussion chapter.

## 3.6. Asymmetry of the odontocete facial skull

The facial skull of odontocetes is highly specialized in comparison to the skull of tetrapods and characterized by a developmental (and phylogenetic) process called "telescoping" by Miller (1923). This term stands for a secondary rearrangement of the skull bones and the backward shift of the bony nares, accompanied by an elongation of the rostrum (anterior projection of the premaxilla and maxilla), and the shortening of the nasal bones (if not reduced as is the case in physeterids). This ontogenetic and phylogenetic process can be described as a backward rotation

of the (bony) nasal passages about 90° and as a result, the bony nasal passages have a vertical orientation (Rommel 1990, Klima 1999). Concomitantly, in odontocete skulls, the premaxillary and maxillary bones have been extended caudalward at both sides of the bony nostrils, sliding over the frontal and parietal bones up to the vertex of the skull. The double layer of bones (maxillary/frontal) and the intermediary layer of connective tissue ("sandwich structure"; Fleischer 1976) may reflect sound generated in the blowhole area to the front (Oelschläger 1990, Aroyan et al. 2000).

The facial skull of toothed whales shows a depression that houses the large epicranial complex. The bony nostrils are situated in the center of this facial depression. The epicranial complex and the facial skull exhibit some asymmetry across the genera and families of toothed whales. The degree of asymmetry varies from slight in phocoenid species up to considerable (extreme) in the sperm whale group (Ness 1967, Clark 1978a, c, Heyning 1989, Cranford et al. 1996). Apart from some exceptions (e.g. the vestibular sacs in most delphinid species as well as the nasal plugs and its muscles in physeterids), the nasal structures of the right hand side are larger than those on the left (Schenkkan 1973).

The asymmetry in the nasal complex of toothed whales is directional and thus consistent in its magnitude and direction across species (Kükenthal 1893, 1908, Steinmann 1912, Ness 1967, Arvy 1977, Yurik and Gaskin 1988, Cranford et al. 1996). Where it has been studied, directional asymmetry is considered to be functional, e.g. in the heart and intestine of tetrapods. The degree of odontocete forehead asymmetry varies in the different species, particularly in the region of the so-called MLDB complexes that are thought to be involved in sonar signal generation (Cranford et al. 1996, Cranford 2000). All extant and extinct physeterids are extremely asymmetric. Every other superfamily has at least one

slightly asymmetric member indicating a possible reversal trend regarding this character in toothed whale evolution. The functional significance of odontocete forehead asymmetry has been pondered for more than a century (Van Beneden and Gervais 1880, Weber 1886, Abel 1902, Kükenthal 1908, Steinmann 1912, Howell 1925, Borri 1932). It has been considered that structural asymmetry may produce an asymmetric sound field in order to reduce left-right ambiguity in the sonar problem and/or has been the result of functional separation (respiration vs. sound production) of the two airways (Norris and Harvey 1972, Cranford et al. 1996, Cranford 2000).

Next to the investigation of Ness (1967), this study is another attempt to analyze the facial (nasal) asymmetry of toothed whales morphometrically and systematically by covering different families. In the following, the preliminary results of a two-dimensional study of small odontocetes are given including a total of 12 species, each of them belonging to separate genus.

### 3.7. The specialized larynx of odontocetes

It was shown in different studies that sonar sound generation in the odontocete nasal complex is pneumatically-driven (Ridgway et al. 1980, Amundin and Andersen 1983, Ridgway and Carder 1988; see Introduction). Whereas muscles of the epicranial complex are probably important for the regulation of air flow along the potential sound-generating structures (monkey lips/dorsal bursae complex), most modern hypotheses consider the larynx and its surrounding musculature to produce the air pressure needed for vocalisations (Cranford et al. 1996). In toothed whales, the larynx is situated in the medioventral vault of the skull base. It is characterized by an elongation of the epiglottic and cuneiform cartilages forming a

goose beak-like spout at its rostral end. The tip of the epiglottis forms a neck and lip which are surrounded and held in position by a strong sphincter muscle suspending the epiglottic spout from the bony nares (choanae) and the skull base, respectively (Fig. 2; Negus 1958, Purves and Pilleri 1983). The laryngeal musculature probably generates much of the pneumatic pressure necessary for sound generation by forcing the larynx in the direction of the choanae. Most prominent is here a strong sphincter muscle which connects the tip of the epiglottic spout with the choanae and the skull base (Purves and Pilleri 1983). But also other muscle groups of the gular region and the skull base, associated with the larynx and the hyoid apparatus, may help force the larynx to the choanae. In this paper we will describe a possible mechanism to pressurize the nasal cavity by synchronized actions of the larynx and hyoid musculature.

# 4. MATERIAL AND METHODS

## 4.1. Harbor porpoise and delphinids

The structures of the upper respiratory tract were investigated in 17 harbor porpoises (*Phocoena phocoena*) by means of macroscopic dissection, cryo-sectioning, x-ray computed tomography (CT), and magnetic resonance imaging (MRI). The MRI scans were usually performed in all three planes; the CT scans in the transverse plane. The occasional measurements of anatomical structures given in the text refer to adult porpoises examined. The surface areas of the vestibular and premaxillary sacs were measured from digital photos in dorsal view using the Amira graphics software package (Indeed - Visual Concepts, Germany).

For comparison, the nasal complex was investigated in 11 delphinid specimens. Further details of the specimens examined can be extracted from Table 1. During the dissections, samples of the nasal complex of three harbor porpoises were taken (Table 1); some of them were cryosectioned at 45 to 55 µm thickness. Smaller samples were embedded in paraffin and cut at 14 to 20 µm. All sections were stained with AZAN (azocarmine and anilin blue), Resorcin-Fuchsin, and/or methylene blue (Romeis 1989). Furthermore, a series of microslides of a 16.7 cm *P. phocoena* fetus (sectional thickness 10 µm, AZAN) were included in the analysis (Table 1). The upper respiratory tract of one harbor porpoise specimen was filled with a contrast argent ($BaSO_4$ solution; Table 1) before CT scanning. For comparison, two specimens of the common dolphin (*Delphinus delphis*), one Risso's dolphin (*Grampus griseus*), one longfinned pilot whale (*Globicephala melas*), one whitebeaked dolphin (*Lagenorhynchus albirostris*) specimen, and seven bottlenose dolphins (*Tursiops truncatus*) heads, including microslides of the rostral region of one *T. truncatus* specimen (conducted by G. Pilleri) were examined (Table 1).

This study includes a comparison of the nasal morphology of the harbor porpoise with the same anatomy in dolphins. The term dolphin refers to members of the family Delphinidae. Most of the anatomical descriptions in the literature refer to the genera *Tursiops*, *Delphinus*, and *Stenella* (e.g. Lawrence and Schevill 1956, Schenkkan 1973, Mead 1975, Cranford et al. 1996). In comparison to these studies, the head of a Minke whale (*Balaenoptera acutorostrata*) was scanned by MRI.

For the scans, the horizontal plane was established by means of a strait line between the two periotic bones (or between the eyes when the ear bones had been removed) and by a strait line from the tip of the rostrum to the most ventral point of the foramen magnum. The medio-sagittal plane was judged by the line between the tip of the rostrum and the midpoint of the foramen magnum in right angle to the horizontal plane; the transverse plane perpendicular to both of them. The planes and lines were set using preliminary scans before the actual scans were conducted.

## 4.2. "River dolphins" (*Pontoporia blainvillei* and *Inia geoffrensis*)

Three formalin-fixed heads of the La Plata dolphin (*Pontoporia blainvillei*) were scanned by MRI in all three planes, one of these by CT in the transverse plane. A fourth formalin-fixed head was dissected macroscopically (Table 1). One formalin-fixed head of the Amazon river dolphin (*Inia geoffrensis*) was scanned by MRI and CT but due to the poor fixation it was of limited value in the analysis. A second formalin-fixed head was examined in transverse cryo-sections of approximately 1.5 cm thickness (Table 1).

## 4.3. Sperm whales (*Physeter macrocephalus* and *Kogia breviceps*)

The description of the giant sperm whale (*Physeter macrocephalus*) nasal complex in this dissertation is based mainly on the examination of two heads of neonate animals. A complete computer assisted tomography (CT) data set was produced of the first specimen, a 4.25 m long male and were kindly provided by Dr. Ted W. Cranford (California State University, San Diego, CA, USA). Further details of the scanning procedure of this specimen can be extracted from Cranford (1999). Please note that the planes of the scans do not match those described before (Fig. 31) and it should be kept in mind that the dataset is color-coded and the colors are correlated to density values of tissues under examination. The color code indicate the following tissues according to the macroscopical dissections: white – bone, purple – tough connective tissue, red – fibrous connective tissue, orange – muscle, yellow – fatty tissue.

Furthermore, a second head of a baby sperm whale was investigated. This formalin-fixed head of a 3.41 m neonate male named "Odie" was kindly provided by Prof. Dr. Sam H. Ridgway (U.S. Navy Marine Mammal Program, San Diego, CA, USA). Further details of this specimen were published by Ridgway and Carder (2001). After the removal of the superficial layers (skin, hypodermal layers and superficial muscles) it was scanned using CT and magnetic resonance imaging (MRI). Afterwards, the head was cryo-sectioned in 13 transverse slices of approximately 5 cm thickness using a band saw. The remaining rear part of the head including the posterior end of the nasal complex was dissected macroscopically.

Out of three transverse slices of "Odie" (frontal surface of slices 4, 8, and 12), representing the front, middle, and rear part of the sperm whale nasal complex, samples of the nasal roof cartilage and the cartilaginous rostrum were taken (Fig.

3). These samples were sectioned in the transverse plane at 10 µm thickness and stained with AZAN (azocarmine and anilin blue) and resorcin. The fixation of the tissue was minor quality so that it could not be examined cytologically. However, the basic arrangement of the cells, their territories as well as the extracellular substance including the elastic material were still in a good condition to give a compete insight into the architecture and developmental stage of the tissues examined.

In addition, the nasal apparatus of two young sperm whale bulls stranded in the Wadden Sea of the German Bight were dissected superficially (monkey lips and distal sac regions) and the ear bones were taken.

Two specimens of the pygmy sperm whale (*Kogia breviceps*) were macroscopically dissected. The findings of these dissections were verified by a set of CT scans of an additional specimen kindly donated by Dr. Darlene Ketten (Department of Biology, Woods Hole Oceanographic Institution, Woods Hole *and* Massachusetts Ear and Eye Infirmary [MEEI], Harvard University, Boston, MA, USA; The scanning was supported by the U.S. Office of Naval Research)

### 4.4. Fetal material

One early fetus of the common dolphin (*Delphinus delphis*, CRL 38 mm) was investigated by magnetic resonance microscopy (MRM). This valuable specimen taken from pregnant female dolphins entangled and drowned as incidental bycatch of the tuna boat fishery in the seventies of the last century by officials of the U.S. Government, was dedicated to our institute by the National Marine Fishery Service (NMFS) in San Diego, CA, USA. Obviously, the specimen was fixed in 4%

formalin and to avoid further parameters, it was scanned in its own preservation fluid.

Image acquisition of the early fetus was performed by high-field MRM. Further details on this method can be found in Haddad et al. (in prep.). The fetus was placed in an upright position to fit in the examination coil and scanned at constant temperature. 3D-spin echo images were used with isotropic nominal resolutions of $(78.1\ \mu m)^3$ with 640 x 256 x 256 voxels. During the processing of the raw data a zero filling of a factor of 2 for each dimension was applied, leading to image resolutions of up to $(39.1\ \mu m)^3$ for the fetus.

Due to the pronounced contrast in the MRM images, it was possible to perform a manual segmentation of several organs and structures in the non-zero filled 3D dataset with the Amira graphics software package (Indeed - Visual Concepts, Germany). Segmentation in this context means the assignment of pixels in a 2D image to specific organs, thus creating an anatomical mask which shows the segmented structures only. After the segmentation was performed for each slice of the 3D dataset, 3D surfaces of the segmented structures were reconstructed on the basis of polygonal surface models. From these surface reconstructions surfaces and volumes of the lung were calculated.

We compared the MRM datasets of the early fetus with series of routine histological sections of a spotted dolphin (*Stenella attenuata*) and a common dolphin (*Delphinus delphis*) of comparable size. The 10 µm sections were performed from paraffin embedding and stained with AZAN (azocarmine and aniline blue; Romeis 1989). For comparison, microslide series of early fetal harbor porpoise (*Phocoena phocoena*) and a narwhal specimen (*Monodon monocerus*) were included.

More detailed information of the examined specimens can be extracted from Table 1.

Furthermore, a total of three perinatal spotted dolphins (*Stenella attenuata)*, were investigated (Table 1). These specimens had been donated by the Southwest Fisheries Science Center in La Jolla (National Marine Fisheries Service, San Diego, U.S.A.) and had been fixed by immersion in 4% buffered formaldehyde solution.

Whereas two heads were dissected macroscopically, the third was used for x-ray computer assisted tomography (CT) and magnetic resonance imaging (MRI) in the transverse and horizontal planes (Somatom Plus, Magnetom SP 63; Siemens Corp., Erlangen, Germany). This head was frozen afterwards and cut transversely with a band saw into slices of 8-12 mm thickness (Rauschmann 1992). The planes orientation of the scans and the band-saw sections are shown in Figure 4. Please note that the planes have slightly different orientation than those of the specimens described before.

Table 1: List of the material examined. Methods of examination: CS – (macroscopical) cryosectioning, CT – computer assisted tomography, DS – macroscopical dissection, HS – histological sections, MRI – magnetic resonance imaging, MRM – magnetic resonance microscopy. CRL – crown-rump length, CBL – condylo-basal length.

| Species (cf. Rice 1998) | Donated by* | ID Number | Age | Body length | Sex | Examined parts | Fixation | Method; application |
|---|---|---|---|---|---|---|---|---|
| *Cephalorhynchus spec.* | SAI | ? | adult | ? | ? | head | Formalin | MRI |
| *Delphinus delphis* | NMNH | ? | adult | ? | ? | nasal complex with skull | Frozen | DS |
| *Delphinus delphis* | SAI | LES 001 | fetal | 38 mm (CRL) | ? | head | Formalin (4%) | MRM (Haddad et al., in prep.) |
| *Delphinus delphis* | SAI | RJO 381 (Dd 14; K 50) | fetal | 40.5 mm (CRL) | ? | head | Ethanol (70%) | HS (10 µm sagittal sections stained with AZAN) |
| *Delphinus delphis (?)* | SAI | ? | fetal | 10.8 cm (CBL) | ? | head | Ethanol | CS (mediosagittal) |
| *Globicephala melas* | coll. G. Pilleri | ? | fetal | ? | ? | head | Formalin | CS (mediosagittal) |
| *Grampus griseus* | NMNH | WJW 012 | adult | ? | ? | nasal complex with skull | Frozen | DS |
| *Inia geoffrensis* | coll. G. Pilleri | ? | ? | ? | ? | head | Formalin | CT, MRI |
| *Inia geoffrensis* | SAI | SAI 53.12 | adult | ? | f | head | Formalin | CS (transverse) |
| *Kogia breviceps* | NMNH | ? | subadult | ? | m | head | Frozen | DS |
| *Kogia breviceps* | NMNH | DAP 033 | adult | ? | ? | head | Frozen | CT, DS |
| *Kogia breviceps* | ? | ? | ? | ? | ? | head | Frozen | CT (by D. Ketten) |
| *Lagenorhynchus albirostris* | DMM | ? | adult | ? | ? | head | Formalin | CS (mediosagittal) |
| *Monodon monocerus* | HL | Hill coll. CE 1 | fetal | 13.7 cm | m | head | Ethanol | HS (40 µm transverse sections stained with hematoxylin-erythrosin) |
| *Neophocaena phocaenoides* | coll. G. Pilleri | ? | adult | ? | ? | larynx | ? | HS (by G. Pilleri) |
| *Phocoena phocoena* | DMM | ? | adult | ? | f | head | Frozen | CT, MRI, CS (mediosagittal) |
| *Phocoena phocoena* | FTZ | 898 | neonate | 78 cm | m | nasal complex with skull | Formalin | MRI |
| *Phocoena phocoena* | FTZ | 903 | fetal | 62 cm | f | nasal complex with skull | Frozen | MRI, HS |
| *Phocoena phocoena* | FTZ | 905 | adult | 161.5 cm | f | nasal complex with skull | Frozen | CT (nasal sacs filled by $BaSO_4$ solution) |
| *Phocoena phocoena* | FTZ | 1281 | subadult | 106 cm | m | nasal complex with skull | Frozen | CT, MRI, DS |
| *Phocoena phocoena* | FTZ | 1321 | adult | 131 cm | m | nasal complex with skull | Formalin | DS |
| *Phocoena phocoena* | FTZ | 1366 | adult | 110 cm | f | nasal complex without melon | Formalin | MRI, HS |
| *Phocoena phocoena* | FTZ | 1367 | adult | 102 cm | m | head | Formalin | DS |
| *Phocoena phocoena* | FTZ | 1369 | adult | 116.5 cm | f | head | Formalin | CT, MRI, DS |
| *Phocoena phocoena* | FTZ | 1370 | adult | 136.5 cm | m | nasal complex with skull | Formalin | DS, HS |
| *Phocoena phocoena* | FTZ | ? | adult | ? | f | nasal complex with skull | Frozen | DS |
| *Phocoena phocoena* | FTZ | ? | adult | ? | f | nasal complex with skull | Frozen | DS |
| *Phocoena phocoena* | SAI | ? | adult | ? | m | head | Frozen | sagittal CS |
| *Phocoena phocoena* | SAI | ? | adult | ? | m | head | Frozen | transverse CS |
| *Phocoena phocoena* | SAI | MK 48 | fetal | 16.7 cm | ? | head | ? | HS (10 µm transv. sections stained with AZAN) |
| *Phocoena phocoena* | SMF | ? | neonate | 72 cm | ? | head | Ethanol | CT, MRI |

| Species | Donated by* | ID Number | Age | Body lenght | Sex | Examined parts | Fixation | Method; application |
|---|---|---|---|---|---|---|---|---|
| *Phocoena phocoena* | ZMUC | CN 138 | fetal | 42 cm | ? | head | Ethanol | CT, MRI |
| *Physeter macrocephalus* | don. S. Ridgway | "Odie" | neonate | 3.41 m | m | nasal complex with skull | Formalin | CT, MRI, DS, CS (transverse), HS |
| *Physeter macrocephalus* | don. T. Cranford | ? | neonate | 4.25m | m | head | Frozen | CT (Cranford 1999) |
| *Physeter macrocephalus* | FTZ | 1922 | adult | 14.8 m | m | nasal complex with skull | Fresh | DS |
| *Physeter macrocephalus* | FTZ | 1924 | adult | 14.6 m | m | nasal complex with skull | Fresh | DS |
| *Platanista gangetica* | coll. G. Pilleri | 473 | adult | ? | ? | head | Formalin | CS (sagittal) |
| *Platanista gangetica* | coll. G. Pilleri | ? | adult | ? | ? | head | Formalin | CT, MRI |
| *Pontoporia blainvillei* | coll. G. Pilleri | ? | adult | (44 cm CBL) | ? | head | Formalin | MRI, DS |
| *Pontoporia blainvillei* | coll. G. Pilleri | ? | adult | ? | ? | head | Formalin | MRI |
| *Pontoporia blainvillei* | coll. G. Pilleri | ? | adult | ? | ? | head | Formalin | CT, MRI |
| *Pontoporia blainvillei* | coll. G. Pilleri | ? | adult | ? | ? | head | Formalin | CT, MRI |
| *Stenella attenuata* | SAI | CWO 813 (Sa 12) | embryo | 12.5 mm (CRL) | ? | head | Ethanol (70%) | MRI (Haddad et al., in prep.) |
| *Stenella attenuata* | SAI | IMC 196 (Sa 50; K 25) | fetal | 43.5 mm (CRL) | ? | head | Ethanol (70%) | HS (10 µm transv. sections stained with AZAN) |
| *Stenella attenuata* | NMFS | BGB 036 | perinatal | ? | ? | head | Formalin | DS (Rauschmann 1992) |
| *Stenella attenuata* | NMFS | RBR 018 (SA 90) | perinatal | 94.5 cm | ? | head | Formalin | CT, MRI, CS (transverse), HS (Rauschmann 1992) |
| *Stenella attenuata* | NMFS | ? | perinatal | ? | ? | head | Formalin | DS (Rauschmann 1992) |
| *Tursiops truncatus* | coll. G. Pilleri | ? | fetal | ? | ? | head | Formalin | CS (mediosagittal) |
| *Tursiops truncatus* | coll. G. Pilleri | ? | adult | ? | ? | rostrum and adjacent melon tissue | ? | HS (by G. Pilleri) |
| *Tursiops truncatus* | NMNH | 01-TTR 031 | adult | ? | ? | nasal complex with skull | Frozen | DS |
| *Tursiops truncatus* | NMNH | MMSC 98-Ø81 | adult | ? | ? | nasal complex with skull | Frozen | DS |
| *Tursiops truncatus* | NMNH | NJ 00-110 | adult | 315 cm | m | nasal complex with skull and throat | Frozen | DS |
| *Tursiops truncatus* | NMNH | REL 017 | adult | ? | ? | nasal complex with skull | Frozen | DS |
| *Tursiops truncatus* | SAI | SAI 7928 | subadult? | ? | ? | head | Formalin | CT, MRI |

* coll. G. Pilleri – collection of Prof. Dr. G. Pilleri, Paciano, Italy (located in SMF); don. S. Ridgway – donated by Prof. Dr. Sam H. Ridgway, U.S. Navy Marine Mammal Program, San Diego, CA, USA; don. T. Cranford – donated by Dr. Ted W. Cranford, California State University, San Diego, CA, USA; DMM – Deutsches Meeresmuseum, Stralsund, Germany; FTZ – Forschungs- und Technologiezentrum Westküste, Büsum, Germany; HL - Hubrecht Laboratory, Utrecht, The Netherlands; NMFS - National Marine Fishery Service, San Diego, CA, USA; NMNH – National Museum of Natural History, Washington, DC, USA; SAI – Dr. Senckenbergische Anatomie, Johann Wolfgang Goethe University, Frankfurt a.M., Germany; SMF – Forschungsinstitut und Naturmuseum Senckenberg, Frankfurt a.M., Germany; ZMUC – Zoological Museum of the University of Copenhagen, Denmark.

## 4.5. Odontocete skull asymmetry

For this study 101 skulls of 12 odontocete species out of 12 genera (*Cephalorhynchus*, *Delphinus*, *Inia*, *Kogia*, *Lagenorhynchus*, *Lissodelphis*, *Phocoena*, *Phocaenoides*, *Pontoporia*, *Steno*, *Stenella*, and *Tursiops*) were examined. Further details on the species and numbers can be extracted from Tables 2 and 4. The skulls are stored in the National Museum of Natural History (Smithsonian Institution in Washington, DC, USA). Each skull was photographed in dorsal view. In order to photograph each skull at the same angle the camera axis was oriented perpendicular to the study table and the dorsal surface of the rostrum of each skull was positioned parallel to the table by using a spirit-level. The color photos were digitized afterwards with a resolution of 96 ppi in which the original photo section was approximately 55 x 37 $cm^2$. In each digital photo, the axis of the skull was determined as the straight line between the midpoint of the tip of the rostrum and the midpoint of the foramen magnum. AS the foramen magnum is not obvious in the photos, the midpoint between the condyles was marked before taking the photograph. Subsequently, two transverse straight lines were taken in each digital image: a posterior line connecting the caudalmost extension of the left and right posterior facial borders (landmarks 23 and 24; Table 3, Figure 5) and an anterior line connecting the left and right antorbital tubercles (landmarks 7 and 8; Table 3). Note that in those species which do not necessarily have an anterior tubercle (because the antorbital notch may be absent as, e.g., in the harbor porpoise; Fig. 5), the anterior line was drawn between the turning points of the left and right lateral skull contours. These two transverse lines border the nasal skull rostrally and caudally, respectively.

After the axis as well as the rostral and caudal border lines of the skull were labeled in the digital images, the 24 landmarks were set (as described in Table 3

and Figure 5) using the tpsDig software (© F.J. Rohlf, 2001, http://life.bio.sunysb.edu/morph/). The Cartesian coordinates of the landmarks were then converted to a coordinate system where landmark 1 was the zero point and the distance between landmarks 1 and 2 was set to 1. Using this conversion the data of each skull were given in relation to the length of the nasal skull along its axis (superimposition or fitting; Rohlf 1999). Correlation of data due to size and age of animals could be ignored that way (but not allometric changes within species). The full dataset was analyzed statistically using a principle component analysis (PCA) of the Statistica software package (© StatSoft, http://www.statsoft.com/). Since the data did not differ conspicuously between sexes (cf. Figures 58 to 64) they were analyzed in species groups.

To analyze the degree of skewing of the skulls (Ness 1967) the distances between the landmarks along the mid-suture (LM 4, 5, 6; Fig. 5) and the axis of the skull (measured perpendicular to the axis) were analyzed in bar plots. This time, there was an distinction between species and sex. Furthermore, the following six bilateral distances (I to VI) were taken perpendicular to the axis of the skull (absolute x values of the two-dimensional coordinates) and plotted in bars:

I. left rostrum width versus right rostrum width; LM 3 - LM 9 : LM 3 - LM 10
II. left premaxillary width versus right premaxillary width at the anterior border of the nasal skull; LM 3 - LM 11 : LM 3 - LM 12
III. left nasal skull width versus right nasal skull width; LM 4 - LM 13 : LM 4 - LM 14
IV. left maximum premaxillary width versus right maximum premaxillary width; LM 4 - LM 15 : LM 4 - LM 16
V. left width versus right width of dorsal openings of bony nasal passages; LM 5 : LM 17 : LM 5 - LM 18
VI. width of left bony nares versus width of right bony nares; LM 5 - LM 21 : LM 5 - LM 22

Table 2: List of the skulls examined including species name, sex, total length, collection number, and abbreviation for species and sex.

| Species | Sex | Total length (cm) | Catalog no. |
|---|---|---|---|
| *Cephalorhynchus commersonii* | F | 132 | 550154 |
| *Cephalorhynchus commersonii* | F | 144 | 550155 |
| *Cephalorhynchus commersonii* | F | 136 | 550449 |
| *Cephalorhynchus commersonii* | M | 136 | 550156 |
| *Delphinus delphis* | F | 186 | 571211 |
| *Delphinus delphis* | F | 195 | 571219 |
| *Delphinus delphis* | F | 200 | 571320 |
| *Delphinus delphis* | F | 206 | 571996 |
| *Delphinus delphis* | F | 202 | 572001 |
| *Delphinus delphis* | M | 210 | 571993 |
| *Delphinus delphis* | M | 217 | 571994 |
| *Delphinus delphis* | M | 206 | 571997 |
| *Delphinus delphis* | M | 208 | 571998 |
| *Delphinus delphis* | M | 225 | 572415 |
| *Inia geoffrensis* | F | 188 | 395415 |
| *Inia geoffrensis* | F | 200 | 395602 |
| *Inia geoffrensis* | F | 136 | 395614 |
| *Inia geoffrensis* | M | 255 | 239667 |
| *Kogia sima* | F | 170 | 504132 |
| *Kogia sima* | F | 237 | 504221 |
| *Kogia sima* | F | 228 | 550471 |
| *Kogia sima* | F | 213 | 550482 |
| *Kogia sima* | M | 234 | 504858 |
| *Kogia sima* | M | 183 | 550345 |
| *Kogia sima* | M | 224 | 550487 |
| *Kogia sima* | M | 187 | 571200 |
| *Kogia sima* | M | 208 | 571663 |
| *Lagenorhynchus acutus* | F | 210 | 571343 |
| *Lagenorhynchus acutus* | F | 228 | 571346 |
| *Lagenorhynchus acutus* | F | 226 | 571387 |
| *Lagenorhynchus acutus* | F | 216 | 571389 |
| *Lagenorhynchus acutus* | F | 224 | 571405 |
| *Lagenorhynchus acutus* | M | 253 | 571347 |
| *Lagenorhynchus acutus* | M | 242 | 571390 |
| *Lagenorhynchus acutus* | M | 260 | 571391 |
| *Lagenorhynchus acutus* | M | 242 | 571395 |
| *Lagenorhynchus acutus* | M | 236 | 571402 |
| *Lissodelphis borealis* | F | 205 | 550026 |
| *Lissodelphis borealis* | F | 211 | 550027 |
| *Lissodelphis borealis* | F | 204 | 571322 |
| *Lissodelphis borealis* | M | 208 | 270981 |
| *Lissodelphis borealis* | M | 268 | 484929 |
| *Lissodelphis borealis* | M | 196 | 550071 |
| *Lissodelphis borealis* | M | 212 | 550188 |
| *Phocoena phocoena* | F | 158 | 571500 |
| *Phocoena phocoena* | F | 175 | 571546 |
| *Phocoena phocoena* | F | 114 | 571715 |
| *Phocoena phocoena* | F | 127 | 571718 |

| Species | Sex | Total length (cm) | Catalog no. |
|---|---|---|---|
| *Phocoena phocoena* | F | 117 | 572019 |
| *Phocoena phocoena* | M | 133 | 571725 |
| *Phocoena phocoena* | M | 106 | 571726 |
| *Phocoena phocoena* | M | 123 | 572012 |
| *Phocoena phocoena* | M | 116 | 572018 |
| *Phocoenoides dalli* | F | 177 | 286864 |
| *Phocoenoides dalli* | F | 189 | 286870 |
| *Phocoenoides dalli* | F | 164 | 286880 |
| *Phocoenoides dalli* | F | 211 | 550190 |
| *Phocoenoides dalli* | M | 184 | 286888 |
| *Phocoenoides dalli* | M | 172 | 286889 |
| *Phocoenoides dalli* | M | 202 | 396304 |
| *Phocoenoides dalli* | M | 211 | 504969 |
| *Pontoporia blainvillei* | F | 135 | 550616 |
| *Pontoporia blainvillei* | F | 99 | 550620 |
| *Pontoporia blainvillei* | F | 147 | 550621 |
| *Pontoporia blainvillei* | F | 158 | 550624 |
| *Pontoporia blainvillei* | F | 110 | 550632 |
| *Pontoporia blainvillei* | M | 115 | 550625 |
| *Pontoporia blainvillei* | M | 120 | 550629 |
| *Pontoporia blainvillei* | M | 117 | 550631 |
| *Pontoporia blainvillei* | M | 109 | 550633 |
| *Pontoporia blainvillei* | M | 120 | 550634 |
| *Stenella attenuata* | F | 192 | 504143 |
| *Stenella attenuata* | F | 138 | 504803 |
| *Stenella attenuata* | F | 185 | 504804 |
| *Stenella attenuata* | F | 201 | 550771 |
| *Stenella attenuata* | M | 194 | 504141 |
| *Stenella attenuata* | M | 145 | 504798 |
| *Stenella attenuata* | M | 186 | 504801 |
| *Stenella attenuata* | M | 165 | 504802 |
| *Stenella attenuata* | M | 164 | 504847 |
| *Stenella attenuata* | M | 180 | 504848 |
| *Steno bredanensis* | F | 215 | 550221 |
| *Steno bredanensis* | F | 207 | 550343 |
| *Steno bredanensis* | F | 208 | 550368 |
| *Steno bredanensis* | F | 212 | 550370 |
| *Steno bredanensis* | F | 230 | 550371 |
| *Steno bredanensis* | M | 212 | 550182 |
| *Steno bredanensis* | M | 216 | 550217 |
| *Steno bredanensis* | M | 193 | 550369 |
| *Steno bredanensis* | M | 228 | 550837 |
| *Steno bredanensis* | M | 173 | 550918 |
| *Tursiops truncatus* | F | 247 | 571016 |
| *Tursiops truncatus* | F | 254 | 571019 |
| *Tursiops truncatus* | F | 250 | 571022 |
| *Tursiops truncatus* | F | 221 | 571025 |
| *Tursiops truncatus* | F | 233 | 571029 |
| *Tursiops truncatus* | M | 228 | 571020 |
| *Tursiops truncatus* | M | 241 | 571023 |
| *Tursiops truncatus* | M | 270 | 571026 |
| *Tursiops truncatus* | M | 258 | 571027 |
| *Tursiops truncatus* | M | 223 | 571032 |

Table 3: List of the landmarks (LM) used in this study (see Figure 5)

| LM | landmark location |
|---|---|
| 1 | junction of artificial midline and connecting line between LM 23 and 24 |
| 2 | junction of artificial midline and connecting line between LM 7 and 8 |
| 3 | junction of connecting line LM 7 - LM 8 and local midpoint of groove of rostral cartilage |
| 4 | local midpoint of bony nasal septum at anterior border of bony nares |
| 5 | ventral (rostral) point of midline between the nasal bones |
| 6 | dorsal (caudal) point of midline between the nasal bones |
| 7 | anterior extremity of left antorbital tubercle |
| 8 | anterior extremity of right antorbital tubercle |
| 9 | junction of left border of rostrum and connecting line LM 7 - LM 8 |
| 10 | junction of right border of rostrum and connecting line LM 7 - LM 8 |
| 11 | junction of left border of premaxilla and connecting line LM 7 - LM 8 |
| 12 | junction of right border of premaxilla and connecting line LM 7 - LM 8 |
| 13 | lateral most extension of left facial border |
| 14 | lateral most extension of right facial border |
| 15 | lateral most extension of left premaxilla |
| 16 | lateral most extension of right premaxilla |
| 17 | lateral most extension of left bony naris |
| 18 | lateral most extension of right bony naris |
| 19 | posterior most expansion of left premaxilla |
| 20 | posterior most expansion of right premaxilla |
| 21 | lateral most extension of left nasal bone |
| 22 | lateral most extension of right nasal bone |
| 23 | posterior most expansion of left facial border |
| 24 | posterior most expansion of right facial border |

## 4.6. The odontocete larynx and hyoid apparatus

The examination of the odontocete larynx and the hyoid apparatus is based mainly on macroscopical dissections, cryo-sections, and MRI scans of eight harbor porpoise specimens ("head" specimens in Table 1). For comparison, a perinatal spotted dolphin head was examined by a complete series of transverse cryo-sections, CT, and MRI scans. In addition, the heads of a bottlenose dolphin (*Tursiops truncatus*) and three La Plata dolphins (*Pontoporia blainvillei*) were studied by MRI whereas another head of the latter species as well as a head of a pygmy sperm whale (*Kogia breviceps*) were dissected macroscopically. Furthermore,

near mediosagittal histological sections of a whole larynx of a porpoise (*Neophocaena phocaenoides*; donated by G. Pilleri) was included in the analysis. For additional information of the specimens examined cf. Table 1.

## 4.7. Terminology

Because the organization of the nasal complex in toothed whales is unique among mammals, there were only minor attempts to establish a valid terminology for these structures. The biggest problem is that there are so few homologous structures in other (terrestrial) mammals (Lawrence and Schevill 1965). Wherever possible, this dissertation follows the terminology of Nickel et al. (1968) but the nomenclature of these nasal structures typical of cetaceans follows Mead (1975). The situation in the terminology of structures associated with the larynx and the hyoid apparatus is more constructive than in the nasal tract because most homologies are clear. A review on the anatomy of this area was done by Schneider (1964), Lawrence and Schevill (1965), and Reidenberg and Laitman (1994) and the terminology in this paper follows the latter description. The taxonomy and systematics on the species level follow Rice (1998) for extant species and Fordyce and Muizon (2001) for fossil groups and higher taxa. For comparison of scientific names of species examined and their common names used in this study see Table 4.

Table 4: List of species examined: scientific nomenclature vs. common name (Rice 1998)

| **Species** | **common name** |
|---|---|
| *Cephalorhynchus commersonii* | Commerson's dolphin, jacobite |
| *Delphinus delphis* | common dolphin, shortbeaked common |
| *Globicephala melas* | longfinned pilot whale |
| *Grampus griseus* | Risso's dolphin |
| *Inia geoffrensis* | Amazon river dolphin, boto |
| *Kogia sima* | dwarf sperm whale |
| *Kogia breviceps* | pygmy sperm whale |
| *Lagenorhynchus acutus* | Atlantic whitesited dolphin |
| *Lagenorhynchus albirostris* | whitebeaked dolphin |
| *Lissodelphis borealis* | northern right-whale dolphin |
| *Monodon monocerus* | narwhal |
| *Neophocaena phocaenoides* | finless porpoise |
| *Phocoena phocoena* | harbor porpoise |
| *Phocoenoides dalli* | Dall's porpoise |
| *Physeter macrocephalus* | giant sperm whale |
| *Platanista gangetica* | Indus and Ganges river dolphins |
| *Pontoporia blainvillei* | La Plata dolphin, franciscana |
| *Stenella attenuata* | (pantropical) spotted dolphin |
| *Steno bredanensis* | rough-toothed dolphin |
| *Tursiops truncatus* | bottlenose dolphin |

# 5. OBSERVATIONS

## 5.1. The nasal complex of the toothed whales

### 5.1.1. Harbor porpoise (*Phocoena phocoena*)

The **skull** of the harbor porpoise is similar to other odontocete skulls (Fig. 6; Noldus and De Klerk 1984, Robineau 1994). Anteriorly, the splanchnocranium is characterized by a beak-like triangulate rostrum whereas, posteriorly, the expanded neurocranium houses the large brain. The nasal skull is situated at the border between the two main cranial components. The bony nasal passage has the same vertical orientation as the soft nasal passage (in Figure 6 perpendicular to the plane of paper). It connects the blowhole situated in front and above the vertex of the skull with the bony nostrils (Figs. 1, 2). The latter are located in the center of a depression and in the center of the skull, respectively, immediately in front of the brain case. This facial depression, also called the **facial fossa** (Heyning 1989), consists mainly of the flat caudal elongations of the premaxillary and maxillary bones. During development the maxillary bones slide over the frontal bones on both sides of the bony nares. This process was termed "telescoping" by Miller (1923) and it results in postnatal animals in a so-called "sandwich structure" where the maxillary and frontal bones are united by large contact surfaces with interposed connective tissue (Figs. 6, 7; Fleischer 1976).

The facial fossa houses the hypertrophied soft nasal complex. The lateral contours of the facial fossa, the facial borders, encircle the nasal skull (Heyning 1989) and join the supraoccipital bone dorsomedially and caudally in the **vertex** This transverse crest is the dorsalmost point of the porpoise skull and shaped by the interparietal, frontal, and supraoccipital bones. Anteriorly, the facial fossa ends in the shallow **antorbital notch**, the indented caudal border of the rostrum where the

facial nerve turns dorsad to innervate the blowhole muscles. The rostrum consists of tooth-bearing maxillae laterally and the premaxillae with the unpaired vomer medially. The median cleft between the premaxillae houses the **rostral cartilage** (cartilaginous rostrum; Fig. 8) which is extends in the gutter-like grove of the vomer. This cartilage attaches caudally to the mesethmoid bone as part of the nasal septum.

The nasal passages at the center of the facial skull are lined rostrally by the premaxilla and in some skulls mediorostrally by the Meckelian ossicles (Klima 1999). Anterior to the nostrils the premaxillary bones form two bulbous convexities, the **premaxillary eminences** or premaxillary bosses (Figs. 6, 11). On each side, the premaxilla extends caudalward at least halfway along the bony naris (Heyning 1989). In some *P. phocoena* skulls, however, this caudal process even reaches the nasal bones. But in all skulls the eminences are raised above the level of the facial fossa. Interestingly, the width of the premaxillae at the bony nares is less than in most delphinid species. Delphinoid premaxillae form smooth and flat surfaces or shelves that expand rostrally and laterally from the bony nares. The dorsal surfaces of the premaxillary shelves form the ventral floor of the premaxillary sacs in all delphinoids (see below). In the harbor porpoise, however, these surfaces (and thus the premaxillary sacs) have a three-dimensional relief caused by the eminences. Between the bony nares (ectethmoid; Fig. 6) and the vertex shallow bilateral depressions can be found immediately lateral to the midline of the skull. It consists of the ethmoid bone immediately caudal to the superior bony nares as well as the ventral part of the nasals and the maxillae. These depressions accommodate the posterior surface of the caudal sac (see below). The asymmetry of the facial skull is less pronounced in the harbor porpoise than in dolphins. In particular, the facial cranial bones of the right hand side are slightly wider and the

midline deviates further to the left (Fig. 6; Ness 1967, Yurick and Gaskin 1988, Heyning 1989; see chapter "*Asymmetry of the facial skull of toothed whales*").

The single external nasal opening (**blowhole**) is situated immediately rostral to the vertex of the head. While being closed the blowhole resembles a transverse semicircular slit, convex rostrally. Only the anterior lip of the blowhole is capable of significant mobility. Below the blowhole, the nasal passage runs vertically i.e., perpendicular to the beak-fluke axis. The dorsal part of the nasal tract consists of a flat, unpaired **vestibulum** (Figs. 2 9) which bulges caudally (Figs. 10, 11). The vestibulum is approximately 1.5 cm deep. The surfaces of the anterior and posterior walls of the vestibulum are in intimate contact with each other and seem to represent a tight closing mechanism ("shutter") at this level (Mead 1975). Below the vestibulum the nasal passage is divided by the soft nasal septum. At the dorsal end of the paired nasal passages, the **monkey lips** are visible (Figs. 2, 9). These lips are represented by a low horizontal ridge on the anterior and posterior walls of the nasal passage and thus stand perpendicular to the air stream and parallel to the monkey lips: according to the macroscopical dissections, delicate horizontal folds on the anterior monkey lip fit in corresponding grooves on the posterior lip. This mortise-tenon complex seems to be another air-tight sealing mechanism of the nasal passage (Fig. 9). Furthermore, parallel to the air stream, a group of approximately 10 to 15 minute dorsoventral wrinkles on the lips are orientated perpendicular to the "closing" (mortise-tenon) folds and grooves (Fig. 9). Below the monkey lips, the nasal passages run directly ventralward to enter the bony nares. Here, the passages are occluded by the **nasal plugs**, paired masses of connective tissue interspersed with muscle fiber bundles. These plugs bulge into each nasal passage from its anterior wall (Figs. 2, 9, 10, 11). In dead animals, the ventrocaudal edge of each plug reaches the posterior border of the bony nares so that it is situated opposite to the opening of the inferior vestibulum (see below). Small

nodes formed largely of connective tissue are located medially at the ventrocaudal edges of the plugs, in contrast to delphinids where the nodes are located on the posterolateral margin of the nasal plugs. In porpoises these nodes and the ventrocaudal border of the plugs form a concave groove (sulcus; Fig. 9). This sulcus of the nasal plugs fits into the opening of the inferior vestibulum (see below) to close it tightly even in dead specimens.

The epithelium lining the vestibulum is black or dark brown, similar to the skin of these animals. The paired soft nasal passages above the monkey lips have a brownish epithelium. Thus, the color of the epithelium changes at the level of the monkey lips (Fig. 9) and continues to have a brighter color in the paired nasal passages. The epithelium on the monkey lips is up to twice as thick as that of the soft nasal passage (Fig. 12). The mucous epithelium of the bony nasal passages, however, appears red and seems to contain glands which are characterized by pinhole-like openings in an elongated area in the ventral part of the bony nasal passage. Unfortunately, there are no data on the structure of the latter epithelium in postnatal animals.

In the harbor porpoise, three pairs of **nasal diverticulae** communicate with the nasal passages. Each of them lies in a separat horizontal level of the epicranial complex (I-III; Fig. 13): from dorsal to ventral the vestibular sacs, the nasofrontal sacs, and the premaxillary sacs. All these air sacs communicate with the soft nasal passage by slit-like apertures.

Each **vestibular sac** as the dorsalmost air sac (Figs. 2, 14, 15) is situated rostrolateral to the nasal passage. The two sacs show a unique configuration in phocoenids (see below) and they are located more rostral to the blowhole than in delphinids (Mead 1975). The slit-like entrances from the nasal passages in these

sacs are orientated horizontally and located in the rostrolateral wall of the nasal passage dorsal to the monkey lips and to the nasal septum, respectively (Fig. 9). The dorsal wall of the vestibular sac is thin and lined by black epithelium but the ventral wall of the sac is composed of thick connective tissue that is deeply (up to 1.5 cm) furrowed (Figs. 2, 9) and lined by a darkly pigmented epithelium (Fig. 11). These furrows (plicae) are arranged concentrically around the entrance (Fig. 16). In all specimens examined a prominent central furrow was visible (coined "ausführender Spalt" by Gruhl 1911 or "hendidura central" by Gallardo 1913) which divides the vestibular sac in an anterior and a posterior portion. Only the central plica is in direct contact with the slit-like aperture in the nasal passage whereas the other plicae contact the central furrow medially within the vestibular sac. The asymmetry of the vestibular sacs was visible in all the *Phocoena* specimens investigated (Figs. 14, 16, 17): Here, the right side is always larger than the left. But the degree of asymmetry of the vestibular sacs varies in harbor porpoises from a nearly symmetrical situation to slight asymmetry (in comparison with other non-physeterid odontocetes[1]; cf. Cranford et al. 1996). Maximal asymmetry in the vestibular sac was found in animal no. 1369 (Fig. 16, see Table 1) where the surface area of the right sac was approximately twice that in the left sac. On an average of the specimens examined, however, the surface of the left vestibular sac is equivalent to about 70% of the right one. (Note that the surface measurements were made form photos in dorsal view and do not include the inner surface of the plicae.) According to the specimens investigated here the degree of asymmetry of the vestibular sac was not age dependent since, e.g., porpoise no. 1369 was an adult but not large (and not old, respectively; Table 1).

[1] Odontoceti which do not belong to the superfamily Physeteroidea. The latter encompass only three living species: *Physeter macrocephalus* (*Physeteridae*), *Kogia sima*, and *Kogia breviceps* (*Kogiidae*; Rice 1998, Fordyce and Muizon 2001).

The **nasofrontal sac** system is situated ventral and caudal to the vestibular sac. A slit-like aperture communicates between the ventrocaudal wall of the soft nasal passage and the posterior part of this air sac system (Fig. 2). This aperture leads first into a small chamber, the **inferior vestibulum**, which connects the posteriormost part of the nasofrontal sac with the nasal passage (Figs. 2, 11, 17). The posterior portion of the nasofrontal sac, however, is divided into an anterior and a posterior part by a thick septum of connective tissue projecting from its dorsal wall. This septum, not found in delphinids (Fig. 18), was called "hintere Klappe" by Gruhl (1911) or the "posterior septum of the blowhole ligament" by Curry (1992). In this description the term "**nasofrontal septum**" is used (Figs. 2, 11). The cavity rostral to the septum is called **posterior nasofrontal sac** whereas the caudal part is termed **caudal sac** (Figs. 2, 11; Moris 1969, Amundin and Cranford 1990). The epithelium of the ventral lip of the septum (on level of the angle and the inferior vestibulum) is non-pigmented and intensively linked with the subepithelial sheet via papillae of connective tissue (Fig. 12d). The caudal epithelium of the caudal sac attaches to the cranium in a bilateral smooth depression between the vertex of the skull and the caudal border of the bony nostrils.

On each side, the ventral connection of the posterior nasofrontal and the caudal sacs project rostralward and encircle the nasal passages in the horizontal plane so that an anterior portion, the **anterior nasofrontal sac**, can be found rostral to the nasal tract (Figs. 17, 19). The lateral junction of the anterior and posterior part of the nasofrontal sac system, called the angle (Figs. 17, 19; cf. Mead 1975), is u-shaped in transverse orientation (Figs. 9, 12) because the nasofrontal septum projects rostrolateralward from the posterior portion of the nasofrontal sac system into the angle up to the level anterior of the nasal passage. At the caudal end of the angle each nasofrontal sac bears a small dorsal extension (Fig. 12e) which may be homologous to the accessory sacs in delphinids (Schenkkan 1971,

Mead 1975). The anterior nasofrontal sac resembles a horizontally flattened tube or gutter (Fig. 17) and is slightly u-shaped in sagittal plane (Figs. 2, 12a). The sac is covered with non-pigmented thin epithelium which is linked via papillae to the underlying connective tissue. The glandular appearance of the epithelium, however, as suggested by Mead (1975), can not be confirmed (Fig. 12).

A thin but tough fold, the so-called **diagonal membrane**, protrudes from the posterior surface of the inferior vestibulum and the caudal sac (Fig. 19). This fold, only 1 to 2 mm wide, stretches through the laterocaudal edge of the nasal passage via the inferior vestibulum to the medioventral border of the nasal bone. It forms a small thin valve directed rostralward in the inferior vestibulum that connects the laterocaudal extension of the premaxillary sac with the caudal sac.

The ventralmost nasal air sac is the **premaxillary sac** which lies on the posterior half of each premaxillary eminence and anterior to the bony nares (Figs. 2, 17). This air sac, 10 to 15 mm deep, opens via a slit-like aperture into the nasal passage (Fig. 2). In the harbor porpoise, this sac is much smaller than in delphinids: in relation to skull size the surface area of the premaxillary sac in the harbor porpoise approximates only 1/5 that in delphinids (Figs. 2, 17, 18). The dorsal epithelium of this sac is linked with the tissue of the nasal plug via papillae of connective tissue as found in parts of the nasofrontal sac (Fig. 12). A lateral extension of the premaxillary sac circles around the bony nares to meet the inferior vestibulum caudally but still is in continuity with the nasal passage (Fig. 13).

Embedded within the anterior and posterior walls of each nasal passage and in lateral position are small ellipsoid fat bodies, the **dorsal bursae** (Cranford 1992; Figs. 2, 7, 10, 11, 12, 14, 15, 17, 19). The paired bursae are associated with the

monkey lips. This juxtaposed structural relationship and a common group of associated structures can be found in a complex within the left and right nasal passages, the so-called monkey lips/dorsal bursae complex (**MLDB complex**; Cranford 1992, Cranford et al. 1996). The two MLDB complexes exhibit slight asymmetry in porpoises (Fig. 17): both dorsal bursae on the right hand side are 10 to 12 mm in width and approximately 4 mm in sagittal diameter. The left bursae are 8 to 10 mm wide and slightly smaller in diameter. Each anterior bursa is slightly smaller (1 mm shorter) in width but little longer than its posterior counterpart.

The dorsal bursae are situated approximately 10 to 12 mm lateral to the nasal midline (nasal septum) and thus encompass the lateral half of each nasal passage (Fig. 7). According to Cranford et al. (1996), the dorsal bursae should be called "bursae cantantes" because of their probable role in sound generation. But in this paper the term "dorsal bursae" is used since their function is not fully understood and so far not tested experimentally.

Bursa cartilages were not found in some harbor porpoise specimens, neither macroscopically nor microscopically, although Cranford et al. (1996) suggested that all odontocetes may possess these small cartilages and also Curry (1992) found these "ovoid cartilages of the blowhole ligament".

Each MLDB complex can be found in the centre of dense connective tissue referred to as the "**porpoise capsule**" (Cranford et al. 1996). The bilateral capsule is surrounded by air spaces: the vestibular sac dorsally, the caudal sac posteriorly and the angle of the nasofrontal sacs laterally but the nasal passage and the nasofrontal sacs project through the capsule (Fig. 13). The capsule is invaded by muscle bundles laterally and dorsocaudally (see below).

A bulbous hypertrophied fat body, the **melon**, is situated anterior to the soft nasal passages (Figs. 2, 7, 8, 10, 11, 14, 15, 17, 20). It is ovoid in shape and flattened dorsoventrally. In the harbor porpoise, the melon is supported ventrally by the maxillary and premaxillary bones and covers the short rostrum for nearly its total length (Fig. 14). Therefore, this fat body is responsible for the typical "beak-less face" of the porpoise and the protruding forehead of many toothed whales. The melon consists of oily or soft fatty tissue. The core of the melon is nearly free of connective tissue fibers but fiber content increases to the entire periphery of the melon (Figs. 7, 10). Ventrolaterally, these fibers of connective tissue (collagen) are interwoven with fiber bundles of the rostral muscles (Fig. 8).

Caudally the melon is embedded in a **theca** of dense connective tissue (Cranford 1992, Cranford et al. 1996; Figs. 7, 10, 11). The overall shape of this theca in *Phocoena* is reminiscent of a megaphone or a short horn (Figs. 7, 8; cf. Cranford et al. 1996). The ventral part of the theca projects into the nasal plug muscle which is rich in connective tissue. Caudal to the theca the subcutaneous tissues are similar to those in the thick blubber beneath the body surface. The posterior extension of the theca is connected with the porpoise capsule (Figs. 7, 8). The posterior end (terminus) of the melon enters the theca and the capsule mediosagittally and is situated dorsal to the nasal plug muscles (Fig. 19). As reported by Cranford et al. (1996), a bilateral low density path exists from the posterior extension of the melon to the area of the anterior dorsal bursae (Fig. 2). This area is located ventral to the anterior nasofrontal sac and is thought to be the potential acoustic pathway (Fig. 12a) which connects the melon with the proposed pulse sound generator, the dorsal bursa. In contrast to delphinids, where the terminus of the melon is in direct contact to the (right) anterior dorsal bursa (Fig. 18), this "pathway" of the harbor porpoise seems to consist of loose connective tissue interspersed with fiber bundles from the nasal plug muscle (Fig. 12). Contraction of

this muscle could therefore alter the shape of the acoustic pathway. According to our macroscopical dissection, this pathway appears to consist of fatty connective tissue. Nevertheless, Figure 12 reveals the differences between the dense connective tissue of the capsule dorsal to the anterior nasofrontal sac and the loose connective tissue ventral to the sac where the low density pathway (potential acoustic pathway) is situated. The connective tissue fibers within the pathway are loose compared to the connective tissue of the porpoise capsule and the fiber direction is parallel to the proposed sound beam (Fig. 12).

As stated before, the MLDB complex is embedded in a capsule of connective tissue. The ribbon-shaped **blowhole ligament** runs on both sides through the porpoise capsule, i.e. from the nasal septum through the lip between the posterior nasofrontal sacs and the nasal passage along the caudal margin of the posterior dorsal bursae (Figs. 2, 12, 19). Therefore, this structure is referred to as "septum of the blowhole ligament" which was named "tissue peninsula" by Cranford et al. (1996). In the porpoise the ligament runs ventrally and caudally and shows the same topographical relations as in dolphins (Mead 1975, Cranford 2000). It ends on both sides in a well defined area on the maxilla exactly laterocaudal to the premaxillary eminences (not shown in figures). The ligament is lined caudally by connective tissue as part of the porpoise capsule (Fig. 12b). Ventral to the ligament, a lip consisting of connective tissue houses a strong intrinsic muscle (Fig. 12c). In dead animals the front part of the ventral lip of the blowhole ligament septum is in contact with the sulcus of the nasal plugs via the opposing epithelium of the nasal passage (Fig. 2) so that the ventrocaudal epithelium of the lip is the dorsal lid of the aperture from the nasal passage into the inferior vestibulum. So it seems that, on the one hand, the lip of the blowhole ligament septum is part of the sealing mechanism of the nasal passage on the level of the nasal plugs and, on the other hand, of the inferior vestibulum.

The **musculature** of the epicranial complex in *Phocoena* is similar to the general pattern seen in the Delphinidae. Different muscle layers form a cone around the soft nasal passages resembling a roofing tile organization in which the single layers lie on top of each other. In the harbor porpoise, the musculature originates from the facial fossa provided by the maxillary bones. Five bilateral fan-shaped muscle layers (facial muscles) originate concentrically from this fossa in more or less dorsomedial orientation around the soft nasal passages. In general, the attachment sites of the muscles describe semicircles on each side around the nasal passages starting from the vertex running in parallel to the facial border to the antorbital region.

Superficial to this cone of five muscle layers a sheet of loose connective tissue is embedded in the subdermal fat deposits and is connected caudally to the subdermal connective tissue sheath (Pabst 1996). The fibers originate from the area dorsal to the vertex of the skull and to the posteromedial part of the facial border and run to the connective tissue theca lateral to the melon. Von Baer (1826) termed this layer "**Galea aponeurotica"** and Curry (1992) "superficial facial tendon". The tendon is up to 4 cm wide and has a thickness of approximately 10 mm when passing over the posterior and ventral part of the vestibular sac (not shown in figures). Here a small muscle is embedded in the tendon. A few fibers diverge in ventral direction and are attached to the supraorbital process posterior to the eye. A thin fascia is connected to the muscle bundle that inserts on the rostrum. Following the terminology of Lawrence and Schevill (1956) this small muscle layer is homologous with the Musculus maxillonasolabialis pars **posteroexternus** (1; Fig. 20) in delphinids (Curry 1992). It is likely that the continuity of the Galea aponeurotica with the p. posteroexternus and the subdermal sheath of connective tissue of the body form a functional unit of locomotion (Curry 1992, Pabst 1996).

The next muscle layer, the M. maxillonasolabialis p. **intermedius** (2; Fig. 19) is situated medial to the p. posteroexternus and the Galea aponeurotica, respectively, and originates from the posterior part of the facial fossa. The fibers are orientated rostralward and insert dorsal in the connective tissue theca. There is a tendinous area superficial to the caudal part of the vestibular sac (Fig. 19a). Together with the small p. posteroexternus, this muscle may pressurize the central part of the nasal complex by pulling the connective tissue theca caudally. This process should compress the air diverticulae and the vestibular sacs should be influenced most by the work of the two muscle groups (Fig. 20). The force of these two muscles exerted to the connective tissue theca in caudal direction should also alter the melon's shape slightly. More specifically, the dorsomedial part of the p. intermedius can retract the posterolateral part of the posterior blowhole lip (Fig. 20).

Medial to the posteroexternus and intermedius components, the **anteroexternus** part of the M. maxillonasolabialis (3; Figs. 16, 19) originates in the typical concentric pattern near the facial border. The muscle of the thicker anterior part of this muscle are orientated perpendicular to the axial course of the p. intermedius and insert on the lateral border of the vestibular sac but some anteriormost fibers blend into the connective tissue anteroventral to the blowhole (Fig. 19a). The thin posterior portion of this muscle is bound by a flat aponeurosis into the connective tissue posterior to the nasal passage and some fibers also into the tissue lateral to the nasal passage and the aperture of the vestibular sac. A separation of this muscle into anterior and posterior portions, as described by Lawrence and Schevill (1956) in dolphins, was not found. In dolphins, the p. anteroexternus is the dilatator of the dorsal unpaired nasal passage (vestibulum). In *Phocoena*, the caudal portion of the p. anteroexternus only dilates the posterior wall of the nasal passage slightly, but its rostral part may open the blowhole lip by

pulling the connective tissue situated anteroventral (Fig. 20). The lateral part of this muscle may control the volume of the vestibular sac (not shown in figures).

The M. maxillonasolabialis p. **posterointernus** (4; Fig. 19) originates medial to intermedius and anteroexternus portions from the facial fossa between the supraorbital process (dorsal to the eye) and the vertex. This muscle is not clearly defined at its anterior end and extends there between the anteroexternus and anterointernus portions (see next paragraph). The rostral layers of the posterointernus insert together with deep fibers of the anteroexternus onto an aponeurosis which is attached to the ventral wall of the aperture of the vestibular sac and may thus control air flow into this sac. In contrast to Curry's description (Fig. 19a), the posterointernus muscle was found to insert further dorsally, in a region of the porpoise capsule roofing the angle and the posterior nasofrontal sac. The lateral fibers of the p. posterointernus may modulate the tension of the nasal passage at the monkey lips and regulate air flow at this level. It also dilate the deeper nasal passage by pulling the wall of the nasal passage caudalward and lateralward. Tension on the posterior portion of this muscle can control the dorsolateral aspects of the posterior nasofrontal and caudal sacs. This muscle action should also cause tension on the blowhole ligament, the accessory septum, and the nasofrontal septum. Therefore, the posterointernus muscle, perhaps with the help of the anteroexternus portion, can control air pressure in the posterior nasofrontal and caudal sacs.

The M. maxillonasolabialis p. **anterointernus** (5; Fig. 19) originates from the maxillary bone, medial to the p. posterointernus. The anterior part of this muscle merges with the overlaying p. anteroexternus and sends a thick bundle connected with the anterior portion of the vestibular sac and the connective tissue directly dorsal to the anterior nasofrontal sac (Fig. 19, 3+5). It borders the p.

posterointernus anteriorly. This bundle originates from the maxilla where the rostrum and nasal skull meet and arises in the strong connective tissue fibers anterior to the antorbital notch. These anterior fibers of the p. anterointernus produce tension in the connective tissue dorsal to the anterior nasofrontal sac and the anterior dorsal bursa (Fig. 19a). As outlined by Lawrence and Schevill (1956) for dolphins, the p. anterointernus of harbor porpoises dilates the deep nasal passage by forcing the plug muscle into the bony nares (Fig. 20). The lateral part of this muscle portion attaches to the connective tissue dorsal to the angle and inferior vestibulum and may control air movement in the angle and the nasofrontal sac (Fig. 20). Moreover, it has a connection lateral to the blowhole ligament and the nasofrontal septum. A distinct intrinsic muscle ventral to the blowhole ligament (Fig. 12) is in contact with the p. posterointernus and can manipulate the tension of the free ventral margin of the lip. The posterior portion of the anterointernus muscle is connected to the dorsal part of the caudal sac and may control the air volume in this sac.

The deepest muscle layer, the M. maxillonasolabialis p. **profundus** (6; Fig. 19), originates on the maxilla beneath the p. anterointernus but does not reach to the base of the vertex (as is true for the p. anterointernus) and is attached to the caudal sac only laterally. The profundus muscle can be divided into an anterior and a posterior portion by means of their fiber orientation (Fig. 19). The anterior portion is bound to the connective tissue theca dorsoventral to the melon terminus and its fibers are orientated in a dorsocaudomedial direction. The fibers of the posterior part run in a rostromedial orientation parallel to the fibers of p. anterointernus. The profundus muscle attaches to the connective tissue lateral and ventral to the angle, the nasofrontal sac, and the caudal sac and thus may control the air volume in these sacs. Additionally, this muscle may also alter the volume of

the laterocaudal extension of the premaxillary sac since its fibers insert into the connective tissue dorsal to the extension.

Curry's description (1992) does not distinguish a separate profundus muscle. She followed the description of Mead (1975) who recognized a fusion of Lawrence and Schevill's (1956) p. anterointernus and p. profundus (Fig. 7 in Curry 1992). In the harbor porpoise specimens examined for this dissertation, the anterointernus and profundus muscles resemble the situation in dolphins (Lawrence and Schevill 1956) but these authors could not find an anterior and posterior division of the p. profundus. In contrast, they described an outer and deeper layer of the p. profundus. According to their figures of bottlenose dolphins (*Tursiops truncatus*) these layers could be homologous to the anterior and posterior portions of this muscle in *Phocoena*. The differences in the descriptions of the medial muscle layers (5 and 6) may, at least in part, be due to different stages of decomposition in the material examined or to different fixation methods since separate profundus and anterointernus portions were found in very fresh or well-fixed specimens only.

The rostrum is associated with two slender bilateral muscles. The **lateral rostral muscle** (5'; Fig. 19) originates mainly from the maxilla and its fibers have a dorsocaudolateral orientation reaching the connective tissue lateral to the melon at each side. It is continuous with the strong muscle bundle formed by the anterior part of the anteroexternus and anterointernus portions (Fig. 19). The narrower part, the **medial rostral muscle** (6'), originates from the dorsal surface of the maxilla and premaxilla and is in contact with the lateroventral sheath of the melon (Fig. 20). Since both lateral and medial rostral muscles insert in the ventral tissue on f the melon these muscles may modulate the shape of the melon. The medial rostral muscle is continuous with the anterior part of the p. profundus (Fig. 19).

The same pattern of continuity of lateral and medial rostral muscles with the maxillonasolabialis musculature could be identified by Mead (1975) but this author did not define a profundus muscle, as stated above, and described the anterointernus muscle to be continuous with the medial rostral muscle in dolphins.

Between the posterior parts of the left and right medial rostral muscles the **nasal plug muscle** (nm; Figs. 2, 12, 19) originates from the premaxillary bones anterior to the spiracular plate (Heyning 1989). These muscle fibers have a slightly dorsocaudal orientation and enter the connective tissue of the nasal plug. The nasal plug muscle is dense and strong but rich in connective tissue fibers (Fig. 12). It borders the dorsal wall of the premaxillary sac. This prominent muscle opens actively and closes passively (shifted by the surrounding tissue and lateral muscles) the air passages at the level of the dorsal entrance into the bony nares. The nasal plug muscle moves the nasal plug and thus the lip of the nasal plug forward. Therefore, air flow in the nasal passage as well as the inferior vestibule can be controlled by this muscle. Pushing the nasal plug into the bony nares by actions of the anterior parts of the anteroexternus and anterointernus muscles, the anterior nasofrontal and premaxillary sacs should become pressurized. In contrast, closing the nasal passage at the level of the monkey lips, the nasal plugs and the blowhole ligament lips control the air flow in the nasofrontal sac and caudal sac. It appears that the diagonal membrane is part of the closing mechanism at the level of the nasal plugs because its ventral part stretches from the nasal passage into the entrance of the inferior vestibulum and is reminiscent of a sealing washer. To open the entire nasal tract completely during respiration, the anterior surface of the nasal passage should be retracted rostralward by the simultaneous contraction of the nasal plug muscle and the strong anteriormost fibers of the intermedius, anteroexternus, and anterointernus muscle portions (Fig. 20).

Curry (1992) reported that the vestibular sac is surrounded by an intrinsic muscle that has no distinct fiber orientation but may be continuous with the p. anteroexternus and p. anterointernus. Probably the same intrinsic muscle was located in the harbor porpoises examined here, but its fiber orientation paralleled that of the p. anteroexternus. The nasofrontal sac is also surrounded by an intrinsic muscle embedded in the connective tissue. A small but prominent muscle fiber bundle ventral in the lip of the blowhole ligament is continuous with the posterointernus portion. A diagonal membrane muscle, as described for dolphins (Lawrence and Schevill 1956, Mead 1975), could not be identified.

The **vascular supply** of the nasal region is achieved by branches of the internal maxillary artery (Mead 1975). Branches, emerging via the infraorbital foraminae together with the infraorbital nerve (Mead 1975, Rommel 1990), supply the epicranial complex and ramify between the layers of nasal musculature.

The rather strong **facial nerve** was found in the harbor porpoise, similar to delphinids (Rauschmann 1992). It runs from the otic region along the slender zygomatic arch to the antorbital notch. Here it turns dorsally. Beyond this point it has a diffuse dorsal and caudal distribution and branches between the different layers of the maxillonasolabialis muscle. A small rostral portion of this nerve is in contact with the rostral muscles. The trigeminal nerve invades the facial complex via the various infraorbital foraminae but the course of this nerve was not traced further.

### 5.1.2. La Plata dolphin (*Pontoporia blainvillei*)

The **skull** of the La Plata dolphin is nearly symmetrical and characterized by a long rostrum resembling a huge pair of tweezers. The facial fossa is relatively small in comparison to skull length and body mass and so is the size of the epicranial complex (Fig. 21). The facial depression is less pronounced than in delphinids so that the vertical nasal passage is relatively short. The concavity of the blowhole projects rostralward and is shifted slightly to the left. Ventralward it continues in a relatively large unpaired vestibulum and further downward the nasal passage is divided by a soft nasal septum. At the dorsal end of the relatively short paired nasal passages (approximately 2 cm below the blowhole but only 0.5 cm above of the bony nostrils) we found the two pairs of **monkey lips** which are characterized only by few small wrinkles oriented parallel to the proposed air stream. The lack of "mortise-tenon" folds (as found in dolphins and the harbor porpoises) could be a post-mortem artifact in the one specimen dissected. According to the short paired nasal passages the nasal plugs, which bulge in the tract from anterior, are relatively small and not characterized by sulci as in *P. phocoena*.

The soft nasal structures are moderately asymmetric. But the most superficial air sacs, the **vestibular sacs**, are extremely hypertrophied on the right side, so that its rostral portion extends over to the left hand side (Fig. 22). The inner surface area of the left vestibular sac is approximately only 8% that of its right counterpart. In the specimen dissected (which had a condylo-basal length of 44 cm) the right vestibular sac had a rostrocaudal extension of 9.8 cm and a maximal width of 6.5 cm. It tapers in the direction of the vestibulum and opens there by means of a horizontal slit, dorsal to the right posterior monkey lip. Near the junction, however, this short corridor widens dorsocaudally into a small additional extension (ca. 1 $cm^2$) which narrows again before entering the vestibular sac. The

right vestibular sac, which, in general, is flattered dorsoventrally, consist of several different parts lying in different planes: On the blowhole level, i.e. at the opening between the vestibulum and the right vestibular sac, there is a fold in the ventral wall of the sac orientated lateralward and dividing it into an anterior and a posterior part (FV; Fig. 22). In some areas, this fold is fused with the dorsal wall of the sac. A second fold in the ventral wall of the anterior portion of the sac projects from the aperture of vestibular sac to its rostrolateral edge (not shown in figures). This fold opens into a small extension, a narrow tube running to the midline of the nasal complex but below the anterior part of the right vestibular sac. The small left vestibular sac is situated lateral to the left nasal passage and opens by a short slit in the vestibulum dorsolateral to the left posterior monkey lip. This sac has a small rostral appendix measuring approximately 1.5 cm (Fig. 22).

At the ventral end of each soft nasal passage, there is a horizontal slit-like opening in the caudal wall. This entrance projects dorsocaudally in a flattened air sac which is situated in the connective tissue between the nasal passages and the vertex of the skull. This sac seems to be homologous to the posterior **nasofrontal sac** in delphinids (Schenkkan 1972). But in contrast to dolphins and porpoises, the sac does not project rostrally, so that we do not have an anterior nasofrontal sac in the La Plata dolphin (not shown in figures).

The **melon** is rather small and slender (Fig. 21) in comparison with other dolphin species (ME; Fig. 18) but has strong and relatively long bilateral extensions which connect the anterior dorsal bursae with the melon. The **dorsal bursae** are found in the same relative position as in dolphins and in the harbor porpoise, respectively, and in association with each monkey lip so that there are two (bilateral) MLDB complexes (Fig. 21). Although there was no blowhole ligament in the one specimen dissected the posterior dorsal bursae are situated in a septum bordered by the

nasal passages anteriorly and the posterior nasofrontal sac ventrally and caudally. As in most non-physeterid toothed whales, the fatty pathway between the melon and the anterior bursa is continuous on the right hand side, whereas on the left there is a short discontinuity in the pathway with loose connective tissue situated between the bursa and the melon's body (Fig. 21). However, concluding from the CT data, a low density pathway from the melon to the left anterior bursa still exists. The anterior portion of the right vestibular sac covers this fatty pathway which connects the proposed sound source to the melon (Fig. 22).

The **musculature** of the epicranial complex in *P. blainvillei* (M. maxillonasolabialis) is similar to the situation in delphinids. The superficial muscle layer on the right side is rather thin and originates from the lateral margins of the maxillary bone (facial border), rostral to the eye, and runs in a dorsocaudal direction converging towards the midline caudal to the blowhole. Only the rostralmost muscle fibers insert on the anterior blowhole lip. On the left side, this muscle layer is thicker than its counterpart on the right, so that a stronger left rostral muscle bundle attaches to the anterior blowhole lip. These muscle fibers seem to be the main components in opening the blowhole. Below these superficial muscle layers the vestibular sacs are situated. Near the midline, a strand dense connective tissue fibers runs from the posterior wall of the vestibulum in a caudal direction to the vertex of the skull. Presumably homologous fiber bundles are found in dolphins and porpoises, too, but in the La Plata dolphin they are developed much stronger (Schenkkan 1972). It seems that these fibers can keep in place the vestibulum and the blowhole, respectively, when the anterior blowhole lip is opened.

Ventral to the vestibular sacs an intermediate but rather thick muscle layer is located. The fibers of this muscle project concentrically from the maxillary bones in a dorsomedial direction into the connective tissue around the nasal passages and

the posterior nasofrontal sac. This muscle may, therefore, control the air volumes in the nasal passages at the level of the dorsal bursae and the posterior nasofrontal sac as well as the entrance to the vestibular sacs. The anteriormost fibers of this muscle are attached to the connective tissue lateral to the low density pathways, i.e. between the melon and the anterior bursae.

The deepest muscle layer is rather small and thin. The orientation of its fibers is parallel to the intermediate muscle layer and they are attached to connective tissue lateral to each nasal passage as well as lateral and caudal to the posterior nasofrontal sacs. This muscle may alter the volume of the air spaces mentioned and thus control air flow in the nasofrontal sac. In contrast to dolphins and harbor porpoises, respectively, we were not able to distinguish more than these three layers of epicranial musculature. This may in part be due to the relatively poor condition of the La Plata dolphin dissected; in fresh material the muscular architecture might have been more detailed. In principle, the three muscle layers seem to be homologous to the six layers proposed in delphinids (Lawrence and Schevill 1956) and harbor porpoises, respectively, although it cannot be decided so far which one is which.

Interestingly, in the La Plata dolphin, there were no rostral muscles inserting in the tissue of the melon. Instead, there is a "spongy" tissue lateroventral to the posterior part of the melon which fills the gap between the melon and the maxillary bones. This "spongy" tissue was not investigated in detail but it might represent a post-mortem artifact.

### 5.1.3. Amazon river dolphin (*Inia geoffrensis*)

One specimen of the Amazon river dolphin (*Inia geoffrensis*) was examined by a series of transverse cryo-sections (slice thickness ca. 1 to 1.5 cm) and another partly decomposed specimen was scanned using MRI and CT. The preliminary results of this study are of great value for a comparison with these taken from other toothed whale species examined.

The skull of the Amazon river dolphin is characterized by an elongated rostrum and the bony structures on both sides of the facial skull are nearly symmetrical but the midline is slightly curved to the left (see chapter "*Asymmetry of the facial skull*"). The lateral facial border is ventrally erupted and there are premaxillary eminences rostral to the bony nares. As is typical for non-physeterid toothed whales, the soft nasal passage is orientated vertically, i.e. perpendicular to the beak-fluke axis. The blowhole is of the type normally seen in dolphins, crescent with the concavity facing rostralward and opens ventrally in a rostrocaudad flattened vestibulum. In the rostral wall of the latter, slightly dorsal to the soft nasal septum, a horizontal slit-like aperture is situated which extends over its whole width. This opening leads into an unpaired diverticulum which is flattened horizontally and covers the epicranial complex dorsally from the nasal passage to the plane of the orbitae. This unilateral diverticulum opens on both sides into an air sac that stretch from the posterior margins of the facial border to the area of the orbitae. These two air sacs seem to be homologous to the vestibular sacs of other toothed whales. The opening into the right vestibular sac is larger than that on the left. This configuration was interpreted by Schenkkan (1977) that the unilateral diverticulum is part of the right sac and that this diverticulum extends up to the smaller left vestibular sac. The vestibular sacs cover the whole posterolateral portion of the nasal musculature. The nasofrontal sacs originate

from a slit-like opening in the ventrocaudal end of each soft nasal passage. Anterior portions of the nasofrontal sacs are lacking, the posterior portion is situated caudal to each nasal passage and extends to a point immediately lateral to the nasal passage. Very similar to the situation in *Phocoena phocoena*, this portion is divided by a septum from the dorsal wall dividing the sac into a caudal and a rostral part ("nasofrontal septum"). Accessory sacs of these nasofrontal sacs were not found. The premaxillary sacs are small but extend over most of the surface of the premaxillary eminences, each of them has a small extension lateral to the bony nares so that they become continuous with the aperture of the nasofrontal sacs caudally. Similar to all other toothed whales the nasal plugs bulge into the nasal passages from anterior and lack lip-like extensions (as is typical for harbor porpoises). The melon is well developed, although it seems to contain more connective tissue than in any of the delphinids examined. The bipartite terminus of the melon stretches posteriorly up to the level of each nasal passage. This terminus is complete on the right hand side whereas the left side shows a discontinuity. Other structures such as the dorsal bursae and the blowhole ligament were not found because of the limits of the methods used and the poor state of preservation of the material. I have not attempted to analyze the structure of the nasal musculature in the Amazon river dolphin, which appears, however, to have a similar general pattern as that of the delphinids. In the transverse cryo-sections, at least four different (horizontal) layers could be distinguished. A thin muscle layer spans over the vestibular sacs. Below these sacs three stronger muscle layers ascend and converge from the facial fossa to the connective tissue around the nasal passages and the nasal air sacs.

### 5.1.4. Giant sperm whale (*Physeter macrocephalus*)

Within the toothed whale order, the **skull** of the sperm whale is unique in its size and shape (Fig. 23). It consists of slender jaws and a stout brain case (Klima 1990). The anterior part of the skull is represented by the elongate rostrum, which is fused broadly to the neurocranium and tapers markedly at the distal end. The face of the skull, where the rostrum is fused to the neurocranium, forms a deep concavity with a steep posterior slope, and is reminiscent of an amphitheater (Figs. 23, 31, 33; cf. Norris and Harvey 1972). The inner surface of this amphitheater is formed predominantly by the caudal elongations of the broadened upper jaw elements (premaxillaries, maxillaries). Due to the telescoping process (Miller 1923) they cover the frontal and parietal bones but obviously are not fused to them but separate from them by means of intermediate connective tissue. As a result, the premaxillary and maxillary bones cover most of the skull roof and may border the steep occipital crest in full-grown sperm whales (Fig. 23). The frontal region of the skull in adult sperm whale specimens seems to be deeply retracted within the skull and lies in the extension of the vomer. Because of algometrical phenomena, larger animals within one taxon have absolutely larger but relatively smaller brains than smaller specimens so that the sperm whale neurocranium houses absolutely largest brain the animal kingdom (10 kg, Oelschläger and Kemp 1998), this brain is at the same time one of the smallest within the Mammalia with respect to body size. As is the case in all extant cetaceans, the brain of the giant sperm whale is wider than it is long. Moreover, the sperm whale seems to have a maximal ratio of cortex mass versus brain stem mass (Oelschläger and Oelschläger 2002). Due to the overwhelming growth of the skull in adult sperm whales, the neurocranium with the brain has dwindled away and is now restricted to the posteriormost part of the skull base. Another reason for the very low position of the brain case is the fact that the nasal complex is huge and needs a high supraoccipital crest for the

positioning of the two hypertrophied fat bodies (see below) and as an abutment for strong muscles originating from the dorsal margin of the amphitheater (facial border) and inserting in the area of the monkey lips.

As in other cetaceans, the **bony nostrils** and the adjacent bony nasal passages in the sperm whales lead to inner nasal openings (choanae). In these animals, however, they differ strongly in size (Figs. 23, 29; see below). In correlation with a general asymmetry of the facial skull in cetaceans, the bony elements on the right side (premaxillary, maxillary bone) are wider and thus shift the region of the bony nares slightly to the left. Concomitantly, this area is somehow twisted clockwise (dorsal aspect) so that the small right bony nostril is situated caudal to the large left bony nostril (Fig. 23).

The **orbita** houses a relatively small eye compared to baleen whales of about the same body mass (Jacobs and Jensen 1964; Oelschläger and Kemp 1998; Zhu et al. 2001; Oelschläger and Oelschläger 2002). However, the zygomatic arch, which is thin and rod-like in other odontocetes, is robust in sperm whales. Obviously, this element, which mediates between the maxillary, frontal and squamosal bones, helps to restrict twisting of the extremely long facial skull against the neurocranium. For the same purpose, the postorbital process of the frontal and the squamosal bones come close to one another and the intermittent gap is bridged by dense connective tissue (secondary zygomatic arch; Oelschläger 1990). Last not least, on both sides of the head, the zygomatic arch is part of an attachment site for the tough connective tissue of the bridle which suspends the rostral part of the nose from the lateral margins of the amphitheater (see below). As in mammals, generally, the stout zygomatic arch serves as an origin for the masseter muscle, which is thin but distinct in the baby sperm whale and contains only little fat in contrast to some dolphins (Rauschmann 1992).

The **lower jaw** is fork-like and equipped with a long mandibular symphysis (Y-shape). In contrast to most other toothed whales, the teeth in the upper jaw do not normally erupt in the sperm whale; in the lower jaw, they are seen as tooth buds in the baby sperm whales examined (Fig. 32). The caudal tips of the fork articulate with the neurocranium in the temporomandibular joints. As in other toothed whales, the alveolar canal has been greatly enlarged within the posterior 1/3 of each mandible and is filled with a fat body thought to serve as an acoustic channel leading to the ear (Figs. 28, 29, 35; c.f. Norris 1968). As a result the medial wall of the mandible is membranous in the posterior part. The lateral wall of the mandible in dolphins thinned out to such a degree that light passes though an isolated and cleaned specimen (acoustic mandibular window, Norris 1968). The position of the zygomatic arch well above the acoustic window suggests that, although the zygomatic arch is relatively thick in the sperm whale, it cannot be regarded an obstacle for sound entering the mandible on its way through the extra- and intramandibular fat bodies to the tympanoperiotic complex (see below).

The **ear bones** strongly resemble the situation in other toothed whales. In odontocetes, these thick, dense and heavy (pachyosteosclerotic) bones have been uncoupled from neighboring bony elements of the skull base (Fig. 30) in order to dampen bone conduction to the ears and thus to isolate the ears acoustically from the skull and from each other (increase of directional sensitivity). In most odontocetes, the tympanoperiotic complex is suspended from the skull via collagenous connective tissue with only one spot-like bony contact to the squamosal element (Oelschläger 1986a, 1990). Therefore, during post-mortem maceration the tympanoperiotic complex of toothed whales usually falls apart from the skull. However, in the sperm whale, this complex is less isolated from the skull than in most other odontocetes because a caudal elongation of the tympanic (posterior process) attaches to the lateral wall of the skull (squamosal).

In contrast to the terminal position of the nostrils in other (terrestrial) mammals, the soft external opening of the respiratory tract in toothed whales (blowhole) has migrated caudalward into a position just above and anterior to the brain case. In the sperm whale, however, it seems that the blowhole has moved again to the tip of the snout whereas the bony nares remain in their posterior but much lower position with respect to the vertex of the skull (Fig. 36). Accordingly, the **nasal passages** have been elongated into long tubes lined by brown or black epithelium which run from the blowhole (or the distal sac and monkey lips in case of the right nasal passage; Fig. 37) in front of the aperture of the bony nares at the rear.

Another peculiarity of odontocetes is the specialized blowhole. In the sperm whale it is located on the left hand side near the dorsal tip of the snout and S-shaped in dorsal view. It opens into a vestibule which is oriented parasagittally and has two additional openings: the anterior corner is continuous via a narrow channel with the distal sac. This sac opens caudalward into the right nasal passage which enters the narrow right bony nares. The posterior corner opens caudalward into the left nasal passage which takes a direct but slightly arching superficial pathway caudalward and ventralward along the left side of the nose into the large left bony naris (Fig. 36). Along most of its course the left nasal passage is C-shaped when seen in cross-section (Fig. 38). This crescentic shape is due to the bulging of the left nasal passage muscle lateroventrally into the lumen of the left nasal passage (Figs. 28, 29).

The right nasal passage runs between the two huge fat bodies (spermaceti organ, junk; Figs. 37, 38) but for the most part of its course it may be collapsed which means that it appears as straight or slightly curved subhorizontal line in the transverse scans (Figs. 25 – 28: RP). As stated before, the right nasal passage opens rostrally into the distal sac which extends as a vertical „mirror" behind the

dorsal tip of the snout (Figs. 31, 37). On the right side, the dorsolateral part of the sac is extended so that, seen from the front, the distal sac appears oval in shape. The distal sac covers the **monkey lips** (museau de singe or phonic lips, cf. Cranford et al. 1996) rostrally (Figs. 24, 36) and continues caudalward through the gape-like aperture ("monkey gape") into the broad and flattened (collapsed) right nasal passage (Fig. 37). The latter courses near the ventral surface of the spermaceti organ and opens dorsalward into another cleft-like air space, the frontal sac (Figs. 31, 37), just before entering the right bony naris. There is a striking disproportionality between the surface areas of the epithelial lining in the two nasal passages, where the right is more than twice as large as the left (Fig. 38). This is in strict contrast to the diameter of the accessory bony nares, where the diameter of the right bony naris is only one third to one fourth that of the left bony naris (Fig. 29). During the dissection of postmortem specimens, we found that the left nasal passage was always partially open whereas the right nasal passage was collapsed except for two narrow lateral channels running to the monkey lips on both sides of the right nasal passage.

Just inside the anterior boundary of the monkey lips, i.e. at the aperture of the valve, there is a mortise-tenon structure (Norris and Harvey 1972) that runs between the angles of the gape in a semicircular arc (Fig. 39). The lower lip forms the mortise and the upper lip represents the tenon. The monkey lips are covered by black epithelium but within the mortise-tenon folds there is a whitish band in fresh animals (note that the whitish band is darkened due to the fixation of the specimen in Fig. 39). Next to the pair of mortise-tenon folds, which seem to form a tight closing mechanism, smaller furrows can be found in the epithelium of these lips. The first set of plicae arises on the dorsal and ventral surface at the right lateral margin of the right nasal passage, approx. 10 - 15 cm caudal to the monkey gape. These plicae fan out in the direction and over the width of the monkey gape.

Additionally, a second and third set of plicae are visible on both inner surfaces of the monkey lips and converge on the first set described above. The second set on the dorsal surface is centered on the right hand side whereas the third set on the ventral surface is centered on the left hand side. From these centers a few plicae diverge parallel to the mortise-tenon folds of the monkey lips. The whitish appearance of the epithelium along the mortise-tenon folds stretches caudally along these delicate grooves (Fig. 39). Near the monkey gape, however, all of these small plicae, which extend over the hole width of the gape, turn rostralward (parallel to the body axis), become deeper and wider, and run across the mortise-tenon folds into the distal sac. Rostral to the mortise-tenon complex at the monkey gape, they turn sharply toward the lateral margins of the distal sac. There, all of the plicae diverge to the right hand side and spread over approximately 1/3 of the inner (caudal) surface area of the distal sac which is represented by the rostral surface of the monkey lips. The monkey gape is slightly inclined to the right side so that its angle stands higher than the right. Accordingly, the plane of the right nasal passage shows the same degree of inclination as the monkey lips but becomes horizontal at the rear end (Fig. 38).

The sperm whale's nose mainly consists of two longitudinal big fat bodies, the spermaceti organ and the junk ventrally (Fig. 37). The **junk** rests on the bony rostrum of the skull (Figs. 27–29, 31, 32, 36-38). Although it forms the ventral tip of the sperm whale snout, the junk is a little shorter than the spermaceti organ because it ends well before the bony nares (Figs. 31, 32). The spermaceti organ extends between the monkey lips just behind the dorsal tip of the snout and the back of the skull amphitheater (Figs. 31, 37). In dorsal view, the spermaceti organ bends slightly to the right (Figs. 33, 34). In transverse sections, it seems to push the dorsalmost part of the junk slightly to the left side but the junk lies symmetrically on the rostrum of the skull (Figs. 25-27) between two lateral thick

ribbons of dense connective tissue (Figs. 26, 27; bridle; see below). Rostrally, the junk hangs over beyond the tip of the rostrum and thus forms the anterior and ventral contour of the sperm whale's nose. Here, the junk is not covered by dense connective tissue (Fig. 31). The junk is a complex structure consisting of loose connective tissue in which lens-like fatty elements are embedded. Each "lens" (referred to as wafers by Møhl 2001), is orientated vertically and the whole set of lenses extends caudalward between the spermaceti organ and the bony rostrum and tapers like a horn with a mouthpiece along the bottom of the skull amphitheater where it ends well before the two nasal passage muscles (Figs. 31, 32, 36). In the posterior third, the junk is separate from the fat of the spermaceti organ only by the right nasal passage and its fatty muscle (Figs. 26, 27). In mediosagittal sections, according to our CT data set, the lenticular elements can be divided into a rostral and a caudal group by the profile of the lenticular surfaces (Figs. 32, 35). The rostral group is characterized by anteriorly convex and posteriorly concave surfaces, the caudal group by anteriorly concave and posteriorly convex surfaces. Both groups seem to be linked by a central biconvex "lens". Interestingly, the rostralmost lenses are confluent ventrally and join in a wedge-shaped mediosagittal fat body which is located ventrally in the protruding part of the nose, just before the tip of the rostrum and thus the gape of the mouth (Fig. 32). Caudally, the connective tissue between the lenticular elements becomes progressively thinner until the lenses merge into a continuous and tapering fatty channel (Fig. 32). This channel (mouth-piece), which consists of a loose conglomeration of fatty and connective tissues (Clarke 1978a, Cranford 1999), turns dorsalward to end between the skull roof, the caudal part of the nasal passage muscles and the posterior portion of the spermaceti organ.

The **spermaceti organ**, which rests on the junk and is enclosed in a tough collagenous sheath (case), spans the entire length of the nose between the monkey

lips rostrally and the frontal sac caudally (Figs. 31, 37). In shape, it approximates a slightly bent horn or cartridge, with the dorsal boundary, which is rather superficial, running nearly straight and the posterior half of the ventral border being somewhat concave (Figs. 33, 34). The apex of the spermaceti organ is located on the right side of the tip of the nose. Caudalward it curves to the left in the horizontal plane, ending posteriorly near the center of the amphitheater, just above the right bony naris and immediately in front of the brain case (Figs. 32, 33). Rostralward the case of the spermaceti organ blends into the collagenous tissue of the monkey lips. Here, the tapering tip of this sausage-like fat body ends in the concave rear end of the dorsal monkey lip (Figs. 24, 25, 31). In its posterior half, the case opens ventrally and to the left; here the spermaceti fat is in contact with fatty connective tissue of the adjacent junk, separated only by the interposed by the flat right nasal passage and its muscle (Figs. 26, 27). The blunt caudal end of the spermaceti organ, being oval in cross-section, rests with its flat surface on the vertical back of the amphitheater. Because here, it is enlarged in diameter, this fat body looks like a drumhead or elephant's foot (Fig. 31). The sole of the foot bears no real case but is covered with relatively thin connective tissue. The smooth surface of the sole opposes another sheet of connective tissue which is covered by small bubbles (Fig. 37) filled with a serous liquid. In the smaller specimen of the two early postnatal sperm whales examined ("Odie"), these bubbles were absent; instead there were many small pinholes in this epithelium. Between the smooth sole of the elephant's foot and the bubble layer extends the **frontal sac** as the dorsocaudal enlargement of the right nasal passage (Figs. 31, 37). It does not extend over the whole sole of the elephant's foot and is larger on the left (as is the distal sac). In the smaller baby sperm whale dissected, the fat of the spermaceti organ does not seem to consist of different layers in concentric arrangement and shows no liquid core as in adult animals. Instead, in its caudal part, the case is interspersed with intrinsic muscle fibers which run from the

dorsal and caudal margins rostroventralward into the fat body (Fig. 38c). Additionally, inside the case the fat of the spermaceti organ is bordered ventrally and laterally by diffuse strands of muscle fibers running perpendicularly to the collapsed right nasal passage (right nasal passage muscle; Fig. 38c). This gives the impression that within the case the right nasal passage may be opened via the spermaceti fat by means of surrounding musculature including the right nasal passage muscle (see below).

According to the CT data, the connective tissue in the baby sperm whale head attains maximal density in the monkey lips which sit at the rostral tip of the spermaceti organ and blend into the thick layer of connective tissue surrounding the fat body of this "organ" referred to as the "**case**" (Raven and Gregory 1933; Fig. 31). The case is a tough criss-cross network of collagenous fibers. The term "case" as well as the terms "spermaceti organ" and "junk" were probably used by historic whalers (Scammon 1874). The case is complete dorsally and to the right but is open ventrally and to the left for most of its length (Figs. 24-29, 31). Thus, in the middle and in the posterior part of the epicranial complex, the case is fenestrated and the spermaceti organ more or less confluent with the adjacent junk with the exception of the collapsed right nasal passage and its fatty muscle (Fig. 27).

The **monkey lips** consist of two thick crescentic bulges which represent the anterior end of the spermaceti organ and are continuous caudally with its collagenous sheath (case). X-ray density of the monkey lips is between that of collagen and bone (Figs. 24, 31). The posterior surface of the upper lip forms a concave interface which houses the fusiform tip of the spermaceti fat (Fig. 31).

The epicranial complex as a whole is surrounded by a sheath of connective tissue called the **bridle** because its two lateral ribbons suspend the soft tissues of the nose from the rear part of the skull (Cranford[2], pers. comm.). In the rostralmost region of the nose (blowhole and monkey lip area), the bridle collagen is immediately subdermal, merges into the case and serves as an abutment for the tendons of the dorsal maxillonasolabialis muscle attaching here (Figs. 24, 34). Otherwise the bridle and the case are separate from each other. Caudalward the lateral ribbons of the bridle approach the margins of the skull roof and are confluent with the dorsal sheet of strong tendons belonging to the maxillonasolabialis muscle which originates from the dorsal crest of the amphitheater (Figs. 25-29, 35). Starting out from the monkey lips, the two lateral tracts of the bridle run in shallow grooves between the spermaceti organ and the junk. Here the tracts are thick, wedge-shaped in cross-section and asymmetric (left tract larger than right). Caudalward the left tract expands dorsalward but does not encompass the case of the spermaceti organ. At half-length of the nose, the two tracts are symmetrical again and now occupy the flanks of the nose below the spermaceti organ and at the sides of the junk. Then the bridle tracts converge in the direction of the skull base, get stronger, run parallel to its lateral margins and finally attach here, on both sides, in the area from rostral to the antorbital notch to the orbita and the anterior part of the zygomatic arch (Figs. 28, 29). It is interesting to note that in the anterior region of the epicranial complex, i.e. distal to the rostrum, the junk is free from the bridle and this is also true for the large areas of the prominent external mandibular fat bodies (Figs. 25-29, 31, 32). Further caudalward, however, the two strands of the bridle unite with a medioventral (interadipose) sheet of connective tissue and form a thick fascia beneath the blubber.

[2] Dr. Ted W. Cranford (California State University, San Diego, CA, USA)

In the sperm whale forehead, there is a perpendicular fork-like cartilaginous structure (Y-shaped, cf. Fig. 41). The short caudal unpaired base of this fork originates from the anterior edge of the mesethmoid bone between the narrow right and the wide left bony naris. As is the case with this small plate of the mesethmoid, the body of the fork is inclined to the left and partially covers the caudomedial half of the left bony naris (Fig. 40).

The lower prong of this fork, the ***rostral cartilage*** (cartilaginous rostrum, rostrum nasi; Klima 1990, 1999), is rod-like and extends along the groove of the vomer (mesorostral canal) between the premaxillary bones as far as the tip of the rostrum (Figs. 23, 26-28, 32, 35, 38, 40, 41). The upper prong of the cartilaginous fork is represented by a thin and narrow perpendicular blade which follows the medial wall of the left nasal passage on its way to the blowhole (Fig. 41). The cartilage describes part of a spiral as it first moves to the left and dorsalward along the concave skull roof, then bends dorsorostrally and runs between the left nasal passage and the case of the spermaceti organ (Fig. 38). In the full-grown sperm whale this **nasal roof cartilage** (Klima 1999) is several meters long, about 32-45 cm in width and 18-35 mm thick (Behrmann and Klima 1985). At its caudal origin this cartilage is fused to the mesethmoid and both structures lean over the left nasal passage (left bony nares). In the direction of the blowhole the nasal roof cartilage tapers markedly and in the adult whale comes close to an ovoid arrangement of about a dozen isolated pieces of cartilage, so-called nostril cartilages, that underlie the sigmoid blowhole (diameter of ovoid arrangement about 80 cm; cf. Klima 1990; Fig. 41). In our early postnatal sperm whales, no such arrangement of cartilaginous elements around the blowhole was found. From the topographical situation it appears that the blade-like nasal roof cartilage probably stabilizes the left nasal passage against the pull of the left nasal passage muscle which opens it (Klima 1990, 1999). The partial insertion of the muscle at the

cartilage (Klima 1990), however, could be verified neither in the macroscopical dissection nor in the histological examination of the baby sperm whales.

Two cartilaginous elements of the nose in a neonate sperm whale, the nasal roof cartilage and the cartilaginous rostrum (rostral cartilage), were examined by routine histology. The topographical relationships of these structures are given in transverse cryo-sections (Fig. 38) , in the short series of transverse MRI scans (Fig. 40), and in a lateral schematic reconstruction of the sperm whale head (Figs. 41, 42d).

In the sperm whale, the nasal area of the skull appears to be shifted far caudalward, behind the deep facial depression of the skull reminiscent of an amphitheater (Norris and Harvey 1972). Rostral to this area, in the medial plane of the rostrum, the fossa mesorostralis is situated between both premaxillary bones and bordered by the vomer ventrally. The volume of this fossa is filled by the massive rod-like cartilaginous rostrum. In the baby sperm whales examined, this cartilage is nearly round and approximately 3 cm in diameter at the frontal end but approximately 2.5 cm wide and 4 cm in height at the rear end where it is fused to the mesethmoid bone (Fig. 38). The nasal roof cartilage and the cartilaginous rostrum are continuous in the area of the bony nares. The bony nares are located in the center of the sperm whale skull (Fig. 23). The left bony nasal opening is bordered by the vomer medially and rostrally, by the left premaxillary bone rostrally and laterally, and by the mesethmoid bone caudally. The right naris is surrounded by the right premaxilla laterally and by the mesethmoid medially (Behrmann and Klima 1985, Gambell 1994). As stated before, the right bony nasal passage is shifted to the left and seems to be rotated clockwise in dorsal aspect in postnatal animals so that in the adult sperm whale it lies not only caudal to the left bony nares but also near the mid-axis of the skull.

In the baby sperm whale, the nasal roof cartilage arises over a length of approximately 8 cm from the dorsocaudal free edge of the cartilaginous rostrum. In contrast to the rostral cartilage, the nasal roof cartilage is flat and only 2 - 3 mm thick. From its caudal origin the nasal roof cartilage projects dorsalward and lateralward (Fig. 40). Near its origin the nasal roof cartilage appears irregular in shape and wavelike (Fig. 40). At the rear end near the bony nostrils, this cartilage has no direct contact with the left nasal passage but is topographically related to it and enclosed by soft tissue. After approximately 10 cm it bends rostralward and accompanies the left nasal passage along its medial wall (Fig. 38). Here, the nasal roof cartilage is nearly vertically orientated and blade-like (approx. 4 - 5 cm wide and 2 - 3 mm thick). At blowhole level the nasal roof cartilage is less in height but slightly wider and its dorsal edge is bent slightly medialward (Fig. 38a). In conclusion, the nasal roof cartilage projects nearly diagonally through the huge nasal complex from the bony nares to the blowhole (Figs. 41, 42d).

From a histological point of view the cartilaginous rostrum consist of hyaline cartilage that showed more or less the same composition in all three transverse planes examined over the total length of this cartilage (Fig. 43). The chondrocytes and their territories are placed individually or in groups. In the center of this cartilage, the territories appear rounded but at the periphery they are slightly flattened. On the one hand, blood vessels, including their typical wall structures, can be found and, on the other hand, lacunas which appear to lack wall structures. Delicate elastic fibers are seen in some layers of the walls of the blood vessels, which probably belong to the tunica intima. However, there are no distinct differences in arterial and venous blood supply. Apart from the fibers in the walls of the blood vessel, there are no elastic fibers in the hyaline cartilage (Fig. 43). The chondrocytes are placed concentrically around these blood vessels and lacunae. The extra-cellular matrix, which comprises approximately 50% of the volume of

the cartilage, appears homogeneous and fibers could not be traced here (Fig. 43). The balanced relation between chondrocytes and matrix is an indication of immature and growing tissue. The perichondrium is narrow which points to high interstitial growth of the cartilage as demonstrated by the high vascularization of the cartilaginous tissue.

The nasal roof cartilage appears to be more complicated both in tissue composition and in structure and shows some peculiarities. In general, it consists of elastic cartilaginous tissue which is structured the same way in all planes examined (Fig. 44). The chondrocytes with their territories are arranged individually, only occasionally in groups. Whereas in the periphery they are small and flattened, they are relatively large and rounded in the center. More than 50% of the volume of the nasal roof cartilage is extra-cellular substance (matrix). Interestingly, this is in contrast to typical elastic cartilage of terrestrial mammals where cellular components predominate over the extra-cellular matrix. But the high proportion of extra-cellular substance in the nasal roof cartilage points to slow interstitial growing in spite of the huge size of the nasal roof cartilage.

The nasal roof cartilage is interwoven with a number of elastic fibers which have a more or less straight orientation (Fig. 44). A wave-like or spiral-like structure, typical for elastic fibers, is nearly absent but the fibers vary in diameter and have a number of ramifications. A higher number of elastic fibers is concentrated at the periphery near the perichondrium. Here, the fibers are relatively thick but ramify into thinner strands and project into the inner cartilage in more or less perpendicular orientation to the surface (Fig. 44). The perichondrium consists of a thick connective tissue layer with numerous collagenous fibers, a network of elastic fibers, and some blood vessels. The connection of the elastic network in the perichondrium to the elastic fibers of the cartilage is a sign of intensive

proliferation of fibers from the perichondrium to the deeper cartilaginous tissue. Therefore, it appears that peripheral (i.e. appositional) growth at the perichondrium is more prominent than the interstitial growth which also correlates with a lack of blood vessels in the nasal roof cartilage (Fig. 44).

The **maxillonasolabialis muscle** of the sperm whale runs more or less in an axial orientation from the lateral and posterior margins of the amphitheater in the rear part of the skull to the blowhole region. The prominent dorsal part originates from the vertex (Fig. 37) and ensheathes the spermaceti organ laterally and dorsally. Halfway to the blowhole this dorsal muscle transforms into a thin layer of numerous gracile but strong tendons which blend into the extremely dense tissue of the upper monkey lip. In cross-section, a slight asymmetry is obvious in that on the right hand side the muscle reaches further ventralward. As a whole, the contraction of this longitudinal part of the maxillonasolabialis muscle is believed to pull the blowhole area and the spermaceti organ caudalward and slightly upward. A second large muscle originates on both sides of the skull along the lateral margin of the amphitheater between the antorbital notch and the infraorbital foramen (Fig. 23). From here, this part of the maxillonasolabialis muscle runs obliquely to the side of the monkey lips where it attaches. Again, a slight asymmetry is obvious: the oblique muscle on the left side, which covers the left nasal passage, is wider in cross section than its counterpart on the right hand side.

Two other muscles accompany one nasal passage each. The **left nasal passage muscle** extends from the area dorsal and left to the monkey lips backward to the left bony naris. On its way it shows a constant topographical relationship to the left nasal passage and the nasal roof cartilage, with the air passage in a more dorsal position and near the surface of the head, the cartilage medial to it and the muscle immediately left and more ventral to the passage. In our sperm whale

specimens, the left muscle bulges into the left nasal passage; its fiber bundles are relatively short and run perpendicular to the lateral wall of the passage ventralward and attach to the connective tissue of the junk. By its contraction, the muscle should be able to open the cavity of the left nasal passage. In the posterior part of the epicranial complex, near the left margin of the amphitheater, the three structures (nasal roof cartilage, left nasal passage, left nasal passage muscle) together curve ventralward and along the surface of the skull roof medialward. Whereas the left nasal passage enters the left bony naris, the nasal roof cartilage broadens together with the left nasal passage muscle. The cartilage attaches to the crest of the wing-like mesethmoid bone which, in an oblique position, roofs over the medial part of the large left bony naris. In this area, the left nasal passage muscle is thick and club-shaped and occupies most of the space to the left of the spermaceti organ. In addition, this part of the muscle seems to have a different fiber orientation: running perpendicular to the corresponding part of the left nasal passage they course in a more rostrocaudal direction. Probably they can pull the transverse rostral wall of the right nasal passage which bulges over the left bony naris rostralward in order to open the entrance into the left bony canal.

The **right nasal passage muscle** is flat, nearly band-shaped and rich in fat. It seems to originate from inside the lower monkey lip and runs below the right nasal passage directly adjacent to the spermaceti organ (Fig. 38) which, for a longer distance in its middle part, lacks the collagenous case ventrally and to the left hand side. The posteriormost part of the right nasal passage is fully enclosed in the case together with the right muscle. The fiber bundles of the right nasal passage muscle run from the lower surface of the case obliquely dorsalward and rostralward and should be able to open the right nasal passage by its contraction.

### 5.1.5. Pygmy sperm whale (*Kogia breviceps*)

In contrast to giant sperm whales (*Physeter macrocephalus*) the blowhole of pygmy sperm whales (*Kogia breviceps*) is not in a terminal (anteriormost) but in a dorsal position. In comparison with other odontocetes the most prominent characteristics of pygmy sperm whales are a) the position of the spermaceti organ caudal to the melon and b) the existence of a large connective tissue "cushion" in the center of the right vestibular sac. Schenkkan and Purves (1973) gave an overview on the nasal morphology and reviewed the extant literature on *Kogia breviceps* and *K. sima*. In general, not much is known on the functional morphology of these two species although, historically, the specialized nasal complex in *Kogia* had been recognized a century ago (Benham 1901, Danois 1910, Kernan and Schulte 1918, Schulte and Smith 1918).

The **skull** of the pygmy sperm whales (*Kogia breviceps*) is unique in shape among the toothed whale order but very similar to the smaller *K. sima* (Fig. 45). Furthermore, its width (in relation to the skull length) is maximal among the toothed whales and the strong nuchal crest projects lateralward to the antorbital notches. The rostrum is triangular in shape but flat and wide at its posterior base. The proximal part of the **mesorostral cartilage** is ossified far to the front as a rostral extension of the mesethmoid bone, a feature specific for young and old animals. Interestingly, we did not find a cartilage similar to Klima's cartilage in *Physeter*.

As in other cetaceans, the **bony nostrils** are in the center of the facial skull (Fig. 45) and the adjacent bony nasal passages project nearly vertically, i.e. perpendicular to the skull base and the beak-fluke axis, respectively. But, similar to the situation found in *Physeter*, the extreme facial asymmetry leads to an unequal cross sectional area of the two sides. The aperture of the left bony nasal

tract is at least six times wider than that of the right one and the right bony naris is shifted to the left and is located near the midline of the skull. Between the two bony nostrils there is a strong curved bony crest consisting of the left maxilla and the mesethmoid (as well as a short process of the right premaxilla; Fig 45). The left border of the ridge is orientated vertically and S-shaped in dorsal view. But the right hand side is characterized by a smooth curved surface of the posterior extension of the right premaxilla around the right bony naris which houses the caudal curvation of the spermaceti organ.

From the bony nares the soft nasal passages extend dorsalward to the **blowhole** which is situated near the vertex of the head but shifted slightly to the left. Its shape is concentric but, in contrast to other odontocetes (except the giant sperm whale), the concavity of the external slit faces caudalward. Immediately below the blowhole the narrow **vestibulum** is situated (not shown in figures). On the right hand side there is a horizontal slit-like opening in the rostral wall of the vestibulum leading into the large **right vestibular sac** (Fig. 46). This air diverticulum circles a large "cushion" of connective tissue resembling a baseball catcher's mitt or a mushroom head. We prefer the term **torus** instead of cushion (Schenkkan and Purves 1973) or catcher's mitt (Cranford et al. 1996). The inner concave surface of the torus faces medialward and ventralward (Fig. 46). Sections through the torus reveal two layers of connective tissue. The medioventral center of the torus, opposite to the entrance into the right monkey lips, is characterized by large and deep crypts originating in a curved arrangement along both sides of the "monkey gape" (cf. chapter above *"The giant sperm whale"*). These crypts within the wall of the torus extend between the two layers of connective tissue. Dorsal and to the sides the torus is characterized by smaller crypts (Fig. 46). The whole torus is fixed in the center of the vestibular sac by a number of thin pillars of connective tissue which attach to the dorsal and side walls of the sac. Near the entrance

between the vestibulum and the right vestibular sac there is a further protrusion of the right vestibular sac consisting of small pouches that extends over the midline to the left hand side (Fig. 46). The **left vestibular sac** is represented by a relatively small evagination from the left hand side of the vestibulum orientated lateralward and caudalward. But this sac consists also of a number of pouches (not shown in figures).

The **right nasal passage** opens dorsolaterally into the right vestibular sac through the aperture of the **monkey lips** (museau de singe) and the ventral surface of the torus covers the dorsal opening of the lips (Fig. 46). The passage is slit-like in transverse orientation so that the monkey lips can be divided in an anterior and a posterior one (Fig. 46c). The lips are up to 3 cm wide in adult specimens and consist of tough connective tissue covered by black epithelium. Both lips are characterized by longitudinal furrows that form a mortise-tenon complex similar to that found in *Physeter*. These furrows are lined by two whitish bands on each lip. At the lips' outer margin, superficial to the mortise-tenon folds, small furrows are arranged parallel to the proposed air stream resembling the pattern of furrows an the shell of scallops. The apex of the spermaceti organ case is consistent with the posterior monkey lip. From the monkey lips the right nasal passage projects in a straight line medioventralward to the right bony naris. Concomitantly, the anterior lip blends medioventrally into the dense connective tissue of the right nasal plug. The deep right nasal tract has a concave cross section because the nasal plug bulges into its lumen from anterior. Ventral to the plug, anterior to the entrance in the bony naris, there is a small diverticulum. This right premaxillary sac was not described by Schenkkan and Purves (1973). Above the right bony nares the right nasal passage bears on its posterior wall the orifice into the large nasofrontal sac that covers most of the spermaceti organ (Fig. 46). The caudal wall of this sac, opposite to the spermaceti organ, attaches to the right concave slope of the mesethmoid

ridge (Figs. 45, 46) and is covered with numerous small knobs or papillae consisting of connective tissue. The right nasofrontal sac is in contact with the right premaxillary sac by a slit-like ventral opening lateral to the entrance into the right bony naris.

The structure of the **left nasal passage** is rather simple when compared to its right counterpart. It is a mere vertical connection between the blowhole and the bony naris. The nasal plug is large and bulges from anterior into the nasal tract (Fig. 46) which gives the tract a convex shape in horizontal plane (facing caudalward), as is the case in most toothed whales. The left premaxillary sac is a relatively small extension of the wide left nasal passage situated on the premaxillary bone rostral and rostrolateral to the nasal tract. A left nasofrontal sac is absent.

The right nasofrontal sac envelops partially a large piriform body, the **spermaceti organ**. The latter is reminiscent of a curved pear or horn the tip of which is situated at the posterior (right) monkey lip and extends medialward and rostralward to the terminus of the melon (Fig. 46). The reddish surface of this "organ" (in fresh specimens) consists of dense connective tissue (case). In contrast to the lateral and posterior surface of the spermaceti organ, where the case is thick, the frontal end of the spermaceti organ, which abuts the melon terminus, is nearly free of dense connective tissue. The shape of the **melon** is responsible for the characteristic "face" of *Kogia* which, in lateral aspect, is reminiscent of a shark. This big fat body projects beyond the tip of the rostrum as is the case in *Physeter* (Cranford et al. 1996) and shows the same layered lipid composition in *Kogia* as in dolphin-like species (Fig. 46). The melon terminus is rather wide, in contrast to the situation in dolphins, and blends with the rostral end of the spermaceti organ. As shown in the CT data the melon and the spermaceti organ

together form a structure resembling a horn with a convex frontal end whereas the caudal end abruptly turns to the (right) posterior monkey lip (Fig. 46).

The **musculature** in the epicranial complex (M. maxillonasolabialis) of *Kogia* is not as complex as in delphinids and phocoenids. Two bilateral rostral muscles originate from the rostrum and enter the melon's connective tissue laterally. These muscles have the same topographical relations to the rostrum and the melon as in dolphins and porpoises and their tension may alter the shape of the ventral melon area.

Layers of fan-shaped muscles from the facial fossa encircle the blowhole region. Their overall pattern is similar to the situation in dolphins but extremely asymmetric. Superficial muscle layers of the right side originate near the facial border from the mesethmoid ridge between the two bony nares (Fig. 45) to the antorbital notch and attach to the connective tissue on the dorsal surface of the right vestibular sac which encompasses the torus. Some fibers reach the thin pillars that fix the torus within the right vestibular sac. Tension of this muscle may control air pressure in the sac. A ventral muscle layer originates caudal on the right facial fossa. It stretches into the dorsocaudal surface of the right nasofrontal sac whereas a few fibers run in direction of the posterior monkey lip and may control the tension of the lips. But in general, the monkey lips are not supplied with strong muscles; only a few weak fibers extend in their direction.

On the left side, the superficial portions of the maxillonasolabialis muscle originate along the whole facial border, project into the connective tissue around the blowhole, and cover the left vestibular sac and the left extension of the right vestibular sac. A strong portion of this muscle attaches to the posterior surface of the vestibulum. It may open the upper nasal passage. A small laterocaudal portion of the left maxillonasolabialis muscle inserts in the dorsal surface of the

nasofrontal sac near the left corner of the (right) monkey lip. Thus, actions of this small muscle portion may alter the tension of the lips. A thin anterior muscle layer stretches from the left antorbital notch area to the left lateral extension of the right nasofrontal sac (ventral to the rostral portion of the mesethmoid ridge) and may control the volume of this sac at its left side.

The bilateral nasal plug muscles are highly asymmetric: the left one is much larger than the right one, a fact which is correlated with the size of the nasal plugs and that of the bony nares, respectively. Both muscles originate rostral to each bony naris and enter the connective tissue of the nasal plugs. The muscle fibers are intercalated by whitish layers of connective tissue, very similar to the situation in the nasal plug muscles in dolphins and porpoises and this muscles may have the same function in these animal groups (*Kogia*, dolphins, porpoises): the contraction of these muscles may open the nasal passages at the level of the nasal plugs (Fig. 46).

## 5.2. Development of the upper respiratory tract in delphinids

In this chapter, the nasal development in early fetuses is briefly described first. Then the situation encountered in perinatal dolphins is evaluated for comparison, on the one hand, to the early fetal material and, on the other hand, to adult dolphins. This comparison is based on results included in this dissertation as well as on existing data in the literature. In the discussion chapter then, the functional and phylogenetic implications of all these data are presented.

The nasal tracts are clearly visible in both the MRI scans and the micro-slides of **early fetuses** (CRL 38 and 40.5 mm) by their fluid-filled spaces (Fig. 47). They are

in nearly vertical in position with respect to the skull base in front of the cranial vault (Fig. 48), a situation typical for adult dolphins. Dorsal to the nasal skull each nasal tube has two small extensions, one directed anteriorly and one posteriorly. The anterior extension seems to represent the rudiment of the premaxillary sac and the posterior extension may be the bud of the nasofrontal sac (Fig. 47). Interestingly, there are no vestibular sac anlagen although these nasal sacs are the largest air spaces in adult dolphins. The same situation was found in the narwhal (13.7 cm total length) and harbor porpoise fetuses (16.7 cm total length) examined, which are in a more mature state than the MRI scanned fetus in Figure 47 and have also nasofrontal and premaxillary sac anlagen but no vestibular sac rudiments.

The nasal cartilages reduced in adult specimens (Klima 1999), are visible in some MRI scans but cartilage is rendered in MRI images similar to fetal bone and connective tissue. Therefore, only part of the structural complexity is visible in the MRI scans (Fig. 47a) but much more detailed in histological slides (Fig. 47b).

Furthermore, the lumina of the larynx and trachea are clearly visible in the MRI images (Fig. 47). But again, in contrast to the micro-sections, the cartilage of these two structures cannot be discriminated in the scans. Shrinkage of the surrounding tissue is not obvious except for a wide connection between the pharyngeal space and the epiglottic spout (see below) seen in both the histological sections and the MRI data. Therefore, for the segmentation an "artificial" boundary between the air passage and the pharynx at the distal tip of the elongated larynx was created to distinguish between the nasal passage and the pharynx in the reconstructions (Figs. 47, 48). This marked elongation of the larynx caused by the long epiglottic and arytenoid cartilages is characteristic for toothed whales and guarantees a complete separation of the air and food passages in postnatal animals (see chapter "*The role of the larynx…*"; Reidenberg and Laitman

1994). Even in these early fetuses the larynx exhibits its typical configuration with the elongated epiglottic spout representing a transitional stage between the mammalian bauplan and the odontocete situation (see below; Fig. 47).

With respect to bone formation, the skull base of **perinatal specimens** is still rather incomplete; rostrolaterally on both sides, there are wide gaps between the presphenoid, orbitosphenoid, and mesethmoid bones and the remaining lateral wall of the skull. The intersphenoidal synchrondrosis, a non-ossified cartilaginous zone in the skull base between the presphenoid and the basisphenoid of adult bottlenose dolphins (Rommel 1990), may be a residue of the cartilaginous gaps. However, this zone is not obvious in radiograms (Fig. 56) because cartilage is rendered similar to bone tissue, but in the T1-weighted MRI scans (Fig. 55b).

The triangular dolphin beak consists of the dorsal rostrum and the ventral mandible and serves as a fish or squid "forceps". The rostrum consists of the premaxillae, maxillae, and of the unpaired vomer. Between the two premaxillae dorsolaterally on both sides and the vomer ventrally in the middle the mesethmoid cartilage represents the axis of the rostrum. The function of this cartilage in toothed whales remains largely unknown. Purves and Pilleri (1983) and Au (1993) suggested that it could be involved in the emission of sonar signals. But this hypothesis could not be confirmed so far. Klima et al. (1986) and Klima (1999) characterized it as the "driving force" in the ontogenetic development of the cetacean rostrum. Whereas the other components of the cartilaginous nasal capsule are clearly visible in early fetal stages of mammals (Fig. 47b), they have disappeared in the perinatal dolphin specimens examined (with the exception of the cartilaginous rostrum; Klima 1999). Although the formation of many components of the nasal complex in toothed whales seems to take place a little later with respect to other main components of the head as, e.g., the ear region (Haddad et al., in

prep., Comtesse and Oelschläger, unpublished), the properties of the rostral cartilage in our perinatal specimens are similar to those in the adult. Due to its high water content, this cartilage is hypodens in the CT but produces an intense signal in MRI scans (Fig. 49). Caudally it is continuous with the mesethmoid bone which separates the two nasal passages from each other; the horizontal CT and MRI scans (Figs. 55a, b) show the boundary between the mesethmoid bone and the cartilage. Although the rostral cartilage is ensheathed by the gutter-like vomer ventrally, both are clearly separated from each other by a distinct gap (Fig. 49). This narrow cleft between the mesethmoid cartilage and the underlying vomer terminates rostral to and below the cribriform plate and thus may be a shrinkage artifact caused by the fixation and/or freezing processes. Dorsolaterally on both sides, however, only the medial rims of the premaxillaries are in contact with the dorsal surface of the cartilage.

In odontocete skulls, as in our perinatal dolphin specimens, the premaxillary and maxillary bones have been extended caudalward, lateral to the bony nostrils and over the frontal bones. This evolutionary and developmental phenomenon is known as the "telescoping process" (Miller 1923) and important for a stable suspension of the viscerocranium (rostrum) from the neurocranium. The double layer of bones (maxillary/frontal) which are interconnected over large contact surfaces via connective tissue (syndesmosis) was called a „sandwich structure" by Fleischer (1976). In the postnatal animal, this composite structure may reflect sound/ultrasound produced in the blowhole area to the front by serial impedance mismatch. The function of this "acoustic shield" (Fleischer 1975) was demonstrated by Aroyan et al. (2000) with computer-based simulation experiments. Apart from that, the sandwich configuration (bone/collagen/bone) could help to acoustically isolate the neurocranium and the ears, respectively, from the rostrum. Nevertheless, in our young specimens, the caudal extensions of the

maxillary bones do not meet the dorsorostral end of the supraoccipital, and there is no trace of a nuchal crest (Rommel 1990) formed in adult spotted dolphins by the frontal, interparietal, and supraoccipital bones.

The facial depression of the dolphin skull houses the large epicranial complex. From the blowhole, the sub-vertical soft nasal passages lead to the bony nostrils situated in the center of the depression. The semicircular blowhole merges into an unpaired vestibulum, which is flattened rostrocaudally and opens ventralward into the two nasal passages. The ventral part of the soft upper respiratory tract is separated by a soft nasal septum. Here, each passage can be closed by its nasal plug (Fig. 50), a cushion consisting of loose connective and muscle tissue, which bulges into its nasal passage from anterior. Three pairs of nasal sacs, each representing a horizontal level of the epicranial complex, communicate with the nasal passages: the vestibular sacs located at the dorsal-most level, the nasofrontal sacs below these, and the premaxillary sacs on the skull roof rostral to the bony nares. As a whole, the nose of our perinatal specimens strongly resembles the situation in the adult in terms of structure and probably also function. Whereas a few decades ago it was speculated that the nasal complex should be the site of sound production in dolphins (Norris et al. 1971 [cited after Norris 1980], Ridgway et al. 1980, Amundin and Andersen 1983), it is rather likely now that the nasal sacs indeed are involved in sonar beam generation and transmission (for review see Cranford et al. 1996, Cranford 2000). Most toothed whales have a rich repertoire of vocalizations (Au 1993, Wartzok and Ketten 1999). These sounds are probably generated near the nasal plugs by vibrations of the monkey lips at the upper (dorsal) end of the paired nasal tracts which oppose each other in the respiratory air-stream and encompass valve-like slits near the transition to the vestibulum (Cranford et al. 1996, Cranford 2000).

The epicranial complex exhibits some asymmetry across the genera and families of toothed whales. The degree of asymmetry varies from slight in phocoenid species up to considerable (extreme) in the sperm whales (Physeteroidea; Ness 1967, Clark 1978a, c, Heyning 1989, Cranford et al. 1996). Apart from at least one exception (e.g., vestibular sac in most delphinid species), the nasal structures of the right hand side are always larger than those on the left (Schenkkan 1973). According to our material, the nasal complex of early fetuses is symmetric (Fig. 48) but the three perinatal specimens show a slight degree of asymmetry and the sagittal midplane of the nasal area is gently shifted to the left (Figs. 49c, 50). We did not measure the degree of asymmetry in these animals but it is less pronounced than in the adult dolphin. With regard to the facial skull (facial depression), the rear end of the rostral cartilage and the bony nasal septum are slightly inclined to the left and the right premaxilla is wider than the left (Fig. 50). Because of their morphological and topographical relations with the elements of the skull roof, the soft tissue components originating here (musculature, nasal sacs) are somewhat larger on the right hand side (Fig. 50). Obviously, facial asymmetry in dolphins arises late in fetal development and gets stronger only during postnatal development.

Due to the fact that, in our perinatal specimens, the accessory sacs of the nasal tract (which contain air in the postnatal animal) were filled with fixation fluid, only part of these spaces can be identified in the scans of our perinatal specimens (Figs. 49, 50). In contrast, the cleft-like soft nasal passages do not give an intensive signal, but appear to have been filled with air in these animals after death, either naturally or artificially.

The dolphin forehead is characterized by a bulbous fat body, the melon, which is located immediately rostral to the nasal tract. This structure, unique to cetaceans,

is already well developed in our perinatal specimens (Fig. 49). In both CT and MRI scans, its structure is inhomogeneous. As seen in the cryo-sections, the melon is embedded in dense connective tissue. Whereas the core of the melon is nearly free from connective tissue, the amount of fibers increases to the periphery of the melon in any direction. Due to this gradient in fiber density and lipid content, the melon is thought to focus the ultrasonic click sounds produced in the nasal complex on their way rostralward (Norris and Harvey 1974, Cranford 2000). The shape of this large fat body can be modulated by means of the rostral nasal musculature (Fig. 49a) in order to vary the shape and direction of the emitted sonar beam (see chapter "*The nasal complex of the harbor porpoise*" above).

## 5.3. Asymmetry of the facial skull in toothed whales

The graphic representation of the principle component analysis (PCA) reveals a clustering of different toothed whale species due to the first and second factors of components (Fig. 57). Factors 1 and 2 of the PCA show that these two factors may explain 52% of the variance of the data (27.9% for factor 1 and 24.3% for factor 2). Factor 3 contains 13.6% of variance. The graphical representation of species (passive variables, factor values; cf. Backhaus 1996) by factors 1 and 2 reveals two clusters (Fig. 57): one cluster consisting of *Cephalorhynchus commersonii* (CC), *Inia geoffrensis* (IG), *Phocoenoides dalli* (PD), and *Phocoena phocoena* (PP) centered in the graph and another cluster formed by *Delphinus delphis* (DD), *Stenella attenuata* (SA), and *Tursiops truncatus* (TT). *Kogia sima* (KS) and *Pontoporia blainvillei* (PB) are far out of these two clusters and clearly distinguished by factor 2. Closer inspection of the active variables (factor loading, cf. Backhaus et al. 1996; Fig. 57: coordinates given by x and y values of the landmarks) characterizes the landmarks which are probably responsible for the

location of the species in the graphical representation. In general, the two clusters (CC, IG, PD, PP as well as DD, SA, TT) and *Pontoporia* (PB) are mainly caused by x values of the facial skull (values in lateral orientation) while the location of *Kogia* (KS) is based on y values (values parallel to the skull axis). This implies that the value of factor 2 of *Kogia* different from those of the other species is based on these axis-parallel landmark values of the skulls.

**5.3. Box 1:**

The graphical representation of factors 1 and 2 of the principle component analysis (PCA; Fig. 57) can be interpreted (without garanty of correctly used mathematical phrases; for further information see Backhaus et al. 1996) as an diagram of "similarities" of species examined with respect to their facial skull shape, i.e. their 2-dimensional landmark topography on the facial skull. According to these data (of the facial skull of species examined) species represented near the center of the graph (0,0) are more generalized toothed whales than those distant from the center. Species far distant from each other are not as similar as toothed whales near by in the graph. The additional representation of the active variables in Fig. 57 (coordinates given by x and y values of the landmarks) can give an optical clue how the values (positions of landmarks) are connected to the position of the species in this graph, i.e. which landmarks are responsible for the position of the species within the graph and thus for the degree of similarity between the species examined.

Figure 58 shows the distance of landmarks (LM) 04, 05, and 06 from the skull axis in lateral axis (right angle to the artificial skull axis). These three landmarks represent three different positions of the mid-suture of the skull in dorsal aspect

and these distances characterize thus the shift of the mid-suture with respect to the skull axis at three different levels along the rostrocaudal axis (skewing; Ness 1967). All these landmarks are shifted to the left with regards to the axis of the skull. In general, the larger the value the larger is the distance to the axis of the skull which means a larger distance from the mid-suture to the skull axis. According to these data the highest degree of skewing (Ness 1967), therefore, can be found in the delphinid species. *Cephalorhynchus commersonii* (Table 2: CCF and CCM) is an exception since its degree of skewing is similar to *Phocoena phocoena* (PPF and PPM). The smallest degree of skewing was found in *Pontoporia blainvillei* (PBF and PBM). In contrast, *Kogia sima* (KSF and KSM) has by far the highest degree of skewing because LM 4 (local midpoint of bony nasal septum at anterior border of bony nares) shows the highest value of all species examined. Although LM 5 and 6 (Table 3) could not be marked for *Kogia* because this species has only one nasal bone, the high degree of skewing can be supported by visual inspection of the skull. In *Kogia*, the mid-suture meanders far to the left from the axis of the skull (Fig. 45). All other skulls examined show that LM 04 has a smaller distance to the axis than LM 5 and 6. This means that the mid-suture of the nasal bones (LM 5 and 6) is shifted more the left than the rostral midpoint between the bony nares (LM 4) so that the degree of skewing is more distinct in the caudal region of the facial skull.

Figure 59 to 64 compare bilateral measurements of both sides. These measurements are distances between landmarks on the mid-suture and bilateral landmarks taken perpendicular to the skull axis (x values of the original coordinate system projected on each skull).

Figure 59 compares the rostrum width at its base to the facial skull of both sides (distance between LM 9 and LM 3 versus LM 10 and LM 3). In all species examined

these values are nearly symmetrical but, in general, the right values are slightly higher than those of the left. The widest rostra are found in *Kogia sima* (KSF and KSM), *Lissodelphis borealis* (LBF and LBF), and *Phocoenoides dalli* (PDM), the narrowest rostrum has *Pontoporia blainvillei* (PBF and PBM).

The width of the premaxillary bones at the transition to the rostrum (distance between LM 11 and LM 3 and between LM 12 and LM 3) exhibits clear asymmetry in *Kogia sima* (KSF and KSM) as shown in Figure 60. In the other species examined these measurements are nearly symmetrical. In general, these values have the same order in *Kogia* and the delphinids but they are slightly smaller in *Inia geoffrensis* (IGF and IGM) and *Phocoena phocoena* (PPF and PPM) and clearly smaller in *Pontoporia blainvillei* (PBF and PBM).

Figure 61 shows that the width of the facial skull on each side (distance between LM 13 and LM 4 versus LM 14 and LM 4) has its highest degree of asymmetry in *Kogia sima* (KSF and KSM). *Cephalorhynchus commersonii* (CCF and CCM), *Inia geoffrensis* (IGF and IGM), *Pontoporia blainvillei* (PBF and PBM), and *Phocoena phocoena* (PPF and PPM) are nearly symmetrical, in contrast to the other delphinids.

Figure 62 implies that the maximal width of the premaxillary bones (distance between LM 15 and LM 4 and between LM 16 and LM 4) is nearly symmetrical in *Inia geoffrensis* (IGF and IGM), *Pontoporia blainvillei* (PBF and PBM), and *Phocoena phocoena* (PPF and PPM) as well as in *Kogia sima* (KSF and KSM). In the latter species, the symmetry of the maximum premaxillary width is in contrast to the premaxillary width at the base of the rostrum (see above) which is caused by the different shapes of the left and right premaxillary bones (Fig. 45). The delphinid species show clear asymmetry in this measurement but *Cephalorhynchus*

*commersonii* (CCF and CCM) is not as asymmetric as the other delphinids investigated here.

The width of the bony naris is larger on the right side in nearly all species examined (Fig. 63). These values are symmetrical only in *Pontoporia blainvillei* (PBF and PBM). The same is true for the width of the nasal bones which is, in general, considerably larger on the right side (Fig. 64). Some exceptions can be found in *Inia geoffrensis* (IGF and IGM), *Pontoporia blainvillei* (PBF and PBM), *Phocoenoides dalli* (PDF), and *Phocoena phocoena* (PPF and PPM) where these bones are nearly equivalent in width.

Comparison of the values of the degree of skewing (Fig. 58) and of the bilateral widths of individual structures in relation to the mid-suture of the skull (Figs. 59 to 64) reveals that asymmetry in the toothed whale skull is caused by both the lateral shift of the mid-suture with respect to the skull axis (skewing) and the increase in width of structures on the right hand side of the skull.

The results of the PCA (Fig. 57), in comparison with the bar plots (Figs. 58 to 64), can be interpreted in such a way that the two clusters, one "dolphin" cluster (*Delphinus*-DD, *Stenella*-SA, and *Tursiops*-TT) and one "porpoise" cluster (*Cephalorhynchus*-CC, *Inia*-IG, *Phocoena*-PP, *Phocoenoides*-PD), which are based on the same dataset, represent different degree of asymmetry. The species of the "porpoise" cluster are generally more symmetric than the "dolphins". *Pontoporia blainvillei* is probably the most symmetric species examined (Figs. 58 to 64; Ness 1967, Heyning 1989) and located near to the "porpoise" cluster but independent (Fig. 57). Interestingly, the location of *Pontoporia* in the PCA graph is based on laterally orientated values (x values) of the left hand side of the skull (Fig. 57). It is possible that this statistical result is correlated with the slight degree of

skewing (Fig. 58) which makes the distances of the left landmarks from the skull axis relatively smaller.

The location of *Kogia* in Figure 57, different of the other species, is based on these axis-parallel landmark values. Therefore, this result does not hold for the analysis of skull asymmetry, in general. But it shows clearly the peculiars character of the facial skull in *Kogia* which is totally different in shape and asymmetry from all other skulls examined (Fig. 45). Nevertheless, in general and most important, all species examined show the same general pattern of facial skull asymmetry: the mid-suture is shifted to the left and the right bony structures are larger than the left.

## 5.4. The larynx of the harbor porpoise (*Phocoena phocoena*)

The **skull base** in the harbor porpoise is symmetrical and the **choanae** are centered in the ventral view of the skull. Anterior to the choanae, the ventral part of the rostrum is formed by the palatine, maxilla, vomer, and premaxilla. Immediately in front of the choanae the bilaterally paired pterygoid hamuli erupt ventrocaudalward. Each of the choanae is bordered laterally by a crest-like projection of the pterygoid hamulus (Rommel 1990), which is interrupted by a deep notch immediately lateral to the choanae. However, the crest projects in a caudal direction and is built by the basioccipital bone that is in lateral contact with the periotic region. Due to these crest-like ventral projections the skull base roofs a medioventral vault. The laryngeal passage runs through this vault where the air passage turns (by means of the larynx) from a vertical course through the bony nares to a horizontal orientation ventral to the brain case. Together with the ventral parts of vomer and basisphenoid, which represents the medial and caudal

borders of the choanae, the pterygoid crest is the anchor of the large pterygoid muscles. These muscles connect the larynx tightly with the bony nares.

The **hyoid apparatus** lies ventral to the skull base. It is C-shaped in lateral aspect and consist of up to four bony elements (Fig. 65). The dorsalmost hyoid bones are the **stylohyals** (SB). They "articulate" by means of the tympanohyal cartilage (Reidenberg and Laitman 1994) to the paroccipital process of the skull. The ventralmost elements of the hyoid are the unpaired **basihyal bone** (BB; rostrally) and the paired **thyrohyal bones** (TB; caudally). In the adult harbor porpoise these bones are fused and reminiscent of a whale fluke in dorsal or ventral view. The anterior horn of the basihyal and the anterior tip of the stylohyals are interconnected by the small **ceratohyal bones** (CB) orientated dorsoventrally. The latter bones "articulate" with each other via cartilage.

The hyoid apparatus forms a framework in which the larynx is moored. In general, the **larynx** of the harbor porpoise shows the typical configuration and shape known of other toothed whales. Furthermore, we found the anatomy of the nasopharyngeal and gular complex to be very similar to dolphins (Figs. 49 to 55, 67). Therefore, we shall restrict our description to a minimum and refer to the extensive literature regarding this subject (Lawrence and Schevill 1965, Green et al. 1980, Reidenberg and Laitman 1994).

With the exception of the so-called **epiglottic spout**, which is reminiscent of a goose beak, the cetacean larynx in principle is similar to that of other mammals, being composed of a cartilaginous framework held together by a number of muscles and connecting tissue (Fig. 65). Via this epiglottic spout the larynx has an intranarial position. Its anterior end (the distal tip of the epiglottic spout) is firmly held within the choanae by a strong sphincter muscle (Fig. 65). The

elongated intranarial larynx (drawn ventrocaudally in Fig. 65 because of didactical reasons) functions to keep the nasal air passages continuous with the glottis while the porpoise sucks in prey (Reidenberg and Laitman 1994).

The **thyroid cartilage** (TC) is the main component of the larynx (Fig. 65). It is made up of right and left laminae fused at their ventral margins (Fig. 66). Each lamina has two well developed processes; the anteriorward directed cranial cornu and the posteriorward directed caudal cornu, the latter being the larger one. Most of the extrinsic muscles, which move the complete larynx, attach to this cartilage. The caudal cornua of the thyroid cartilage articulates with the superior laterocaudal margins of the cricoid cartilage via small oval synovial joints. Rostrally the thyroid cartilage articulates with the epiglottic cartilage.

As in *Tursiops* and *Stenella*, the **cricoid cartilage** (CR; Lawrence and Schevill 1965, Green 1980; Figs. 65, 66) in the harbor porpoise is not a complete ring as in some cetaceans (e.g. in *Physeter macrocephalus*; Hosokawa 1950), but it is open ventrally, forming two rather long lateral cornua which project caudalward. These cornua almost fill the posterior lateral notch in each thyroid lamina. In addition to the joints formed between the cricoid and thyroid cartilages mentioned above, there are articulations between the anterior lateral margins of the cricoid cartilage and the arytenoid cartilages.

The **epiglottic cartilage** (EC) in all the toothed whales examined so far is much longer than that of most mammals. It is concave medially and forms a trough with thin lateral margins. The latter projects caudalward to wrap around the anterior borders of the cuneiform and arytenoid cartilages thereby forming the "laryngeal beak" (Figs. 65, 66).

The **arytenoid cartilages** (*AC*; Fig. 66) articulate with the anterior lateral margins of the cricoid cartilage by well formed oval-shaped synovial joints. Each has a well-developed muscular process projecting lateralward, but no vocal processes are evident. The arytenoid cartilages also articulate with the cuneiform cartilages.

The **cuneiform cartilages** (*CU*) are elongated blade-like processes of the arytenoid cartilage that face each other medially and lie in the trough formed by the epiglottic cartilage (Figs. 65, 66). Two or more small cartilages, probably representing the corniculate cartilages, attach to the caudolateral end of each cuneiform cartilage and also to the caudal two-fifths of the ventral edge of the arytenoid (not shown in figures).

The odontocete larynx is characterized by an intralaryngeal unilateral "midline fold" standing in the mediosagittal plane (Hosokawa 1950, Reidenberg and Laitman 1988). In the harbor porpoise the fold is relatively thick and stretches between the rostral ends of the arytenoid cartilages and the mediorostral end of the thyroid cartilage. Lateral to this midline fold is a set of smaller folds, in the harbor porpoise usually only one or two on each side. These folds project oblique along the midline fold and give way into a system of small sacculi between them (Fig. 66).

As stated above, the larynx is suspended from the musculoskeletal framework of the hyoid apparatus but is connected to the hyoid itself and to the sternum by a set of only five muscles (Fig. 65):

The unpaired **hyoepiglottic muscle** (he) originates from the mid-dorsal basihyal and from the ventrocaudal surface of the ceratohyal and attaches to the epiglottic cartilage and more specific to the inferior half of its anterior edge (Figs. 10, 65,

66). This muscle probably functions to pull the epiglottal cartilage forward so as to enlarge the size of the anterior passageway in the laryngeal beak (Green et al. 1980).

The **thyrohyoid muscle** (th) arises from the rostrolateral surface of the thyroid cartilage, anterior to the attachment of the sternothyroid muscle. It attaches to the posterior margin of the basihyal and thyrohyal bones (Fig. 65) and probably pulls the laryngeal apparatus rostralward, thus anchoring the tip of the laryngeal beak within the choanae (Green et al. 1980).

The **sternothyroid muscle** (sd) originates from the rostroventralmost part of the sternum and inserts on the lateral surface of the thyroid cartilage (Fig. 65), just superior to and anterior to the insertion of the cricothyroid muscle. The sternothyroid muscle probably pulls the complete laryngeal apparatus caudalward (Green et al. 1980).

Furthermore, there is a set of muscles which interconnect the different cartilaginous parts of the larynx to each other:

The **cricothyroid muscle** (cr) has its origin on the lateral posterior surface of the lateral horn of the cricoid cartilage. It attaches to the thyroid cartilage along the inferior margin of the caudolateral part, i.e. to the posterior notch and to the lateral surface of the thyroid lamina just below the posterior notch (Fig. 65).

The **cricoarytenoid muscle** (cy) originates from the dorsal surface of the cricoid cartilage, extends laterad to the medial surface of the caudal horn of the thyroid cartilage and attaches to the dorsal muscular process of the arytenoid cartilage

(Figs. 65, 66). It probably rotates the arytenoids lateralward and posterodorsalward (Fig. 65).

The **thyroarytenoid muscle** (ta) originates from the dorsal midline and the medial surface of the thyroid cartilage. The fibers pass dorsad to insert on the arytenoid cartilage, more precisely on the ventral surface of its muscular process (Fig. 66). The anterior fibers pass lateralward, over the posterior angle of the epiglottic cartilage. The thyroarytenoid muscles probably pull the arytenoid and cuneiform cartilages ventrad and mediad to decrease the angle between their medial surfaces. If the arytenoid and cuneiform cartilages are already approximated the thyroarytenoid muscles probably pull the arytenoids and cuneiforms deeper into the epiglottal trough (Green et al. 1980). Thus, these muscles may control the closing of the epiglottic spout.

The **interarytenoid muscle** (ia; M. arytenoideus transversus; Figs. 65, 66) connects the dorsal margins of the cuneiform cartilages and to a lesser degree the arytenoid cartilages. Some of the posterior fibers join the anterior edge of the dorsal cricoarytenoid muscle. These muscles apparently increase the inter-arytenoid space between the edges of the arytenoids and thus the inter-cuneiform space between the anterior edges of the cuneiform cartilages (Green et al. 1980). Simultaneous contraction of the cricoarytenoid muscle may, therefore, open the inter-cuneiform space. Rostral movement of the epiglottic (by the hyoepiglottic muscle) could then widen the connection between the nasal and the laryngeal air passages (Fig. 65).

The larynx is suspended from the base of the cranium by a complex of muscles, the thyropalatine, the occipitothyroid and the thyropharyngeal muscles (Fig. 65). These muscles arise from the dorsal margin and anteromedial surface of the

thyroid cartilage, and then pass dorsad and rostrad to attach to the base of the cranium. The anteriormost of these muscles is the **thyropalatine**, (tl; a posterior part of the palatopharyngeal muscle, see below), which attaches the medial surface of the thyroid lamina and the thyroid ligament. The middle muscle, the **occipitothyroid** (ot; Lawrence and Schevill 1965), attaches to the dorsal margin of the cranial cornu of the thyroid cartilage. This muscle is not found in terrestrial mammals (Schneider 1964) and in *Physeter macrocephalus* (Hosokawa 1950). Nevertheless, in the harbor porpoise as well as in dolphins, it appears that the occipitothyroid muscle is part of the thyropharyngeus muscle that is connected to the skull base. The **thyropharyngeus** muscle (tp) is the posteriormost muscle connecting the larynx with the skull base and attaches to the dorsal margin of the posterior cornu of the thyroid cartilage.

A strong sphincter muscle, a complex of the **palatopharyngeus** and **pterygopharyngeus** muscles, suspends the epiglottic spout from the bony nares and the skull base and is responsible for the secure intranarial position of the larynx and the reliable separation of the respiratory and digestive tracts (Figs. 10, 65, 67). This sphincter muscle is reminiscent of a strong hose which arises in the bony nares and attaches to the epiglottic spout. In general, each palatopharyngeus muscle originates from the rostral and lateral surface inside the bony nasal passages (Figs. 50, 51, 55a, b), both muscles together forming the "soft palate" and surrounding the ventral part of the epiglottic spout as a loop (Fig. 65). The pterygoid hamulus (PH; cf. Rommel 1990) as a posterior elongation of the bony nasal passage is extended rostralward; it may serve as an additional origin for the palatopharyngeus muscle, which largely displaces the lumen of each bony nasal passage even in dead animals. The pterygopharyngeus muscles originate from the lateral and caudal walls of the choanae as well as from the caudal area of the pterygoids and the rostral parts of the basioccipital and encircle the dorsal part

of the spout. The palatopharyngeus muscle has a high (dorsorostrad) intranarial area of origin and reaches nearly as far as the dorsal bony nares (Fig. 50). In contrast, only the lateral fibers of the pterygopharyngeus muscle originate intranarially to meet fibers of the palatopharyngeus (Fig. 51)

The larynx and hyoid apparatus are covered by the massive gular musculature. The **sphincter colli** (not shown in figures) is the distalmost muscle of the gular region and is situated superficial to the mylohyoideus. It is clearly separated from this underlying muscle posteriorly as these two muscles are here divided by the digastric. The **digastric muscle** (dm) originates from the intramandibular fat pad and the ventral posterior half of the mandible. It attaches to the lateroventral edge of the basihyal and thyrohyal bones (Fig. 65).

The **hyoglossus muscle** (hg; Figs. 8, 10, 65) is a thin, broad muscle which originates from the lateral surface of the rostral third of the thyrohyal bone. Its origin is deep to the digastricus and superficial to the hyoid muscle. This muscle extends rostrally and fuses with the ventral fibers of the genioglossus.

The **mylohyoid muscle** (mh; Figs. 8, 10, 65, 68) is located entirely anterior to the hyoid bones. This muscle originates ventrally from the mandible and stretches medioventrally. The mylohyoideus is less than 0,5 cm thick but broad and both muscles meet ventrally between the mandibles. Caudal fibers attach to the lateral edge of the basihyal.

The **geniohyoid muscle** (gh; Figs. 8, 10, 65) originates as a thin, flat tendon from the anterior horn of the basihyal just ventral to the origin of the hyoglossus. Some fibers originate from the rostral surface of the ceratohyal bone. The fleshy body of this muscle has a wide attachment on the medioventral surface of the mandible,

caudal to the symphysis and along the anterior third of the mandible (Fig. 68). The **genioglossus muscle** (gg; Fig. 68) arises from the posterolateral surface of the tongue and extends along its lateral surface. Some ventral fibers are continuous with those of the geniohyoid muscle and attach to the medial surface of the mandible near the symphysis. The insertion is primarily along the ventral median raphe of the tongue, but further caudally some fibers extend dorsolateralward over the esophagus and are continuous to the palatoglossus muscle. The **palatoglossus muscle** (pg; Fig. 68) surrounds the oropharynx and runs to the bony palate on each side.

As in delphinids (Lawrence and Schevill 1965), the **styloglossus muscle** (sg; Figs. 8, 10, 65, 68) originates from the ventrolateral surface of the stylohyal bone (not from the styloid process). It extends anteriorly and medially as a rather cylindrical muscle until it stretches into the tongue where it fuses with the lateral head of the hyoglossus (Fig. 68). The intrinsic muscles of the tongue are quite complex, as is typical for mammals, but were not dissected in detail in the course of this study. The **stylopharyngeus muscle** (sp; Figs. 65, 68) originates from the medial surface of the stylohyal bone, in its distal (ventral) half and inserts onto the pharynx at the level of the epiglottic spout.

The **sternohyoid muscle** (sm; Figs. 10, 65, 68) is a massive muscle in most cetaceans which is part of an unpaired median muscle complex because right and left portions lie side by side. It originates from the ventral surface of the basihyal and thyrohyal bones and inserts on the rostral margin of the sternum. If the mouth is closed, contraction of this muscle may pull the ventral part of the hyoid apparatus caudalward: This movement is probably the antagonistic movement to that of the hyoglossus, digastric, mylohyoid, and geniohyoid muscles (Fig. 65).

Since the hyoid apparatus is "articulated" to the skull base via the tympanohyal cartilage the resulting movement of the apparatus is reminiscent of a swing.

There are two muscles connecting the dorsal and ventral wings of the hyoid apparatus with each other. The first is the short **ceratohyoid muscle** (ch; Fig. 68; interhyoideus muscle after Lawrence and Schevill 1965) which is very similar to that found in delphinids (Lawrence and Schevill 1965). It connects the stylohyal with the thyrohyal bone. The caudal fibers of the ceratohyoid muscle in the harbor porpoise appear to be distinct and may be homologous to the **stylohyoid muscle** (Reidenberg and Laitman 1994). This muscle spans between the caudal tip of the thyrohyal bone and the tympanohyal cartilage and the adjacent areas of the skull base and the stylohyal respectively. The second "interhyoid" muscle is the small **hyoid muscle** (not shown in figures) which connects the ceratohyal bones near their "articulation" with the basihyal bones.

# 6. DISCUSSION

## 6.1. Functional morphology of the nasal complex in toothed whales

### 6.1.1. Harbor porpoise (*Phocoena phocoena*)

As in other mammals, the primary and main function of the nasal tract in toothed whales (Odontoceti) is respiration. However, only a minor part of the structures seems to be involved in opening and closing of the nasal passage although a water-proof sealing of the respiratory tract is the precondition for the aquatic life style of these mammals. Two muscle strands may open the dorsal part of the nasal tract including the blowhole and the vestibulum. Caudally, the dorsomedialmost fibers of the intermedius and anteroexternus portions of the maxillonasolabialis muscle (Figs. 19, 20) pull the posterior wall of the vestibulum and the posterior lip of the blowhole slightly caudalward. In front, the strong bundle of the anteroexternus and anterointernus muscles pulls the anterior wall of the vestibulum and the anterior lip of the blowhole rostroventralward. Thus, simultaneous actions of both (rostral and caudal) muscle antagonists should open the blowhole and the vestibulum, respectively. The ventral (paired) section of the nasal passage is opened on both sides by the nasal plug muscle which pulls the nasal plug rostralward (Fig. 20). In addition, the intermedius muscle may pull the area of the melon terminus and surrounding connective tissue caudalward. This action should close the vertically orientated nasal tract tightly (Fig. 20). The opening mechanism proposed above is similar to that described by Mead (1975) but, according to the results presented in this study, it seems unlikely that the anteroexternus and posterointernus muscles contribute significantly in closing the passage in the harbor porpoise as suggested for dolphins by this author (Mead 1975). Closing of the nasal passage seems to be mainly passive by the sliding back of the muscles

active during opening and by the tension of the other tissues as fat bodies, air spaces, and connective tissue.

An important additional function of the nasal complex in toothed whales (next to respiration) is sound generation (Cranford et al. 1996, Cranford 2000). Whereas the repertoire of vocalizations seems to be restricted in harbor porpoises (narrow frequence spectrum of clicks, no general use of whistles; Au et al. 1999, Kastelein et al. 1999), their nasal architecture is as complex as in non-physeterid toothed whales (Odontoceti except the genera *Physeter* and *Kogia*) although in a different way. Nevertheless, the MLDB complex has a similar configuration as in dolphins which, in principle, implies comparable functional properties of their components in sound production. Other structures as, e.g., the existence of the spherical porpoise capsules, however, differ significantly between these two families of toothed whales.

The morphological observations presented here reveal that nasal structures potentially involved in sound generation have the same topographical relationships to each other in the harbor porpoise as in delphinids. Therefore, the unified sound generation mechanism for odontocetes as suggested by Cranford et al. (1996) could be substantiated and enlarged by this detailed morphological study of *P. phocoena*. Piston-like movements of the larynx are thought to create positive air pressure in the area of the bony nares. Due to that pressure air quanta are driven dorsalward through the nasal passage and into the vestibular sacs. Thus, on each side between the bony nares and the vestibular sacs, the air stream passes between the monkey lips and causes them to open and then to slap together in a series of events. The blowhole ligament septum (Fig. 2; referred to as "tissue peninsula" in Cranford et al. 1996) acts like a hammer that slaps in a well defined area at the level of the dorsal bursae (monkey lips) against the adjacent rostral

epithelium of the nasal passages. The frequency and amplitude of these events are, among others factors, controlled by the tension of the blowhole ligament and by the maxillonasolabialis muscles, respectively (see below). Each clapping event causes the anterior bursa to vibrate, creating an initial sound wave that is guided via the low density pathway (potential acoustic pathway) and the melon into the water (Cranford et al. 1996). The expanded air in the vestibular sacs should be recycled as shown by Norris et al. (1971 [cited after Norris 1980]) by contraction of the superficial layers of the M. maxillonasolabialis which control the volume of the sacs (see below): Pulling the nasal plugs out of the bony nares and the larynx being returned in its "resting" position by the sternohyoid and thyrohyoid muscles (cf. Figure 65) should guide the air back in the bony nasal passage and the throat.

The bilateral spherical porpoise capsule of connective tissue situated in the nasal complex of the harbor porpoise is not found in dolphins. It was shown here and by Cranford et al. (1996) that this capsule no structural unit, since it is interposed by the nasal passages and air sacs, but, because of its homogeneous density, probably a functional (acoustical) unit (Figs. 2, 13). It may be involved in the formation of the characteristic porpoise clicks since the material of the capsule is rather stiff so that the dorsal bursae, which are embedded in it, have only limited potential to oscillate during sound generation. As one prerequisite for the narrow-band and high-frequency click signals of harbor porpoises, the capsule and the connective tissue theca seem to work as a functional unit due to the topographical relationships to the low density pathway: Sound produced by vibrations of the anterior dorsal bursae is trapped in the low density channel the latter beeing surrounded by tough connective tissue of the capsule and the theca and by air sacs. Thus, the impedance mismatch should be very high between the low-density tissue of the potential acoustic pathway and the surrounding dense connective tissue (Fig. 12). The sound waves are presumable guided into the melon which lies

caudally in the connective tissue theca, which is here reminiscent of a megaphone (Fig. 10; see below; Cranford 1992, Cranford et al. 1996)

Bursae cartilages could not be identified in the nasal complexes of the harbor porpoises examined here. These small cartilages are located exactly caudal to both posterior dorsal bursae in most non-physeterid toothed whales, and Cranford et al. (1996) hypothesized that they may be remnants of the tectum nasi in the odontocete embryo (Klima 1999). The same authors (Cranford et al. 1996) stated that these cartilages possibly serve as stiffening devices for the posterior dorsal bursae. The absence of these cartilages in the harbor porpoise examined here supports their idea since the bursae are embedded in dense connecting tissue and may not need stiffening structures for their function. Nevertheless, the absence of the bursae cartilages in our porpoise material could be explained by differences between individuals or even populations.

In 1964, Norris reported the idea developed by Forrest G. Wood and Paul Asa-Dorian that the melon of dolphins couples the sound from inside the animal's the nasal complex into the surrounding water and that parts of the nasal diverticulae serve as an acoustic reflector to guide the sound to the melon. The structure and topography of the air sacs in the harbor porpoise suggest similar functional properties: the premaxillary, the posterior nasofrontal, and the caudal air sacs may reflect sound in the direction of the melon. Besides, they help insulate the neurocranium and, above all, the ears from sound traveling caudally. In this respect, the "sandwich structure" consisting of the maxillary and frontal bones are thought to constitute an additional "acoustic shield" in this area (Fleischer 1975, 1976, Oelschläger 1990). In contrast, the folded ventral surface of the vestibular sac (Figs. 11, 16), only found in phocoenids (Mead 1975, Curry 1992), does not look like a sound reflector: presumably, sound is muffled at this heavily folded surface

which is reminiscent of a sound absorbing device in sound-proof chambers. This structure (the folded ventral surface of the vestibular sac) may help to avoid sound reflection as a possible source of interferences influencing the porpoise sound beam. The anterior nasofrontal sac in the harbor porpoise is situated directly in front of the anterior bursa as the proposed sound generator and has a larger horizontal extension than in most dolphins. Because of its close topographical relation to the "low density pathway" from both anterior bursae to the melon it is likely that the sac may help to modulate the directionality of the sound beam. But it has to be kept in mind that the anterior nasofrontal sac is close to the proposed near-field of the sound beam (Fig. 12). However, since the near-field structure in the odontocete nasal complex is not known (Cranford 2000) the function of this sac may be hard to interpret without further data.

Premaxillary eminences are typical for *Phocoena* but they can also be found in *Inia* and *Pontoporia*. So this character is not unique for phocoenids as was suggested by Heyning (1989). In *Phocoena*, these bulbous protuberances raise the premaxillary sac dorsalward above the rostrum level and thus approache the proposed structures of sound generation and the low density pathway, respectively. The shape of the smooth dorsal and ventral walls and the position of this sac should influence the emission of the sound beam which makes it a likely candidate for being a sound reflector. Due to its position, the premaxillary sac narrows the potential acoustic pathway dorsoventrally and may, therefore, help to focus the sound beam before it enters the melon. At the same time, the premaxillary sacs may represent facets on which the nasal plugs can slide rostralward to open the nasal passages.

The nasal complex of porpoises and dolphins resembles a three-level system of muscles and connective tissue in which each storey, comprising one of the three

pairs of air sacs (Fig. 13), each of which can be controlled more or less independently by a complex of six muscle layers (1 to 6, Figs. 2, 13, 19, 20). Accordingly, each nasal passage may be controlled on these three levels independently: Three dorsal muscle layers (Fig. 20; 1, 2, and 3, including the anterior fibers of 5) are responsible for air flow at the level of the vestibular sacs and operate the blowhole. The next muscle layer (4) may control air flow at the level of the monkey lips and, probably, air pressure in the caudal sacs and posterior nasofrontal sacs. These muscles should also control the tension of the blowhole ligament and its septum (Fig. 17) and thus air flow through the nasal passages and into the posterior nasofrontal sacs. The deepest layers (5 and 6) regulate air flow into the premaxillary sacs and the nasofrontal sacs (Fig. 17). In addition, the bilaterally symmetrical muscle complexes of the rostrum (5' and 6') presumable modulate the melon's shape by pulling its lateroventral part in a ventral direction (Mead 1975; Fig. 20), i.e. they flatten the melon with respect to the rostrum. Furthermore, the intermedius muscle may pull the dorsal part of the melon caudalward. Strong posterior fibers of the lateral rostral muscle, where it becomes continuous with the muscle bundle of anteroexternus and anterointernus, attach to an aponeurosis rostral to the anterior blowhole lip and should cause the opening of the blowhole (Fig. 20).

Facial structures are innervated by the sensory (maxillary) division of the trigeminal nerve. The diverticulae and the melon do not appear to be heavily innervated (Mead 1975). The motor innervation of the nasal musculature is provided by the facial nerve (Mead 1975, Rauschmann 1992). In general, the highly differentiated nasal musculature should have the capacity of very complex movement patterns. The function of the epicranial complex in toothed whales, to some degree, can be explained by its three-dimensional pattern. However, only the basic principles can be taken into consideration here. Thus, the degree of

complexity is reminiscent of the situation in primates. In these animals, the facial musculature as a multi-component system (innervated by the facial nerve) is thin and widely distributed across the largely hairless skin of the face and able to change its topographical features in many different ways resulting in highly expressive possibilities of visual communication for members of their group. Dolphins live in a comparatively dense medium in permanent locomotion, sometimes at high speeds (Fish 2000). Here the terrestrial (primate) principle of facial expression would be inefficient, particularly because of water resistance (loss of hydrodynamics) and at night or in deep and murky waters where visual controle is inefficient. The facial musculature in odontocetes has been concentrated around the upper respiratory tract which was transformed into the epicranial (nasal) complex together with additional (and maybe phylogenetically new) structures as, e.g., the melon, the dorsal bursae, the blowhole ligament, and the accessory nasal air sacs. Now most of the facialis musculature is united in a flattened cone around the nasal air spaces. As to the amount and distribution of the musculature, the two sides are more or less symmetrical in the porpoise. However, this cone is subdivided on both sides into different muscle layers, the texture of which is more or less the same throughout the different layers. Nearly all of the muscle fiber bundles run from the facial fossa concentrically and ascend dorsalward to the different parts of the nasal passage and its diverticulae. Looking closer, it seems likely that single layers of the nasal muscles or parts of these layers are innervated by individual brunches or fiber bundles of the facial nerve and that these axons belong to specific neuron populations in the facial motor nucleus of the brain stem as is true for the various components of the facial muscles in tetrapods (Papez 1927). This hypothesis has to be tested in future by careful comparative investigations of ungulates and cetaceans. Such a detailed functional organization within the facial musculature and its layers so similar in dolphins and porpoises would allow highly complicated changes in the shape of the air spaces and related

components so that toothed whales would possess fine control of sound production, as evidenced by their proficiency at vocal mimicry (Reiss and McCowan 1993). This is all the more plausible because, in principle, the organization and functional implications of the epicranial complex seem to be valid for all the toothed whales (Cranford et al. 1996). Quantitative analysis of the facial nerve revealed that dolphins have three to nine times more axons in their facial nerve than the human (*Phocoena phocoena*: 4 times more; Jacobs and Jensen 1964, Blinkov and Glezer 1968, Morgane and Jacobs 1972, Pilleri and Gihr 1970, Oelschläger and Oelschläger 2002). Thus, dolphins and porpoises should be able to make "facial expressions" of considerable subtlety not for visual communication but for auditory purposes and facial asymmetry in most odontocetes may even increase their potency of "acoustical facial expression" (Oelschläger and Huggenberger, unpublished).

The musculature of the epicranial complex in toothed whales is derived from the Musculus maxillonasolabialis in mammals (Huber 1934). On the one hand, it can be subdivided topographically and functionally in two major portions: the rostral musculature associated with the melon and the caudal muscles controlling the nasal passages and their diverticulae (Fig. 19). On the other hand, the paired nasal musculature can be divided structurally into two portions on each side (Fig. 19): a medial part consisting of the medial rostral muscle (6') and the p. profundus (6) and a lateral part. The latter group consists of the lateral rostral muscle (5') and the anterointernus (5), posterointernus (4), anteroexternus (3), intermedius (2), and posteroexternus (1; not shown in Fig. 19) portions. As suggested by Mead (1975), it is likely that the continuity of the medial muscles are derivates of the M. maxillonasolabialis p. nasalis. The lateral division should be derivates of the M. maxillonasolabialis p. labialis. This suggestion is in contradiction to Huber (1934) who considered the posterior nasal musculature to be homologous with the p. nasalis and the rostral muscles with the p. lateralis. But the results presented here

do not contribute new findings to the question of the homology of the nasal muscles in comparison to terrestrial mammals. Rodionov and Markov (1992) presented an extensive study of the nasal musculature in the bottlenose dolphin (*Tursiops truncatus*). But their suggestions regarding the homology of nasal muscles in odontocetes cannot be proved here because, first, their muscle description of the bottlenose dolphin cannot be verified by the presented results of the harbor porpoise and, second, their work is based on a Russian examination of mammals that was not available for this study. Nevertheless, closer inspection of the development of toothed whale fetuses could bring light to this problem since the analysis of cranial innervation so far did not provide answers to this question (Mead 1975, Rauschmann 1992).

Norris and Harvey (1974) tested the acoustical properties of the melon's tissue and demonstrated that the melon transmits and focuses acoustic energy into the water. Concomitantly, Au (1993) stated that the melon of harbor porpoises works as an impedance transformer which couples the tissue-borne sound to the surrounding water. The modulation of the sound by the shape of the melon is probably the last step in the formation of the sound beam in the toothed whale head (Norris 1975). But by itself the melon cannot account for the directional beam of toothed whales (Au 1993, Aroyan et al. 2000). The melon oil was found to have a low sound velocity compared with other oils and also a lower velocity than that of the surrounding sea water (Norris and Harvey 1974, Blomberg and Lindholm 1976). Since the topographic relationships and the lipid composition of the melon in the harbor porpoise are similar to those in delphinids (Litchfield and Greenberg 1974, Cranford et al. 1996) it is most likely that this structure has the same acoustic function in both groups. But a striking difference between porpoises and dolphins remains in the structure of the melon terminus and the low density pathway (Cranford et al. 1996) which connects the melon tissue with the anterior

bursae. In general, porpoises have a unilateral terminus of the melon that is not connected via fatty tissues to the anterior bursae (but via a low-density pathway of connective tissue). In dolphins, the terminus of the melon is bilateral (often with a discontinuity on the left side of the animal; Cranford et al. 1996) and it is in direct contact with the anterior bursae. As stated above, in the harbor porpoise the posterior terminus of the melon enters the bilateral capsule mediosagittally and it does not have a fatty connection to the anterior dorsal bursae. But, nevertheless, as suggested by Cranford et al. (1996), a potential acoustic pathway exists probably here since the connective tissue in the area ventral to the anterior nasofrontal sacs is not as dense as the capsule but rather loose (Fig. 12) and the fiber texture is parallel to the potential acoustic pathway supporting an acoustic coupling of the anterior dorsal bursae and the melon (Fig. 12). Tension of the nasal plug muscle may modulate the shape of the potential acoustic pathway but it is not clear whether or how this action would influence the sound field.

Cranford et al. (1996) proposed a regulation mechanism of the sound beam by an interference pattern between sound waves from both left and rigiht monkey lips/dorsal bursae complex (MLDB complex) using controlled timing of the initial sound generation process. However, the assumption of such a mechanism brings up some questions: A pressure cycle within a harbor porpoise click has a duration of approximately 10 $\mu$s only (Au et al. 1999). Due to the pneumatic nature of the proposed sound generation mechanism it is difficult to imagine that harbor porpoises are capable to produce a controlled interference pattern of two clicks generated in the two MLDB complexes within such a small time window.

As stated before, the MLDB complexes are positioned nearly symmetrical in the harbor porpoise. In contrast, dolphins are more asymmetric in this respect which points to a functional asymmetry. Cranford et al. (1996, 2001) presented the

hypothesis that each MLDB complex generates a slightly different frequency range according to its size. Therefore, in the harbor porpoise, the nearly symmetrical nasal complex could explain their narrow-band clicks by the symmetry of both proposed pulse sound generators and of the accassory potential acoustic pathways. From a phylogenetic point of view, the slight asymmetry in the harbor porpoise may point to a plesiomorphic condition. In contrast, however, the nasal connective tissue capsule (porpoise capsule) and the plicae of the vestibular sac are potentially new soft tissue structures only found in Phocoenidae. Therefore, in spite of the fact that the function of the nasal complex is not fully understood, these structural features of the nasal complex in *Phocoena* point to a specialized type of biosonar. In comparison with most dolphin species studied so far, the sonar system of the harbor porpoise should have a higher resolution of its sonar due to higher frequencies used in the clicks which may be an adaptation to coastal habitats.

Some individual differences could be found in the proposed structures of sound generation and emission of the harbor porpoise; e.g., asymmetry was more marked in some animals than in others or the arrangement of the plicae in the vestibular sac differed slightly. With regard to these differences it seems likely that also the harbor porpoise click sounds differ slightly from individual to individual. It seems possible that these sounds include kind of an individual signature component, thus, compensating for the lack of specific communication sounds (whistles of dolphins). On the other hand, anatomical differences exist between some specimens examined here and the descriptions in the literature (e.g., the structure of the deep layers of the nasal muscles or the existence of bursae cartilages; Curry 1992, Cranford et al. 1996). These differences may be explained by potential morphological peculiarities of individuals or on the population level. But it is not likely that these characteristics imply functionally significant differences.

Similar to those of porpoises, the pulses of Commerson's dolphins (*Cephalorhynchus commersonii*) are also known to be polycyclic (Kamminga and Wiersma 1982, Cranford 2000). If our hypothesis is correct that the dense and stiff porpoise capsule is the major component responsible for the production of high frequencies, *C. commersonii* should have a similar device stiffening the sound generation apparatus. Unfortunately, not much is known on the anatomy of this species but there are some similarities in *Phocoena* and *Cephalorhynchus* that set them apart from most delphinids. In both species, the anterior nasofrontal sacs are similar in shape (Amundin and Cranford 1990) and the posterior terminus of the melon is unilateral with respect to the mediosagittal plan (Heyning 1989). Furthermore, the dorsal aspect of the cranium shows the same slight degree of asymmetry (Schenkkan 1973). Nevertheless, there is no report of a structure in *C. commersonii*, which may have similar properties as the porpoise capsule. Also the plicae in the floor (ventral surface) of the vestibular sacs are absent in *Cephalorhynchus* suggesting that the plicae themselves are not responsible for the polycyclic click sounds of the harbor porpoise.

Evidence from high-speed video endoscopy suggests that whistles are produced in the nasal passages of dolphins (Cranford 2000, Cranford et al. 2001). These sounds are likely generated at the nasal plugs (Mead 1975, Ridgway et al. 2001) which are good candidates for this function morphologically since each nasal passage acts as a pipe on this level with a variable narrow opening at the monkey lips. Even if whistles are not part of the normal sound repertoire of harbor porpoises, the general potential to produce sounds other than pulses would explain the deviating vocalizations recorded by Verboom and Kastelein (1995, 1997). So far, however, it is not clear whether whistles are produced by the sweeping of air along the nasal plugs or as a high rate of pulsed sounds as outlined by Killebrew et al. (2001) which may be produced by the monkey lips.

In conclusion, the morphological differences in the nasal complex between delphinids and *Phocoena* may be explained by specializations of the sonar signal generating apparatus responsible for the characteristic polycyclic clicks of the harbor porpoise. To test the recent hypotheses on the production of sonar signals in toothed whales, basic experimental approaches of the physical properties of the tissues involved are needed. Their combination with modern imaging techniques as CT and MRI as well as standard histological procedures may lead to valuable new insights into mechanisms of sound generation and emission in toothed whales.

### 6.1.2. La Plata dolphin (*Pontoporia blainvillei*)

The anatomical and topographical similarities of the proposed sound-generating and -emitting structures in the La Plata dolphin, the harbor porpoise, and delphinids points to the fact that, for production of ultrasonic click sounds, the same general mechanism is used in these groups. In the La Plata dolphin, the fat bodies of the epicranial complex and the potential acoustic pathway (melon terminus) are in the same relative position to each other as in delphinids and porpoises as are the posterior dorsal bursae situated in a septum between the nasal passages and the posterior nasofrontal sacs. This septum may act as a hammer, activated by flowing air, that claps in the well defined area of the monkey lips against the adjacent rostral wall of each nasal passage. As described before, this clapping mechanism could generate the initial sound wave in the anterior dorsal bursae that is guided via the low-density pathway and the melon into the water (Cranford et al. 1996).

A striking difference between *P. blainvillei* and delphinids is the length of the bilateral terminus of the melon. In the La Plata dolphin, the terminus is elongated parallel to the beak-fluke axis but meanders like an old river (Cranford et al.

1996). From each anterior dorsal bursa it projects in the direction of the melon, at first dorsomedialward then it extends rostralward and finally ventralward where merges with the main body of the melon. This pathway, however, is incomplete on the left side where a "gap" filled with loose connective tissue is situated halfway between the bursa and the melon's body. With regard to the function as a potential acoustic pathway in non-physeterid toothed whales, this feature in *Pontoporia* means an enormous elongation of the sound emission structures in relation to the size of the remaining epicranial complex. The absolute size of the nasal complex in the La Plata dolphin is rather small, as are the volume of the melon (Cranford et al. 1996) as well as the neurocranium with the small brain of only about 200 ml (Oelschläger, pers. comm.). Therefore, it is probable that the elongation of the melon terminus helps to focus the sound before it enters the melon. On the other hand, it seems possible that the (right) potential acoustic pathway in *Pontoporia* with its relatively small diameter serves as a low-frequency filter. Unfortunately, not much is known about the frequency composition of the click sounds of *Pontoporia* except for one paper by Busnel et al. (1974) nearly 30 years old.

Cranford et al. (1996) found the size (i.e. the width) of the monkey lips/dorsal bursae (MLDB) complex correlated with the wavelength of the peak frequency in the emitted clicks. According to the small size of the sound-generating apparatus (MLDB), the La Plata dolphin should emit a strong high-frequency component. However, Busnel et al. (1974) recorded only sounds in the low-frequency range (0.3 to 24 kHz). But technical equipment of that time probably did not have the capacity to detect high frequencies. Here, it becomes clear that future acoustic research is needed, particularly because the La Plata dolphin exhibits some morphological peculiarities in its sound production apparatus (see below) and comparative morphology of the acoustic system will lead to new insights into the toothed whale sound generation process, in general. The same is true for some

other species. For example, the acoustic lifestyle of most beaked whale species (ziphiids) is nearly unknown because these animals living in the open ocean are difficult to explore.

Interestingly, the La Plata dolphin does not have rostral portions of the maxillonasolabialis muscle associated with the melon. Considering the function of the melon as an acoustic lens (Norris and Harvey 1974) this fact implies that the sound beam cannot be modulated by actions of these muscle portions connected with the melon. Apart from that, extreme differences in the morphology of some acoustic structures between the left and right side in the La Plata dolphin point to considerable functional specialization. Thus, the organization of the air sacs and fatty acoustic pathways may indicate refined acoustic properties and bilateral specialization. It seems possible that the structures on the right hand side are capable of more extensive focusing of the sonar beam while the structures on the left may produce a wider beam. This two-way system, therefore, could compensate for the potentially limited functional properties of the melon as a sound-conducting medium and focussing device. Furthermore, the nasal musculature should be able to modulate the shape of the fatty (and low-density) pathways which project from the anterior dorsal bursae to the melon. By this the La Plata dolphin may be able to focus the sound beam to some degree. Unfortunately, too little information is available on the acoustic beam configuration in the La Plata dolphin (Busnel et al. 1974, Wartzok and Ketten 1999) to test the hypothesis outlined here.

Harbor porpoises and La Plata dolphins belong to distantly-related systematic groups but both live in coastal areas. They are also known to be opportunistic feeders. Their skulls differ morphologically but are nearly symmetrical. The same is true for the nasal complex except that in *Pontoporia* the right dorsal nasal air sac (vestibular sac) shows "hyperdevelopment" (Schenkkan 1972). Thus, *Pontoporia*

shows clear asymmetry of the superficial storey of the nasal complex, while this region is more symmetrical in *Phocoena.* The nasal morphology in both harbor porpoises and La Plata dolphins is as complex as in delphinids but differs strongly in these two species. It appears that some features of the nasal complex in *Phocoena* and *Pontoporia* correlate with a specialized type of biosonar adapted to different but coastal habitats (Wartzok and Ketten 1999). This could be an interesting example of parallel evolution.

### 6.1.3. Amazon river dolphin (*Inia geoffrensis*)

One of the most interesting observations in the anatomy of the Amazon river dolphin in comparison with the dolphin and porpoise specimens examined is that, so far, dorsal bursae have not been found in this species, neither in this study nor in the few short descriptions found in the literature (Mead 1975, Schenkkan 1977). But it is likely that structures homologous to the dorsal bursae can found if the morphology of the head is studied carefully. The general structure of the epicranial complex of *Inia* is so similar to that in most non-physeterid toothed whales examined so far so that unified sonar beam generation mechanism is likely in toothed whales (Cranford et al. 1996).

Closer inspection of structures potentially emitting the sonar beam (e.g. the melon) would be of great interest since this kind of comparative examination can give insight into the mechanism of sound emission in toothed whales, in general. *Inia* and *Pontoporia* are both different from delphinids with respect to single potential structures of sound emission. But in contrast to the La Plata dolphin, there are some recent data on the sonar beam pattern of the Amazon river dolphin (Kamminga et al. 1993) so that comparison of their vocalization with respect to

nasal morphology could offer important information on the mechanisms involved in both groups. For example, the width of the aperture of the right vestibular sac to the left hand side of the vestibulum and the left vestibular sac, respectively, are unique in the toothed whales examined so far. Moreover, the structure of these sacs strongly supports their function in reflecting the sound as proposed for other dolphin-like species (Cranford et al. 1996, Aroyan et al. 2000).

### 6.1.4. Giant sperm whale (*Physeter macrocephalus*)

This study focuses mainly on the soft parts of the huge facial area of the sperm whale head which is equivalent to an extremely hypertrophied and asymmetric odontocete nasal region. In the huge sperm whale head, the skull is relatively small and only comprises about 12% of the total head mass (of as much as 20 tons; example: adult male of 18 m length, estimated age 27 years and 57 t total body mass; after Behrmann and Klima 1985). The rest of the head (88% of its weight) is represented by mostly soft tissue of the nose and its accessory structures. Thus the skull "is degraded to an insignificant marginal structure" (Klima 1990), which can only incompletely seat this huge epicranial complex serving respiration and phonation.

Sperm whales use so-called click sounds for their active sonar system and for communication. These sounds can be, at least, divided into two types: highly directional clicks and click sounds with low directionality. It has been suggested that the highly directional usual clicks are involved in echolocation (Weilgart and Whitehead 1988, Jaquet et al. 2001) whereas stereotyped patterns of clicks, termed codas, are less directional and may serve communication and social interaction (Watkins and Schevill 1977, Weilgart and Whitehead 1993). A potential

third class of so-called slow clicks are also low-directional and only produced by males (Madsen et al. 2002b). The generation mechanism of these sounds will be discussed later in this chapter. All click sounds (except the slow clicks) of sperm whales typically consist of trains of regularly spaced, decaying pulses (Backus and Schevill 1966, Møhl 2001). According to the theory of Norris and Harvey (1972) the pulse pattern within the clicks is the result of one initial pulse generated by the monkey lips and its multiple reflections between two acoustic mirrors (frontal and distal sacs) and thus repetitive propagation within the spermaceti organ. Therefore, the inter-pulse interval should represent the two-way sound travel time between the mirrors (Cranford 1999, Møhl et al. 2000, Møhl 2001, 2003). In view of the fact that the right nasal passage is associated with the spermaceti organ, it is plausible that this tract is specialized in phonation whereas the left nasal passage mainly serves respiration (Norris and Harvey 1972). Within the huge nose of the sperm whale, the central and dominant structure (geometrically, volumetrically, and functionally) is the spermaceti organ. It is so large that by its size it contributes much to the shape of the sperm whale skull and forehead as a whole.

Pouchet and Beauregard first described the enigmatic museau de singe (monkey lips) in 1885. In the sperm whale, this bipartite valve is believed to be the main source of sound generation (Cranford et al. 1996, Cranford 1999, Ridgway and Carder 2001, Møhl 2001, Møhl et al. 2002). The initial pulse of a sperm whale click is probably produced by a pneumatically-driven clapping mechanism of the monkey lips in which air is transported distalward from the right nasal passage via the monkey lips into the distal sac (Norris and Harvey 1972). After Cranford et al. (1996) the air stream "... passes between the monkey lips, causing them to open and then slap together in a series of events whose repetition rate is regulated by factors such as air pressure and/or muscle tension on vibratory elements".

Vibrations of the monkey lips caused by high pressure injection of air from the right nasal passage into the distal sac via the aperture of the lips are believed to be transferred to the tip of and into the spermaceti organ. The concentric organization of the spermaceti organ, as well as the impedance mismatch (high acoustic resistance) at the boundary of the case may help to channel the acoustic energy of the monkey lip vibrations backward in the direction of the frontal sac. The discontinuity between the acoustic impedance values of the drumhead surface of the spermaceti organ, the adjacting air in the frontal sac and the high bony crest (back) of the skull amphitheater form a multi-layered surface where sound should be reflected. From there, according to the theory of Norris and Harvey (1972) and Møhl (2001), the sound waves are guided into the junk (Fig. 69a). By means of different acoustical properties of the connecting tissue and the fatty lenses in the junk, the sound should be focused, guided to the front of the head and emitted into the water. Any acoustic energy produced by the initial sound generation process at the monkey lips that cannot be reflected from the frontal sac and skull amphitheater surfaces would enter the cranium and therefore be lost for the intended purpose. In addition, it might even interfere with the hearing apparatus by bone conduction (Fleischer 1976, Oelschläger 1990).

From a morphological point of view, the Norris and Harvey (1972) theory (Møhl 2001) is most likely since the topography and the tissue properties support a sound-generation mechanism by the monkey lips and a propagation (acoustic) pathway via the spermaceti organ. Due to the morphological continuity between the spermaceti organ and the junk, sound propagation this way is plausible (Cranford 1999, Møhl 2001, Møhl et al. 2002). On its way through the junk the sound may be focused probably by the lenticular fatty structures (Møhl 2001) since fatty tissue has lower sound propagation velocities than the connective tissue of the junk. The function of these fatty lenses of the junk as acoustic lenses was first outlined by

Kenneth S. Norris in the 1980ies (cf. Cranford 1999). As a whole, the two fat bodies (spermaceti organ and junk) resemble a bent acoustic horn (Møhl 2001) in which the sound is reflected by air filled cavities (distal and frontal sacs). But the reason why the right nasal passage crosses the potential acoustic pathway between the spermaceti organ and the junk is still enigmatic. This issue will be discussed later in this chapter.

The stack of lenticular fat bodies within the junk seems to suggest a sound propagation pathway along the axis of this system. In the anteroventral region of the junk, the density is more or less homogeneous and the fatty connective tissue is confluent with the lenticular bodies of the junk. In this area the junk tapers from the sides in the ventral direction with the superficial fat being located at ventral-most part of the nose just in front of the tip of the rostrum (Figs. 25, 26, 32). This rostroventral "terminal acoustic window" is potentially very important and there are at least two possibilities of sound emission in that area, one in a more or less anterior direction and another in a more ventral direction just in front of the gape. Careful inspection shows that dense connective tissue covers the entire region in front of the museau and spermaceti organ but is completely absent in the region of the anterior and ventral regions of the junk. A potential interpretation of this observation is that the region superficial to the anterior and anteroventral parts of the junk is an excellent candidate for an acoustic window guiding the sound out of the sperm whale's head (Cranford and Oelschläger[3], per. comm.).

[3] Dr. Ted W. Cranford (California State University, San Diego, CA, USA), Prof. Dr. Helmut A. Oelschläger (J. W. Goethe-University, Frankfurt a.M., Germany)

As stated before, the two prominent fat bodies in the sperm whale head (spermaceti organ and junk) together seem to form a bent acoustic horn (Møhl 2001, 2003). The primary axes of both fat bodies, however, are offset from one another. More specifically, reviewing the potential sound path through the fat bodies, the center of the spermaceti organ does not lie in a sagittal plane but is rotated about 30° counterclockwise (seen from in front) against the center of the junk. This is consistent with the fact that the right nasal passage, in its frontal part, is rotated about approximately the same angle out of the horizontal plane. The potential sound path from the spermaceti organ through the conduit to the junk has to swing back from the left hand side of the head throughout the junk to the midline in order to terminate about the ridge along the ventral-most part of the nose which is believed to serve as the terminal acoustic window. Caudal to the spermaceti organ, in the frontal sac, the caudal surface is equipped with a field of densely packed knobs containing serous fluid. Norris and Harvey (1972) saw the function of these knobs in the capture and even distribution a small volumes of air (remaining at depths during diving) in a filigree of air spaces. Thus, the incompressible knobs may help to resist total collapse of the frontal sac under high pressure during deep dives.

The acoustic fats in the spermaceti organ and the junk are significantly different from the the blubber fat chemically. The spermaceti oil consists of a mixture of wax esters and triglycerides (Morris 1973, 1975). The wax esters in the spermaceti organ of the giant sperm whale (as well as those in the melon of *Inia geoffrensis*) are unique among the toothed whales. In contrast to wax ester composition in the melon of delphinoid species, they are dominated in the spermaceti organ by long chain fatty acids and by the virtual absence of isovaleric acids (Lichtfield et al. 1975). The spermaceti oil of adult animals has a transition temperature between the solid and liquid state of 26 to 30° C (Clarke 1978b) which

means that the sperm whale, with a mean body temperature of 36°C, probably carries liquid wax. While wax esters are also found in the melons of delphinid odontocetes, the sperm whale has the largest store of wax in the animal kingdom. Interestingly, the wax esters in both the spermaceti organ and the junk are not evenly distributed but their content differs between the various compartments of the two fat bodies. The highest fraction of up to 88% of wax esters is found in the anterior and central parts of the junk and in the core of the spermaceti organ; the lowest fraction, down to 58%, in the periphery of the same compartments (Morris 1973). Flewellen and Morris (1978) observed an inverse correlation between wax ester content and sound speed and inferred from these findings a reduced sound speed in the core of these compartments due to the high wax ester fractions. Although sound speed increases with temperature and pressure, there is no sudden change in sound velocity during the phase change of the spermaceti oil from liquid to solid and vice versa (Goold et al. 1996). According to Ahlborn[4] (pers. comm.), it seems possible that a phase change from fluid to solid is induced by the high pressure circle of a sound wave. In turn, the reverse phase change could increase the amplitude of the wave while it travels through the spermaceti organ and may, thus, lead to an amplification of the sperm whale click sounds.

The lipids of the melon in delphinids reportedly are toxic to the animal (Morris 1986) and the same could be true fur the spermaceti organ of *Physeter*. Old and starved sperm whale specimens retain the size and volume of the spermaceti compartments, implying that the wax esters are metabolically inaccessible. Thus, the fat bodies in the nasal complex of sperm whales does not serve as an energy store that can be metabolized when needed (Madsen 2002). These facts indicate the functionally derived character of the "acoustics fats" in odontocetes as well as the importance of these structures for the aquatic life style.

[4] Prof. Dr. Boye K. Ahlborn (University of British Columbia, Vancouver, B.C., Canada)

One of the most interesting characters in the sperm whale forehead is the asymmetry of the two nasal passages. The considerable difference in the size of the two external bony nasal openings of the sperm whale can be correlated with their presumed function: Whereas the left (large) naris is part of the left nasal passage running directly to the blowhole and being responsible for efficient respiration during surfacing, the right naris leads to the monkey lips via the right nasal passage and is responsible for phonation (Norris and Harvey 1972, Møhl 2001). The fact that the right bony naris is only about one third of the left naris in diameter (which correlates with the anterior opening of the right nasal passage into the blowhole) contrasts with the diameter of the (collapsed) soft right nasal passage. Thus, whereas the left nasal passage has to transfer large quantities of air very quickly during respiration at the sea surface, the right passage could deal with relatively small quantities of air during phonation at the surface and during diving, when the water pressure may shrink air spaces to tiny volumes.

As a whole, the forehead (epicranial complex) of the sperm whale is so huge that it is suspended by the skull only incompletely. It appears that the bridle out of connective tissue stabilizes the nasal complex in keeping its shape and suspending it from the skull (Cranford[5], pers. comm.). Nevertheless, the bridle is somewhat asymmetric in that one branch on the left side in front extends as far as the blowhole. With this attachment, the bridle might help to open the blowhole in breathing via the contraction of the longitudinal facial muscles. At its rear end the bridle attaches on both sides to the area of the zygomatic arch which is rather thick and strong in the sperm whale in relation to skull size. In contrast, the zygomatic arch of dolphins may have evolved its thin profile in order to guarantee the continuity of the fatty acoustic pathway in the lower jaw in the direction of the ear complex (Van Beneden and Gervais 1880, Norris 1968) and to reduce bone

[5] Dr. Ted W. Cranford (California State University, San Diego, CA, USA)

conduction (Fleischer 1976, Oelschläger 1990). Inspection of the CT scans of the neonate sperm whales shows that the extramandibular and intramandibular fat bodies (including the intermediate acoustic window within the "pan bone" of the mandible) lie well below the level of the zygomatic arch. The dissection of "Odie" (Table 1) revealed that here the masseter muscle is still fleshy (light red) and obviously not interspersed with fat, i.e. this muscle is still active and needs a stable origin. In the giant sperm whale, the distortional forces on the long and heavily loaded visceral cranium (rostrum) require a strong bilateral bracing between the viscero- and the neurocranium by means of zygomatic arches which consist of bony elements relatively thick for odontocetes, including a stout zygomatic (malar) bone. The heavy postorbital process of frontal opposes the thick squamosal process of the temporal bone (secondary zygomatic arch; Oelschläger 1990), both components being united via intercalated dense connective tissue that stabilizes the secondary zygomatic arch but presumably has a high impedance mismatch for sound (Oelschläger[6], pers. comm.).

The huge size and the organization of the sperm whale nose seems to reflect the necessity to produce and to transmit high intensity sound for orientation, communication, and hunting. The size of the nasal apparatus is so large and the signals are so intense that the sperm whale has been suspected of using its sound machine to debilitate or immobilize its prey (Norris and Møhl 1983). In the stomachs of harpooned deep-diving sperm whales whalers often found living prey items. This suggests that the prey may have only been stunned temporarily. This stunning hypothesis is astonishingly complementary to the suction feeding hypothesis: Odontocetes do not chew their prey, they swallow it whole by strong negative pressure created in the pharyngeal space (Reidenberg and Laitman 1994).

[6] Prof. Dr. Helmut A. Oelschläger (J. W. Goethe-University, Frankfurt a.M., Germany)

It seems plausible that it would be very difficult for sperm whales to swallow a large squid struggling to survive.

Recently, Madsen et al. (2002a) studied sperm whale sounds with a recording system in a fixed position relative to the whale's body using a hydrophone and depth recording system attached with a suction cup to the back of the animal. They recorded differences in waveforms between the proposed coda clicks and the usual (echolocation) clicks. The sound level of the coda clicks recorded was significantly lower than that of usual clicks. A distinct difference between these two click types can also be seen in the decay rate between the successive pulses within one click. In usual clicks the decay rate is significantly higher so that the initial pulse is followed by one or a few echoes only. Most of the energy of these clicks is put into the (first) single pulse ($p_0$) and the following individual pulses in the usual clicks are approximately 1/3 shorter in duration. Interestingly, no depth-dependent spectrum difference has been recorded in the two click types by Madsen et al. (2002a) as was shown in some other papers where recordings could perhaps be more prone to artifacts like surface reflections (Papastravrou et al. 1989, Thode et al. 2002). Furthermore, the coda clicks of sperm whales express less directionality than the echolocation clicks making the former better suited for communication (Madsen et al. 2002a).

Sperm whales are capable of diving to enormous depths in pursuit of their prey, which has profound effects on the volume of air available for sound production. Today it is still enigmatic how sperm whales can produce click sounds by means of a pneumatically driven mechanism with rapidly shrinking volumes of air during dives down to more than 1000 meters (Papastravrou et al. 1989, Wahlberg 2002). In dolphins, air in the nasal complex is probably pressurized by piston-like movements of the larynx in order to drive click production (Cranford et al. 1996). But it has to

be kept in mind that in a diving 15 meter sperm whale with a lung capacity of approximately 750 liters at surface level (Clarke 1978a) only a residual volume of about 7.5 liters is left at 1000 meters depth for the production of sonar signals. It is plausible that the animals transfer at least some air (if not all) from the lung into the nasal system during dives. But it is not likely that sperm whales can drive the whole right nasal passage (which has approximately the same length as the head) including the right bony naris and the laryngeal area with such small volumina. Thus, it is plausible from an anatomical point of view, that the pressure to generate the pulsed sounds may be produced only by structures associated with the right nasal passage where the monkey lips are located. Controlled retraction of the oblique lateral maxillonasolabialis muscle may build up pressure in the spermaceti organ and thus compress the air in the right nasal passage causing its mid and rear portion to collapse ("pressure pump"; Fig. 69a). This mechanism may be similar to the idea mentioned by Norris and Møhl (1983) but these authors did not describe the alleged mechanism in detail. Concomitantly, residual air could be squeezed in the direction of the monkey lips where the pulsed sounds are generated. Fine tuning of the air flow to generate the click sounds may be controlled by the nasal passage muscle. Therefore, it seems likely that the right nasal passage serves as an air-collecting system forcing small quanta of air in the direction of the monkey lips (Fig. 69). This process can be figured as the squeezing of toothpaste out of a tube (from the rear to the front; Huggenberger and Oelschläger, unpublished). A similar mechanism seems likely for non-physeterid toothed whales where air pressure produced by movements of the larynx should drive the initial sound generation process: Here, the air stream at the monkey lips/dorsal bursae complex may be tuned by movements of the nasal plug muscles. This mechanism could even allow an independent control of air in each nasal passage when the bony nares are closed by the palatopharyngeus muscle complex (see chapter "*The role of the larynx...*"). In a collapsing right nasal passage of sperm

whales the residual air may be transported distalward along two lateral canaliculi in the right nasal passage. According to our morphological examinations, these small channels should contain the residual air volume of the pressurized tract, guiding the air to the monkey lips by the action of the "pressure pump" mentioned above. As a result, even small amounts of pressurized air, collected and conducted in the left and right residual canals of the collapsed right nasal passage can stream at high velocity through the museau, distributed evenly by a system of branching thin, capillary-like airways which join each other at the aperture of the museau. Here the opposed soft and unpigmented areas in the epithelial lining on the corresponding lips cooperate in sound production. The fluid-filled knobs in the posterior wall of the frontal sac have to withstand such a pressure exerted on the spermaceti organ in an axial direction and are believed to maintain a "reticular" system of air spaces representing a posterior acoustic mirror. Whenever the longitudinal muscles contract to shift air in the right nasal passage in the direction of the monkey lips, the air in the frontal sac should be pressurized simultaneously (Fig. 69). The bubbles in the frontal sac may prevent the total collapse of this air sac during these pressurizing events and thus maintain the caudal acoustic mirror.

After a sound generation cycle the air may be recycled directly from the distal sac through backward suction via the monkey lips into the right nasal passage by the contraction of muscles associated with the right nasal passage. Tension of the dorsal portion of the maxillonasolabialis muscle should open the monkey lips while contractions of the right nasal passage muscle should increase the volume of the nasal tract. The potential for a circular pattern of air movement in the nose of a sperm whale (Norris and Harvey 1972) is theoretically possible since the left and right nasal passages are interconnected via the vestibulum (of blowhole) and the distal sac rostrally and via the inner nasal openings (choanae) caudally. Thus a continuous air flow in one direction would pass the right nasal passage through the

monkey lips in the distal sac, then via the vestibulum, the left nasal passage, and the laryngeal space back into the right nasal passage. This possibility seems intriguing but fit only the situation in a non-diving whale since the hydrostatic pressure during diving may compress the resident air volume to such a degree that an air recycling from the distal sac through the monkey lips into the right nasal passage is more likely. This recycling pattern, which is reciprocal to the air movement during sound generation, is seen also in dolphins (Norris et al. 1971 [cited after Norris 1980]). During dives there has to be a change in the function of the nasal passages because the pressure increases so dramatically that at greatest depths, only isolated acoustic mirrors may remain in the distal and frontal sacs as well as in the frontal part of the right nasal passage.

As stated before, the pulsed sounds of sperm whale clicks may be produced by a clapping mechanism of the monkey lips (Cranford et al. 1996). The inner surface of the lips exhibits some anatomical features that support this hypothesis. The small plicae of the monkey lips cause a distal air stream to spread over the inner surface of the lips. On the two opposing lips these plicae turn in opposite directions. This implies that the plicae of the upper lip are fed by air from the left margin of the right nasal passage and those of the lower lip are fed from the right margin of the right nasal passage. As a result, air can stream evenly over the total inner surface of the lips and, therefore, the lips can clap together over their entire inner surface. This action should produce an even and broad (sound) wave in the surrounding tissue. Such a sound wave with an even wave front may be the main prerequisite for the emission of loud and focused pulses that serve echolocation.

According to the theory of Norris and Harvey (1972) the higher number of successive pulses in the coda clicks of sperm whales point to a higher number of reflections within the spermaceti organ between the acoustic mirrors (i.e., distal

and frontal sacs; Møhl 2001). Therefore, it is likely that the higher numbers of pulses in the coda clicks are generated by changing the shape of sound mirrors in comparison with the emission mechanism of the usual clicks. Accordingly, Madsen et al. (2002a) proposed that a change in the conformation of the sound emission structures may create the differences in these two click types. From an anatomical point of view it is feasible that the right nasal passage may serve as an additional acoustic structure. This flat passage is situated rostroventral to the spermaceti organ and crosses the potential sound path between the latter and the junk. It is interesting to note that the two huge fat bodies are more or less in contact with one another in the area of a "window" in the case through which sound could be transmitted from one fat body into the other (Fig. 27, not labeled). In this "acoustic window" within the nose, only the right nasal passage and its fatty muscle are interposed between the two fat bodies. A small volume of air (air film) in this part of the right passage may reflect and, therefore, "trap" most of the energy of a sound wave in the spermaceti organ because of the impedance mismatch between air and tissue and thus produce the multiple cycles of pulses. In this situation, only part of the sound energy would be transmitted via the junk into the water (Fig. 69b). In contrast, a collapsed right nasal tract may let pass most of the sound energy into the junk. In this case, additional echoes produced within the spermaceti organ would be less energetic. This mechanism could generate the usual clicks where most of the energy is put into the $p_0$ pulse (Fig. 69a).

The pulling force of the maxillonasolabialis muscle was estimated for 100 kN in adult males (Norris and Møhl 1983) and the contraction of this muscle system may build up considerable tension within the spermaceti organ. The amphitheater of the skull (i.e. its facial fossa) serves as an abutment for both the spermaceti organ and the muscles. The maxillonasolabialis muscle insert upon the bridle and can pull the dorsal part of the the facial complex caudalward to build up pressure in the right

nasal passage (Fig. 69a). If a relatively small air volume is present in the right nasal passage, this action is believed to cause a collapse of the mid and rear portion of the tract, i.e. in the area of the large foramen within the case between the spermaceti organ and the junk. This is a scenario involving a sound emission mechanism similar to that described above and used for the production of usual clicks at depth. If a larger volume of air is trapped in the right passage, the movement of the spermaceti organ by muscle force would create air pressure without a collapse of the tract as proposed for the production of coda clicks. This hypothesis implies that a relatively larger air volume would be needed to produce coda clicks and it is supported by the fact that coda clicks were only recorded in depth down to 250 m where more than 4% of the initial air volume is still present (Madsen et al. 2002a). Larger air volumes can be controlled by piston-like movements of the larynx in its surrounding musculature in order to switch between the two types of click emission. We are not able at the moment to decide whether the differences in directionality of the two click types (directional usual clicks and less directional coda clicks) is a result of (controlled) changes in the configuration of the elevant air spaces. But this scenario seems possible. This model proposed can explain why coda clicks have a higher number of successive pulses with higher amplitude but does not clarify why coda clicks are less directional than usual clicks. The form of the distal and frontal sacs manipulated by the variation of their air volume, however, may play an important role in focusing click sounds. In contrast, the broad distal (anteroventral) part of the junk which protrudes beyond the tip of the bony rostrum may not be affected by the movements of the spermaceti organ and the right nasal passage, respectively, and thus keep its shape and functional properties as a terminal acoustic window.

As stated before, the frontal sac could serve as an acoustic mirror with a minimum of air (Norris and Harvey 1972). The fact that the mean diameter of the knobs in

the frontal sac is shorter than the wavelength of the peak frequency of adult sperm whale sounds may be correlated with the acoustic function of the sac. The described knobs were found in the adult animals but not in the smallest of the neonate sperm whales ("Odie"). In this young neonate animal caudal epithelium of the the frontal sac has a rough surface which may reflect an early developmental stage of the "mirror" in this animal. This fact points out that the knobs are adaptations to deep-diving since young sperm whales do not dive as deep as adults (Papastavrou et al. 1989) but stay at the surface while their mothers hunt at great depths and are "baby-sitted" by other adult females (Madsen et al. 2003).

In conclusion, from a morphological point of view it is likely that the hypertrophied epicranial complex of sperm whales may have evolved to maximize directionality and source levels of echolocation clicks. Their 15 kHz pulses with low absorption and sufficient resolution seem to be ideal for long-range biosonar detection of (larger) cephalopod prey with low target strength resulting in a low echo (Madsen et al 2002b). The size and shape of the fat bodies and their air sac system in the nasal complex are good candidates for this proposed specialized function. The adaptation to long-range echolocation may have been the main factor in sperm whale evolution that led to this unique and big sound "cannon". In contrast to the mechanism described for dolphins (Cranford et al. 1996), sperm whales may drive the initial pulse generation process with air pressurized by structures associated with the right nasal passage. This can be seen as an adaptation to deep-diving when shrinking air volume may restrict sonar sound production. Moreover, the right nasal passage may control the transmission of sound signals from the spermaceti organ into the junk (and thus the signals which are emitted into the environment) by manipulating the volume and position of air within the tract. In this theoretical scenario the right nasal passage serves as an "acoustic valve" to switch between to modes of click production: one mode for coda click production and a second for the

generation of echolocation clicks. So, the same structural complex in the sperm whale nose (monkey lips, spermaceti organ, right nasal passage, and junk) serves both communication and echolocation. It seems that the central position and the sub-horizontal orientation of the right nasal passage within the sperm whale head (as an interface between the two gigantic fat bodies) is related to the mechanism of sound production with changing volumes of air.

From the fossil record it appears that the facial skull of cetacean ancestors was bilaterally symmetrical (Fordyce and Muizon 2001). The Archaeoceti, fully adapted to aquatic life, had subterminal bony nostrils. In these animals, they had already started to migrate caudalward, leading to more efficient surfacing for respiration between dives. Their skull roof was still symmetrical, as is the case in all fossil and extant baleen whales. The first odontocetes of the Oligocene with their posterior position of the bony nostrils and a facial depression indicative of a melon and thus the ability to echolocate started to shift the bony nares slightly to the left by means of a stronger broadening of right skull roof elements (and to twist the area clockwise as seen from above; Fordyce and Muizon 2001). This asymmetry of the skull roof, typical for toothed whales, obviously brought the right bony naris and its monkey lips in an axial position, a fact which could be related in all non-sperm whale odontocetes with mediosagittal sound and ultrasound emission through the melon. In sperm whales, this primary asymmetry was even increased by the expansive development of the spermaceti organ out of the right posterior dorsal bursa and the shift of this fat body to the left into a near-sagittal position. But here, again, the axis of the potential sound path is orientated sagittally running through the rostroventral part of the junk.

Whereas in dolphins both pairs of monkey lips seem to be active in sound production (Cranford 2000), there is a beginning segregation as to their functional

properties since right and left sound generators (MLDB-complexes) may produce slightly different peak frequencies (Cranford et al. 1996, Cranford 2000, Cranford et al. 2001). In sperm whales, only the right pair of monkey lips has been retained whereas the left pair has vanished. This interpretation that the sperm whale exhibits an extreme in the functional segregation of the two nasal tracts seen in other toothed whales helps to understand why asymmetry in most odontocetes is restricted to the epicranial complex and to the skull roof. Other parts of the skull do not exhibit such a degree of asymmetry which is obvious if we turn around a dolphin skull to see the ventral aspect. In the most asymmetric skulls of odontocetes (dwarf and pigmy sperm whales, *Kogia sima* and *K. breviceps*), asymmetry in the ventral aspect of their skulls is restricted to the shape and size of the choanae and bony nasal tubes as well as the vomer area.

The biological significance of the spermaceti organ as an acoustic structure was probably so important that it became tremendously hypertrophied during the evolution of the sperm whale tribe. As a result, the blowhole region was shifted to the tip of the nose (secondary terminal position of the single nasal opening), thus increasing the travel time of the sound pulses between the two proposed acoustic mirrors (distal and frontal sacs). The soft parts of the upper respiratory tract which are rather short comparatively in other toothed whales and orientated in a vertical position, became much elongated dorsorostrally in the sperm whale: thus they run in a paraxial direction from the bony nostrils at the caudal base of the amphitheater to the blowhole region. By this transformation, the organization of the sperm whale nose became extremely asymmetric, so that the right hand side of the epicranial complex, with the spermaceti organ extending far to the left in the posterior half of nasal region, leaves the anatomically left part of the nose as a regressive wedge-like region. The asymmetry of the upper airways results in the situation that the caudal part of the right nasal passage runs between the two

huge fat bodies (spermaceti organ/junk) in a more or less axial (but sub-horizontal) orientation. In contrast, the course of the left nasal passage is rather superficial below the left dorsolateral surface of the head. This superficial course and the lack of any accessory structures imply that the left nasal passage is used in respiration only.

In contrast to other cetaceans, sperm whales have two large nasal cartilaginous structures, i.e. the rostral cartilage (cartilaginous rostrum) which is part of the rostrum in all adult cetaceans and the nasal roof cartilage which is typical for the sperm whale and extends diagonally through their nasal complex (Behrmann and Klima 1985, Klima 1999).

It is interesting to note that, whereas the rostral cartilage consists of hyaline cartilage, the nasal roof cartilage running along the left nasal passage is an intermediate between hyaline and elastic cartilage (Klima et al. 1986). In view of its delicateness, the upper cartilage cannot support the nasal complex as a whole but seems to serve the operation of the left nasal passage. Its equipment with fibroelastic material may indicate repetitive deformation of the nasal passage and cartilage via the nasal passage muscle during inhalation and exhalation.

Ontogenetically, the rostral cartilage goes back to the lower edge of the embryonic nasal septum and is seen in all cetaceans examined so far (Klima 1999). During embryonic and early fetal stages this cartilage is the driving force in the development of the cetacean rostrum or upper jaw (Klima 1987, Klima et al. 1986), followed at some distance by the much slower growth and elongation of the desmal premaxillary, maxillary, and vomer bones. In contrast, the blade-like upper cartilage of sperm whales is unique and equivalent to the nasal roof (tectum nasi) of embryonic and fetal stages (Behrmann and Klima 1985, Klima 1999). As a

secondary structure (secondary elongation), this cartilage seems to have its maximum in rostral outgrowth later than the rostral cartilage. In its mature situation, the cartilage is extremely modified and unparalleled throughout the animal kingdom. This nasal roof cartilage was discovered and interpreted by Klima (1990); therefore and because of the heuristic value of this structure for the understanding of the sperm whale nose it is referred to as "**Klima's cartilage**" (Oelschläger and Cranford, pers. comm.).

In previous studies on embryos and early fetuses of sperm whales specific cartilaginous structures were found during morphogenesis of the nasal complex which are unique among cetaceans (Klima et al. 1986). These cartilages are part of the embryonic nasal septum and consist mainly of material of the former tectum nasi but also contain of material of the embryonic left and right cupula nasi anterior. This cartilaginous structure of sperm whales was termed "nasal roof cartilage" (Klima 1999).

The embryonic septum nasi of the cetaceans forms a massive wall in the median plane dividing the nasal capsule into bilaterally symmetrical halves. The septum consists of a vertical cartilaginous plate, triangular in shape and orientated in the mid-sagittal plane. Its lower anterior tip projects in a long cartilaginous rostrum, typical for all cetaceans. In the sperm whale, the dorsal edge of the embryonic septum releases a branch of the tectum nasi and forms the nasal roof cartilage (Fig. 42). The outgrowth of this prominent structure extending diagonally through the forehead seems to be responsible for the organization of the soft nasal complex and, therefore, the typical sperm whale head contour (Klima et al. 1986, Klima 1999). The appearance of this structure in larger fetal stages led to the assumption that, at least, the rudimentary nasal roof cartilage may be present in adult sperm whales as well. This assumption was indeed confirmed by the

anatomical dissection of a 18 m male sperm whale (Figs. 41, 42) that stranded near Bremerhaven (Germany) in 1984 (Behrmann and Klima 1985). Comparison of the histological pattern of the nasal roof cartilage in fetal and adult specimens, however, showed some substantial differences (Klima 1990). In the fetuses examined, this structure consists of embryonic hyaline cartilage which is fast-growing and thus well-suited for morphogenetic processes. In the adult sperm whale, however, the hyaline cartilage has been transformed into a special kind of elastic cartilage.

There is an immense disproportion of the cartilaginous rostrum and the nasal roof cartilage in the neonate sperm whale examined in this study. Although both are similar in length, they differ significantly in mass. Whereas the nasal roof cartilage is thin and blade-like, the cartilaginous rostrum is conical so that the volume of the nasal roof cartilage is approximately only 1 % that of the rostrum cartilage. In contrast, in embryos and early fetuses, the volume of these two cartilages is nearly identical. In fetuses of 10 to 90 cm total length, the nasal roof cartilage is as massive as the cartilaginous rostrum (Klima et al. 1986). The relative size of these fetal cartilages may reflect their important role during the developmental arrangement and fast growth of the sperm whale forehead.

After birth these nasal cartilages lose their developmental significance: The nasal roof cartilage seems to be "degenerated" to a supporting structure of the left nasal passage. Its mass is reduced in relation to tissues of the huge epicranial complex while the relative mass of the cartilaginous rostrum is more or less constant throughout the whole developmental process. This fact may be explained by the role of the cartilaginous rostrum as one of the main components of the elongated upper jaw but the functional reason why it does not ossify during

development and persists as such a prominent cartilaginous structure is still unknown.

The nasal septum delineates the mid-plane of the nasal skull in mammals. The nasal roof cartilage of postnatal sperm whales, however, the former embryonic septum and tectum nasi, is shifted to the left hand side in the nasal complex. Therefore, this structure indicates the extreme asymmetry of the sperm whale facial area which is caused by the hypertrophy of structures on the right hand side, particularly the spermaceti organ. The shape and position of the nasal roof cartilage in ontogenetic stages may therefore represent important steps in sperm whale evolution such as the occurrence of hypertrophy in nasal structures of the right hand side as well as the concordant forward projection of the blowhole region (Klima 1999) leading to a functional specialization of each nasal passage. The left nasal passage may serve mainly respiration and the right passage sound generation (Norris and Harvey 1972).

In general, the supportive tissue in aquatic mammals seems to be adapted to their aquatic lifestyle. This was shown for the specific construction of cetacean bones with respect to bony tissues in terrestrial mammals (Felts and Spurrel 1965, Felts 1966, Madar 1998, Klima 1999). But the function of the cartilaginous rostrum is still unknown. The high content of water, the proposed pressure resistance, and the "elasticity" of cartilaginous tissue seems to be advantageous for an aquatic lifestyle but it is not clear how these mechanical properties can be relevant for the cartilaginous rostrum which is embedded into dense and stable skull bones. An acoustic function of the cartilaginous rostrum as outlined by Pilleri and coworkers (Pilleri et al. 1983, Purves and Pilleri 1983, Pilleri 1990) is unlikely because of the poor acoustic coupling between the proposed (click) sound generator (monkey lips)

and the rostrum (Norris 1968, Cranford et al. 1996, Cranford 1999, Cranford 2000, Madsen et al. 2003).

The cartilaginous rostrum of the neonate sperm whale examined here consists of mature hyaline cartilage. There are no characteristics of embryological hyaline cartilage except the relatively high blood supply. In this context, vascularization may not be interpreted as a prenatal feature but as an allometrical phenomenon of the mature cartilaginous rostrum since such a massive structure cannot be supplied per diffusion from the superficial perichondrium only. An internal blood supply seems necessary as is typical for large cartilaginous structures (Wilsman and Van Sickle 1972).

Cartilaginous tissue can adapt to different mechanical stimuli by developing into different types of cartilage. Pressure stress favors the development of hyaline cartilage, tension fiber cartilage, and shearing stress induces elastic cartilage (Roux 1895, Benninghoff 1925, Kummer 1959, 1985). In the the nasal roof cartilage of the adult sperm whale, the arrangement of the chondrocytes, their territories as well as the amount of extra-cellular substance correspond to those in hyaline cartilaginous tissue. The occurrence and arrangement of elastic fibers, however, correspond to elastic cartilaginous tissue. According to these findings, pressure and deformation should be the main source of stress for the persistence of the nasal roof cartilage (Klima 1990, 1999).

The nasal roof cartilage does not serve (stabilize) the components of the sperm whale forehead in the sense of a true skull strut. This is plausible because of the proportions in the huge sperm whale head (Klima 1990, 1999). The bony tissue is only ca. 12 % of the total head mass (Clarke 1978a, b, 1979). The remaining 88 % soft tissue may weigh 20 t and attain up to one third of the total body mass. After

loosing its important function in the nasal formation during early prenatal development (Klima 1999), the nasal roof cartilage seems to be reduced in postnatal animals but supports the left nasal passage life-long throughout its entire length. Since the left nasal tract probably serves mainly respiration (the right nasal passage may serve sound production; Norris and Harvey 1972, Cranford 1999) it is likely that the close association of the nasal roof cartilage and the left nasal passage benefit the function of rapid air exchange during respiration. The left nasal passage is embedded in the soft tissue of the nasal complex. Therefore, it is likely that the nasal roof cartilage may stabilize the passage during respiration (Klima 1990, 1999). The left nasal passage muscle which inserts onto the lateroventral wall of the left nasal passage opens it while the medial wall of the passage with the cartilage remains in place. This cartilage may prevent the nasal passage from collapsing during the high negative pressure event of inhalation. During this event the cartilage would undergo deformation stress mainly.

The nasal roof cartilage seems to serve the attachment of a muscle which originates at the perichondrium in regularly arranged fiber strands (Klima 1990). The nasal complex of sperm whales is covered dorsolaterally by the very strong maxillonasolabialis muscle that stretches from the dorsal crest of the frontal bone anteriorward (Norris and Harvey 1972). Tension of this muscle, that may pull the monkey lip area caudally, would be another source of stress of the nasal roof cartilage which could explain both hyaline and elastic components. However, the interpretation that the elastic component of this cartilage may be an adaptation to high pressure during dives as outlined by Klima (1990) seems unlikely since hydrostatic pressure would not deform the soft tissues of the sperm whale nose since the air tract system would be collapsed in depth.

The nasal roof cartilage in fetuses of up to 90 cm total length consists of hyaline cartilage without elastic fibers and in adult sperm whales of a peculiar type of elastic cartilage (Klima 1990). In the neonate sperm whale of 3.41 m total length examined in this study, the structure of the nasal roof cartilage is similar to that found in the adult which points to similar functional properties in neonate and adult animals. Therefore, also the implications of the nasal roof cartilage in the neonate sperm whale should be similar to that of adults. But the histological analysis revealed some differences between these two stages. First, the perichondrium of the nasal roof cartilage is thicker in the neonate than in the adult indicating that the growth process is completed in the adult and that cartilage may be replaced only by regeneration. Second, there are differences in the concentration, structure, and arrangement of the elastic fibers within the matrix. The neonate sperm whale has more elastic fibers in the nasal roof cartilage than the adult. This is probably caused by a change in the activity of the mature perichondrium that seems to reduce the proliferation of elastic fibers. The straight or slightly-undulating course of the elastic fibers as well as their parallel arrangement near the center of the cartilage in the neonate sperm whale could be caused by the lack of mechanical stress in the immature tissue. The postnatal use of the cartilaginous tissue in respiration may then lead to the adult-like arrangement of the fibers in the nasal roof cartilage where the elastic fibers become wound and orientated in different directions according to their topography and proposed function.

The two cartilaginous structures in the forehead of the adult sperm whale have both important implications to reconstruct the evolution and development of their nose. The mesorostral cartilage was described as an ontogenetic "pacemaker" in the formation of the cetacean upper jaw (rostrum), in general because, as a central structure, it seems to drive the elongation of the upper jaw anteriorward by the strong cartilaginous tissue proliferation and thus longitudinal growth (Fig. 42; Klima

1990). At least as important intellectually is Klima's cartilage (tectum nasi) because it can shed light on the evolution of the cetacean rostrum. In the terrestrial ancestors of the cetaceans, which are suspected among fossil mammals near the origin of the even-toed hoofed animals (Artiodactyla; Gingerich et al. 2001, Thewissen et al. 2001), as well as in the first cetaceans obviously fully adapted to aquatic life (Archaeoceti), the nostrils were still in a more or less terminal position. In contrast, advanced cetaceans shifted these nasal openings backward along the mid-line of the upper jaw to a position just before the brain case. This shift was part of a total reorganization of the nasal region accompanied by the elongation of the upper jaw bones and their "backward-sliding" past the bony nostrils and over the bony elements of the forehead (telescoping, Miller 1923), and the nasal canals were rotated about 90° upward and backward so that in all extant non-physeterid toothed whales they stand perpendicular to the skull base (Klima 1987). In odontocetes, the reorganization of the nose led to the reduction of the peripheral olfactory system (Oelschläger and Buhl 1985, Oelschläger and Oelschläger 2002) and left over respiratory tubes which secondarily equipped with accessory air sacs used for the generation and emission of sonar signals for orientation and communication. However, whereas in most extant odontocetes, the blowhole and the bony nostrils are situated immediately before the brain case of the skull, the sperm whale shows a highly derived situation. In the course of the development of the spermaceti organ as a huge "new" acoustic fat body out of the small right posterior dorsal bursa (Cranford et al. 1996), the blowhole with the phonetic apparatus (monkey lips) was shifted anteriorward. By that, the nasal passages interconnecting between the blowhole and the bony nostrils were strongly elongated. Taking into account all this, the course of Klima's cartilage throughout the epicranial complex may stand for the evolutionary shift of the blowhole with the phonetic apparatus in a terminal position, i.e. its course can be seen as a trajectory during this process which, in principle, is repeated during the fetal

period of sperm whale development. In this respect, the similarities of the nasal cartilages of prenatal sperm whales and baleen whales may be interpreted as symplesiomorphies.

The impressive sexual dimorphism of the nasal complex in giant sperm whales (Nishiwaki et al. 1963, Berzin 1972) was interpreted by Cranford (1999) in terms of acoustic sexual selection since larger males have longer inter-pulse intervals than smaller animals which is in agreement with the theory of Norris and Harvey (1972). Another hypothesis by Carrier et al. (2002) interprets the huge nose of sperm whales as a possible weapon specialized in male-male aggression. But in the light of the proposed acoustic function, the use of the spermaceti organ as a battering ram (Carrier et al. 2002, Lusseau 2003) is not plausible. The sonar system is so important for the survival of sperm whales that these animals would probably not risk the damage of this vulnerable device in regular competetive fights. Furthermore, there are no skeletal structures, neither in the skull nor in the spine, that could divert the forces which would arise during ramming.

### 6.1.5. Pygmy sperm whale (*Kogia breviceps*)

In all odontocetes the blowhole is concave, except in *Physeter macrocephalus*. But only in *Kogia spec.* the concavity points caudally. Therefore, the mechanism to open the upper nasal passage is different in *Kogia*. In all dolphin-like species examined so far the blowhole is opened by muscle layers rostral of the upper respiratory tract shifting the mobile anterior blowhole lip rostrad. In *Kogia*, the blowhole is opened by caudalward orientated muscles moving the posterior blowhole lip that seems to be extremely mobile. Furthermore, the blowhole of *Kogia* is shifted slightly to the left. According to its orientation it can be opened by a strong caudal

portion of the left maxillonasolabialis muscle. The right maxillonasolabialis muscle is involved insignificantly in blowhole opening. These differences between *Kogia* and non-physeterid toothed whales may be explained by the functional differentiation of the two nasal passages and the development of the spermaceti organ. The left nasal passage of *Kogia* seems not involved in sound generation but in respiration mainly. Therefore, the structures and muscles on the left hand side are specialized in breathing so that the mechanism to open the left nasal passage widely is optimized. Interestingly, a small portion of the left maxillonasolabialis muscle is connected to the left corner of the (right) monkey lips (Fig. 5 in Schenkkan and Purves 1973). So, the functional differentiation of the nasal passages is not as complete as in *Physeter*.

According to our morphological findings a sound generation mechanism at the monkey lips analogous to the procedure described for *Physeter* in the chapter before is most likely which is consistent with the unified hypothesis of sound generation in toothed whales mentioned by Cranford et al. (1996). The monkey lips act as a clapping system driven by a distal air stream (from the right nasal passage into the vestibular sac). Each clapping event causes the posterior monkey lip to vibrate. This initial sound wave is than guided via the spermaceti organ into the melon.

The right bony nares is situated near the midline of the skull but the monkey lips in *Kogia* are shifted far right. This fact may be interpreted in terms of air sac and spermaceti positioning so that the right nasal passage, the nasofrontal sac, and the spermaceti organ became elongated relatively to the size of the nasal complex. Due to the inward and forward curvation of the spermaceti organ the two nasal passages are widely separated.

The torus may function as a very potent acoustic isolator, first, because of the proposed high impedance mismatch between its dense connective tissue and the surrounding air and, second, because of the irregular surface build mainly by the deep crypts. These crypts and pouches may muffle the sound significantly so that reflected sound waves would not influence the initial sound guided through the spermaceti organ.

Circular air recycling during sound production seems possible. Similar to the situation in *Physeter* the two nasal passages are connected via the vestibulum and the laryngeal space. But this mechanism is not plausible because it would require a large amount of air. So, it is likely that the air is recycled by backward sucking from the vestibular sac through the monkey lips into the right nasal passage. Muscles of the vestibular sac and the monkey lips support this mechanism that is similar to the air recycling procedure described by Norris et al. (1971 cited after Norris 1980) in dolphins. However, air is probably pressurized by the piston-like movement of the larynx (not by a pressurizing process of the right nasal passage as mentioned before for *Physeter*) since the right nasal passage appears to lack muscles associated with the tract that could pressurize the air volume.

As stated before, there are strong evidence that the monkey lips are the primary sound generator in the *Kogia* head. Therefore it is likely that the spermaceti organ acts like an acoustic funnel or horn (Cranford, pers. comm.) that couples the monkey lips acoustically with the melon. Accordingly, it is possible that the spermaceti organ focuses the sound beam by reflections at its surface (case and air sacs). To reach the required length to support the focusing process the spermaceti organ is curved. We are not able to decide whether the structure of the spermaceti organ may amplify the sound beam but that additional function seems possible.

Despite the fact that the knobs of the nasofrontal sac in *Kogia* contain connective tissue and are not fluid-filled as in *Physeter* we postulate that they have the same primary function. The gaps between the knobs enclose a continuous air film so that the spermaceti organ is covered by a functional acoustic mirror that requires a minimum of air.

The left premaxillary sac may have no acoustic function since the left nasal passage does not serve sound production and the sound path (spermaceti organ) from the generator in the right passage is nearly completely isolated acoustically by the nasofrontal sac. Therefore, it is likely that the left premaxillary sac creates the surface on which the nasal plug muscles can move.

The fact that the rostral muscle are in similar topographical relation to the melon may point to a similar function of this muscles as proposed for non-physeterid odontocetes in sound beam formation. The curvature (shape) of the head surface probably contributes to the focusing of sound (Bel'kowitsch and Nesterenko 1972). So we can speculate that the external frontal shape of the melon may be an important factor in sound emission. That means that differences in the frontal "face" of the melon in different species could explain specializations of the melon's shape, in general. Species with nearly vertical (genus *Physeter* and *Kogia*) or steep foreheads (genus *Pontoporia*) have elongated sound paths either due to the existence of a spermaceti organ or because of the elongation of the terminus of the melon. But we are not able to decide so far whether these are causal correlations or not.

Stomach contents of *Kogia breviceps* indicate that this species dives regularly to depth of more than 100 m (Ross 1979). Shrinking air volumes during dives should

limit the sonar sound generation. The specializations of the nasal tracts in *Kogia* and *Physeter* – the left passage in respiration and the right one in sound generation – may be an adaptation to sound production in great depth since the number and volume, respectively, of the accessory air sacs can be reduced that way. In ziphiids, which are also known to be deep divers (Pitman 2002), a reduction of the number of air sacs was found (vestibular sacs are absent) but the nasal complex exhibits more symmetric than in physeterids (Heyning 1989).

## 6.2. Homologies in odontocete forehead structures

Schenkkan and Purves (1973) confirmed that the monkey lips of physeterids are the homologue of the lips in the right naris in conventional odontocetes. Cranford et al. (1996) reviewed the discussion on homology in the toothed whale nasal complex and stated that the right posterior dorsal bursa of non-physeterid toothed whales is probably homologous to the spermaceti organ in *Physeter* and *Kogia*. This fatty structure has the same relative position in all odontocetes; it is bound to the caudal part of the right nasal passage and corresponds to the posterior monkey lip (and the dorsal monkey lip in *Physeter*, respectively). The same is true for the melon and the junk, respectively. These two fat bodies rest on the rostrum anterior to the nasal passages in both physeterids and non-physeterids. Another striking similarity in all odontocetes is the position of the monkey lips. Despite the fact that the extreme asymmetry in physeterids leads to the development of only one pair of lips it is also in the same topographical relation as the right pair of lips in non-physeterid toothed whales. Nevertheless, it is surprising that the monkey lips in *Kogia* are partially "parasitized" (Schenkkan and Purves 1973) by some superficial fibers of the left maxillonasolabialis muscle. They insert near the left corner of the lip's slit.

The two cartilaginous structures in the forehead of adult sperm whales (nasal roof and rostral cartilages) have both important implications for the reconstruction of the sperm whale nose during evolution and during development (Klima et al. 1986, Klima 1995, 1999). The rostral cartilage was described as „pacemaker" in the ontogenesis of the cetacean upper jaw (rostrum), in general, because, as a central structure, it appears that this structure induces the elongation of the upper jaw anteriorward by strong cartilaginous tissue proliferation and thus longitudinal growth (Klima 1990) but this point of view is not tested experimentally. At least as important (intellectually) is the nasal roof cartilage (tectum nasi) because it can shed light on the evolution of the cetacean rostrum. In the terrestrial ancestors of the cetaceans, which are suspected among fossil mammals near the origin of the even-toed hoofed animals (Artiodactyla), as well as in the first cetaceans obviously fully adapted to aquatic life (Archaeoceti) the nostrils were still in a terminal position (Fordyce and Muizon 2001). In contrast, advanced cetaceans shifted these nasal openings backward along the midline of the upper jaw to a position just before the brain case. This shift was part of a total re-organization of the nasal region accompanied by the telescoping process of the skull (Miller 1923), and the backward rotation of the nasal canals so that they project dorsally perpendicular to the skull base (Klima 1987). In odontocetes, the reorganization of the nose led to the reduction of the peripheral olfactory system (Oelschläger and Buhl 1985, Oelschläger and Oelschläger 2002) and left over the respiratory tube which was equipped secondarily with accessory air sacs used for the generation and emission of sonar signals for orientation and communication. Whereas in most extant odontocetes the blowhole and the bony nostrils are situated immediately before the brain case of the skull, the sperm whale shows a highly derived situation. In the course of the development of the spermaceti organ as a huge „new" acoustic fat body out of a small rudiment of fat body (right posterior dorsal bursa, Cranford et al. 1996), the blowhole with the phonetic apparatus (monkey

lips/dorsal bursae complex - MLDB complex) was shifted anteriorward. By that the interconnecting nasal passages between the blowhole and the bony nostrils were strongly elongated. Taking into account all this, the course of the nasal roof cartilage throughout the epicranial complex may stand for the evolutionary shift of the blowhole with the phonetic apparatus in a terminal position, i.e. its course can be seen as a trajectory during this process which, in principle, is repeated during the fetal period of sperm whale development (Behrmann and Klima 1985, Klima 1990).

According to the development of the cartilaginous nasal skull, the cetacean order can be divided into three groups at least: baleen whales, sperm whales, and toothed whales (except sperm whales). In this context, sperm whales show similar pattern than baleen whales and both groups are different from the non-physeterid toothed whales in some respects (Klima 1995, 1999). These findings can be interpreted as to an closer relationship of sperm whales with baleen whales than with the remaining odontocetes (Klima 1995, 1999) which was also outlined by Milinkovitch (1995) based on genetic studies. In contrast, comparisons of nasal soft structures presented in this study and by Cranford et al. (1996) reveal a closer relationship of sperm whales to other toothed whales than to baleen whales. Thus, the similarities of the nasal cartilaginous structures between sperm whales and baleen whales found by Klima (1995,1999) can be explained by synplesiomorphism and the development of the nasal roof cartilage in *Physeter* may be apomorphic.

The assumption made by Cranford et al. (1996) that the bursa cartilages found in some odontocetes are homologous to the unilateral nasal roof cartilage of *Physeter* seems not to be true for all purposes. The tectum nasi is divided into several cartilaginous parts and only one unilateral develops to the nasal roof cartilage (Klima 1990, 1999). Therefore, it is likely that the bursa cartilages may be

homologous to tectum nasi components lateral to the one leading to the nasal roof cartilage.

Mead (1972 cited after Cranford et al. 1996) recognized the unilateral vestibulum directly ventral to the blowhole as an entity in delphinids that becomes highly modified in some odontocete groups. In comparison with *Physeter* we can conclude that the vestibulum became modified that way that it is differentiated in the distal sac, the blowhole cavity, and the connection between these two structures. Therefore, the term vestibular sac is referred to for the distal sac in *Physeter*. In *Kogia* this sac is prominent only on the right hand side (as in *Physeter*) and characterized by the torus (catchers mitt). Interestingly, the sac is in the same relative position as the vestibulum of non-physeterid toothed whales, dorsal of the monkey lips, but highly modified by bilaterally asymmetric outpockets (vestibular sacs). In conclusion, it is likely that all these structures formally called vestibular sacs in delphinids, phocoenids, *Kogia spec.* and the distal sac of *Physeter* are modification of the vestibulum and therefore a unified character of odontocetes. Furthermore, the posterior nasofrontal sac in non-physeterid species, the (right) nasofrontal sac in *Kogia spec.*, and the (right) frontal sac in *Physeter* are all in the same relative position to the fat bodies (posterior dorsal bursae and spermaceti organ, respectively) and to the skull. Therefore, it appears that these sacs are homologous structures found throughout the odontocete sub-order and are homologous to the right posterior nasofrontal sac in non-physeterid toothed whales.

Because of the extreme morphogenetic distance between sperm whales and other toothed whales (Fordyce and Muizon 2001), it is rather difficult to derive or homologize single components of the **maxillonasolabialis muscle** complex between these groups. However, it is very likely that, as a whole, the epicranial muscles in

all odontocetes go back to one ancestral configuration and that, in the sperm whale, they reflect the profound phylogenetic modifications alterations of the epicranial complex which led to a unique situation in the morphology of the head. In parallel to the (secondary) shift of the blowhole to the new dorsal tip of the sperm whale head the course of the muscle fiber bundles from the margins of the skull roof to the blowhole has changed from a more concentric (radial) to a more longitudinal orientation. Besides the specific course of the nasal roof cartilage from the bony naris to the blowhole area this is another hint for this secondary shift of the external nasal opening into a terminal position during ontogenesis and evolution.

The musculature in the epicranial complex is probably homologous to that of dolphins and innervated by the facial nerve (Rauschmann 1992). In contrast to the situation in non-cetacean mammals, this cranial nerve runs without considerable ramification from the tympanoperiotic complex and below the orbita and turns upward around the lateral margin of the skull roof via the antorbital notch, ramifies strongly and innervates the blowhole musculature. In the sperm whale, not only the diameter but also the number of axons is much higher than in other odontocetes investigated so far, and also in baleen whales of the same size (Oelschläger and Kemp 1998, Oelschläger and Oelschläger 2002). This correlates, on the one hand, with the extreme absolute and relative size of the head and the epicranial (blowhole) musculature and, on the other hand, with the fact that baleen whales do not echolocate and possess a much less developed nasal area (no epicranial complex).

Nevertheless, beside the problems to consider the homology of the different parts of the maxillonasolabialis muscle, it is very likely that the nasal passage muscles found in sperm whale is the equivalent to the nasal plug muscles in other

odontocetes. In all toothed whale groups examined so far this muscle is positioned rostral to each nasal passage and it functions (at least) as an dilator of the tract.

The significance of the spermaceti organ as an acoustic structure was probably so important, that it tremendously hypertrophied during evolution of the spermaceti tribe. As a result, the blowhole region was shifted to the tip of the nose (secondary terminal position of the single external nostril). The soft parts of the upper respiratory tract which are rather short comparatively in other toothed whales and in a vertical position, became much elongated dorsorostrally in the sperm whale: thus they run in a paraxial direction from the bony nostrils at the caudal base of the amphitheater to the blowhole region. By this transformation, the organization of the sperm whale nose became extremely asymmetric, so that the right hand side of the epicranial complex, with the spermaceti organ, extends far to the left in the posterior half of nasal region, leaving the anatomically left part of the nose as a small wedge-like region. The asymmetry of the upper airways brings up the situation that the caudal part of the right nasal passage runs between the two huge fat bodies (spermaceti organ/junk) in a more or less central and parahorizontal orientation. Instead, the course of the left nasal passage is rather superficially below the dorsolateral surface on the left side of the head. Because of the relative position of the junk in *Physeter* anterior to the right nasal passage and ventrally to the ventral monkey lip, respectively, there are two logical possibilities of its homologous structures in non-physeterid odontocetes: the melon and the right anterior dorsal bursa. But comparison with *Kogia spec.*, which has a melon very similar to that of dolphins and porpoises, leads to the assumption that the junk is the homologue to the melon. The unique structure of the junk may be caused by the elongation of the spermaceti organ during evolution. The connective tissue pillars intercepted by numerous fatty lenses may function not only as

impedance transformer of the outgoing sound beams but also as base to stabilize the spermaceti organ.

If the hypothesis of Cranford et al. (1996) is correct that the spermaceti organ is homologous to the posterior dorsal bursa of other odontocetes, this would imply that the ancestors of all extant toothed whales were echolocators. All non-physeterid toothed whale species investigated so far for this detail have this fat body in the same topographical relationship and this relationship suggests an acoustic function of this structure. The proposed homology of nasal structures within the toothed whale group corresponds with the fact that the nasal asymmetry shows the same general pattern (see chapter "*Asymmetry of the facial skull of toothed whales*"). These findings imply the monophyly of all odontocetes including sperm whales which is in contradiction to some interpretation based on genetic analyses (Milinkovitch 1995).

Heyning and Mead (1990) reported of a fatty structure just anterior of the nasal passage in mysticetes. They speculated that this structure appears to be the homologue of the odontocete melon. We did not find a fat body in the nasal complex of the 52 cm *Balaenoptera* fetus (Table 1) but this fact is not surprising since fatty tissue mature late in mammalian development. The authors believe that the original function of this fat body in cetacean ancestors and recent mysticetes was to allow free movement of the nasal plugs to open the nasal passages during respiration. The fat body could have been hypertrophied during odontocete evolution as it obtained an secondary function in sound transmission (Heyning and Mead 1990). The original function of this fat body in toothed whales as surface on which the nasal plug can move could be taken over by the premaxillary sacs as additional function next to their primary role during sound emission.

Interestingly, all these proposed homologous structures (air sacs and fat bodies) are thought to have similar functions each in sound production and emission. These findings are consistent with observations that all odontocetes from their earliest origins show evidence for echolocation (Fordyce and Muizon 2001). This implies that the active sonar system had been developed once during odontocete evolution. The proposed evolutionary trend entails that echolocation could be the main driving force in toothed whale evolution.

## 6.3. Developmental aspects of the upper respiratory tract in toothed whales

Interestingly, the epicranial complex of toothed whales develops in late fetal stages, later than the ear complex and its accessory mandibular fat body, the second functional unit of the active sonar system (Haddad et al. in prep, Comtesse and Oelschläger unpublished). This could be shown by the comparison of the morphology of perinatal dolphins with the microslide series and magnetic resonance microscopy datasets of early fetal stages in this paper. The nasal air sacs are nearly fully grown in the perinatal animals examined but in early fetuses only anlagen of the nasofrontal and premaxillary sacs can be found. The vestibular sacs, the largest diverticulae in adults, are absent in these early stages. Thus, these large and important structures are still in a surprisingly immature state in early fetuses. These facts may demonstrate some parallels in the sequence of ontogenetic and phylogenetic events. The ear complex of the cetacean ancestors was obviously largely adapted to aquatic hearing when the first osteological hint for echolocation sound production, i.e. the facial depression, appeared in the fossil record (Fordyce and de Muizon 2001).

According to the specimens examined, it is not possible to determine at which stage in dolphin ontogenesis the acoustic fat bodies (melon and mandibular fat body) reach their structural maturity. In early fetuses the fat tissue is not yet visible as such but still at the level of immature loose connective tissue and in our perinatal dolphins the acoustic fat bodies are fully grown and differentiated. Unfortunately, we could not investigate specimens of intermediate fetal stages histologically. It would be interesting to see how these specialized fat bodies develop with respect to the blubber fat. But it seems that the acoustic fat bodies grow simultaneously to the blubber fat which is indicated by a late *Delphinus delphis* fetus in Figure 67.

The degree of differentiation in the nasal structures of the perinatal dolphins, among other criteria, points to the fact that neonate animals have to produce and emit whistle-like sounds for adequate communication with their mothers. This correlates with the findings of Reiss (1988) and Killebrew et al. (2001) that young bottlenose dolphins vocalize similar to adults shortly after birth. The epicranial complex and the head, in general, of the perinatal spotted dolphins examined is rather similar morphologically to that of the adult and this precocial situation is reflected in the behavior of newborn dolphins (Cockcroft and Ross 1990). This highly precocial nature of dolphin (and whale) newborn may have lead to specializations in timing of fetal development in comparison to terrestrial mammals.

## 6.4. Asymmetry of the facial skull in toothed whales

All toothed whale skulls examined show the same pattern of asymmetry: the mid-suture is "skewed" (Ness 1967) to the left and the right bony structures are larger than the left. Therefore, it is likely that asymmetry in the toothed whale skulls (at

least of the groups examined) did not arise numerous times independently in odontocete evolution as outlined by Heyning and Mead (1990). This would also imply that the cranial asymmetry and the reduced vertex is lost secondarily in *Pontoporia* (Heyning and Mead 1990) and that the specialized asymmetric features in the facial skull of *Kogia spec.* (and probably *Physeter macrocephalus*), e.g. the lost of the right nasal bone, are apomorphic. Some authors stated that the facial skull of *Pontoporia blainvillei* is truly symmetrical (Ness 1967, Barnes 1985). The combined results of this study show that the skull of this species is asymmetric but the most minor degree of all species examined. These results are in agreement with Heyning (1989). But it was not possible to test Ness' (1967) statement that skewing increases with body size since only relatively small species were analyzed.

Cranial asymmetry is not universal in the toothed whale group. It is absent in some extinct groups (Heyning 1989, Fordyce and Muizon 2001). But at least in the late Oligocene Waipatiidae, which are probably closely related to the platanistoids, the skull exhibits very similar pattern of asymmetry as most extant odontocetes (Fordyce 1994) but other Oligocene toothed whales, e.g. Squalodontidae, Eurhinodelphinidae, and Kentriodontidae, have symmetrical skulls (Fordyce and Muizon 2001). In general, if asymmetry is present in odontocete skulls it shows the same pattern. Thus, it appears more parsimoniously that asymmetry evolved only once in the common ancestors of all modern toothed whales. A lesson to learn from the examination of *Pontoporia* skulls is that the form of asymmetry in the skulls is not always to detect clearly. Therefore, it is possible that at least some fossil groups have slightly asymmetric skulls but it is not possible to detect it in the fossil material.

Visual inspection of the nasal skull of odontocetes show that shape and location of the bony nares and surrounding structures appears to be rotated around a center

near the bony nasal septum. This rotation seems to be significant in *Kogia* (Fig. 45) but is also visible in delphinids (Fig. 56). It was not possible to document the rotation in the morphometric data of this study because the sample size was probably to small to show clear trends.

The nasal complex of toothed whales is known to be involved in the generation and emission of echolocation sounds (for review see Cranford 2000). This complex is characterized by directional asymmetry which shows, in general, the same pattern in most odontocete species (Cranford et al. 1996). Therefore, this asymmetry must be interpreted in functional terms. Accordingly, Cranford et al. (1996) hypothesized that at least the frequency of the sonar beam may be correlated with the asymmetry pattern. The facial bony structures represent some of the asymmetry of the over-laying nasal complex. After Fleischer (1975, 1982, Oelschläger 1990) the facial skull functions as an acoustic shield where the sound, generated in the epicranial complex, may be reflected. Thus, it is likely that the cranial asymmetry contribute to the formation of sonar beams (Norris 1964, 1968, Dubrovskii and Zaslavskii 1975).

Nevertheless, it can be combined that odontocete asymmetry may be a result of specialization in sonar signal type and/or sound generation mechanism for a particular environment. There are strong correlations between habitat types, social behavior, and sonar sound peak spectra as well as cochlear morphology in toothed whales. According to Wartzok and Ketten (1999) and Ketten 2000 there are two different types of odontocete echolocators: type I emits peak frequencies above 100 kHz and type II is characterized by peak frequencies below 80 kHz. Type I echolocators are mainly inshore or riverine species living in a complex environment; e.g. *Phocoena phocoena* or *Inia geoffrensis*. Offshore and near-shore species belong typically to type II operating in a less complex surroundings and are

characterized by a more social behavior than type I species. A typical example is *Tursiops truncatus* as well as *Physeter macrocephalus*. Cochlea parameter are correlated with these two types of sonar signals each (Wartzok and Ketten 1999, Ketten 2000). These to types of echolocators are at least in parts represented in the statistical analysis of skull measurements. In the "porpoise" cluster are species that are type I echolocators and the "dolphin" cluster is taken by species of the type II group. According to the PCA, *Kogia* and *Pontoporia* do not fit in this system since they are not clustered with either of the group types. Unfortunately, it is not enough known on the structure of echolocation sounds in *Pontoporia* to put it in one type of echolocators but it appears that this species is more like a type I echolocator since its correlation values (factor 1 and 2, Figure 57) is close to the "porpoise" cluster. *Kogia*, however, has no direct neighboring cluster since shape and asymmetry in the skull of this species seem to be significantly different. Nevertheless, there are no data on vocalizations of this species but comparisons with the related species *Kogia breviceps*, which is very similar in nasal morphology, points to a type I grouping because of its peak frequency of approximately 120 kHz (Wartzok and Ketten 1999).

As stated before, this study contains preliminary results of a two-dimensional morphometric analysis. According to the promising results it appears adequate to extend this kind of examination to a larger sample size that includes most of the extant toothed whale species. For example, it would be interesting to know how beaked whales (Ziphiidae) would fit into the proposed system of asymmetry (Fig. 57). Furthermore, three-dimensional data would contain far more information than the dataset used in this study. If and how the vertex height is correlated to the degree of asymmetry is still enigmatic but it was suggested by Heyning and Mead (1990) that the degree of asymmetry and the vertex height may have a positive relation.

## 6.5. The role of the larynx in odontocete sound production

This study is mainly based on the examination of the larynx and hyoid regions in the harbor porpoise but the results were compared to the situation found in other species (*Kogia breviceps*, *Neophocaena phocaenoides*, *Pontoporia blainvillei*, *Stenella attenuata*). However, because of the similarities of the laryngeal complexes in odontocetes examined in this study and described in literature (Lawrence and Schevill 1965, Reidenberg and Laitman 1994), the observations and interpretations intended here may hold for all members of the group. In toothed whales, the larynx is situated in the medioventral vault of the skull base. It is characterized by an elongation of the epiglottic and cuneiform cartilages forming a goose beak-like spout at its rostral end. The tip of the epiglottis forms a lip that is surrounded and held in position by a strong sphincter muscle. This muscle, a complex of the palatopharyngeus and pterygopharyngeus muscles, connects the epiglottic spout with the bony nares. The sphincter muscle is attached on the skull base as well as in the ventral part of the bony nasal passages and the pterygoid hamuli. The long spout in connection with the sphincter muscle is responsible for the secure intranarial position of the larynx and the total (waterproof) separation of the respiratory and pharyngeal tract so that the nasal air passages stays continuous with the glottis while the animal sucks in prey (Reidenberg and Laitman 1987, 1994). Because the respiratory and the digestive tracts are completely separated, the diet pass the narrow pharyngeal cavities on larynx level, i.e. left or right of the epiglottic spout. Anterior-posterior movement of the larynx might help the food to pass by and pushes the food in posteriorlly direction. The muscular connection between the larynx and the mandible, the hyoid apparatus as well as the sternum may be responsible for these movements (Fig. 65).

Because the odontocete larynx is unique in shape among the Mammalia, various hypothesis came in favor regarding its function. As stated above, the major function of the larynx is to keep the respiratory and the digestive tract separated. Furthermore, during the 1980$^{th}$ some scientist established the idea that the larynx of toothed whales is the source of the pulsed sounds which are used in echolocation. This "larynx hypothesis" implied a similar mechanism of sound production as in other mammals (Purves and Pilleri 1983, Reidenberg and Laitman 1988, 1994). Nevertheless, it was shown that the echolocation signals are generated in the nasal complex of toothed whales. According to modern sound generation hypotheses, the larynx and its associated musculature produces the air pressure for the air flow in the nasal complex where the (echolocation) sound generation takes place in toothed whales (Norris 1969, Norris and Harvey 1972, Ridgway et al. 1980, Amundin and Andersen 1983, Marten et al. 1988, Cranford et al. 1996, Cranford 2000). The mechanism of sound generation in the nasal complex as described by Cranford et al. (1996) does not require a large air volume but high pressure. From an anatomical point of view, the larynx and the sphincter muscle complex are very good candidates for the production of the responsible pressure. Here, the larynx functions like a piston that is pulled by the sphincter muscle in direction of the choanae. Simultaneously, the sphincter muscle closes the larynx tightly at level of the tip of the epiglottic spout. Furthermore, the larynx is framed by the hyoid apparatus and connected to it by a set of different muscles (Fig. 65). The strong gular musculature connecting the hyoids with the mandible and the skull base may force the larynx additionally in direction of the choanae. Figure 65 demonstrates schematically favored pulling directions of the musculature of the hyoid apparatus and the larynx. Strong muscle complexes force these structures rostrodorsalward but only two muscle (sternohyoid and sternothyroid) backward. Therefore, it is likely that the laryngeal pressure pump is not conducted by the very strong palatopharyngeal sphincter muscle only but also,

at least in parts, by the muscles associated with the hyoid apparatus. After a sound generation cycle the air in the nasal system can be recycled (Norris et al. 1971 [cited after Norris 1980]). Here, the sternohyoid and sternothyroid muscles can retract the larynx from its intranarial position to help sucking in the air from the nasal air sacs in the nasal passage down to the nasal plugs (Fig. 65). Interestingly, the hyoid apparatus is bilaterally "articulated" only by the thyroid cartilage to the skull. Thus, the capability of movements resemble to a swing moving in rostrocaudal directions but also rostrodorsalward in direction of the choanae (Fig. 65). These potencies of movements support the mechanism of the larynx during odontocete sound production since the larynx may "swing" in its hyoid framework from its caudal and post-pterygoidal position to the intranarial and rostral location.

So-called bangs or "jaw" pops are another type of loud impulse sound frequently recorded in dolphins (Connor and Smolker 1996). These low-frequency sounds (peak frequency around 1 to 8 kHz) lasting generally for several milliseconds are thought to function in social interactions (Connor and Smolker 1996) and/or prey capture (Norris and Møhl 1983, Marten et al. 2001). Although the bangs are likely generated in the nasal complex the mechanism seems to be correlated with rapid closure of the jaws (Marten et al. 1988). Cranford et al. (1993) suggested a generation mechanism similar to that used for echolocation pulses, except that the (nasal) tissue region involved is larger and the air pressure considerably higher. Inspections of the gular musculature in dolphins and porpoises support this hypothesis (but phocoenids are not known to produce bangs so far) since the mandible is strongly connected to the hyoid apparatus and the larynx, respectively. Opening of the jaws would, therefore, enable the larynx to be retracted to a far caudal position by the sternohyoid and sternothyroid muscles. This movement could, in turn, enlarge the air space between the nasal plugs (dorsal bony nares) and

the tip of the epiglottic spout. Simultaneous contraction of, first, the palatopharyngeal sphincter complex, second, the muscular connection of the larynx and the mandible (Fig. 65), and, third, the closing musculature of the jaw (temporalis, masseter, and pterygoid muscles) should force this large air volume rapidly into the nasal complex to produce the bang.

As stated before, the larynx is thought to build up the air pressure needed for high-frequency sound production in the nasal complex by a piston-like movement. In order to facilitate this movement, the sphincter muscle seems to close the tip of the larynx and forces it into the choanae (Norris 1969). From here, the dorsalward directed contraction of the strong intranarial portion of the pterygopharyngeus and palatopharyngeus muscles (Fig. 55) and the concordant shortening of the muscle may shift air in the direction of the nasal structures and may lead to an additional increase of air pressure by filling the space of the bony nasal tubes. The intranarial position of the palato- and pterygopharyngeus muscles and their presumed function could be important for deep-diving when shrinking air volumes may limit the sound generation process.

In dolphins, the jaw apparatus (rostrum and lower jaw) are designed for the catch of living fish and squid. The prey, however, is not chewed but swallowed whole. Thus, the strong hyoid apparatus and its massive musculature (Fig. 65) probably play an important role in creating considerable negative pressure in the oral cavity and pharynx that helps to suck in prey (Reidenberg and Laitman 1994). This suction-feeding behavior, apart from vocalization by pressurized air streaming in and through the nasal passages, may be another reason for the tight connection of the larynx and the nasal passages by the strong sphincter muscle. Even if the gular area is pulled ventralward to create negative pressure in the oral cavity, the larynx

stays in position and there is no weakening of the respiratory connection (Reidenberg and Laitman 1994).

It was shown before that the hyoid framework may contribute to the piston-like movements of the larynx to drive the air flow in the odontocete nose. But whether the size and shape of the hyoid apparatus means another adaptation to high-frequency sound generation is difficult to tell. So, it is a matter of speculation whether the appearance of the typical odontocete hyoid apparatus during the radiation of toothed whale ancestors can be added to the sonar-related skull features as, e.g. the facial depression since hyoid bones are rarely seen in the fossil record.

The respiratory and the digestive tracts are separated completely. But sound production and swallowing of food should not be possible simultaneously. The dorsalward movement of the larynx for the production of high air pressure in the nares to drive the click generator (MLDB complex) should close the pharyngeal passages since the larynx is pushed in direction of the skull base and the pharynx should be collapsed this way. But in addition to its function during sound production, the larynx and its musculature plays maybe an important role in a special prey capture behavior called "suction feeding" (Reidenberg and Laitman 1994). The muscles of the tongue and the floor of the mouth create a strong negative pressure in the oral cavity, which, in turn, may draw in water and thus the targeted prey. Also during this behavior the structure of the larynx and its sphincter muscle prevent the water to enter the air passages. To swallow prey the larynx is probably forced ventralward by the strong gular musculature (Fig. 65) to give way for the prey. But, simultaneously, the sphincter muscle may seal the laryngeal connection although the larynx is in a ventral position.

But more interesting, the respiratory and digestive tracts need to be securely separated during rapid respiration which is typical for cetaceans (Kooyman 1973, Pabst et al. 1999). A strong negative pressure in the lung, and therefore also in the respiratory tract, is the precondition for rapid inspiration. But this negative pressure would also force in water from the digestive tract if there is no secure sealing. During the inspiration phase the sphincter can not be closed tightly around the spout of the larynx since the respiration tract needs to be open. Here, it is likely that the pharynx is collapsed during the respiration phase. A possible mechanism to close the pharynx could be to force the larynx in direction of the skull base. The musculature which connects the hyoid apparatus with the skull base, the stylohyoid and the ceratohyoid muscles, can force the larynx in dorsal direction.

In conclusion, the function of the larynx and its surrounding structures is hard to determine since this complex is a multi-functional system serving respiration, feeding, and sound production. From an anatomical point of view, it is likely that the role of the larynx in odontocete sound production is the piston-like movement to create the initial air pressure for click sound generation in the nasal complex. Contraction of the strong palatopharyngeal muscle complex, which links the choanae with the rostral tip of the larynx (epiglottic spout), may provide most of the power for this process. But in addition, muscles that connect the larynx/hyoid complex with the mandibles and the skull base may support these laryngeal movements. All these muscles may be also important for the secure intranarial position of the larynx during feeding and respiration. The importance of sound generation in toothed whales seems to be represented in the morphology of the laryngeal complex (next to other peculiarities), which is unique in the mammalian tribe.

# 7. RELATED FINDINGS

## 7.1. Topographic anatomy of the harbor porpoise: comparison of some morphological methods

The harbor porpoise (*Phocoena phocoena*) is a cetacean well documented in the scientific literature and the anatomy of this animal was documented by many different methods (e.g. Tyson 1680, Slijper 1936, Cranford et al. 1996, Kastelein et al. 1997). Macroscopic dissection of tissues and organs is a prerequisite for the identification of body structures, whereas x-ray computed tomography (CT) and magnetic resonance imaging (MRI) data give an interpretation of the different tissues within scanned slices. The CT method converts tissue densities into digital values and images, respectively (Brouwers et al. 1990, Hartmann et al. 1992). In contrast, MRI uses the proton density in tissues to reconstruct corresponding digital images. To demonstrate the power of different morphological methods, an adult female harbor porpoise was documented by CT and MRI. Afterward it was sectioned frozen in the mediosagittal plane by means of a band saw. The animal was photographed and fixed using the "Kaiserling" method (Romeis 1989).

CT and MRI are well-established diagnostic methods in life science. In anatomical research, dealing mostly with post-mortem specimens, these methods face some problems. One problem using MRI in dead animals is the recognition of artifacts (Fig. 71). So, hematomas or fluid-filled spaces may be mistaken for parts of structures. X-ray methods are more robust against this kind of artifacts. But often soft tissues are not rendered good enough because of minor differences in tissue densities (Rauschning et al. 1983). On the other hand, invasive methods as cryo-sections or macroscopic dissection for partial analysis may alter the topography of the target structures (Fig. 70).

In the magnetic resonance microscopy (MRM) images of a dolphin fetus (*Delphinus delphis*, CRL 38 mm) the skull and other skeletal structures, e.g. the spine are visible (Fig. 47). Due to their similar spin densities, fetal bony tissue, cartilage, and connective tissue lead to the same contrast in the MRI images. Therefore, it is difficult to distinguish between them. Thus, it is necessary to use color stained histological sections for additional information about these tissues (Fig. 47).

As non-invasive methods, CT and MRI demonstrate the topography of organ systems better than any other technique and 3-d computer reconstruction of the scans is a powerful tool to understand complicated structures (Figs. 71). Our synthetic study is one of the few that present the topographic relation of the skeleton within the body, e.g., the pelvic bones in a porpoise (Knauff 1905, Kastelein et al. 1997; Fig. 71). In conclusion, only the combination of modern imaging techniques and traditional gross anatomical methods (slice cryosectioning, dissection) including routine histology will show the complete picture of morphology and topography and help to interpret the functional implications of the tissues and structures in question. Nevertheless, CT and MRI scans even of high end systems (e.g. MRM) cannot compete with the resolution and brilliance shown in photos of gross sections or histological slices (Haddad et al., in prep.).

## 7.2. Eye

The ellipsoid shape of the eye, elongated in rostrocaudal orientation, is in contrast with the spherical appearance of the lens (Fig. 55). Whereas the spherical lens is an adaptation to vision under water (analogous to the situation in fishes), the ellipsoid shape of the eyeball may serve two different focal distances independently. Thus, the eye of a dolphin is normal-sighted for axial directions of view but short-sighted for rostral directions (Kröger and Kirschfeld 1993). It is unlikely that dolphins can compensate for the frontal myopia (nearsightedness) because the ciliary muscle is rudimentary or absent (Pütter 1903, Pilleri 1964, Dral 1972) as is the case in ruminantia (Dyce et al. 1991). It is therefore plausible that the sonar system, being less efficient at close ranges, and the eye support each other in the rostral direction whereas near-field vision in other directions seems to be impossible (Kröger and Kirschfeld 1993).

## 7.3. Lung

The toothed whale lung is located dorsally in the thoracic cavity and the diaphragm is positioned in an oblique orientation with respect to the beak-fluke axis (Reynolds et al. 2002). Both features may be adaptations to passive thorax compression during deep-diving (Kooyman and Andersen 1969). In the fetal specimen segmented in this study (Fig. 48) the lungs are already in their final (dorsal) position but rather small so that the wide fluid-filled pleura cavity creates an intense signal in comparison to the dark-rendered tissue of the lung, facilitating graphical segmentation. The wide pleura cavity, cleft-like in postnatal animals, is probably no shrinkage artifact of the early fetal lung because, generally, in mammals the lungs "attack" to the inner surface of the thorax only during late fetal development

(Duncker 1990). In toothed whales, the two parts of the lung are asymmetric, the right larger than the left (Arvy 1977). This fact is also represented by surface and volume measurements of the fetus' lungs (Table 5). In contrast to most mammals including the human, the MRI images show that the lung is not lobated; a situation typical for cetaceans (Robineau 1994). Furthermore, the diaphragm is not as oblique in our fetus as in adults because the liver is still very large and the straightening and elongation of the body is not yet completed (Fig. 48).

Table 5: Surface area and volumes of segmented lung parts of an early fetus (LES 001, Table 1)

| Structure | Surface area [$mm^2$] | Volume [$mm^3$] |
|---|---|---|
| Left lung | 58.8 | 24.9 |
| Right lung | 63.6 | 26.9 |

## 8. CONCLUSIONS

This dissertation project deals with the anatomy (macroscopical dissection, cryo-sectioning), histology, and modern imaging techniques (CT, and MRI, including 3-d computer reconstruction) of the sound generator and transmitter in the head of toothed whales. As most marine mammals rely heavily on acoustic cues, it is important to understand how these animals produce, hear, and use sounds with regard to their normal life style and in order to cope with sound pollution in the oceans of the world.

Despite our restricted knowledge on the biosonar of animals, only very little research is currently conducted on this important aspect of mammalian biology. This study is dedicated to a better understanding of the mechanisms of sound generation and emission in toothed whales on a morphological basis and on bio-acoustical interpretations.

In general, the morphological data presented here prove the unified "phonic lips" hypothesis of sound generation in toothed whales presented by Cranford et al. (1996). Their hypothesis identifies a valve-like structure in both nasal passages (in physeterids only in the right nasal passage), the monkey lips/dorsal bursae (MLDB) complex, as the sound generator. The underlying principle is a pneumatically-driven clapping mechanism at the monkey lips (phonic lips) which creates the initial tissue-borne sound vibration. This vibration is conducted and focused into the water by the melon, a hypertrophied fat body in the toothed whale forehead. Nasal air sacs, nasal musculature, and other specific features of the skull and connective tissue may contribute to focus the sound to the front.

Whereas the emitted signals of harbor porpoises (*Phocoena phocoena*) are rather specialized and thus differ from those of other toothed whales, their sound generating system (epicranial complex) reaches the same degree of complexity as in dolphins and in river dolphins as well. The correspondence of their nasal structures as to topography and shape points to the same general functional principles in both groups regarding sound generation and emission serving echolocation. But there are some morphological peculiarities in the porpoise nasal complex that could explain their unique click structure. It can be hypothesized that specializations found in the nasal morphology of the harbor porpoise are adaptations of the sonar system to the specific requirements of their coastal habitat. Moreover, the morphological results presented here suggest that not only the MLDB complex but also the air sac system is homologous throughout the toothed whale sub-order. Since all these structures (nasal tract with MLDB complex, melon, air sacs, facial musculature) are involved in sound production and emission, it is likely that the sonar system arose only once in odontocete evolution and, thus, that the toothed whale group is monophyletic which is supported by the fossil record.

It was shown that the process of echolocation sound generation in the epicranial complex of toothed whales is pneumatically-driven (Norris 1968, Cranford et al. 1996). Whereas the muscles of the epicranial complex are probably important for the regulation of air flow along the potential sound-generating structures in the odontocete nose, most of the modern hypotheses consider the larynx and its surrounding musculature to produce the initial air pressure needed for nasal vocalization (Cranford et al. 1996). The functional implications of the larynx and the surrounding structures, however, are hard to determine since this complex is a multi-functional system serving respiration, feeding, and sound production. But from an anatomical point of view it is likely that, in odontocetes, sound production

is caused by piston-like movements of the larynx in the direction of the choanae inducing air flow into and throughout the nasal complex. Contraction of the strong sphincter muscle complex which links the choanae with the epiglottic spout of the larynx, may provide most of the power needed for this process. But in addition, muscles that connect the larynx/hyoid complex with the mandibles and the skull base may support these repetitive movements of the larynx. These muscles are probably also important for the secure intranarial position of the larynx during respiration and feeding.

The most striking difference in the nasal morphology of the giant sperm whale (*Physeter macrocephalus*) and of the non-physeterid toothed whales is the high degree of asymmetry in physeterids. Here, the right nasal passage carries a valve-like structure (monkey lips) that is very likely the site of click sound generation (Norris and Harvey 1972, Cranford et al. 1996, Cranford 1999, 2000). In contrast, the left nasal passage lacks this structure and, therefore, is not involved in sound generation but mainly serves respiration. It is plausible that, in giant sperm whales, the hypertrophy of the epicranial complex may have maximized the directionality and source levels of their echolocation clicks. In these animals, the topography and shape of the huge fat bodies (spermaceti organ, junk), reminiscent of a bent acoustic horn (Møhl 2001), and their peculiar air sac system are good candidates for this proposed specialized function. Moreover, the adaptation to long-range echolocation may have been the main factor in sperm whale evolution that led to this unique and big "sound cannon". In contrast to the mechanism described for dolphins, sperm whales may drive the initial pulse generation process with air pressurized by structures associated with the right nasal passage (and not by the laryngeal structures). Contraction of the longitudinal muscles that cover the nasal complex should lead to the squeezing of air out of the right nasal passage from rear to front through the monkey lips. This mechanism could be an adaptation to

deep-diving when shrinking air volume may restrict sonar sound production. Additionally, the right nasal passage may control the transmission through the acoustic fat bodies and thus the signals which are emitted into the environment by manipulating the volume and position of air within the tract. In this theoretical scenario the right nasal passage serves as an "acoustic valve" to switch between two modes of click production: one mode for coda (communication) click production while the passage is air-filled and a second one for the generation of echolocation clicks while the nasal tract is nearly collapsed. Thus it seems that the central position and the sub-horizontal orientation of the right nasal passage within the sperm whale head as an interface between the two gigantic fat bodies is related to the mechanism of sound production with changing volumes of air.

The results of this study hold implications for further physiological experiments as well as behavioral tests. Future research dedicated to the analysis of the mechanisms involved in the toothed whale sonar system will have to include functional models for testing the existing hypotheses and to explain the functional principles of the system, in general. Computer-supported modeling techniques will probably lead to new insights into this important field of biological research (Aroyan et al. 2000).

Small cetaceans are often victims of fishery activities and the entanglement in fishing gear is a major factor in the mortality even of large whales (Reeves and Reijnders 2002). Obviously, the animals are not able to recognize the danger of the fishing nets. Attracted by fish, the porpoises get entangled and suffocate. Apparently, their sonar system has the capacity to detect the thin nylon material of the nets, but probably not in time to avoid collision (Kastelein et al. 2000). These findings are reflected in the by-catch statistics of the fishery industry (Benke 1994, Reeves et al. 2003). In order to reduce by-catch it is necessary to

understand the mechanism of the sonar system. Insights into the ultrasound generation and emission mechanisms can therefore support the development and use of adequate remedy. So-called "acoustic harassment devices" or "pingers" are tested to keep small whales away from the nets by acoustic signals, but these alarms may not have the expected effect since long-term habituation may still cause problems (Culik et al. 2001, Bordino et al. 2002, Olesiuk et al. 2002, Barlow and Cameron 2003). Moreover, efforts are made to develop nets that are detectable for the sonar of whales due to the material density or mesh geometry (Trippel et al. 2003).

Whale strandings, for example those of sperm whales at the North Sea coast during the last few years, are also believed to be caused by failures of the echolocation system (Simmonds 1997, Jauniaux et al. 1998, Tougaard 1999). A better understanding of the principles in whale orientation might also help to explain and prevent mass strandings and thus rescue the animals.

Furthermore, insights into biosonar function offer the opportunity for new technical applications because the principle of ultrasound generation and emission in whales differs basically from modern technologies. The benefit may be the development of ultrasonic transducers with fully adjustable frequency modulation for material inspection, in advanced processing of industrial materials (e.g. drilling), and in medical diagnostics and therapy (e.g. sonography). Toothed whales outclass our technological equipment for material discrimination because they may use a wide frequency range (Au 1993, Ridgway and Au 1999). They have probably larger sound fields than modern man-made systems, which are limited by the necessity to choose a frequency and by the size of the oscillator (Schlegermann 1986, Hassler and Soldner 1995). A better understanding of how toothed whales focus their sound field, again, could improve ultrasound applications. So far, the focusing of

industrial equipment is limited by the physical traits of lenses and lens materials, respectively (Schlegermann 1986, Mooney and Wilson 1994, Hassler and Soldner 1995). In this respect, co-operations with research laboratories outside the universities are essential to combine the results of basic research including physical models with technical applications.

## 9. REFERENCES


Abel O. 1902. Die Ursache der Asymmetrie des Zahnwalschädels. Sitzungsberichte der mathematisch-naturwissenschaftlichen Classe der kaiserlichen Akademie der Wissenschaften 111:510-529.

Amundin M. 1991. Helium effects on the click frequency spectrum of the harbour porpoise, *Phocoena phocoena*. J Acoust Soc Am 90:53-59.

Amundin M, Andersen SH. 1983. Bony nares air pressure and nasal plug muscle activity during click production in the harbour porpoise, *Phocoena phocoena*, and the bottlenosed dolphin, *Tursiops truncatus*. J exp Biol 105:275-282.

Amundin M, Cranford TW. 1990. Forehead anatomy of *Phocoena phocoena* and *Cephalorhynchus commersoni*: 3-dimensional computer generated reconstructions with emphasis on the nasal diverticula. In: Thomas J, Kastelein RA, editors. Sensory Abilities of Cetacea. New York: Plenum Press. p. 1-18.

Aristoteles 350BC. Tierkunde. In: Gohlke P, editor. 1949. Aristoteles – Tierkunde. Paderborn: Ferdinand Schoningh.

Aroyan JL, McDonald MA, Webb SC, Hildebrand JA, Clark D, Laitman, JT, Reidenberg, JS. 2000. Acousic models of sound production and propagation. In: Au WWL, Popper AN, Fay RR, editors. Hearing by Whales and Dolphins. New York: Springer. p. 409-470.

Arvy L. 1977. Asymmetry in Cetaceans. In: Pilleri G, editor. Investigations on Cetacea. Vol. 8. Berne, Switzerland. p.161-212.

Au WWL. 1993. The Sonar of Dolphins. New York: Springer Verlag.

Au WWL. 2000. Echolocation in dolphins. In: Au WWL, Popper AN, Fay RR, editors. Hearing by Whales and Dolphins. New York: Springer. p. 364-408.

Au WWL, Benoit-Bird KJ. 2003. Automatic gain controle in the echolocation system of dolphins. Nature 423:861-863.

Au WWL, Kastelein RA, Rippe T, Schooneman NM. 1999. Transmission beam pattern and echolocation signals of a harbor porpoise (*Phocoena phocoena*). J Acoust Soc Am 106:3699-3705.

Backhaus K, Erichson B, Plinke W, Weiber R. 1996. Multivariate Analysemethoden. Berlin, Heidelberg: Springer.

Backus RH, Schevill WE. 1966. *Physeter* Clicks. In: Norris K, editor. Whales, Dolphins and Porpoises. Berkeley: University of California Press. p. 510-528.

Barlow J, Cameron GA. 2003. Field experiments show that acoustic pingers reduce marine mammal bycatch in the California drift gill net fishery. Mar Mammal Sci 19:265-283.

Barnes LG. 1985. Fossil Pontoporiid dolphins (Mammalia: Cetacea) from the Pacific coast of North America. Contributions in Science 363:1-34.

Behrmann G, Klima M. 1985. Knorpelstrukturen im Vorderkopf des Pottwals *Physeter macrocephalus*. Z Säugetierkunde 50:347-365.

Bel'kowitsch WM, Nesterenko JI. 1972. Das Ortungsorgan der Delphine. Naturwiss Rdsch 25:143-147.

Benham WB. 1901. On the anatomy of *Cogia breviceps*. Proc Zool Soc Lond 2:107-134.

Benke H. 1994. Menschlicher Einfluß und Schutzmaßnahmen. In: Niethammer J, Krapp F, editors. Handbuch der Säugetiere Europas. Wiesbaden: Aula-Verlag. p. 112-122.

Benninghoff A. 1925. Form und Bau der Gelenkknorpel in ihrer Beziehung zur Funktion. Erste Mitteilung: Die modellierenden und formerhaltenden Faktoren des Knorpelreliefs. Z Anat Entwickl Gesch 76:43-63.

Berzin AA. 1972. The Sperm Whale. Jerusalem: Israel Program for Scientific Translations.

Blinkow SM, Glezer II. 1968. Das Zentralnervensystem in Zahlen und Tabellen. Jena: Gustav Fischer.

Blomberg J, Lindholm LE. 1976. Variations in lipid composition and sound velocity in melon from the North Atlantic pilot whale, *Globicephala melaena melaena*. Lipids 11:153-156.

Boenninghaus G. 1903. Der Rachen von *Phocoena communis* Less. Zoologische Jahrbücher 17:1-99.

Bordino P, Kraus S, Albereda D, Fazio A, Palmerio A, Mendez M, Botta S. 2002. Reducing incidental mortality of franciscana dolphin *Pontoporia blainvillei* with acoustic warning devices attached to fishing nets. Mar Mammal Sci 18:833-842.

Borri C. 1932. L'asimmetria del cranio dei Cetacei. Archivio Zoologico Italiano 16:751-759.

Brouwers MEL, Kaminga C, Klooswijk AIJ, Terry RP. 1990. The use of computed tomography in cetacean research. Airsacs determination of *Lagenorhynchus albirostris*; Part 1. Aquat Mamm 16:145-155.

Busnel RG, Dziedzic A, Alcuri G. 1974. Études préliminaires de signaux acoustiques du *Pontoporia blainvillei* Gervais et D'Orbigny (Cetacea, Platanistidae). Mammalia 38:449-459.

Carrier DR, Deban SM, Otterstrom J. 2002. The face that sank the Essex: potential function of the spermaceti organ in aggression. J exp Biol 205:1755-1763.

Clarke MR. 1970. Function of the spermaceti organ of the sperm whale. Nature 228:873-874.

Clarke MR. 1978a. Buoyancy control as a function of the spermaceti organ in the sperm whale. J Mar Biol Assoc UK 58:27-71.

Clarke MR. 1978b. Physical properties of spermaceti oil in the sperm whale. J Mar Biol Assoc UK 58:19-26.

Clarke MR. 1978c. Structure and proportions of the spermaceti organ in the sperm whale. J Mar Biol Assoc UK 58:1-17.

Clarke MR. 1979. Der Kopf des Pottwals. Spektrum der Wissenschaft 3:20-28.

Cockcroft VG, Ross GJB. 1990. Observations on the early development of a captive bottlenose dolphin calf. In: Leatherwood S, Reeves R, editors. The Bottlenose Dolphin. New York: Academic Press. p. 461-478.

Connor RC, Smolker RA. 1996. "Pop" goes the dolphin: a vocalization male bottlenose dolphins produce during consortships. Behaviour 133:643-662.

Cranford TW. 1992. Functional morphology of the odontocete forehead: Implications for sound generation. Dissertation, University of California, Santa Cruz, pp. 276.

Cranford TW. 1999. The sperm whale's nose: sexual selection on a grand scale. Mar Mammal Sci 15:1133-1157.

Cranford TW. 2000. In search of impulse sound sources in odontocetes. In: Au WWL, Popper AN, Fay RR, editors. Hearing by Whales and Dolphins. New York: Springer. p. 109-155.

Cranford TW, Takaki L, Hudson M, Ramires K. 1993. Do "jaw" pops originate in the dolphins nose? Am Zool 33:106.

Cranford TW, Amundin M, Norris KS. 1996. Functional morphology and homology in the odontocete nasal complex: implication for sound generation. J Morphol 228:223-285.

Cranford TW, Bonn WG van, Chaplin MS, Carr JA, Kamolnick TA, Carder DA, Ridgway SH. 1997. Visualizing dolphin signal generation using high speed video endoscopy. J Acoust Soc Am 102:3123.

Cranford TW, Elsberry WR, Blackwood DJ, Carr JA, Kamolnick TA, Bonn WG van, Carder DA, Ridgway SH. 2001. Anatomy and physiology of bilateral sonar signal generation in the bottlenose dolphin. Talk at the 14th Biennial Conference on the Biology of Marine Mammals in Vancouver, B.C., Canada.

Cranford TW, Huggenberger S, Oelschläger HHA. (in prep). Functional morphology of the sperm whale nose: a 3-dimensional study. Biol Rev.

Culik BM, Koschinski S, Tregenza N, Ellis GM. 2001. Reactions of harbor porpoises *Phocoena phocoena* and herring *Clupea harengus* to acoustic alarms. Mar Ecol Prog Ser 211:255-260.

Curry BE. 1992. Facial anatomy and potential function of facial structures for sound production in the harbour porpoise (*Phocoena phocoena*) and Dall's porpoise (*Phocoenoides dalli*). Can J Zool 70:2103-2114.

Danois E. 1910. Recherches sur l'anatomie de la tête de *Kogia breviceps* Blainv. Arch de Zool Exp et Gen 6:149-174.

Dawson SM. 1988. The high frequency sounds of free-ranging Hector's dolphins, *Cephalorhynchus hectori*. Rep Int Whal Commn Special Issue 9:339-341.

# REFERENCES


Dormer KJ. 1979. Mechanism of sound production and air recycling in delphinids: Cineradiographic evidence. J Acoust Soc Am 65:229-239.

Dral ADG. 1972. Aquatic and aereal vision in the bottlenosed dolphin. Neth J Sea Res 5:510-513.

Dubrovskii NA, Zaslavskii GL. 1975. Role of the skull bones in the space-time development of the dolphin echolocation signal. Soviet Physics/Acoustics 21:255-258.

Duncker HR. 1990. Respirationstrakt. In: Hinrichsen KV, editor. Human-Embryologie. Berlin: Springer. p. 571-606.

Dyce KM, Sack WO, Wensing CJG. 1991. Anatomie der Haustiere. Stuttgart: Ferdinand Enke.

Evans WE, Awbrey FT, Hackbarth H. 1988. High frequency pulses produced by free-ranging Commerson's dolphins (*Cepholorhynchus commersonii*) compared to those of phocoenids. Rep Int Whal Commn special issue 9:173-181.

Felts WJL. 1966. Some functional and structural characteristics of cetacean flippers and flukes. In: Norris KS, editor. Whales, Dolphins, and Porpoises. Berkeley and Los Angeles: University of California Press. p. 255-276.

Felts WJL, Spurrell FA. 1965. Structural orientation and density in cetacean humeri. Am J Anat 116:171-204.

Fish FE. 2000. Biomechanics and energetics in aquatic and semiaquatic mammals: Platypus and whales. Physiol Biochem Zool 73:683-698.

Fleischer G. 1975. Über Beziehungen zwischen Hörvermögen und Schädelbau bei Walen. Säugetierkundliche Mitteilungen 24:48-59.

Fleischer G. 1976. Hearing in extinct cetaceans as determined by cochlear structure. Journal of Paleontology 50:133-152.

Fleischer G. 1982. Hörmechanismen bei Delphinen und Walen. HNO 30:123-130.

Flewellen CG, Morris RJ. 1978. Sound velocity measurements on samples from the spermaceti organ of the sperm whale (*Physeter catodon*). Deep-Sea Res 25:269-277.

Fordyce RE. 1994. *Waipatia maerewhenua*, new genus and new species (Waipatiidae, new family) an archaic late Oligocene dolphin (Cetacea: Odontoceti: Platanistoidea) from New Zealand. Proc San Diego Soc Hist 29:147-176.

Fordyce RE, Muizon C de. 2001. Evolutionary history of the cetaceans: a review. In: Mazin JM, Buffrénil V de, editors. Secondary Adaptation of Tetrapods to Life in Water. München: Verlag Dr. Friedrich Pfeil. p. 169-234.

Gallardo A. 1913. Notas sobre la anatomia del aparato espiracular, laringe y hioides de dos delfines: *Phocaena dioptrica* Lahille y *Lagenorhynchus fitzroyi* (Waterhouse) Flower. Anales del Museo Nacional de Historia Natural de Buenos Aires 23:235-245.

Gambell R. 1994. *Physeter catodon* Linnaeus, 1758 – Pottwal. In Niethammer J, Krapp F, editors. Handbuch der Säugetiere Europas. Vol. 6. Meeressäuger. Wiesbaden: Aula-Verlag. p 625-646.

Gingerich PD, Haq M ul, Zalmout IS, Khan IH, Malkani MS. 2001. Origin of whales from early artiodactyls: Hands and feet of Eocene Protocetidae from Pakistan. Science 293:2239-2242.

Goodson AD, Datta S. 1995. Investigating the sonar signals of the harbour porpoise, *Phocoena phocoena*. Journal of the Acoustical Society of India 23:205-211.

Goodson AD, Kastelein RA, Sturtivant CR. 1995. Source levels and echolocation signal characteristics of juvenile harbour porpoises (*Phocoena phocoena*) in a pool. In: Nachtigall PE, Lien J, Au WWL, Read AJ, editors. Harbour Porpoises - Laboratory Studies to Reduce Bycatch. Woerden: De Spil Publishers. p. 41-54.

Goold JC, Jefferson TA. 2002. Acoustic signals from free-ranging finless porpoises (*Neophocaena phocaenoides*) in the water around Hong Kong. Raffles B Zool 10 (Supp.):131-139.

Goold JC, Bennell JD, Jones SE. 1996. Sound velocity measurements in spermaceti oil under combined influences of temperature and pressure. Deep-Sea Res 43:961-969.

Green RF, Ridgway SH, Evans WE. 1980. Functional and descriptive anatomy of the bottlenosed dolphin nasolyngeal system with special reference to the musculature associated with sound production. In: Busnel RG, Fish JF, editors. Animal Sonar Systems. New York: Plenum Press. p. 199-238.

Gruhl K. 1911. Beiträge zur Anatomie und Physiologie der Cetaceennase. Jenaische Zeitschrift für Naturwissenschaft 47:367-414.

Haddad D, Huggenberger S, Haas-Rioth M, Kossatz LS, Oelschläger HHA, Haase A. (in prep). MR microscopy of prenatal dolphins: a documentation of internal structures and comparison with routine histology. J Comput Assist Tomogr.

Hartmann MG, Kamminga C, Klooswijk AIJ, Fleischer G. 1992. The use of computer tomography in odontocete morphology - preliminary results. In: Symoens JJ, editor. Whales: Biology - Threats - Conservation. Brussels, Belgium: Royal Academy of Overseas Sciences. p. 157-166.

Hassler D, Soldner R. 1995. Ultraschalltechnik. In: Morneburg H, editor. Bildgebende Systeme für die Medizinische Diagnostik. Erlangen: Publics MCD. p. 191-225.

Hatakeyama Y, Soeda H. 1990. Studies on echolocation of porpoises taken in salmon gillnet fisheries. In: Thomas J, Kastelein R, editors. Sensory Abilities of Cetaceans. New York: Plenum Press. p. 269-281.

Heyning JE. 1989. Comparative facial anatomy of beaked whales (Ziphiidae) and a systematic revision among the families of extant odontoceti. Contributions in Science 405:1-64.

Heyning JE, Mead JG. 1990. Evolution of the nasal anatomy of cetaceans. In: Thomas JA, Kastelein RA, editors. Sensory Abilities of Cetaceans. New York: Plenum Press. p. 67-79.

Hosokawa H. 1950. On the cetacean larynx, with special remarks on the laryngeal sac of the sei whale and the aryteno-epiglottideal tube of the sperm whale. Sci Rep Whales Res Inst 3:23-62.

Howell AB. 1925. Asymmetry in the skulls of mammals. Proc US Nat Mus 67:1-18.

Huber E. 1934. Contribution to palaeontology IV: Anatomical notes on pinnipedia and cetacea. Publ Carnegie Inst, Washington 447:105-136.

Jacobs MS, Jensen AV. 1964. Gross aspects of the brain and a fiber analysis of cranial nerves in the great whale. J Comp Neurol 123:55-72.

Jaquet N, Dawson S, Douglas L. 2001. Vocal behavior of male sperm whales: Why do they click? J Acoust Soc Am 109:2254-2259.

Jauniaux T, Brosens L, Jacquinet E, Lambrigts D, Addink M, Smeenk C, Coignoul F. 1998. Postmortem investigations on winter stranded sperm whales from the coasts of Belgium and the Netherlands. J Wildlife Dis 34:99-109.

Kamminga C. 1988. Echolocation signal types of odontocetes. In: Nachtigall PE, Moore PWB, editors. Animal Sonar. New York: Plenum Press. p. 9-22.

Kamminga C, Wiersma H. 1981. Investigations of cetacean sonar II: acoustical similarities and differences in odontocete sonar signals. Aquat Mamm 8:41-62.

Kamminga C, Wiersma H. 1982. Investigations of cetacean sonar V: the true nature of the sonar sound of *Cephalorhynchus commersonii*. Aquat Mamm 9:95-104.

Kamminga C, Hove MT van, Engelsma FJ, Terry RP. 1993. Investigations on cetacean sonar X: a comparative analysis of underwater echolocation clicks of *Inia* and *Sotalia* spp. Aquat Mamm 19:31-43.

Kastelein RA, Dubbeldam JL, Luksenburg J, Staal C, Immerseel AAH van. 1997. An anatomical atlas of an adult female harbour porpoise (*Phocoena phocoena*). In: Read AJ, Wiepkema PR, Nachtigall PE, editors. The Biology of the Harbour Porpoise. Woerden: De Spil Publishers. p. 87-178.

Kastelein RA, Au WWL, Haan D de. 2000. Detection distances of bottom-set gillnets by harbour porpoises (*Phocoena phocoena*) and bottlenose dolphins (*Tursiops truncatus*). Mar Environ Res 49:359-375.

Kastelein RA, Au WWL, Rippe HT, Schooneman NM. 1999. Target detection by an echolocating harbor porpoise (*Phocoena phocoena*). J Acoust Soc Am 105:2493-2498.

Kernan JD, Schulte H von W. 1918. Memoranda upon the anatomy of the respiratory tract, foregut, and thoracic viscera of a foetal *Kogia breviceps*. Bull Am Mus Nat Hist 38:231-267.

Ketten DR. 2000. Cetacean ears. In: Au WWL, Popper AN, Fay RR, editors. Hearing by Whales and Dolphins. New York: Springer. p. 43-108.

Killebrew DA, Mercado III E, Herman LM, Pack AA. 2001. Sound production of a neonate bottlenose dolphin. Aquat Mamm 27:34-44.

Kinkel MD, Thewissen JGM, Oelschläger HA. 2001. Rotation of the middle ear ossicles during cetacean development. J Morphol 249:126-131.

Klima M. 1987. Morphogenesis of the nasal structures of the skull in toothed whales (Odontoceti). In: Kuhn HJ, Zeller U, editors. Morphogenesis of the Mammalian Skull. Hamburg: Paul Parey. p. 105-122.

Klima M. 1990. Histologische Untersuchungen an Knorpelstrukturen im Vorderkopf des Pottwals *Physeter macrocephalus*. Gegenbaurs Morph Jahrb 136:1-16.

Klima M. 1995. Cetacean phylogeny and systematics based on the morphogenesis of the nasal skull. Aquat Mamm 21:79-89.

Klima M. 1999. Development of the cetacean nasal skull. Advances Anat Embryol Cell Biol 149:1-143.

Klima M, Seel M, Deimer P. 1986. Die Entwicklung des hochspezialisierten Nasenschädels beim Pottwal (*Physeter macrocephalus*). Gegenbaurs Morph Jahrb 132:245-284, 349-374.

Knauff M. 1905. Ueber die Anatomie der Beckenregion beim Braunfisch (*Phocoena communis* Less.). Jenaische Zeitschrift für Naturwissenschaft 40:253-318.

Kooyman GL. 1973. Respiratory adaptations in marine mammals. Am Zool 13:457-468.

Kooyman GL, Andersen HT. 1969. Deep diving. In: Andersen HT, editor. The Biology of Marine Animals. New York and London: Academic Press. p. 65-93.

Kröger RHH, Kirschfeld K. 1993. Optics of the harbor porpoise eye in water. J Opt Soc Am A 10:1481-1489.

Kükenthal W. 1893. Vergleichend-anatomische und entwicklungsgeschichtliche Untersuchungen an Walthieren. Denkschr med-naturwiss Ges Jena 3:1-448.

Kükenthal W. 1908. Ueber die Ursache der Asymmetrie des Walschädels. Anat Anz 33:609-618.

Kummer B. 1959. Bauprinzipien des Säugerskeletes. Stuttgart: Thieme.

Kummer B. 1985. Kausale Histogenese der Gewebe des Bewegungsapparates und funktionelle Anpassung. In: Benninghoff A, editor. Makroskopische und mikroskopische Anatomie des Menschen. Bd. 1. München: Urban & Schwarzenberg. p 199-213.

Lawrence B, Schevill WE. 1956. The functional anatomy of the delphinid nose. Bull Mus Comp Zool 114:103-151.

Lawrence B, Schevill WE. 1965. Gular musculature in delphinids. Bull Mus Comp Zool 133:1-65.

Litchfield C, Greenberg AJ. 1974. Comparative lipid patterns in the melon fats of dolphins, porpoises and toothed whales. Comp Biochem Physiol 47:401-407.

Litchfield C, Greenberg AJ, Caldwell DK, Caldwell MC, Sipos JC, Ackman RG. 1975. Comparative lipid patterns in acoustical and nonacoustical fatty tissues of dolphins, porpoises and toothed whales. Comp Biochem Physiol 50:591-597.

Lusseau D. 2003. The emergence of cetaceans: phylogenetic analysis of male social behaviour supports the Cetartiodactyla clade. J Evol Biol 16:531-535.

Mackay RS, Liaw HM. 1981. Dolphin vocalisation mechanisms. Science 212:676-678.

Madar SI. 1998. Structural adaptations of early archaeocete long bones. In: Thewissen JGM, editor. The Emergence of Whales. New York: Plenum Press. p. 353-378.

Madsen PT. 2002. Sperm whale sound production. Dissertation, Department of Zoophysiology, Biological Institute, University of Aarhus, Denmark.

Madsen PT, Payne R, Kristiansen NU, Wahlberg M, Kerr I, Møhl B. 2002a. Sperm whale sound production studied with ultrasound time/depth-recording tags. J Exp Biol 205:1899-1906.

Madsen PT, Wahlberg M, Møhl B. 2002b. Male sperm whale (*Physeter macrocephalus*) acoustics in a high-latitude habitat: implications for echolocation and communication. Behav Ecol Sociobiol 53:31-41.

Madsen PT, Carder DA, Au WWL, Nachtigall P, Møhl B, Ridgway SH. 2003. Sound Production in neonate sperm whales (L). J Acoust Soc Am 113:2988-2991.

Marten K, Norris KS, Moore PWB, Englund KA. 1988. Loud impulse sounds in odontocete predation and social behavior. In: Nachtigall PE, Moore PWB, editors. Animal Sonar. New York: Plenum Press. p. 567-579.

Marten K, Herzing D, Poole M, Newmann Allman K. 2001. The acoustic predation hypothesis: linking underwater observations and recordings during odontocete predation and observing the effects of loud impulsive sounds on fish. Aquat Mamm 27:56-66.

Mead JG. 1972. Anatomy of the external nasal passages and facial complex in the Delphinidae (Mammalia: Cetacea). Dissertation, University of Chicago. [7]

Mead JG. 1975. Anatomy of the external nasal passage and facial complex in the delphinidea (Mammalia: Cetacea). Smithson Contrib Zool 207:1-72.

Milinkovitch MC. 1995. Molecular phylogeny of cetaceans prompts revision of morphological transformations. Trends Ecol Evol 10:328-334.

Miller GS. 1923. The telescoping of the cetacean skull. Smithson Misc Collect 76:1-71.

Møhl B. 2001. Sound transmission in the nose of the sperm whale *Physeter catodon*. A post mortem study. J Comp Physiol A 187:335-340.

[7] Citation after Cranford et al. 1996

Møhl B. 2003. The monopulse-nature of sperm whale sonar clicks. Talk at the Conference of the European Cetacean Society in Las Palmas de Gran Canaria, Spain.

Møhl B, Andersen S. 1973. Echolocation: high-frequency component in the click of the harbour porpoise (*Phocoena ph.* L.). J Acoust Soc Am 54:1368-1372.

Møhl B, Wahlberg M, Madson PT, Miller LA, Surlykke A. 2000. Sperm wale clicks: Directionality and source level revisited. J Acoust Soc Am 107:638-648.

Møhl B, Madsen PT, Wahlberg M, Au WWL, Nachtigall PE, Ridgway SH. 2002. Sound transmission in the spermaceti complex of a recently expired sperm whale calf. ARLO 4:19-24.

Mooney MG, Wilson MG. 1994. Linear array transducers with improved image quality for vascular ultrasonic imaging. Hewlett-Packard Journal 10: 43-51.

Morgane PJ, Jacobs MS. 1972. Comparative anatomy of the cetacean nervous system. In: Harrison RJ, editor. Functional Anatomy of Marine Mammals. London: Academic Press. p. 117-244.

Moris F. 1969. Etude anatomique de la region céphalique du marsouin, *Phocoena phocoena* L. (Cetace, Odontocete). Mammalia 33:666-705.

Morris RJ. 1973. The lipid structure of spermaceti organ of the sperm whale (*Physeter catodon*). Deep-Sea Res 20:911-916.

Morris RJ. 1975. Further studies into the lipid structure of spermaceti organ of the sperm whale (*Physeter catodon*). Deep-Sea Res 22:483-489.

Morris RJ. 1986. The acoustic faculty of dolphins. In: Bryden MM, Harrison R, editors. Research on Dolphins. Oxford: Clarendon Press. p. 369-399.

Negus V. 1958. The Comparative Anatomy and Physiology of the Nose and Paranasal Sinuses. Edingburgh and London: Livingstone.

Ness AR. 1967. A measure of asymmetry of the skulls of odontocete whales. J Zool (Lond) 153:209-221.

Nickel R, Schummer A, Seiferle, E. 1968. Lehrbuch der Anatomie der Haustiere. 3. Auflage. Berlin und Hamburg: Paul Parey.

Nikaido M, Matsuno F, Hamilton H, Brownel RL, Cao Y, Ding W, Zuoyan Z, Shedlock AM, Fordyce RE, Hasegawa M, Okada N. 2001. Retroposon analysis of major cetacean lineages: the monophyly of toothed whales and paraphyly of river dolphins. PNAS 98:7384-7389.

Nishiwaki M, Ohsumi S, Meada Y. 1963. Change of form in the sperm whale accompanied with growth. Sci Rep Whales Res Inst 17:1-17

Noldus LPJJ, De Klerk RJJ. 1984. Growth of the skull of the harbour porpoise, *Phocoena phocoena* (Linnaeus, 1758), in the North Sea, after age determination based on dental growth layer groups. Zool Meded (Leiden) 58:213-239.

Norris KS. 1964. Some problems of echolocation in cetaceans. In: Tavolga UN, editor. Marine Bio-Acoustics. Oxford: Pergamon Press. p. 317-336.

Norris KS. 1968. The evolution of acoustic mechanisms in odontocete cetaceans. In: Drake ET, editor. Evolution and Enviroment. New Haven: Yale University Press. p. 297-324.

Norris KS. 1969. The echolocation of marine mammals. In: Andersen HT, editor. The Biology of Marine Mammals. New York & London: Academic Press. p. 391-423.

Norris KS. 1975. Cetacean biosonar - Part I: Anatomical and behavioral studies. In: Malins DC, Sargent JR, editors. Biochemical and Biophysical Perspectives in Marine Biology. New York: Academic Press. p. 215-236.

Norris KS. 1980. Peripheral sound processing in odontocetes. In: Busnel RG, Fish JF, editors. Animal Sonar Systems. New York: Plenum Press. p. 495-509.

Norris KS, Harvey GW. 1972. A theory of the function of the spermaceti organ of the sperm whale (*Physeter catodon*). In: Galler SR, Schmidt-Koenig K, Jacobs GJ, Belleville RE, editors. Animal Orientation and Navigation. Washington, D.C.: Scientific and Technical Information Office, National Aeronautics and Space Administration (NASA). p. 397-417.

Norris KS, Harvey GW. 1974. Sound transmission in the porpoise head. J Acoust Soc Am 56:659-665.

Norris KS, Møhl B. 1983. Can odontocetes debilitate prey with sound? Am Nat 122:85-104.

Norris KS, Prescott JH, Asa-Dorian PV, Perkins P. 1961. An experimental demonstration of echolocation behavior in the porpoise, *Tursiops truncatus* (Montagu). Biol Bull 120:163-176.

Norris KS, Dormer KJ, Pegg J, Liese GJ. 1971. The mechanisms of sound production and air recycling in porpoises: a preliminary report. Proceedings of the 8th Annual Conference Biol. Sonar and Diving Mammals, Menlo Park, CA, Stanford Research Institute: 113-129. [8]

Oelschläger HA. 1986. Comparative morphology and evolution of the otic region in toothed whales (Cetacea, Mammalia). Am J Anat 177:353-368.

Oelschläger HA. 1990. Evolutionary morphology and acoustics in the dolphin skull. In: Thomas J, Kastelein RA, editors. Sensory Abilities of Cetaceans. New York: Plenum Press. p. 137-162.

Oelschläger HHA. 2000. Morphological and functional adaptations of the toothed whale head to aquatic live. Historical Biology 14:33-39.

Oelschläger HA, Buhl EH. 1985. Development and rudimentation of the peripheral olfactory system in the harbor porpoise *Phocoena phocoena* (Mammalia, Cetacea). J Morphol 184:351-360.

Oelschläger HA, Kemp B. 1998. Ontogenesis of the sperm whale brain. J Comp Neurol 399:210-228.

Oelschläger HHA, Oelschläger JS. 2002. Brain. In: Perrin WF, Würsig B, Thewissen JGM, editors. Encyclopedia of Marine Mammals. San Diego: Academic Press. p. 133-158.

Olesiuk PF, Nichol LM, Sowden MJ, Ford JKB. 2002. Effect of the sound generated by an acoustic harassment device on the relative abundance and distribution of harbor porpoises (*Phocoena phocoena*) in retreat passage, British Columbia. Mar Mammal Sci 18:843-862.

Pabst DA. 1996. Morphology of the subdermal connective tissue sheath of dolphins: a new fibre-bound, thin-walled, pressurized cylinder model for swimming vertebrates. J Zool (Lond) 238:35-52.

Pabst DA, Rommel SA, McLellan WA. 1999. The functional morphology of marine mammals. In: Reynolds JE, Rommel SA, editors. Biology of Marine Mammals. Washington: Smithsonian Institution Press. p. 15-72.

Papastavrou V, Smith SC, Whitehead H. 1989. Diving behaviour of the sperm whale, *Physeter macrocephalus*, off the Galapagos Islands. Can J Zool 67:839-846.

Papez JW. 1927. Subdivisions of the facial nucleus. J Comp Neurol 43:159-191.

Pilleri G. 1964. Zur Morphologie des Auges vom Weisswal, *Delphinapterus leucas* (Pallas). Hvalråd Skr 47:3-16.

Pilleri G. 1990. Adaption to water and the evolution of echolocation in the Cetacea. Ethol Ecol Evol 2:135-163.

Pilleri G, Gihr M. 1970. The central nervous system of the mystecete and odontocete whales. In: Pilleri G, editor. Investigations on Cetacea. Vol. 2. Berne, Switzerland. p. 89-128.

Pilleri G, Gihr M, Kraus C. 1983. Near field, interference, far field and rostrum structure in the echolocation system of cetaceans. In: Pilleri G, editor. Investigations on Cetacea. Vol. 15. Berne, Switzerland. p. 11-142.

Pitman RL. 2002. Mesoplodont whales. In: Perrin WF, Würsig B, Thewissen JGM, editors. Encyclopedia of Marine Mammals. San Diego: Academic Press. p. 738-742.

Podos J, Silva VMF da, Rossi-Santos MR. 2002. Vocalisations of Amazon river dolphins, *Inia geoffrensis*: insights into the evolutionary origins of delphinid whistles. Ethology 108:601-612.

Pouchet G, Beauregard H. 1885. Note sur "l'organe des spermaceti". Comptes Rendus de la Société de Biologie Paris 8:342-344.

Purves PE, Pilleri G. 1983. Echolocation in Whales and Dolphins. London: Academic Press.

Püttner A. 1903. Die Augen der Wassersäugetiere. Zoologische Jahrbücher 17:99-402.

Rauschmann MA. 1992. Morphologie des Kopfes beim Schlanken Delphin *Stenella attenuata* mit besonderer Berücksichtigung der Hirnnerven. Dissertation, Johann Wolfgang Goethe-Universität Frankfurt am Main.

Rauschmann MA, Huggenberger S, Kossatz LS, Oelschläger HHA. (in prep.). Perinatal development of the head of spotted dolphins (*Stenella attenuata*). Evol Dev.

Rauschning W, Bergström K, and Pech P. 1983. Correlative craniospinal anatomy studies by computed tomography and cryomicrotomy. J Comput Assist Tomogr 7:9-13.

Raven HC, Gregory WK. 1933. The spermaceti organ and nasal passages of the sperm whale (*Physeter catodon*) and other odontocetes. Am Mus Novit 677:1-17.

[8] Citation after Norris 1980 and Cranford et al. 1996

Rawitz B. 1900. Die Anatomie des Kehlkopfes und der Nase von *Phocoena communis* Cuv. Intern Monatsschr Anat Physiol 17:245-354.

Reeves RR, Reijnders PJH. 2002. Conservation and management. In: Hoelzel AR, editor. Marine Mammal Biology: An Evolutionary Approach. Malden: Blackwell Science Ltd. p. 388-416.

Reeves RR, Smith BD, Crespo EA, Notarbartolo di Sciara G (compilers). 2003. Dolphins, Whales and Porpoises: 2002–2010 Conservation Action Plan for the World's Cetaceans. IUCN/SSC Cetacean Specialist Group. Gland and Cambridge: IUCN.

Reidenberg JS, Laitman JT. 1987. Position of the larynx in Odontoceti (toothed whales). Anat Rec 218:98-106.

Reidenberg JS, Laitman JT. 1988. Existence of vocal folds in the larynx of Odontoceti (toothed whales). Anat Rec 221:884-891.

Reidenberg JS, Laitman JT. 1994. Anatomy of the hyoid apparatus in Odontoceti (toothed whales): Specialisations of their skeleton and musculature compared with those of terrestrial mammals. Anat Rec 240:598-624.

Reidenberg JS, Laitman JT. 2002. Prenatal development in cetaceans. In: Perrin WF, Würsig B, Thewissen JGM, editors. Encyclopedia of Marine Mammals. San Diego: Academic Press. p. 998-1007.

Reiss D. 1988. Observations on the development of echolocation in young bottlenose dolphins. In: Nachtigall PE, Moore PWB, editors. Animal Sonar. New York: Plenum Press. p. 121-127.

Reiss D, McCowan B. 1993. Spontaneous vocal mimicry and production by bottlenose dolphins (*Tursiops truncatus*): evidence for vocal learning. J Comp Psych 107:301-312.

Reynolds JE, Rommel SA, Bolen ME. 2002. Anatomical dissection: thorax and abdomen. In: Perrin WF, Würsig B, Thewissen JGM, editors. Encyclopedia of Marine Mammals. San Diego: Academic Press. p. 21-30.

Rice DW. 1998. Marine Mammals of the World, Systematics and Distribution. (special publication number 4 of the Society for Marine Mammalogy) Lawrence: Allen Press.

Richardson MK, Oelschläger HHA. 2002. Time, pattern, and heterochrony: a study of hyperphalany in the dolphin embryo flipper. Evol Dev 4:435-444.

Ridgway SH, Carder DA. 1988. Nasal pressure and sound production in an echolocating white whale, *Delphinapterus leucas*. In: Nachtigall PE, Moore PWB, editors. Animal Sonar. New York: Plenum Press. p. 53-60.

Ridgway SH, Au WWL. 1999. Hearing and echolocation: Dolphin. In: Adelman G, Smith BH, editors. Elsevier's Encyclopedia of Neuroscience. New York: Elsevier Science. p. 858-862.

Ridgway SH, Carder DA. 2001. Assessing hearing and sound production in cetacean species not available for behavioral audiograms: experience with sperm, pygmy sperm, and gray whales. Aquat Mamm 27:267-276.

Ridgway SH, Carder DA, Green RF. 1980. Electromyographic and pressure events in the nasolaryngeal system of dolphins during sound production. In: Busnel RG, Fish JF, editors. Animal Sonar Systems. New York: Plenum Press. p. 239-249.

Ridgway, S. H., Carder, D. A., Kamolnick, T., Smith, R. R., Schlundt, C. E., Elsberry, W. R. 2001. Hearing and whistling in the deep sea: depth influences whistle spectra but does not attenuate hearing by white whales (*Delphinapterus leucas*) (Odontoceti, Cetacea). *J. Exp. Biol.* 204: 3829-3841.

Robineau D. 1994. Anatomie. In: Niethammer J, Krapp F, editors. Handbuch der Säugetiere Europas. Wiesbaden: Aula-Verlag GmbH. p. 83-102.

Rodionov VA, Markov VI. 1992. Functional anatomy of the nasal system in the bottlenose dolphin. In: Thomas JA, Kastelein RA, Supin AY, editors. Marine Mammal Sensory Systems. New York: Plenum Press. p. 147-177.

Rohlf FJ. 1999. Shape statistics: Procrustes superimpositions and tangent spaces. J Classif 16:197-223.

Romeis B. 1989. Mikroskopische Technik. 17th ed. München: Urban.

Rommel SA. 1990. Osteology of the bottlenose dolphin. In: Leatherwood S, Reeves RR, editors. The Bottlenose Dolphin. San Diego: Academic Press. p. 29-50.

Ross GJB. 1979. Records of pygmy and dwarf sperm whales, genus *Kogia*, from Southern Africa, with biological notes and some comparisons. Ann Cape Prov Mus (Nat Hist) 11:259-327.

Roux W. 1895. Gesammelte Abhandlungen über Entwicklungsmechanik der Organismen. Leipzig: Engelmann.

Scammon CM. 1874. The Marine Mammals of the Northwestern Coast of North America. San Francisco and New York: John H. Carmany and Company and G.P. Putnam's Sons. Republication 1968. New York: Dover Publications.

Schenkkan EJ. 1971. The occurrence and position of the "connecting sac" in the nasal tract complex of small odontocetes (Mammalia, Cetacea). Beaufortia 19:37-43.

Schenkkan EJ. 1972. On the nasal tract complex of *Pontoporia blainvillei* Gervais and D'Orbigny, 1844 (Cetacea, Platanistidae). In: Pilleri G, editor. Investigations on Cetacea. Vol. 4. Berne, Switzerland. p. 83-90.

Schenkkan EJ. 1973. On the comparative anatomy and function of the nasal tract in odontocetes (Mammalia, Cetacea). Bijdr Dierkd 43:127-159.

Schenkkan EJ. 1977. Notes on the nasal tract complex of the bouto, *Inia geoffrensis* (De Blainville, 1817) (Cetacea, Platanistidae). Bijdr Dierkd 46:275-283.

Schenkkan EJ, Purves PE. 1973. The comperative anatomy of the nasal tract and the function of the spermaceti organ in physeteridae (Mammalia, Odontoceti). Bijdr Dierkd 43:93-112.

Schlegermann U. 1986. Möglichkeiten zur Fokussierung von Ultraschallfeldern - ein Überblick. Materialprüfung 28:137-141.

Schneider R. 1964. Der Larynx der Säugetiere. In: Helmcke JG, Lengerken HV, Starck D, Wermuth H, editors. Handbuch der Zoologie. Vol. 8. Berlin: Walter De Gruyter. p.1-128.

Schulte HVW, Smith FM de. 1918. The external characters, skeletal muscles, and peripheral nerves of *Kogia breviceps* (Blainville). Bull Am Mus Nat Hist 38:7-72.

Sedmera D, Mišek I, Klima M. 1997a. On the development of cetacean extremities: I. Hind limb rudimentation in the spotted dolphin (*Stenella attenuata*). Eur J Morphol 35:25-30.

Sedmera D, Mišek I, Klima M. 1997b. On the development of cetacean extremities: II. Morphogenesis of the flippers in the spotted dolphin (*Stenella attenuata*). Eur J Morphol 35:117-123.

Sibson F. 1848. On the blowhole of the popoise. Philos Trans R Soc Lond:117-123.

Simmonds MP. 1997. The meaning of cetacean strandings. Smithson Contrib Zool 67:29-34.

Slijper EJ. 1936. Die Cetaceen, vergleichend-anatomisch und systematisch. Amsterdam: Asher & Co.B.V.

Steinmann G. 1912. Über die Ursache der Asymmetrie der Wale. Anat Anz 41:45-54.

Thewissen JGM, Williams EM, Roe LJ, Hussain ST. 2001. Skeletons of terrestrial cetaceans and the relationship of whales to artiodactyls. Nature 413:277-281.

Thode A, Mellinger DK, Stienessen S, Martinez A, Mullin K. 2002. Depth dependent acoustic features of diving sperm whales (*Physeter macrocephalus*) in the Gulf of Mexico. J Acoust Soc Am 112:308-321.

Tougaard S, Kinze CC. 1999. Sperm Whale Strandings in the North Sea. Esbjerg: Fisheries and Maritime Museum.

Trippel EA, Holy NL, Palka DL, Shepherd TD, Melvin GD, Terhune JM. 2003. Nylon barium sulphate gillnet reduces porpoise and seabird mortality. Mar Mammal Sci 19:240-243.

Tyson E. 1680. *Phocaena* or the anatomy of a porpess dissected at Grefham Colledge: with a praeliminary discourse concerning anatomy, and a natural history of animals. In: Pilleri G, editor. Investigations on Cetacea. Vol. 10 Supp. (1980). Berne, Switzerland. p. 11-65.

Van Beneden PJ, Gervais P. 1880. Ostéographie des Cétacés Vivants et Fossiles. Paris: Arthus Bertrand.

Verboom WC, Kastelein RA. 1995. Acoustic signals by harbour porpoises (*Phocoena phocoena*). In: Nachtigall PE, Lien J, Au WWL, Read AJ, editors. Harbour Porpoises - Laboratory Studies to Reduce Bycatch. Woerden: De Spil Publishers. p. 1-40.

Verboom WC, Kastelein RA. 1997. Structure of harbour porpoise (*Phocoena phocoena*) click train signals. In: Read AJ, Wiepkema PR, Nachtigall PE, editors. The biology of the harbour porpoise. Woerden: De Spil Publishers. p. 343-362.

Von Baer KE. 1826. Die Nase der Cetaceen erleutert durch Untersuchung der Nase des Braunfisches *Delphinus Phocoena*. Isis 19:811-847.

Wahlberg M. 2002. The acoustic behaviour of diving sperm whales observed with a hydrophone array. J Exp Mar Biol Ecol 281:53-62.

Wartzok D, Ketten DR. 1999. Marine mammal sensory systems. In: Reynolds JE, Rommel SA, editors. Biology of Marine Mammals. Washington: Smithsonian Institution Press. p. 117-175.

Watkins WA, Schevill WE. 1977. Sperm whale codas. J Acoust Soc Am 62:1485-1490.

Weber M. 1886. Ueber Asymmetrie der beiden Körperhälften bei Cetaceen. In: Studien über Säugethiere - Ein Beitrag zur Frage nach dem Ursprung der Cetaceen. Jena: Gustav Fischer. p. 181-183.

Weilgart LS, Whitehead H. 1988. Distinctive vocalisations from mature male sperm whales (*Physeter macrocephalus*). Can J Zool 66:1637-1931.

Weilgart LS, Whitehead H. 1993. Coda communication by sperm whales (*Physeter macrocephalus*) off the Galapagos Islands. Can J Zool 71:744-752.

Williams TM, Worthy GAJ. 2002. Anatomy and physiology: the challange of aquatic living. In: Hoelzel AR, editor. Marine Mammal Biology: An Evolutionary Approach. Malden, MA: Blackwell Science Ltd. p. 73-97.

Wilsman NJ, van Sickle DC. 1972. Cartilage canals, their morphology and distribution. Anat Rec 173:79-94.

Yurick DB, Gaskin DE. 1987. Asymmetry in the skull of the harbour porpoise *Phocoena phocoena* (L.) and its relationship to sound production and echolocation. Can J Zool 66:399-402.

Zhu Q, Hillmann DJ, Henk WG. 2001. Morphology of the eye and surrounding structures of the bowhead whale, *Balaena mysticetus*. Mar Mammal Sci 17:729-750.

## 10. ACKNOWLEDGMENTS

This dissertation project was only possible with the help of so many people along the way. My sincere thanks go to Prof. Boye K. Ahlborn for the interesting discussions on the physics of odontocete sound production; Dr. Harald Benke and Dr. Ursula Siebert for the donation of harbor porpoise specimens; Dr. Ted W. Cranford for his help in preparing and rewieving the manuscript, the donation of sperm whale material under his care, and, most of all, his enormous input in my understanding of the odontocete bio-sonar; Dipl. Inf. Marc Gillmann and Cand. Biol. Sonja Leidenberger for their help in morphometrical analysis of toothed whale skulls; Prof. Dr. Axel Haase and Dipl. Phys. Daniel Haddad for the capture and interpretation of MRI datasets of a fetal dolphin; Dipl. Biol. Michaela Haas-Rioth and Dipl. Biol. Lars S. Kossatz for the numerous discussions about cetacean biology and their help in creating and resolving computer problems; Prof. Dr. Darlene Ketten for the donation of a set of CT scans of a pygmy sperm whale; Irmgard Kirschenbauer for her help in preparing the histological sections; Prof. Dr. Milan Klima for his help in preparing the manuscript of sperm whale head structures; Georg Matjasko for his help in preparing the cryo-sections; Prof. Dr. Helmut A. Oelschläger, especially, for his continuos impact on my understanding on cetacean morphology and evolution as well as for advising this dissertation project; Dr. Michael A. Rauschmann, Dr. Jan Schmitt, Prof. Dr. Thomas J. Vogl, and the staff of the Institute for Diagnostic and Interventional Radiology for the enormous help in the capture of MRI and CT datasets of postnatal toothed whale material; Dr. Sam H. Ridgway for the donation of a sperm whale calf specimen; Dr. James G. Mead and Dr. Charles Potter for the warm welcome in the National Museum of Natural History in Washington, DC, and their input in my understanding of cetacean biology; Prof. Dr. Giorgio Pilleri and Dr. Gerhard Storch for the donation of toothed whale material under their care; Prof. Dr. Jürgen Winckler for the continous support of this project; Prof. Dr. Dr. h.c. Christian Winter for advising this dissertation.

This project depended very heavily on the financial support of the "Graduiertenförderung" of the Johann Wolfgang Goethe-University and the "Deutscher Akademischer Austauschdienst".

## 11. FIGURES

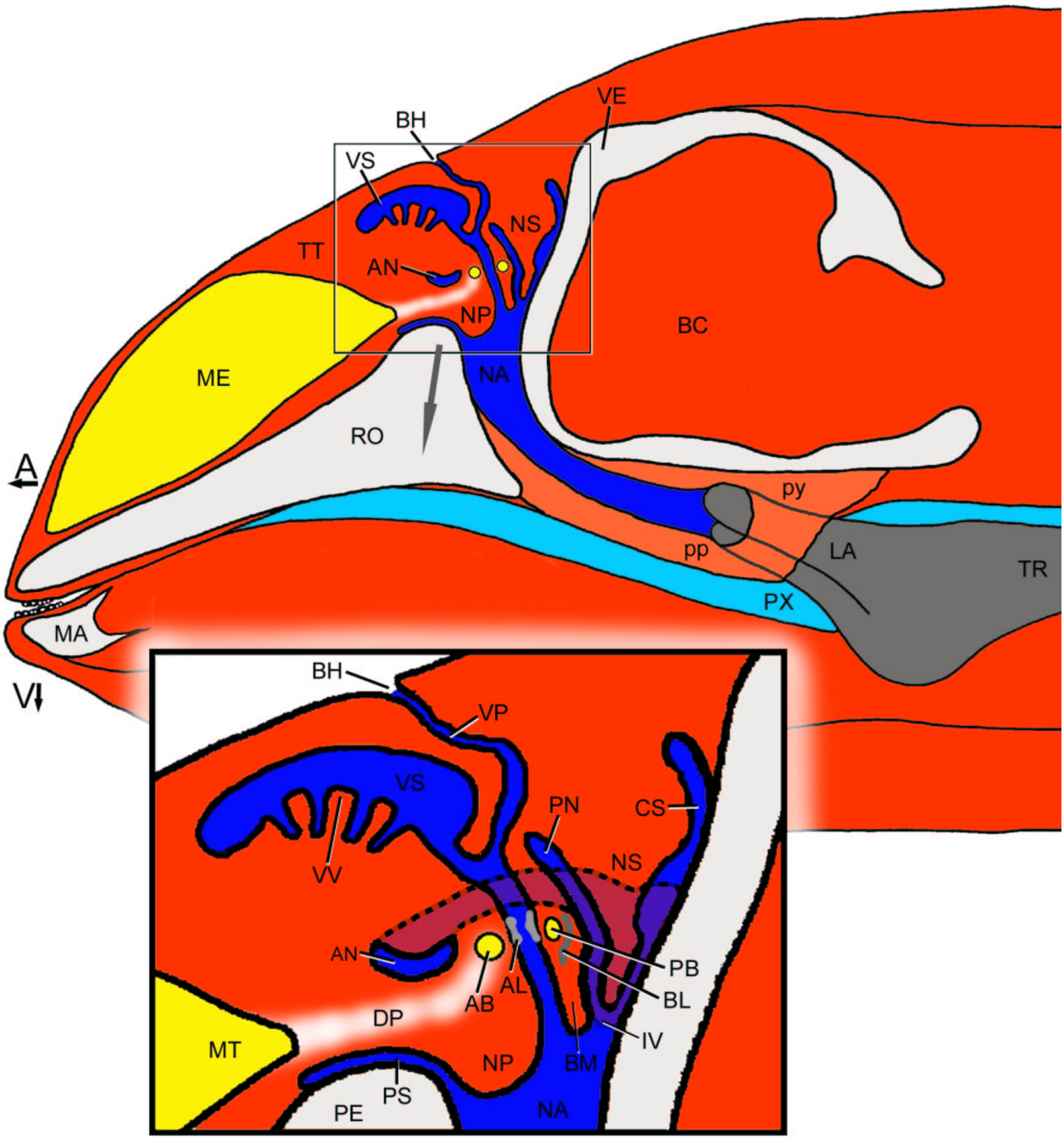


Figure 2: Sagittal schematic reconstruction of a harbor porpoise (*Phocoena phocoena*) head showing the nasal structures and the position of the larynx. A-anterior, AB-anterior dorsal bursa, AL-anterior monkey lip, AN-anterior nasofrontal sac, BC-brain cavity, BH-blowhole, BL-blowhole ligament, BM-blowhole ligament septum, CS-caudal sac, DP-low density pathway, IV-inferior vestibulum, LA-larynx, MA-mandible, ME-melon, MT-melon terminus, NA-nasal passage, NP-nasal plug, NS-nasofrontal septum, PB-posterior dorsal bursa, PE-premaxillary eminence, PN-posterior nasofrontal sac, pp-palatopharyngeus muscle, PS-premaxillary sac, PX-pharynx, py-pterygopharyngeus muscle, RO-rostrum, TR-trachea, TT-connective tissue theca, V-ventral, VE-vertex of skull, VP-vestibulum of nasal passage, VS-vestibular sac, VV-folded ventral wall of vestibular sac.

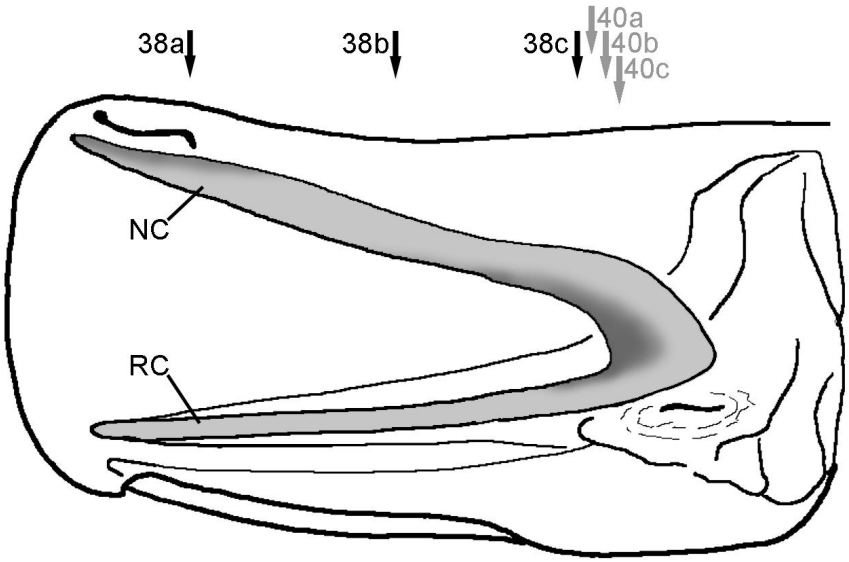


Figure 3: Outline drawing of the head of a neonate sperm whale in left lateral view showing the position of the nasal roof cartilage (NC) and the cartilaginous rostrum (RC). The arrows indicate planes of the cryo-sections in Figure 38 of which the tissue samples of both cartilaginous structures were taken and planes of the MRI scans in Figure 40.

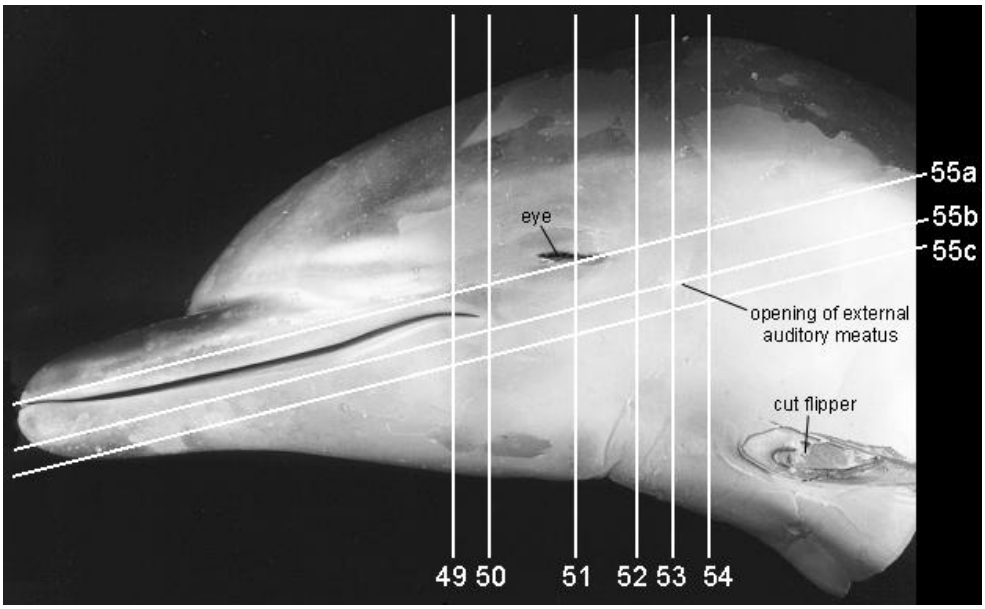


Figure 4: Lateral photograph of a perinatal spotted dolphin (*Stenella attenuata*) showing orientation of planes in Figs. 49 - 55. Modified after Rauschamnn et al. (in prep.).

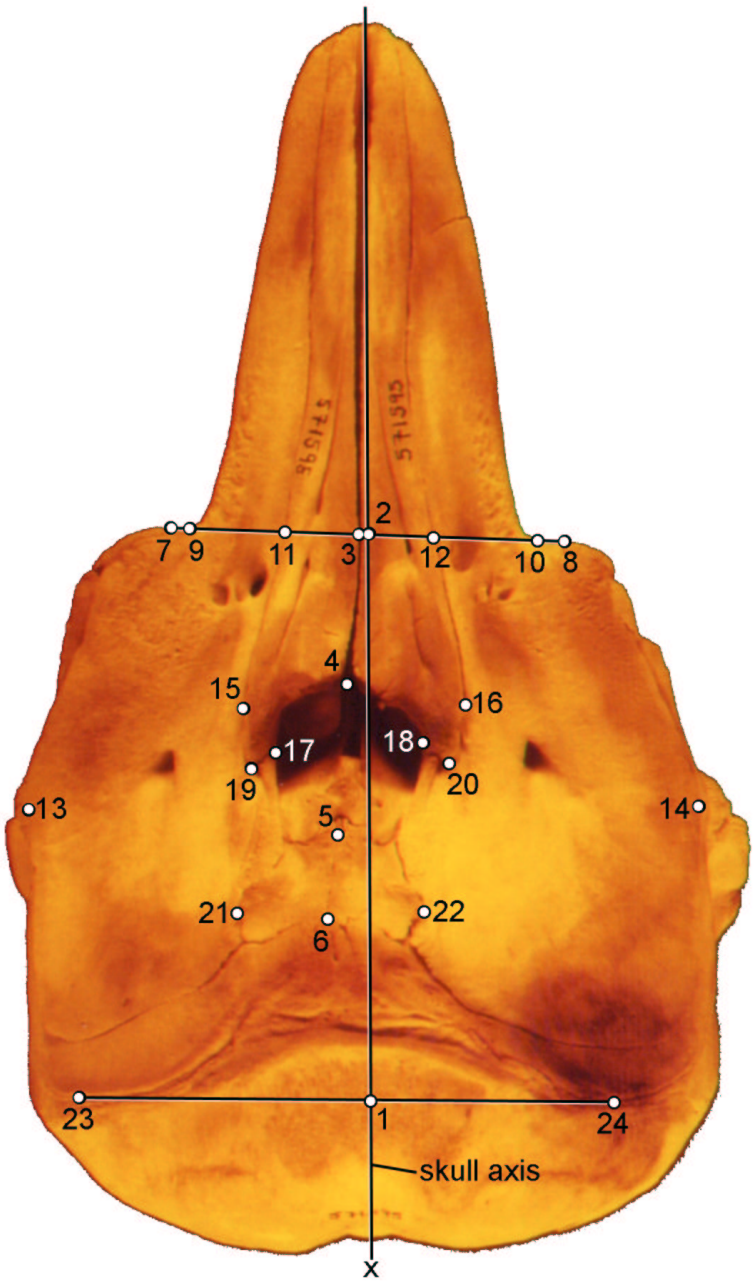


Figure 5: Location of landmarks on a toothed whale skull (harbor porpoise, *Phocoena phocoena*) in dorsal view (x-position mark of midpoint between occipital condyles, description of landmark position in table 3). Discription of main bony structures in Fig. 6.

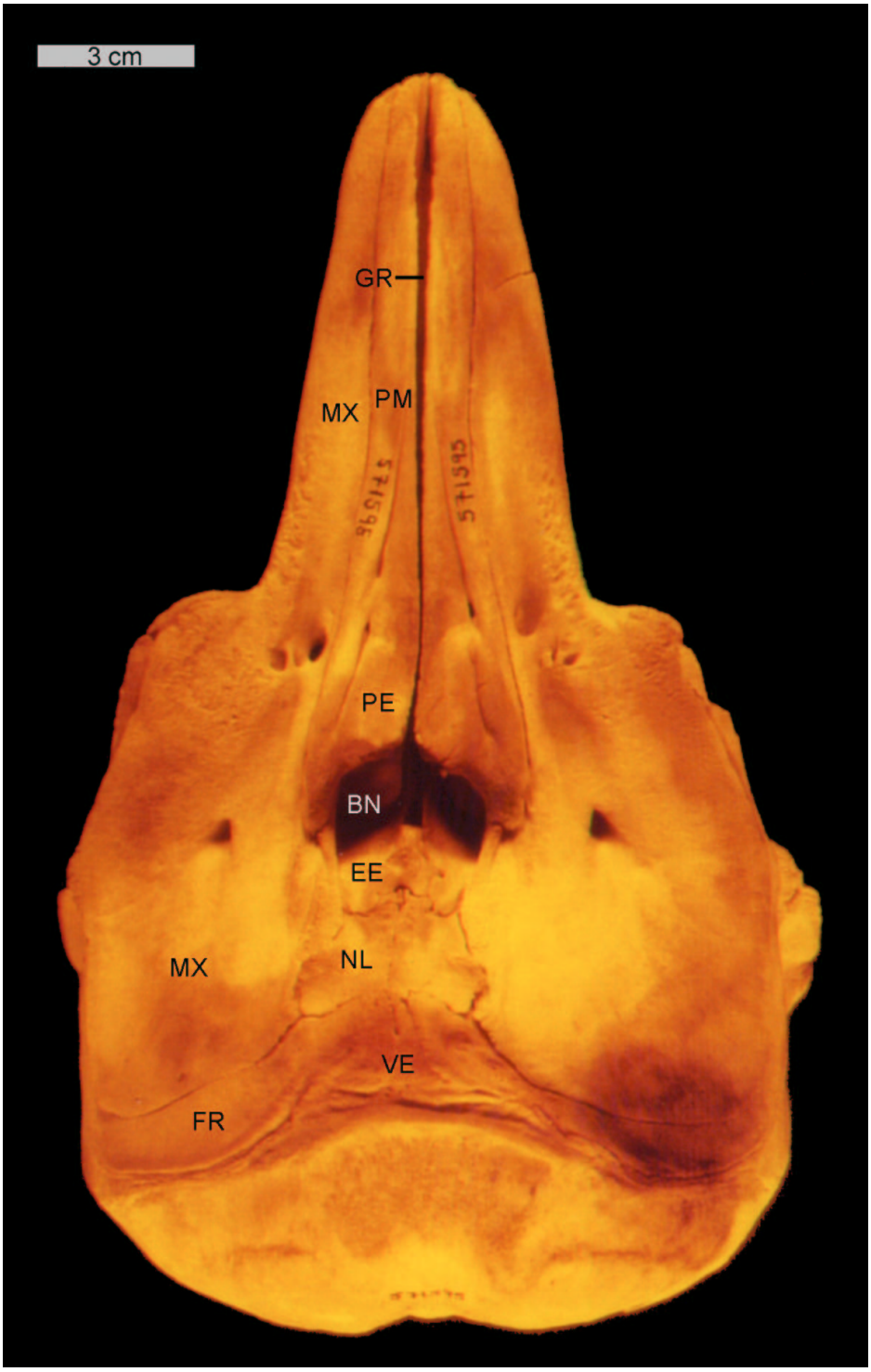


Figure 6: Dorsal view of a harbor porpoise (*Phocoena phocoena*) skull showing its main components and the "telescoping" phenomenon. BN-bony naris, EE-ectethmoid, FR-frontal, GR-groove of rostral cartilage, MX-maxilla, NL-nasal, PE-premaxillary eminence, PM-premaxilla, VE-vertex of skull.

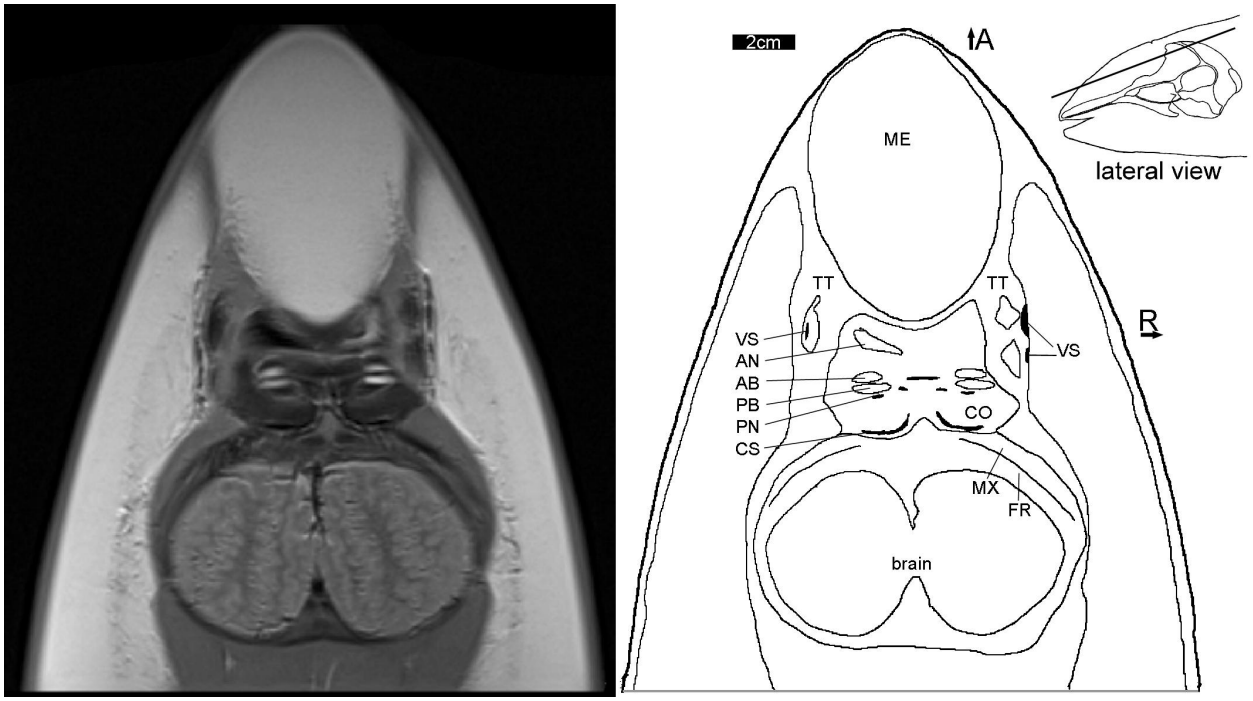


Figure 7: Horizontal T2-weighted MRI scan of the nasal complex in the harbor porpoise (*Phocoena phocoena*) at level of the dorsal bursae. The maxilla (MX) and the frontal bone (FR) are united in a "sandwich structure" (Fleischer 1982). A-anterior, AB-anterior dorsal bursa, AN-anterior nasofrontal sac, CO-connective tissue of porpoise capsule, CS-caudal sac, ME-melon, PB-posterior dorsal bursa, PN-posterior nasofrontal sac, R-right, TT-connective tissue theca, VS-vestibular sac.

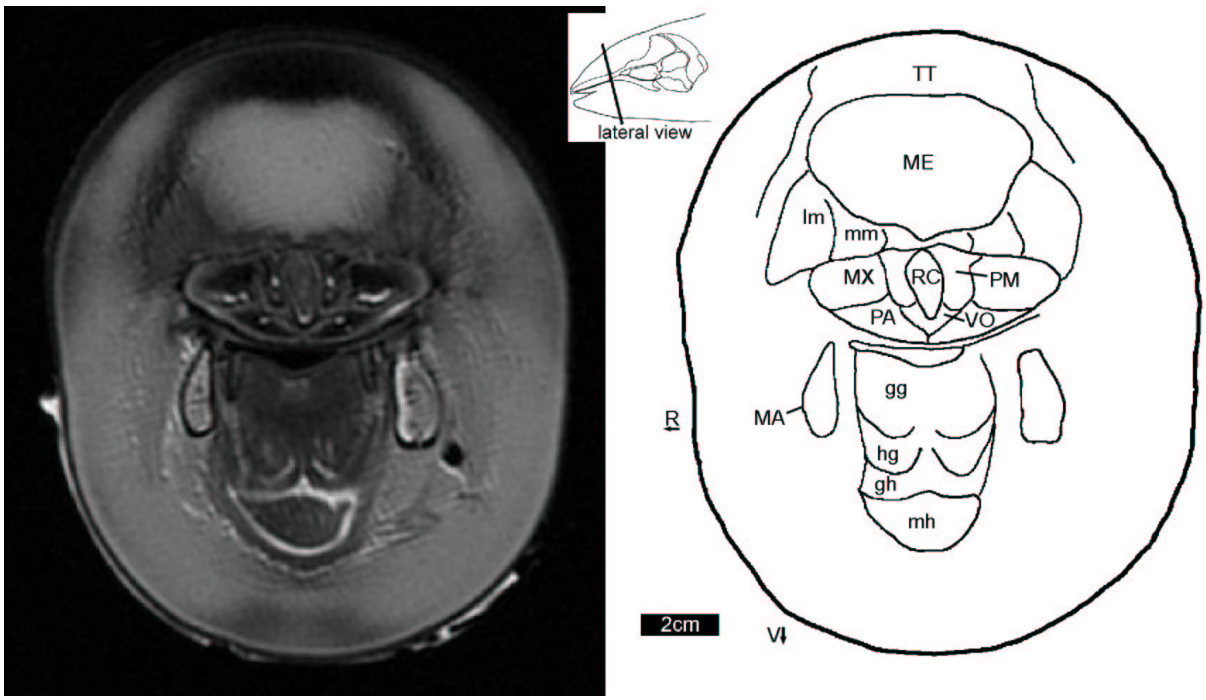


Figure 8: Transversal T1-weighted MRI scan of the rostral region in the harbor porpoise (*Phocoena phocoena*) anterior to the antorbital notch showing the melon (ME) and the rostral musculature. 5'-lateral rostral muscle, 6'-medial rostral muscle, gg-genioglossus muscle, gh-geniohyoid muscle, hg-hyoglossus muscle, MA-mandible, mh-mylohyoid muscle, MX-maxilla, PA-palatine, PM-premaxilla, RC-rostral cartilage (cartilaginous rostrum), R-right, TT-connective tissue theca, V-ventral, VO-vomer.

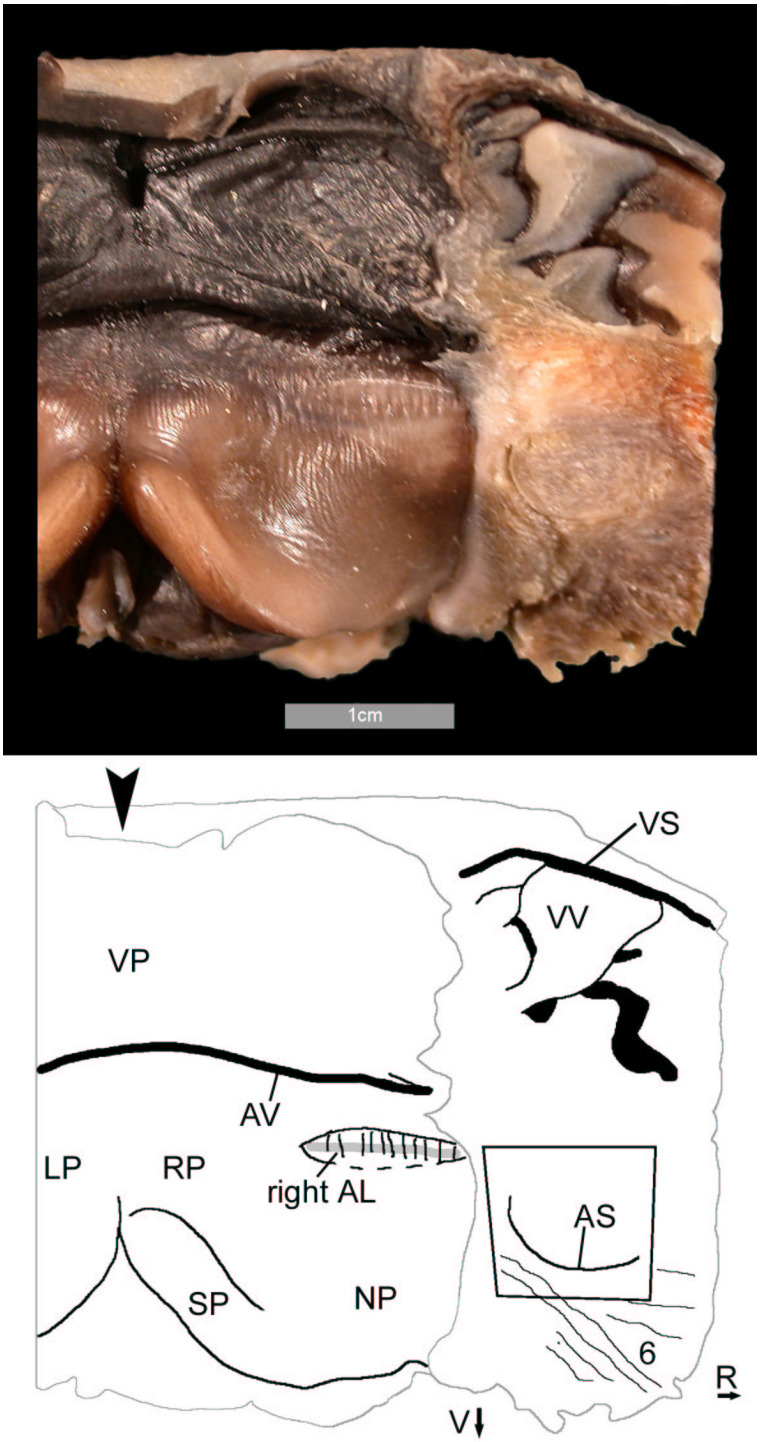


Figure 9: Caudal view of a transversal dissection parallel to the soft nasal passage in the harbor porpoise. View on the anterior wall of the right nasal passage (*Phocoena phocoena*) showing the anterior monkey lips and the angle. The arrow head marks the mediosagittal plane. The rectangle marks the section of Fig. 12e. 6-M. maxillonasolabialis p. profundus, AL-anterior monkey lip (note the vertical "wrinkles" [black] and the horizontal "mortise-tenon fold" [light gray] within the monkey lips), AS-angle of nasofrontal sac, AV-aperture of vestibular sac, LP-left nasal passage, NP-nasal plug, R-right, RP-right nasal passage, SP-sulcus of nasal plug, V-ventral, VP-vestibulum of nasal passage, VS-vestibular sac, VV-folded ventral wall of vestibular sac, WL-"wrinkles" of monkey lips.

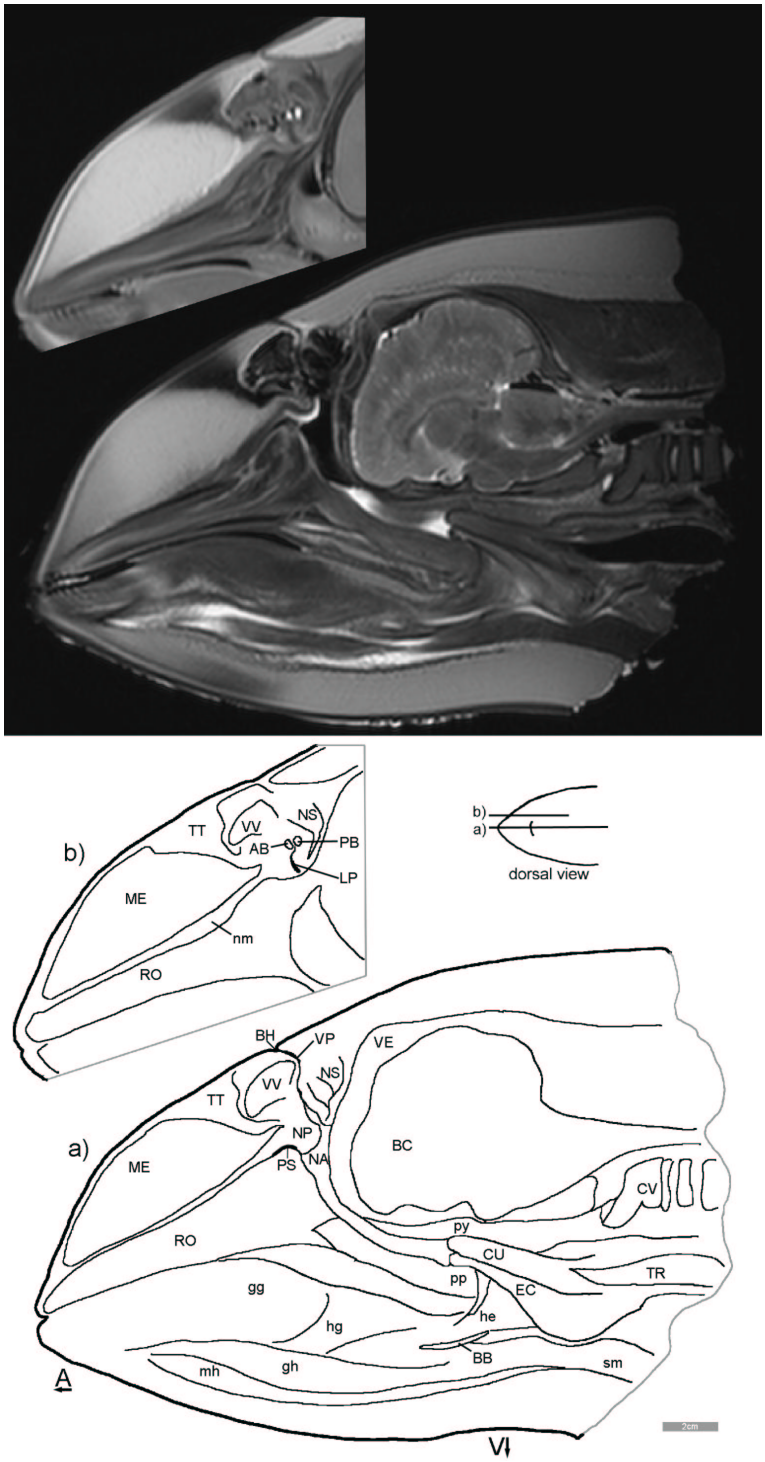


Figure 10: Sagittal MRI scan of the harbor porpoise (*Phocoena phocoena*) head. a) mediosagittal T1-weighted scan of an entire head. b) right parasagittal T2-weighted scan of the nasal complex at the level of the dorsal bursae. A-anterior, AB-anterior dorsal bursa, BB-basihyal bone, BC-brain cavity, BH-blowhole, CU-cuneiform cartilage, CV-cervical vertebrae, EC-epiglottid cartilage, gg-genioglossus muscle, gh-geniohyoid muscle, he-hyoepiglottic muscle, hg-hyoglossus muscle, LP-left nasal passage, mh-mylohyoid muscle, ME-melon, NA-nasal passage, nm-nasal plug muscle, NP-nasal plug, NS-nasofrontal septum, PB-posterior dorsal bursa, pp-palatopharyngeus muscle, PS-premaxillary sac, py-pterygopharyngeus muscle, RO-rostrum, sm-sternohyoid muscle, TR-trachea, TT-connective tissue theca, V-ventral, VE-vertex of skull, VP-vestibulum of nasal passage, VV-folded ventral wall of vestibular sac.

Figure 11 (next page ➔): Mediosagittal (a) and left parasagittal (b) cryosections of a harbor porpoise (*Phocoena phocoena*) head and neck showing the nasal structures and the position of the larynx. 1st -first tracheal cartilage, A-anterior, AB-anterior dorsal bursa, AS-angle of nasofrontal sac, AV-aperture of vestibular sac, BB-basihyal bone, BC-brain cavity, BH-blowhole, CM-core of melon, CR-cricoid cartilage, CS-caudal sac, CU-cuneiform cartilage, CV-cervical vertebrae, EC-epiglottic cartilage, ES-esophagus, gg-genioglossus muscle, gh-geniohyoid muscle, he-hyoepiglottic muscle, hg-hyoglossus muscle, ia-interarytenoid muscle, IF-left infraorbital foramen, IV-inferior vestibulum, LP-left nasal passage, MA-mandible, mh-mylohyoid muscle, NA-nasal passage, nm-nasal plug muscle, NS-nasofrontal septum, PB-posterior dorsal bursa, PE-premaxillary eminences, PH-pterygoid hamulus, PN-posterior nasofrontal sac, pp-palatopharyngeus muscle, PX-pharynx, RC-rostral cartilage (cartilaginous rostrum), RO-rostrum, RP-right nasal passage, sm-sternohyoid muscle, ST-sternum, SY-symphysis of mandibles, TO-tongue, TR-trachea, TT-connective tissue theca, V-ventral, VE-vertex of skull, VS-vestibular sac, VV-folded ventral wall of vestibular sac.

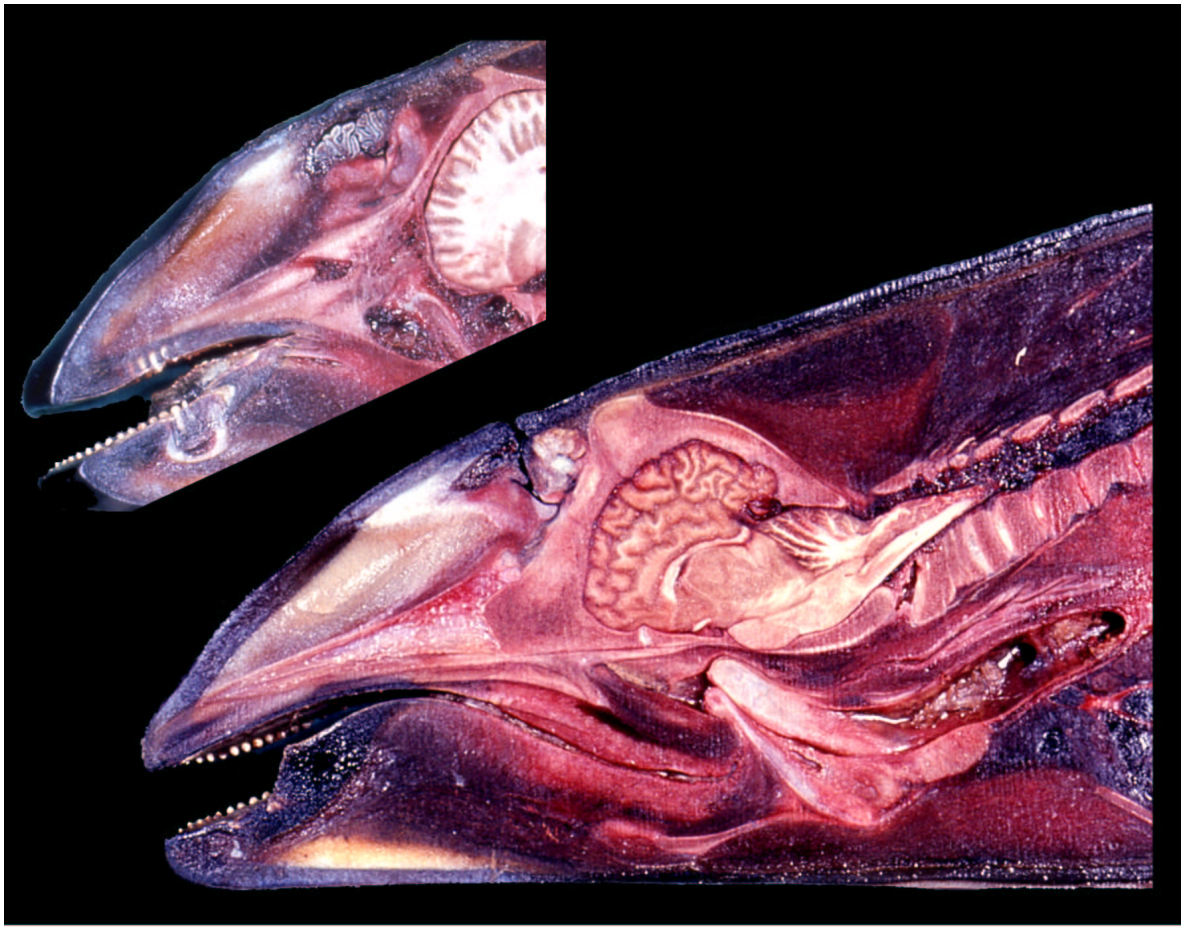

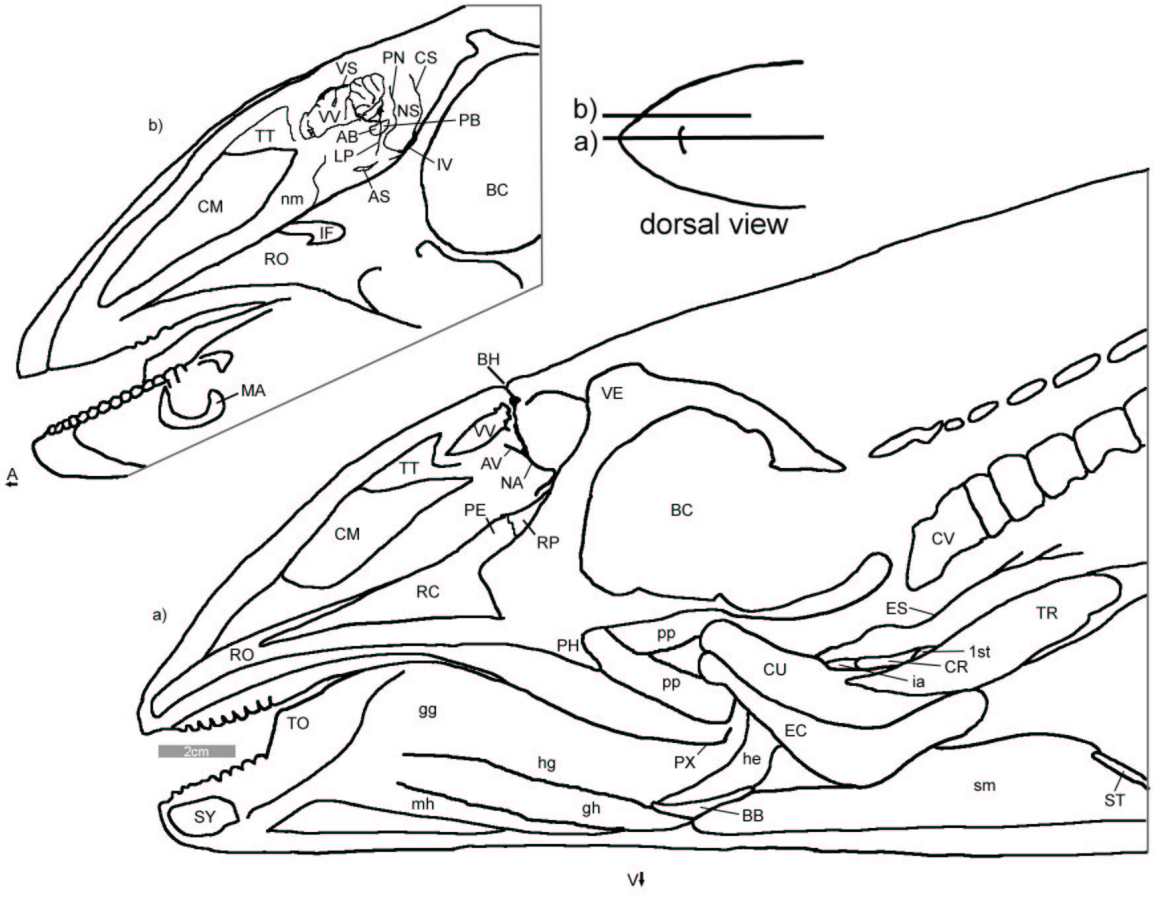
b)
VS
PN
CS
NS
PB
TT
AB
LP
IV
CM
nm
AS
BC
IF
RO
MA
A
BH
VE
VV
TT
AV
NA
PE
RP
BC
CM
CV
RC
a)
ES
TR
PH
pp
RO
CU
1st
CR
ia
pp
TO
gg
EC
2cm
hg
PX
he
sm
ST
SY
mh
gh
BB
V
b)
a)
dorsal view

Figure 12 (next page ➔): Parasagittal histological sections of the harbor porpoise (*Phocoena phocoena*) nasal complex stained with AZAN (for orientation cf. Fig. 2):
a) block of tissue including the left nasal plug (NP), anterior dorsal bursa (AB), and anterior nasofrontal sac (AN). Note that artificial boundaries are drawn in light gray in the "raod-maps".
b) left blowhole ligament septum with its ligament (BL) including the posterior dorsal bursa (PB). Note that a) and b) are different histological sections but arranged in their natural orientation and separated by an artificial wide left nasal passage.
c) ventral lip of blowhole ligament septum (sagittal plane medial to a and b) septum showing the intrinsic muscle (red reticulated material).
d) close-up of the rostral epithelium of the posterior nasofrontal sac showing the subepithelial papillae.
e) Transverse histological section of the angle of nasofrontal sac (AS); the orientation of the section is shown in Fig. 9. Note the u-shaped cross section and the small dorsal extension of the air sac (asterisk).
6-M. maxillonasolabialis p. profundus, A-anterior, AS-angle of nasofrontal sac, AV-aperture of vestibular sac, CO-connective tissue of porpoise capsule, DP-low density pathway, EN-epithelium of nasofrontal sac, EP-dorsal epithelium of premaxillary sac, LP-left nasal passage, mf-muscle fiber, ms-intrinsic muscle of blowhole ligament septum, P-posterior, V-ventral, x-artifact.

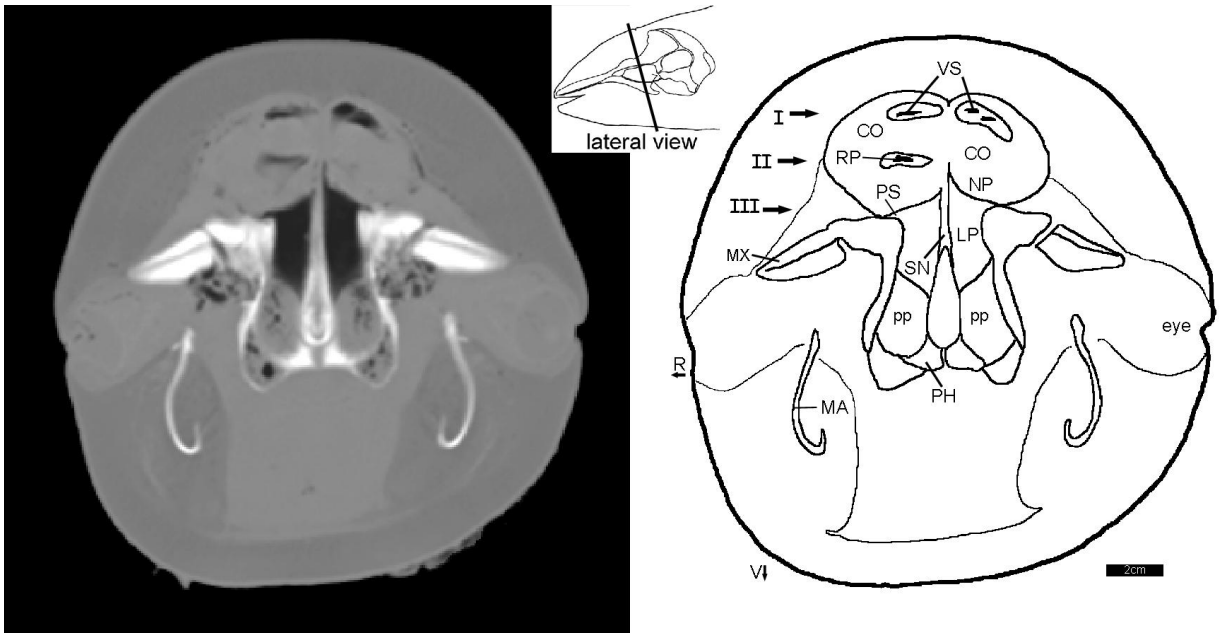


Figure 13: Transverse CT scan of the harbor porpoise (*Phocoena phocoena*) head at the level of the bony nares showing the "porpoise capsules" (left and right). I – III mark the three levels of nasal air sacs. CO-connective tissue of "porpoise capsule", LP-left nasal passage, MA-mandible, MX-maxilla, NP-nasal plug, PH-pterygoid hamulus, pp-palatopharyngeus muscle, PS-premaxillary sac, R-right, RP-right nasal passage, SN-nasal septum, V-ventral, VS-vestibular sacs.

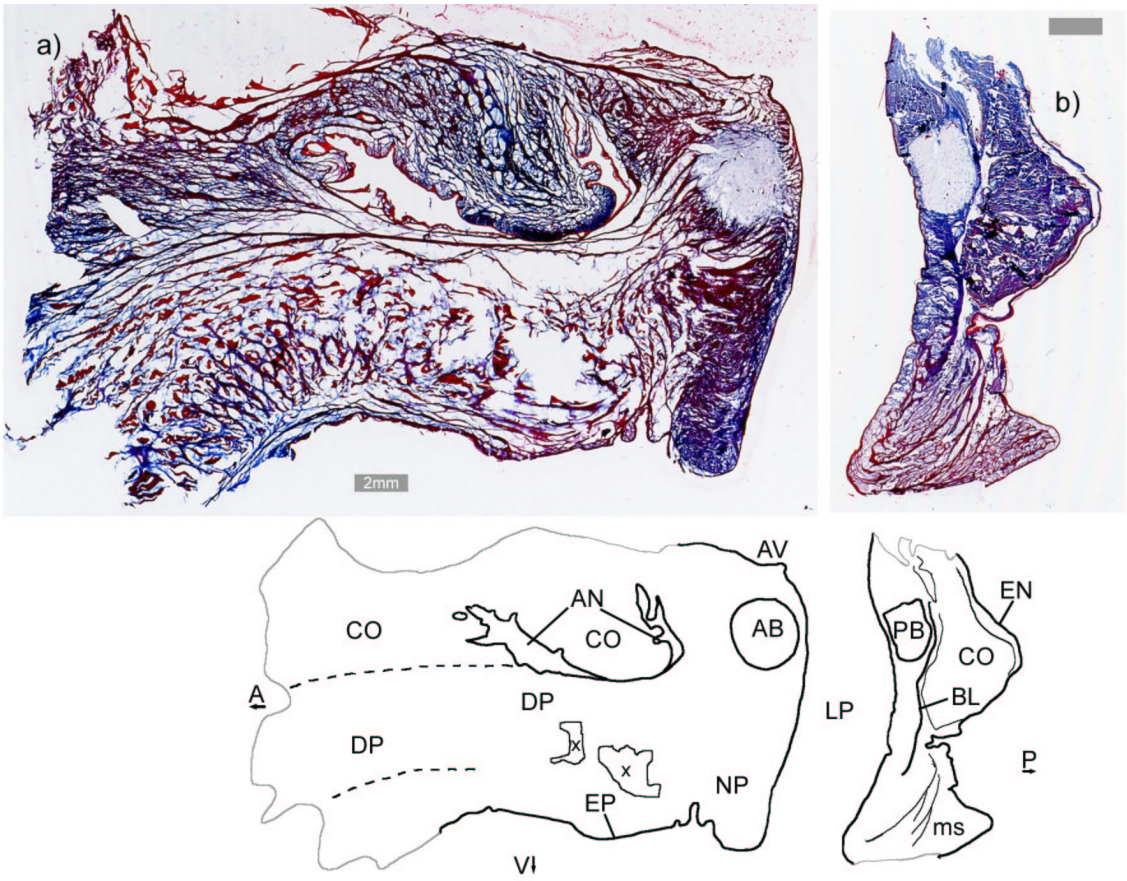
a)
2mm
b)
AV
AN
CO
CO
AB
A
DP
DP
x
x
NP
EP
VI
EN
PB
CO
BL
LP
P
ms
CO
EN
A
c)
ms
VI
mf
d)
0.6mm
e)
6
AS
CO
mf
2mm

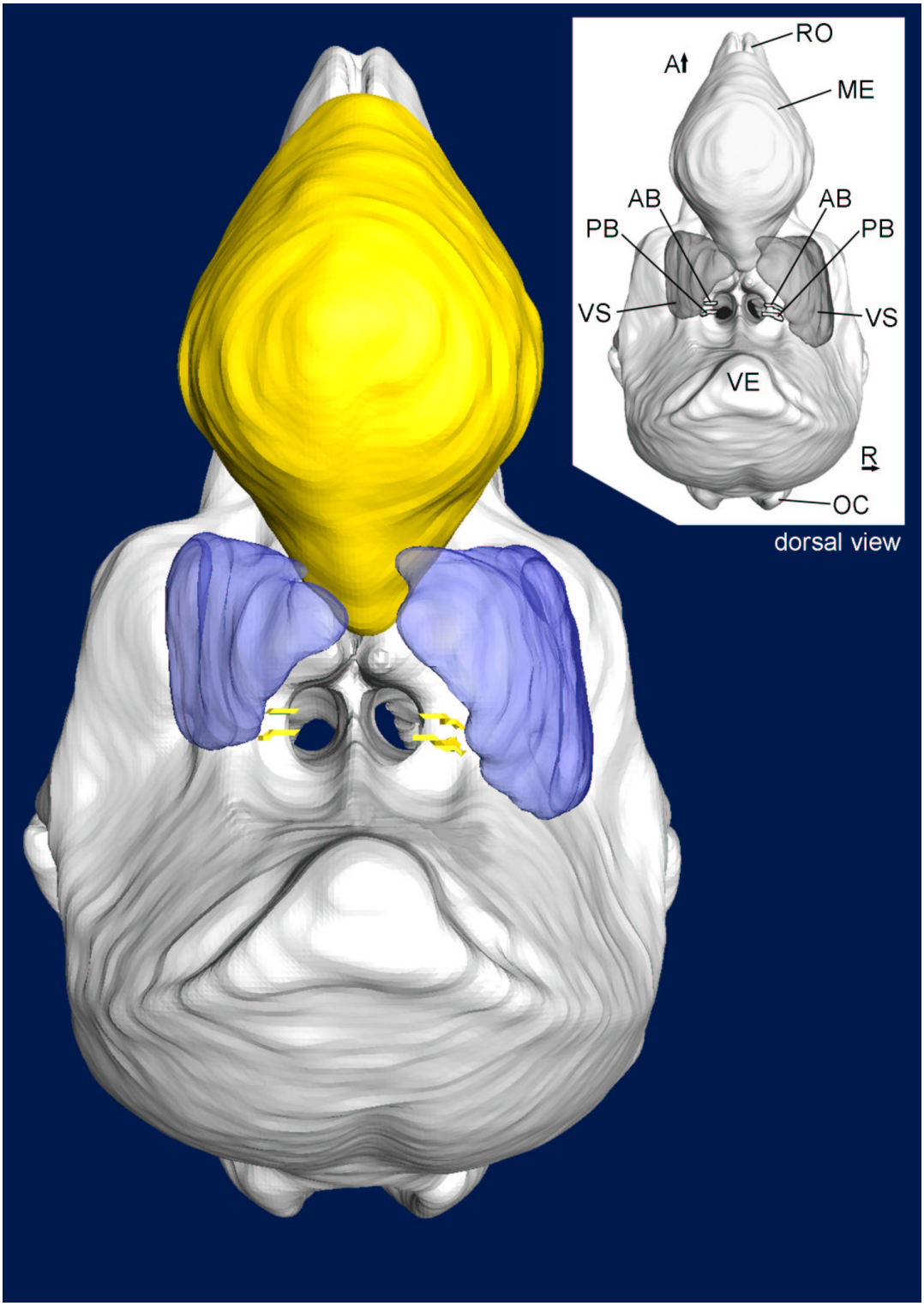


Figure 14: 3D-reconstruction of the harbor porpoise (*Phocoena phocoena*) nasal complex in dorsal view showing the topographic relations of the skull, melon, dorsal bursae, and vestibular sacs. A-anterior, AB-anterior dorsal bursa, ME-melon, OC-occipital condyle, PB-posterior dorsal bursa, R-right, RO-rostrum, VE-vertex of skull, VS-vestibular sac.

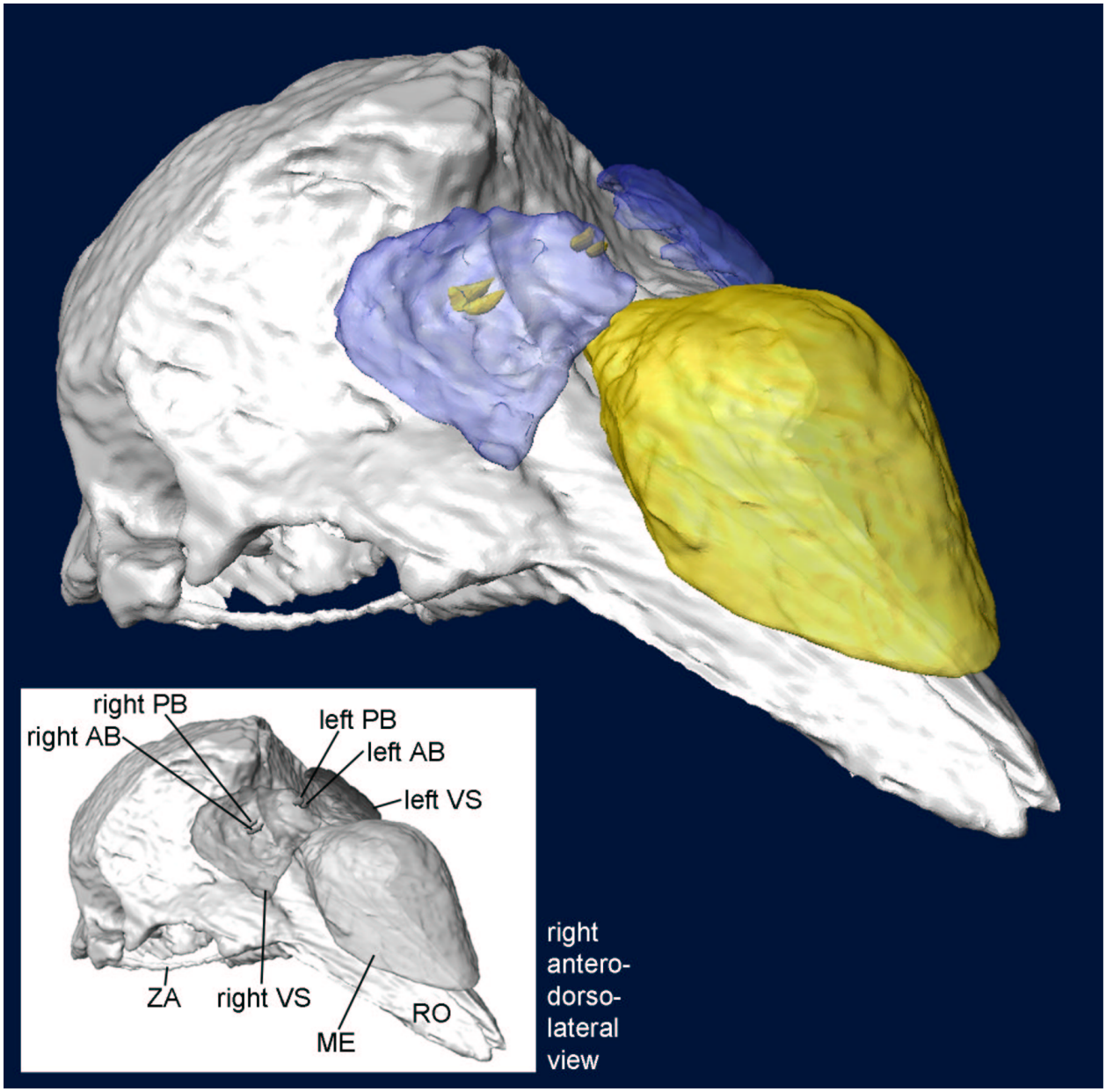


Figure 15: 3D-reconstruction of the harbor porpoise (*Phocoena phocoena*) nasal complex showing a right frontal dorsolateral view with the topographic relation of the skull, melon, dorsal bursae, and vestibular sacs. AB-anterior dorsal bursa, ME-melon, PB-posterior dorsal bursa, RO-rostrum, VS-vestibular sac, ZA-zygmatic arch.

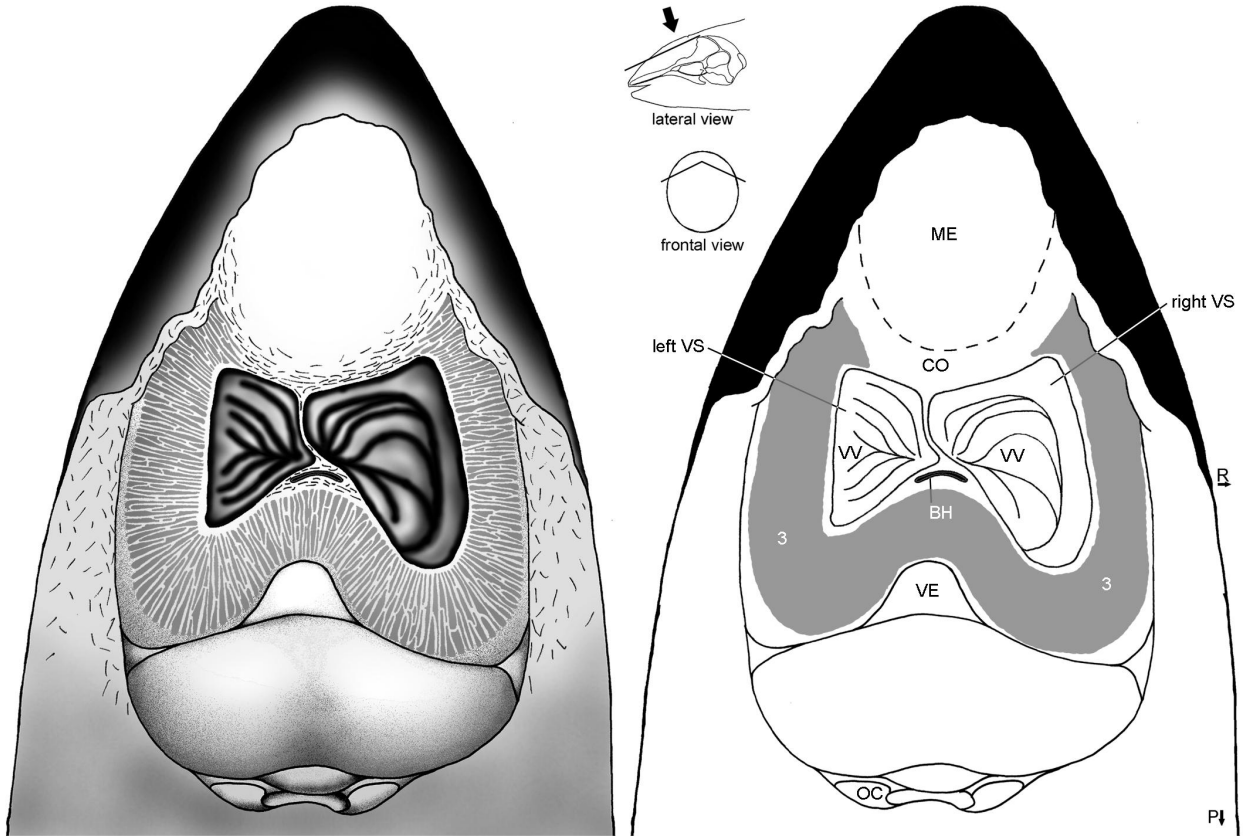


Figure 16: Schematic horizontal reconstruction of the vestibular sacs (VS) and anteroexternus muscle in the harbor porpoise (*Phocoena phocoena*) based on a macroscopical dissection of animal no. 1396 (Table 1) which showed the highest degree of asymmetry in the vestibular sacs of all specimens examined. 3-M. maxillonasolabialis p. anteroexternus, BH-blowhole, CO-connective tissue of porpoise capsule, ME-melon, OC-occipital condyle, P-posterior, R-right, VE-vertex of skull, VV-folded ventral wall of vestibular sac.

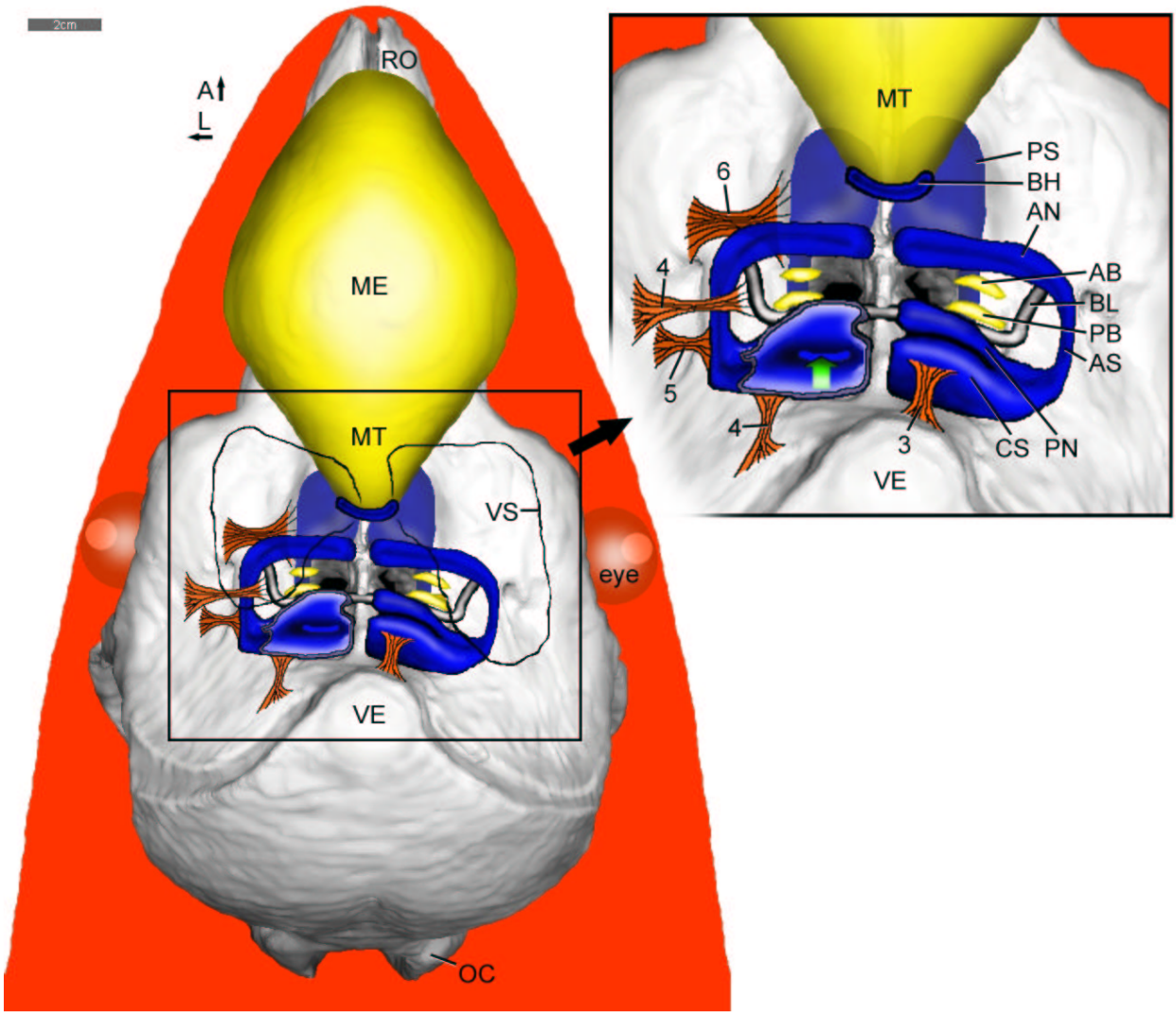


Figure 17: 3D-reconstruction of the harbor porpoise (*Phocoena phocoena*) nasal complex in dorsal view showing the topographic relations of the skull, melon (ME), dorsal bursae, the nasofrontal and premaxillary sacs (PS). The vestibular sacs (VS), which are superficial (dorsal), are shown by black contours. The left caudal and posterior nasofrontal sacs are opened to show their entrance in the inferior vestibulum and the nasal passage, respectively (green arrow). The facial musculature, which is organized in sheets, is shown here in the form of a rope scheme in order to indicate the functional properties of the different parts 3-M. maxillonasolabialis p. anteroexternus, 4-M. maxillonasolabialis p. posterointernus, 5-M. maxillonasolabialis p. anterointernus, 6-M. maxillonasolabialis p. profundus, A-anterior, AB-anterior dorsal bursa, AN-anterior nasofrontal sac, AS-angle of nasofrontal sac, BH-blowhole, BL-blowhole ligament, CS-caudal sac, L-left, MT-melon terminus, OC-occipital condyle, PB-posterior dorsal bursa, PN-posterior nasofrontal sac, RO-rostrum, VE-vertex of skull.

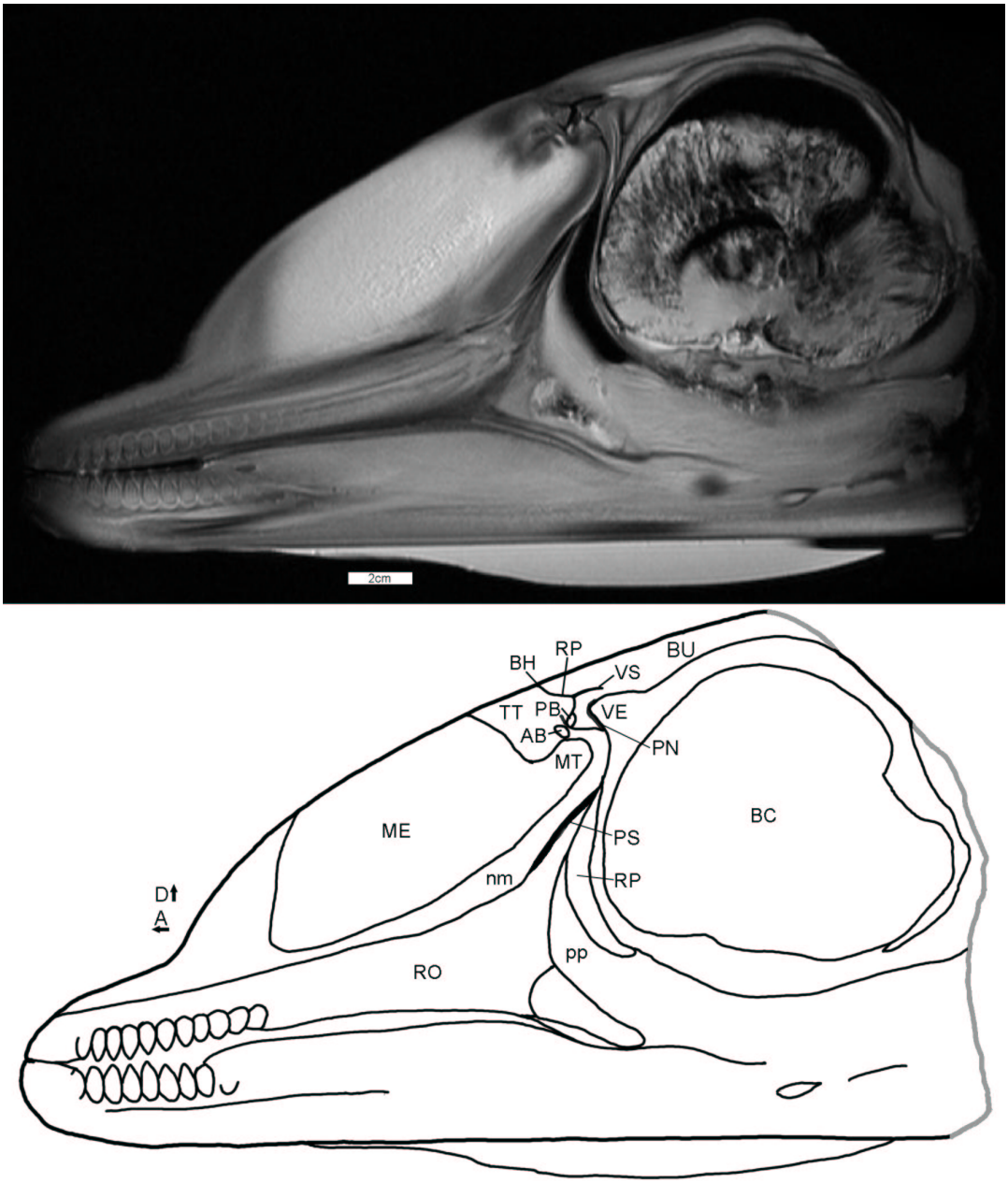


Figure 18: Parasagittal MRI scan of a subadult bottlenose dolphin (*Tursiops truncatus*) head in the plane of the right bony nasal passage and dorsal bursae. A-anterior, AB-anterior dorsal bursa, BC-brain cavity, BH-blowhole, BU-blubber, D-dorsal, ME-melon, MT-melon terminus, nm-nasal plug muscle, PB-posterior dorsal bursa, PN-posterior nasofrontal sac, pp-palatopharyngeus muscle, PS-premaxillary sac, RO-rostrum, RP-right nasal passage, TT-connective tissue theca, VE-vertex of skull, VS-vestibular sac.

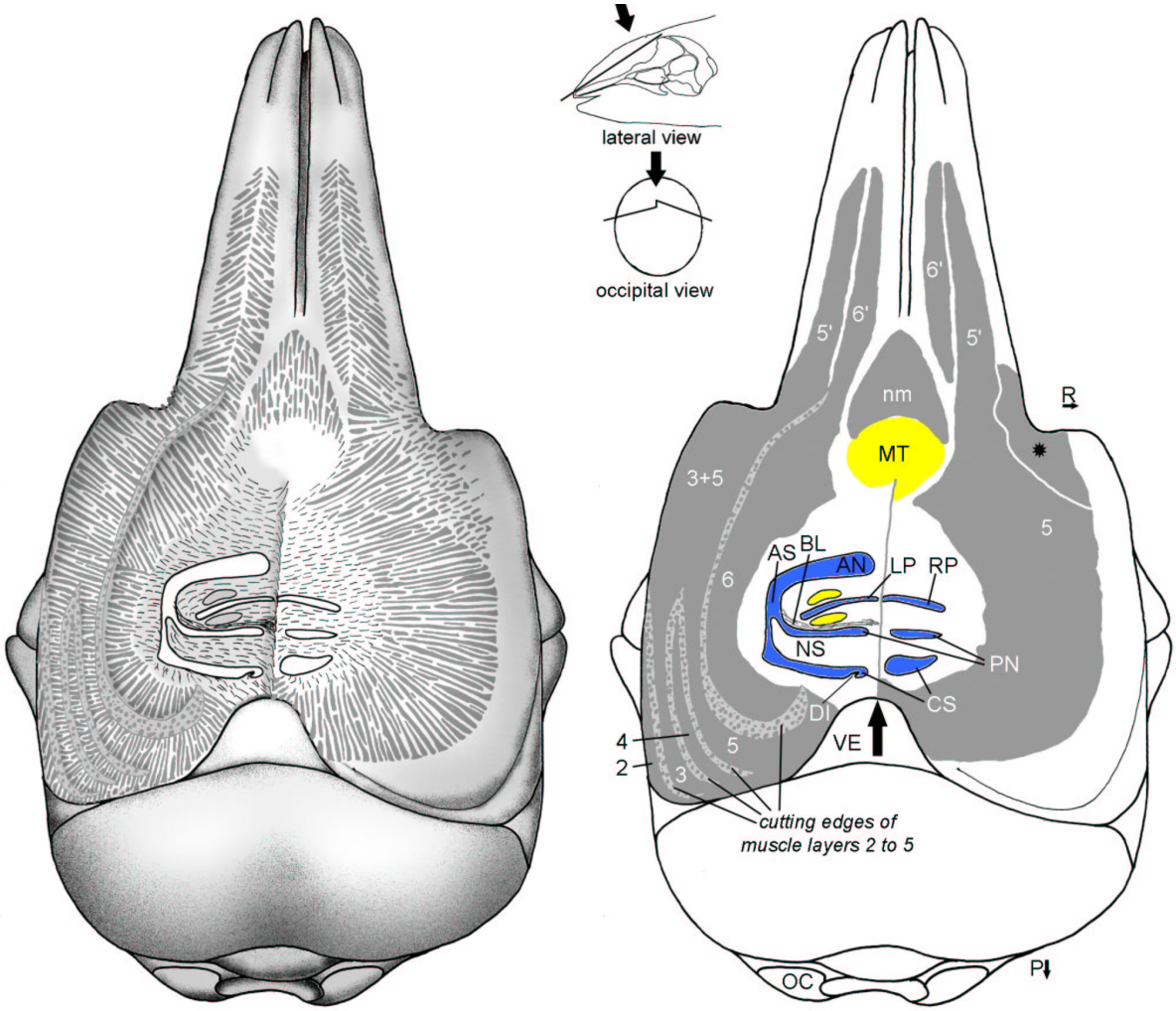


Figure 19: Schematic horizontal reconstruction of the nasal musculature of the harbor porpoise (*Phocoena phocoena*) in two different oblique planes (cf. insets). The air spaces are marked in blue. The nasal diverticulae of the subhorizontal planes are shown divided by the midline (arrow): On the right side the level passes dorsal to the dorsal bursae and the anterointernus (5) and lateral rostral muscles (5') are complete. At the antorbital notch fibers of the anteroexternus muscle are shown that build a strong muscle bundle together with the anterointernus (asterisk; see text). On the left hand side, the plane of which corresponds to that on the right but cuts further ventral, the nasal sacs on the level of the dorsal bursae (small yellow elypsoids) are visible. Whereas the superficial muscles are partly cut the complete profundus (6) and medial rostral muscles (6') is shown here. Fiber orientation of muscle 2, 3, and 4 are shown in lateral view in Fig. 7 in Curry 1992 (Appendix 1). Rostrally, the base of the nasal plug muscle and the oblique cut of the terminus of the melon (MT in yellow) are shown. The vestibular sacs and the Galea aponeurotica are not shown. 2-M. maxillonasolabialis (mnl) p. intermedius, 3-mnl p. anteroexternus, 4-mnl p. posterointernus, AN-anterior nasofrontal sac, AS-angle of nasofrontal sac, BL-blowhole ligament, CO-connective tissue of "porpoise capsule", CS-caudal sac, DI-diagonal membrane, LP-left nasal passage, nm-nasal plug muscle, OC-occipital condyle, P-posterior, PN-posterior nasofrontal sac, R-right, RP-right nasal passage, VE-vertex of skull.

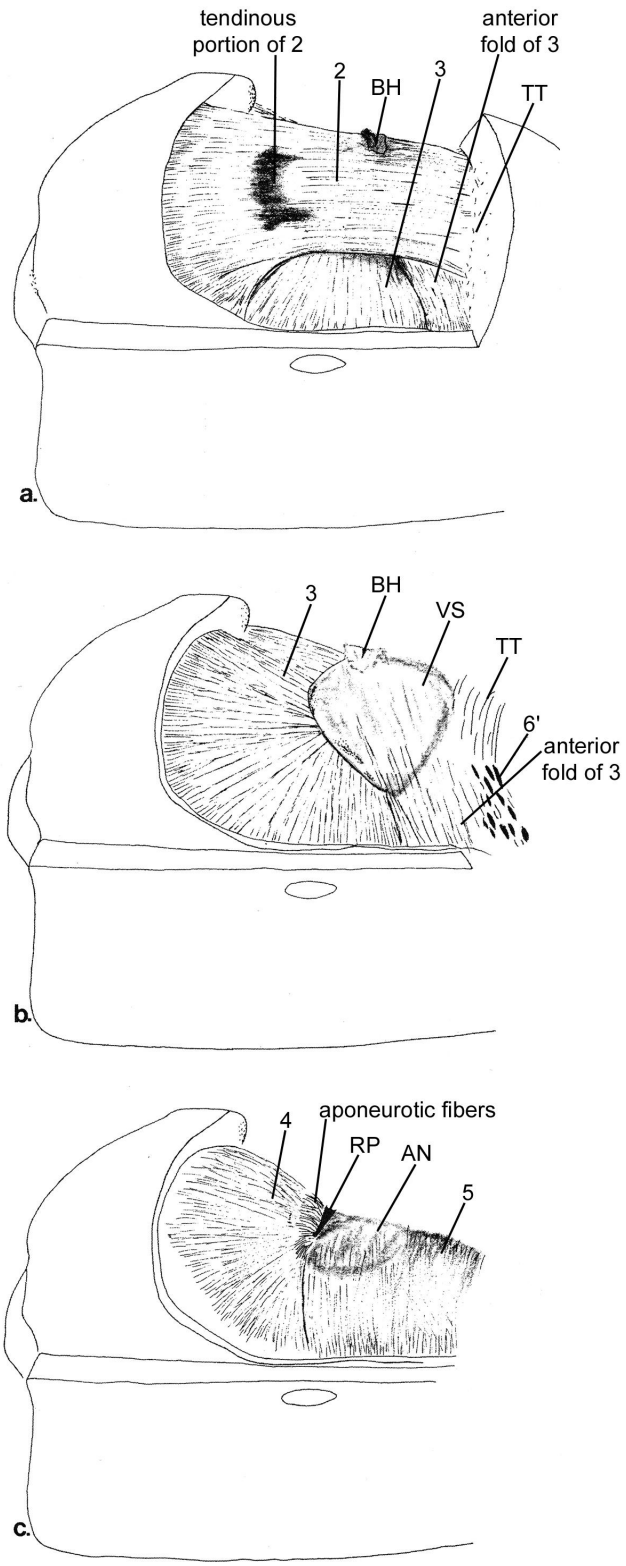


Figure 19a: Right lateral views of the nasal musculature of the harbor porpoise (*Phocoena phocoena*) from superficial (a) to proximal (c) muscle layers. a) the pars intermedius muscle (2). Note that the Gale aponeurotica was removed. b) the pars anteroexternus muscle (3) and the vestibular sac. c) the pars posterointernus muscle (4) on top of the anterior nasofrontal sac (AN). 5-M. maxillonasolabialis p. anterointernus, 6'-medial rostral muscle, BH-blowhole, RP-right nasal passage, TT-connective tissue theca (modified after Curry 1992, Fig. 7).

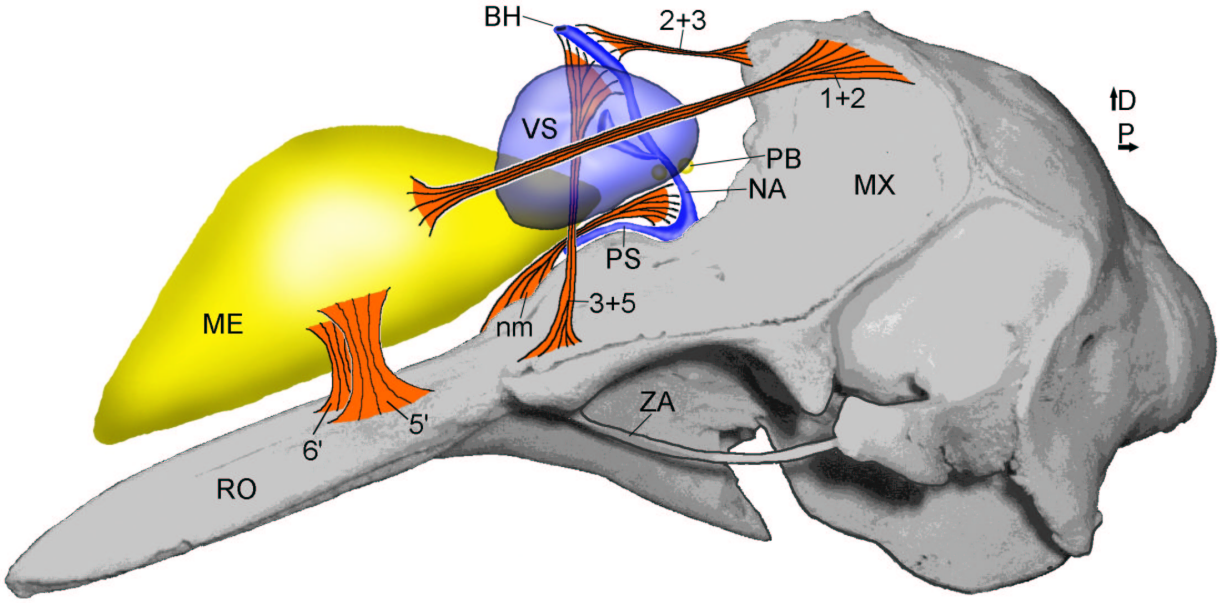


Figure 20: 3D reconstruction of the harbor porpoise (*Phocoena phocoena*) nasal complex in left side view showing the topographic relation of the skull, melon, dorsal bursae, the vestibular sac as well as proposed functional muscle tensions. 1-M. maxillonasolabialis p. posteroexternus, 2-M. maxillonasolabialis p. intermedius, 3-M. maxillonasolabialis p. anteroexternus, 5-M. maxillonasolabialis p. anterointernus, 5'-lateral rostral muscle, 6'-medial rostral muscle, BH-blowhole, D-dorsal, ME-melon, nm-nasal plug muscle, MX-maxilla, NA-nasal passage, P-posterior, PB-posterior dorsal bursa, PS-premaxillary sac, RO-rostrum, VS-vestibular sac, ZA-zygmatic arch.

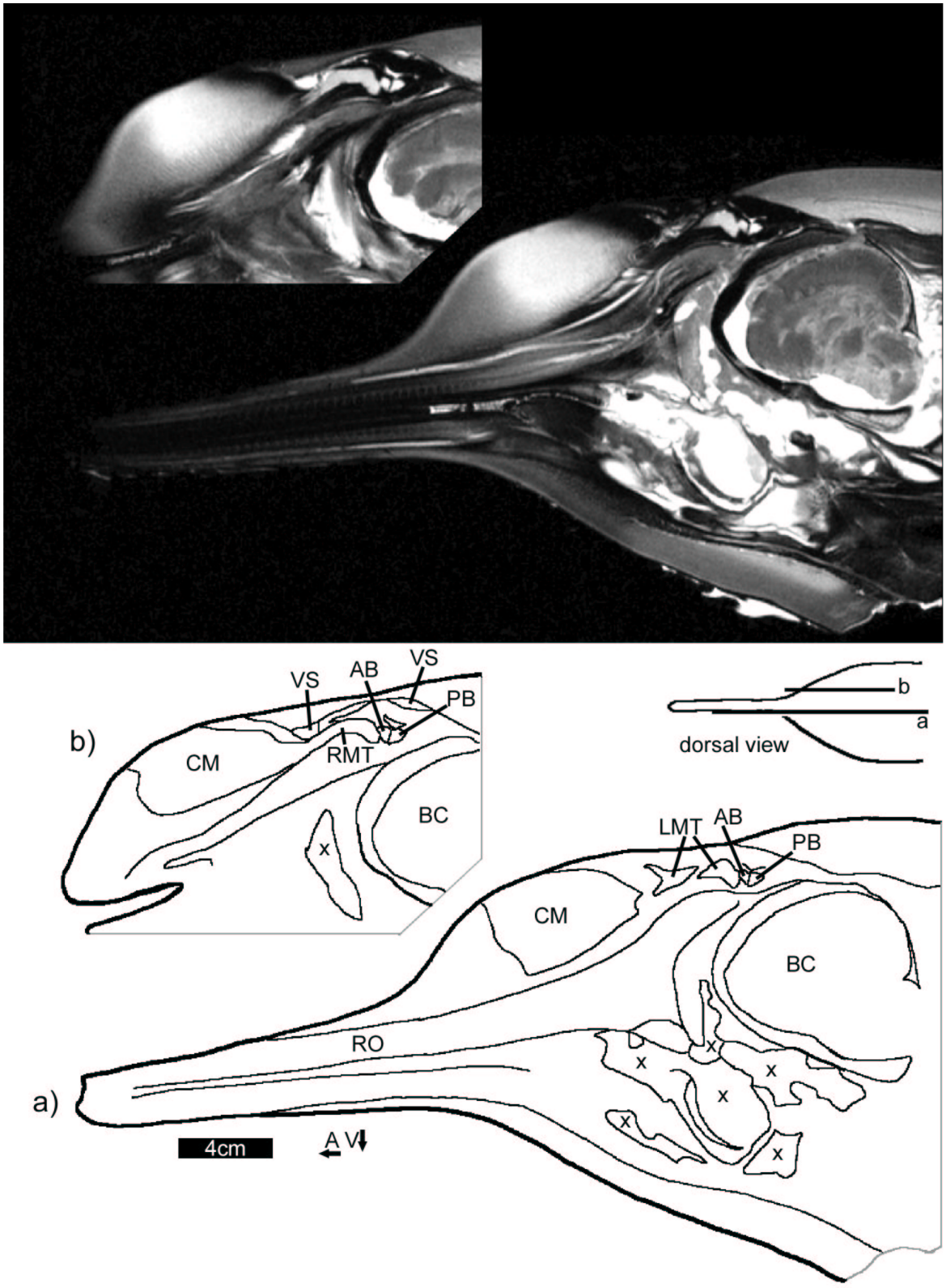


Figure 21: MRI scan of a La Plata dolphin (*Pontoporia blainvillei*) head. a) mediosagittal scan of a entire head. b) right parasagittal scan of the nasal complex at the level of the dorsal bursae. A-anterior, AB-anterior dorsal bursa, BC-brain cavity, CM-core of melon, LMT-left melon terminus, PB-posterior dorsal bursa, RMT-right melon terminus, RO-rostrum, V-ventral, VS-vestibular sac, x-artifact.

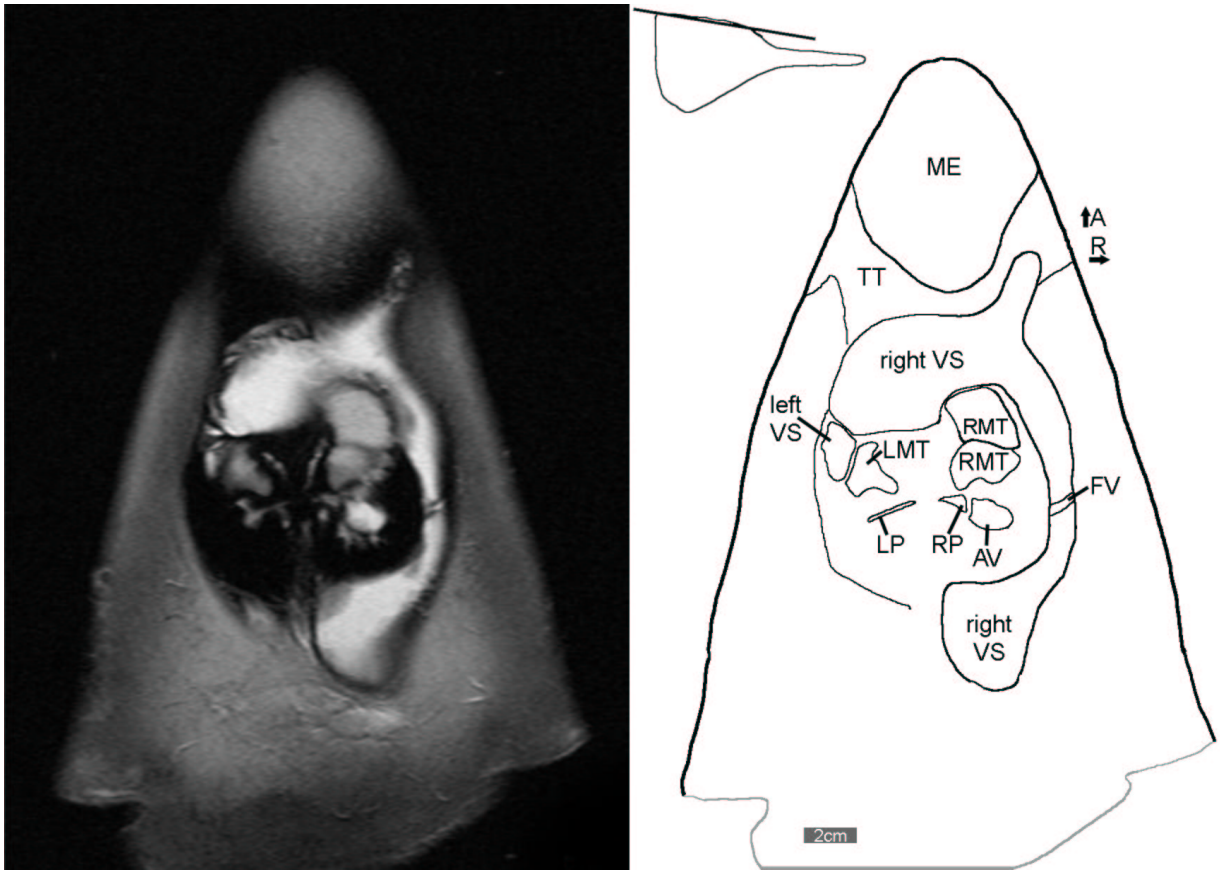


Figure 22: Horizontal MRI scan of the nasal complex of a La Plata dolphin (*Pontoporia blainvillei*) head at the level of the vestibular sacs. A-anterior, AV-aperture of vestibular sac, FV-transverse fold in vestibular sac, LMT-left melon terminus, LP-left nasal passage, ME-melon, R-right, RMT-right melon terminus, RP-right nasal passage, TT-connective tissue theca, VS-vestibular sac.

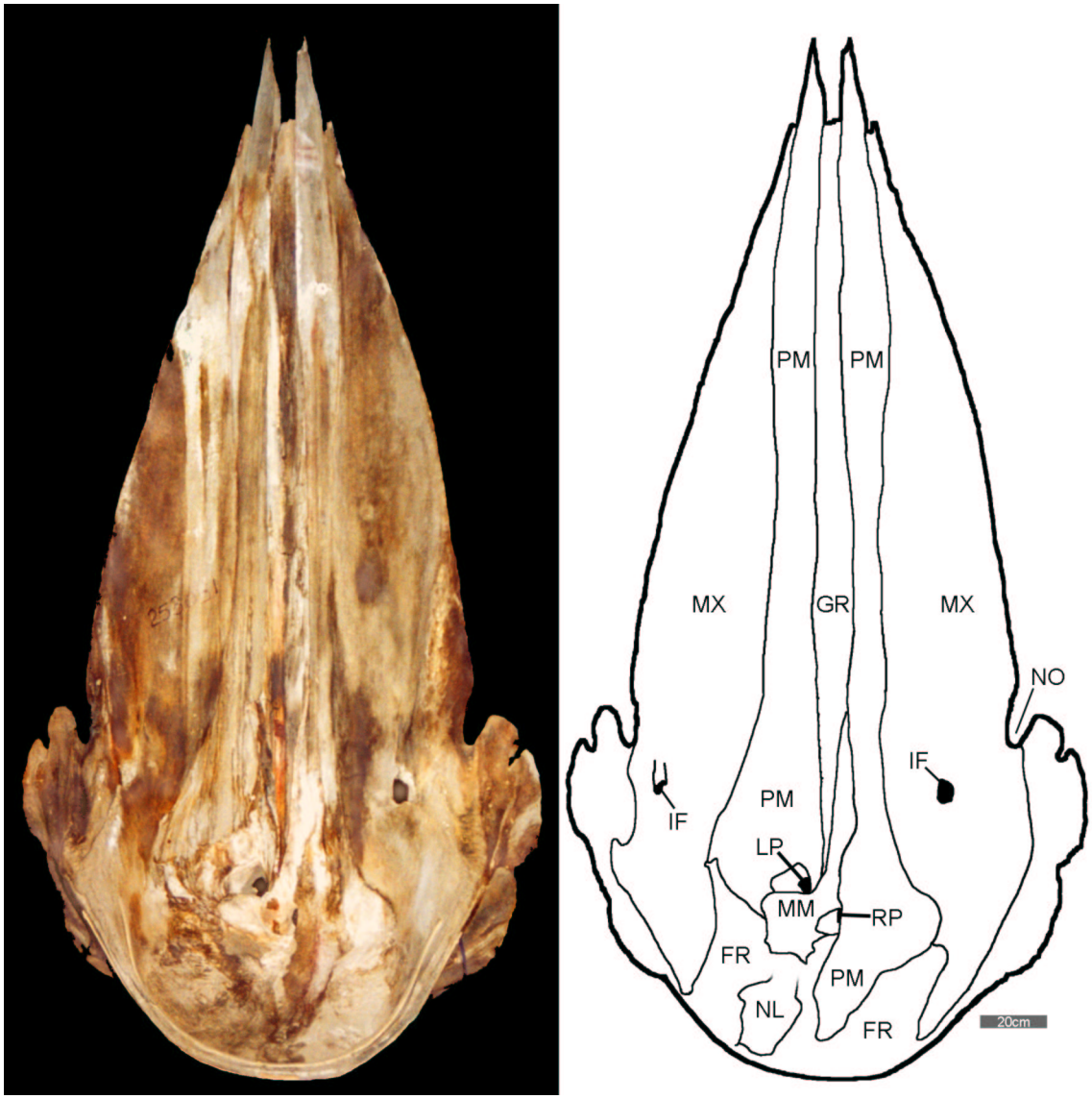


Figure 23: Dorsal view of a sperm whale (*Physeter macrocephalus*) skull showing its main components. FR-frontal, GR-groove of rostral cartilage on the vomer, IF-infraorbital foramen, LP-left nasal passage, MM-mesethmoid, MX-maxilla, NL-nasal, NO-antorbital notch, PM-premaxilla, RP-right nasal passage.

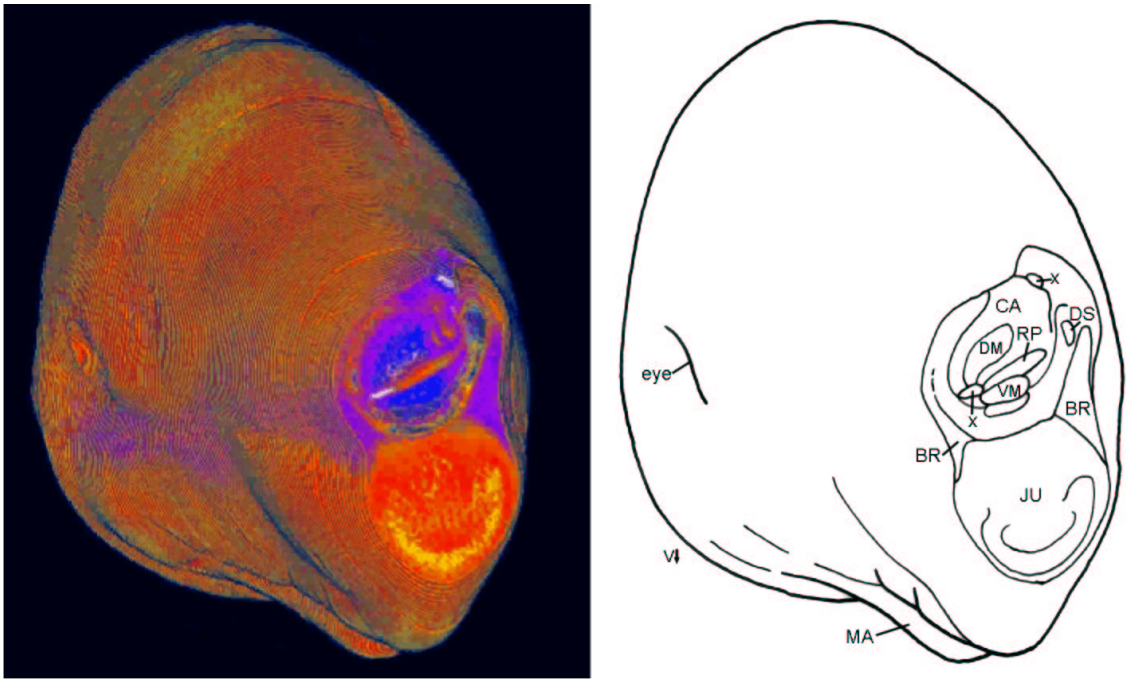


Figure 24: Reconstructed transverse CT scan of a neonate sperm whale (*Physeter macrocephalus*) head through the tip of the nose with the blowhole complex and the anterior end of the junk, seen slightly from the right. For plane orientation and scale see Fig. 31. Modified after Cranford, Huggenberger and Oelschläger (in prep). BR-bridle, CA-case of spermaceti organ, DM-dorsal monkey lip, DS-distal sac, JU-junk, MA-mandible, RP-right nasal passage, V-ventral, VM-ventral monkey lip, x-artifact.


Figure 25: Reconstructed transverse CT scan (caudal to Fig. 24) of a neonate sperm whale (*Physeter macrocephalus*) head through the rostral tip of the spermaceti organ and junk. For plane orientation and scale see Fig. 31. Modified after Cranford, Huggenberger and Oelschläger (in prep). BR-bridle, CA-case of spermaceti organ, JU-junk, LE-fatty lenses in junk, LP-left nasal passage, SO-spermaceti organ.

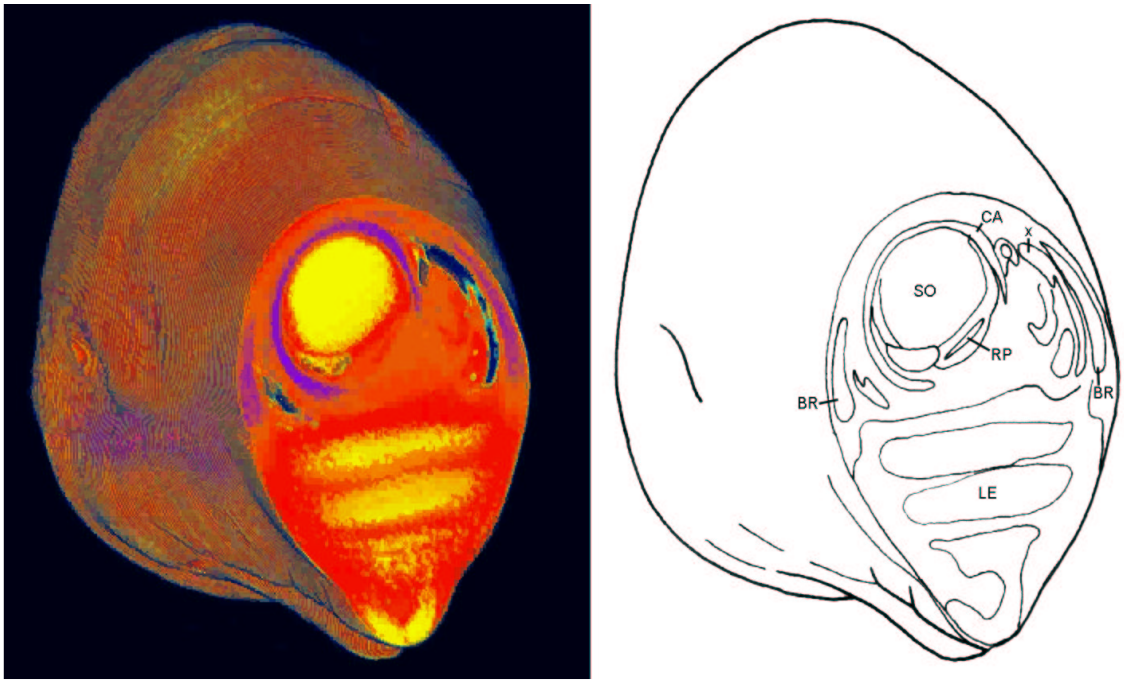


Figure 26: Reconstructed transverse CT scan (caudal to Fig. 25) of a neonate sperm whale (*Physeter macrocephalus*) head showing the lamination of the junk. For plane orientation and scale see Fig. 31. Modified after Cranford, Huggenberger and Oelschläger (in prep). BR-bridle, CA-case of spermaceti organ, LE-fatty lenses in junk, RP-right nasal passage, SO-spermaceti organ, x-artifact.

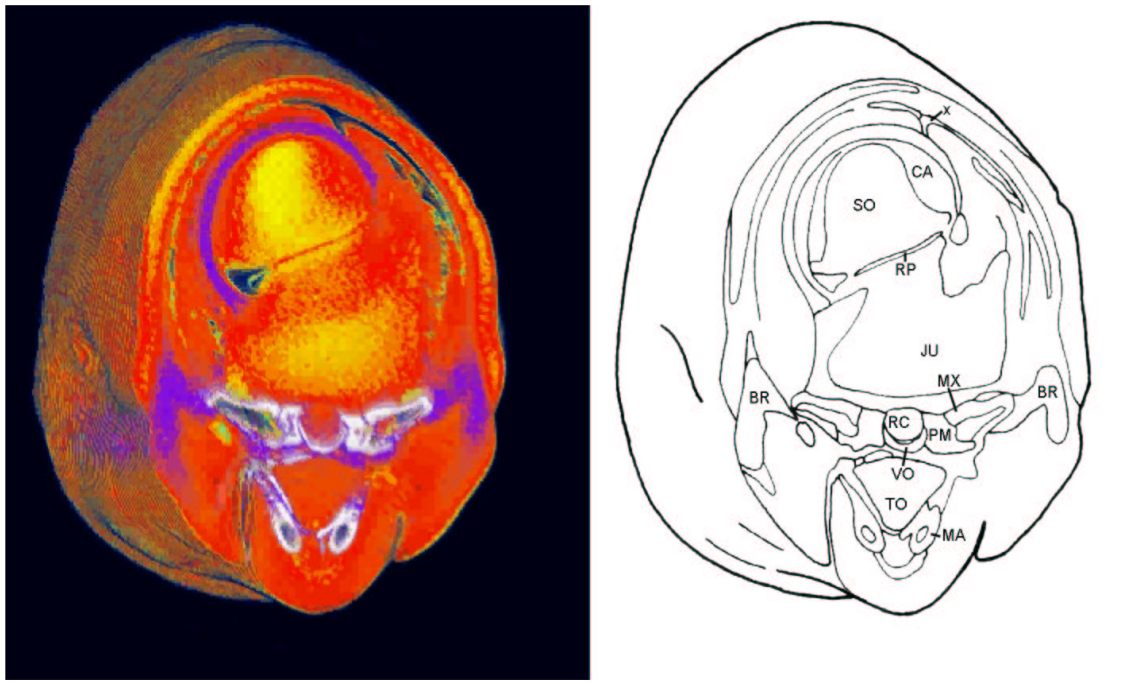


Figure 27: Reconstructed transverse CT scan (caudal to Fig. 26) of a neonate sperm whale (*Physeter macrocephalus*) head showing the rostral part of skull with mesorostral cartilage. Lower jaw is largely separate from the rest of the head by narrow clefts. The spermaceti organ and junk are only separated from each other by the right nasal passage. For plane orientation and scale see Fig. 31. Modified after Cranford, Huggenberger and Oelschläger (in prep). BR-bridle, CA-case of spermaceti organ, JU- junk, MA-mandible, MX-maxilla, PM-premaxilla, RC-rostral cartilage (cartilaginous rostrum), RP-right nasal passage, SO-spermaceti organ, TO-tongue, VO-vomer, x-artifact.

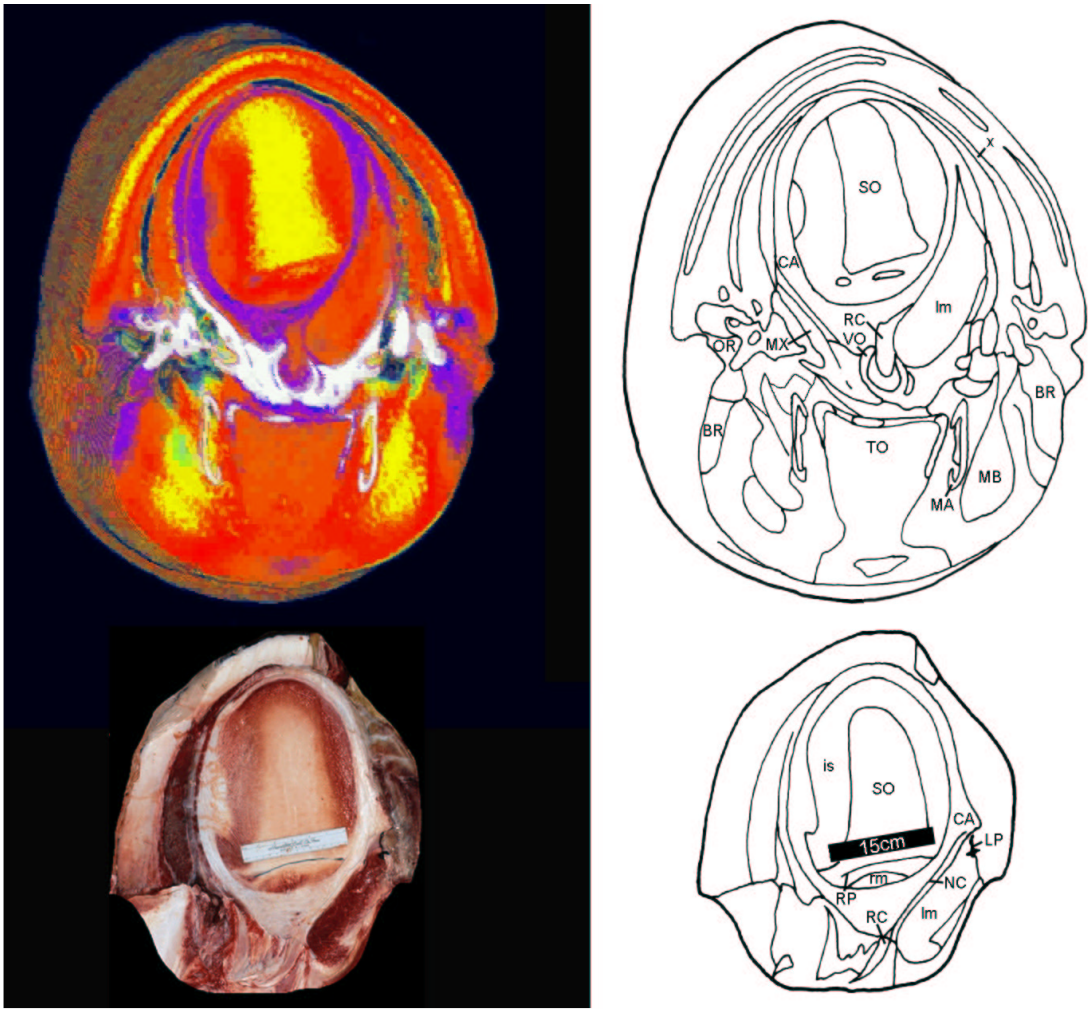


Figure 28: Reconstructed transverse CT scan (caudal to Fig. 27) of a neonate sperm whale (*Physeter macrocephalus*) head through the cranial basin with the spermaceti organ and the area of the bony nostrils with mesorostral cartilage and nasal plug muscles, the orbita, and tongue. For plane orientation and scale see Fig. 31. Modified after Cranford, Huggenberger and Oelschläger (in prep). BR-bridle, CA-case of spermaceti organ, is-intrinsic muscle of spermaceti organ, lm-left nasal passage muscle, LP-left nasal passage, MA-mandible, MB-mandibular fat body, MX-maxilla, NC-nasal roof cartilage, OR-orbita, RC-rostral cartilage (cartilaginous rostrum), rm-right nasal passage muscle, RP-right nasal passage, SO-spermaceti organ, TO-tongue, VO-vomer, x-artifact.

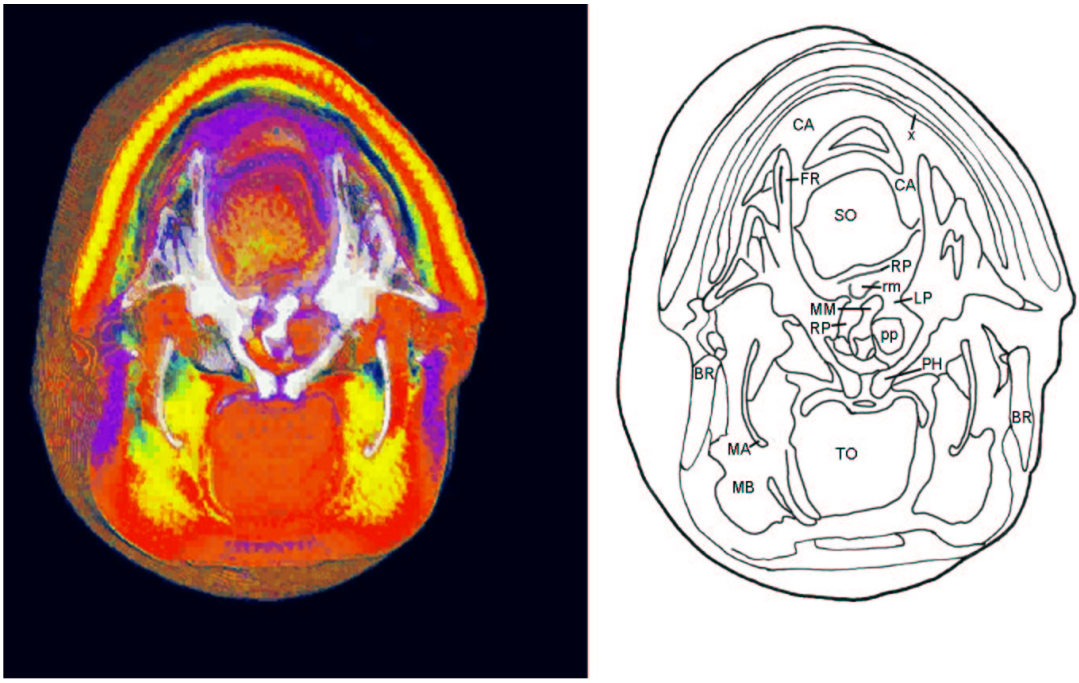


Figure 29: Reconstructed transverse CT scan (caudal to Fig. 28) of a neonate sperm whale (*Physeter macrocephalus*) head through the cranial basin with the spermaceti organ and the area of the bony nostrils with mesorostral cartilage, tongue, and the shell-like mandibular ramus with the external and internal mandibular fat bodies. For plane orientation and scale see Fig. 31. Modified after Cranford, Huggenberger and Oelschläger (in prep). BR-bridle, CA-case of spermaceti organ, FR-frontal, LP-left nasal passage, MA-mandible, MB-mandibular fat body, MM-mesethmoid, PH-pterygoid hamulus, pp-palatopharyngeus muscle, rm-right nasal passage muscle, RP-right nasal passage, SO-spermaceti organ, TO-tongue, x-artifact.

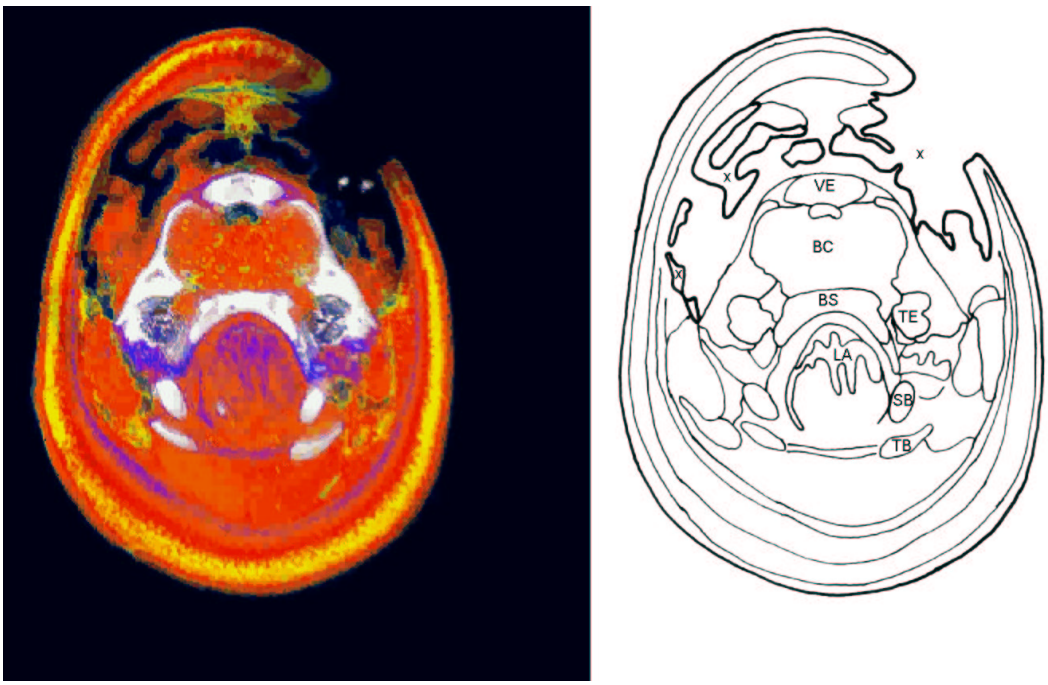


Figure 30: Reconstructed transverse CT scan (caudal to Fig. 29) of a neonate sperm whale (*Physeter macrocephalus*) head through the posterior part of head with cranial vault and brain, ear region (tympanoperiotic complex), larynx and hyoid. Upper third of scan incomplete, with artificial spaces and contours (x). For plane orientation and scale see Fig. 31. Modified after Cranford, Huggenberger and Oelschläger (in prep). BC-brain cavity, BS-basisphenoid, LA-larynx, SB-stylohyal bone, TB-thyrohyal bone, TE-tympanoperiotic bone, VE-vertex of skull, x-artifact.

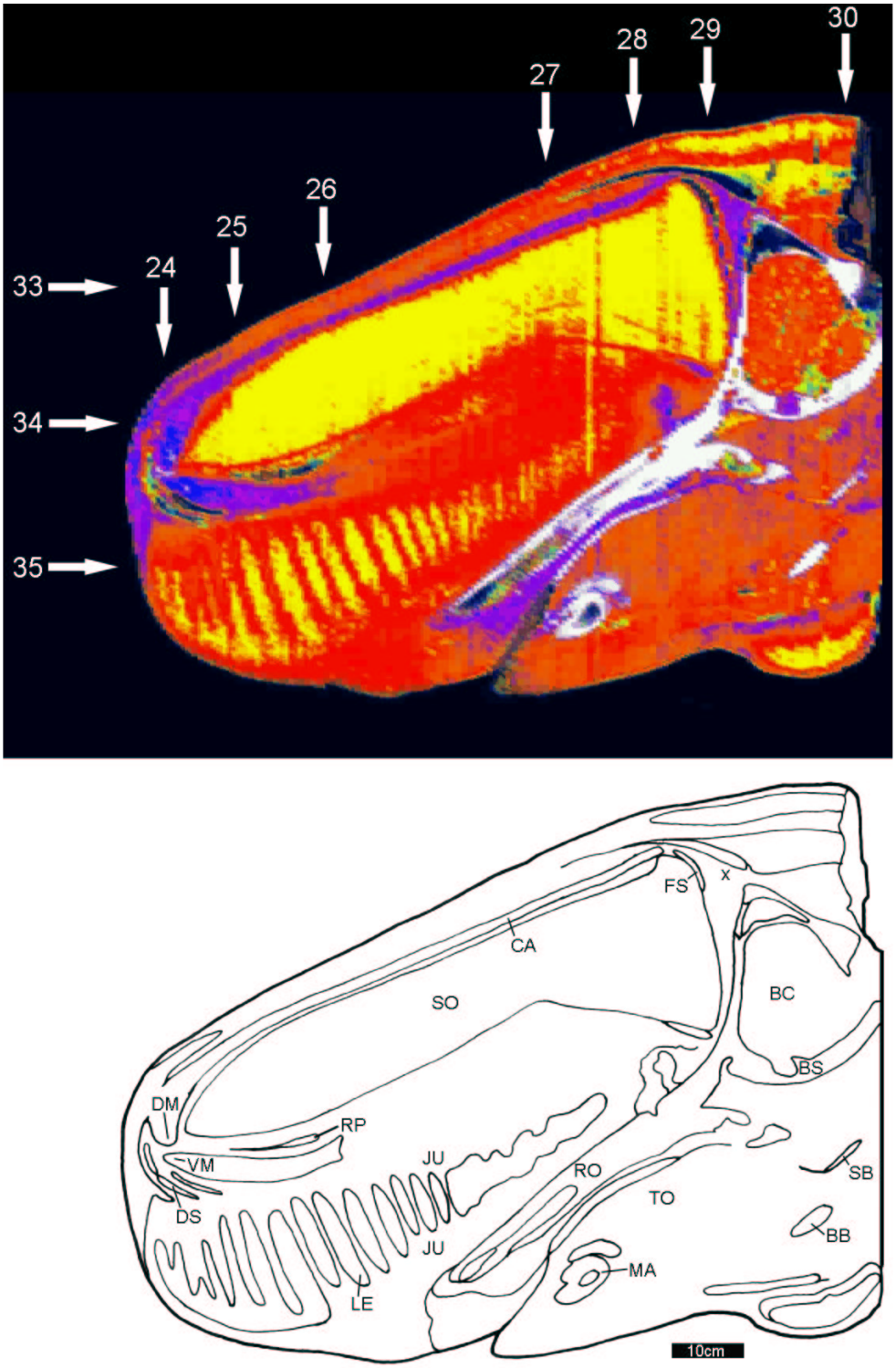


Figure 31: Reconstructed near-midsagittal scan of a neonate sperm whale (*Physeter macrocephalus*) head showing the topographical relations between the skull, fat bodies, and the air spaces. Area of the left osseous nasal tube with nasal plug muscles. The lenticular structure of the junk and the size of the tongue are obvious. Modified after Cranford, Huggenberger and Oelschläger (in prep). BB-basihyal bone, BC-brain cavity, BS-basisphenoid, CA-case of spermaceti organ, DM-dorsal monkey lip, DS-distal sac, FS-frontal sac, JU-junk, LE-fatty lenses in junk, MA-mandible, RO-rostrum, RP-right nasal passage, SB-stylohyal bone, SO-spermaceti organ, TO-tongue, VM-ventral monkey lip, x-artifact.

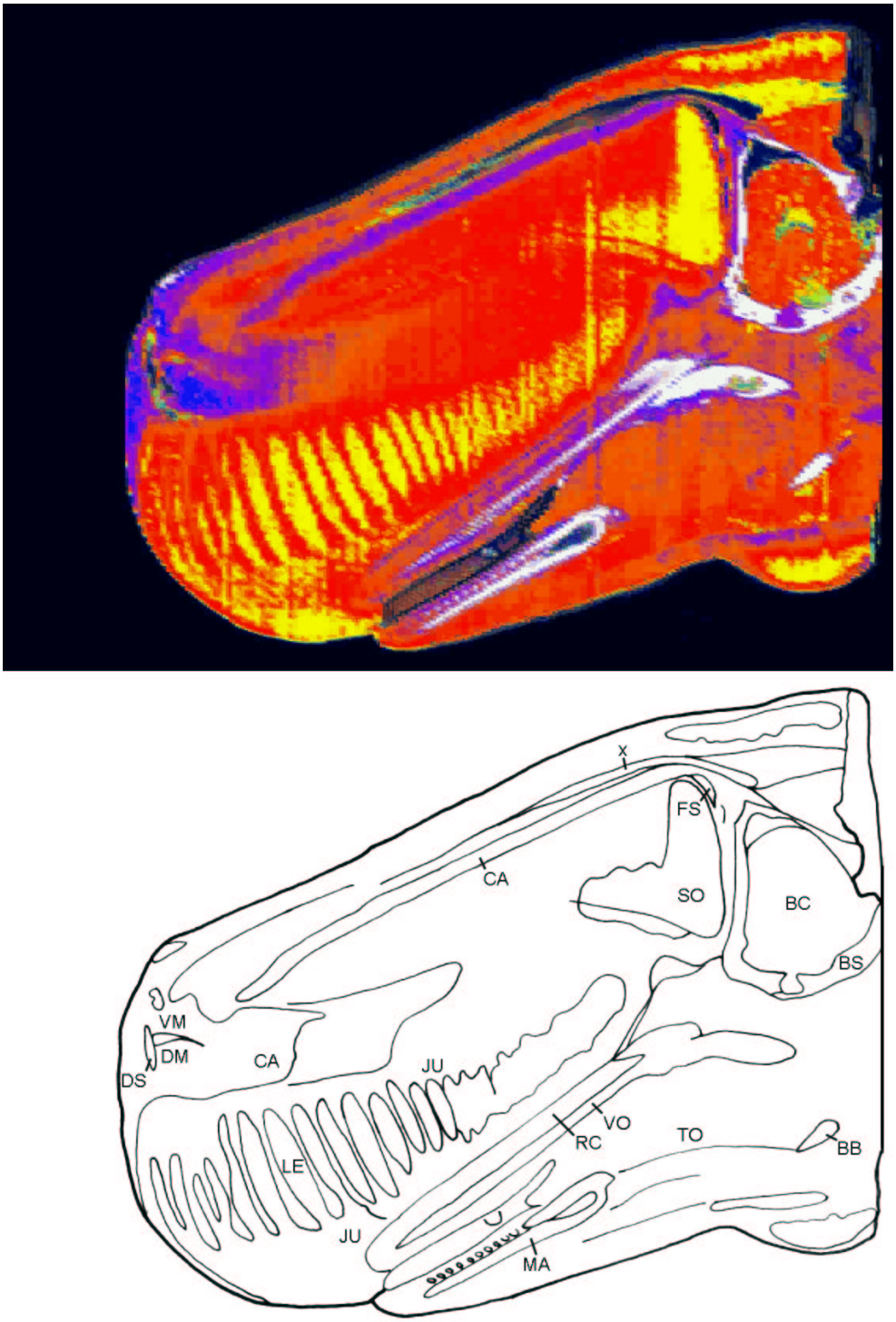


Figure 32: Reconstructed left lateral sagittal scan of a neonate sperm whale (*Physeter macrocephalus*) head. For scale see Fig. 31. Modified after Cranford, Huggenberger and Oelschläger (in prep). BB-basihyal bone, BC-brain cavity, CA-case of spermaceti organ, DM-dorsal monkey lip, DS-distal sac, FS-frontal sac, JU-junk, LE-fatty lenses in junk, MA-mandible, RC-rostral cartilage, SO-spermaceti organ, TO-tongue, VM-ventral monkey lip, VO-vomer, x-artifact.

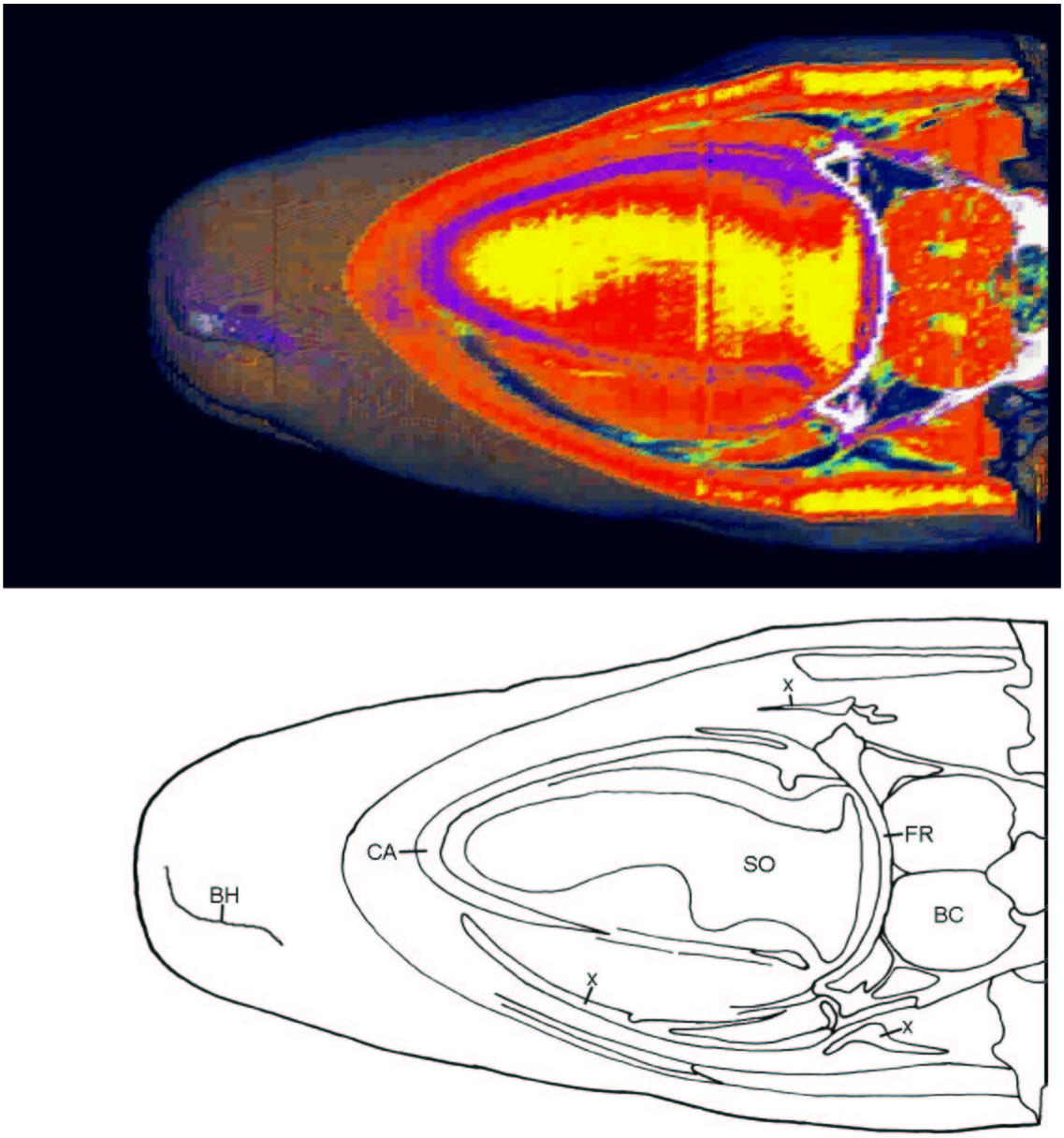


Figure 33: Reconstructed uppermost of three horizontal scans of a neonate sperm whale (*Physeter macrocephalus*) head through the top of the head showing the spermaceti organ enclosed in the case and the brain within the cranial vault. The posterior end of the spermaceti organ is in contact with the concave anterior wall of the skull. Blowhole with some artificial sand, seen in dorsal aspect. x indicate shearing artifacts. For plane orientation and scale see Fig. 31. Modified after Cranford, Huggenberger and Oelschläger (in prep). BC-brain cavity, BH-blowhole, CA-case of spermaceti organ, FR-frontal, SO-spermaceti organ, x-artifact.

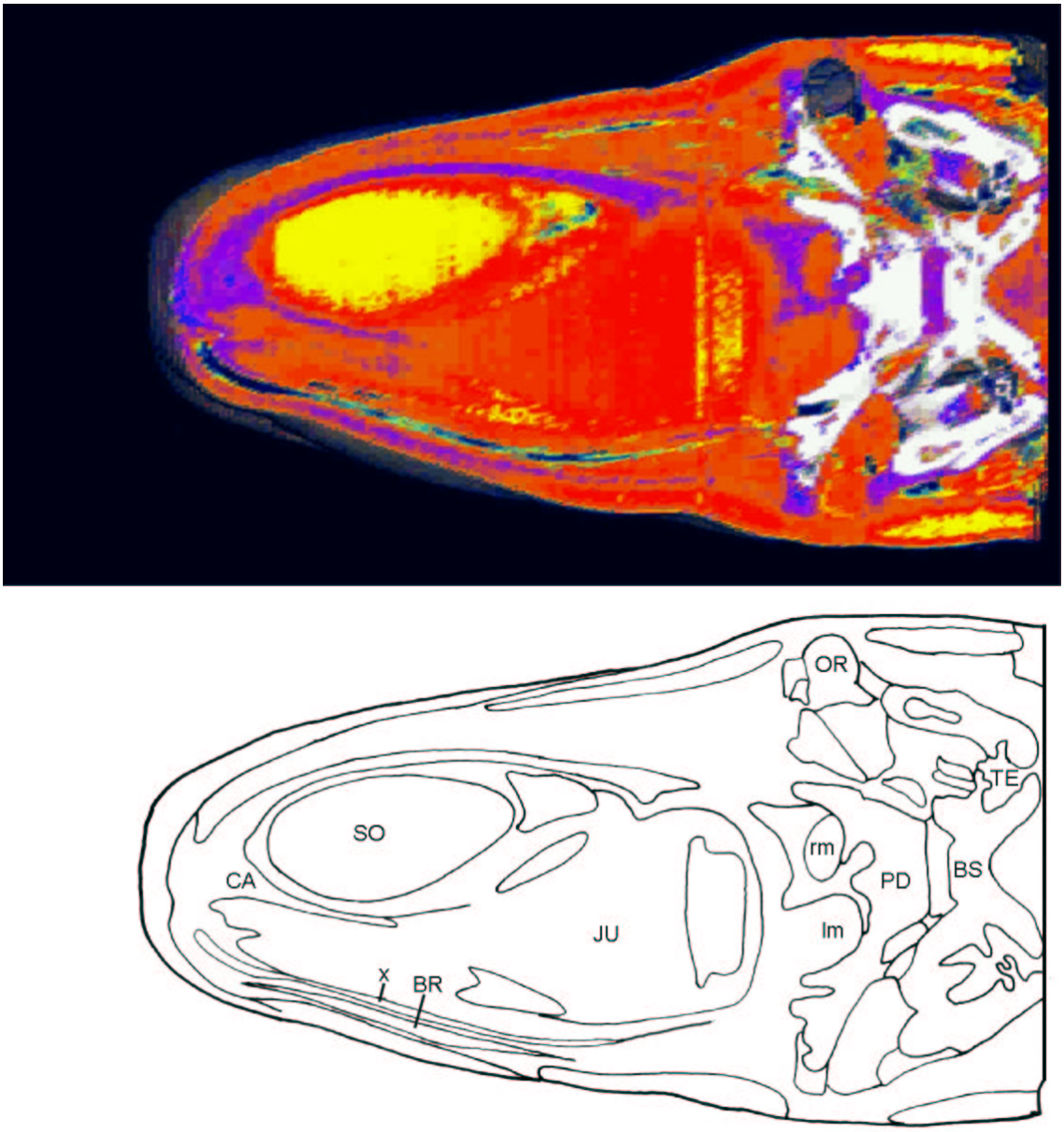


Figure 34: Reconstructed middle horizontal scan of a neonate sperm (*Physeter macrocephalus*) whale head through the spermaceti organ, junk, and the base of neurocranium (with tympanoperiotic complex). Both fat bodies are joined in the middle of the forehead. For plane orientation and scale see Fig. 31. Modified after Cranford, Huggenberger and Oelschläger (in prep). BR-bridle, BS-basisphenoid, CA-case of spermaceti organ, JU-junk, lm-left nasal passage muscle, OR-orbita, PD-presphenoid, rm-right nasal passage muscle, SO-spermaceti organ, TE-tympanoperiotic bone, x-artifact.

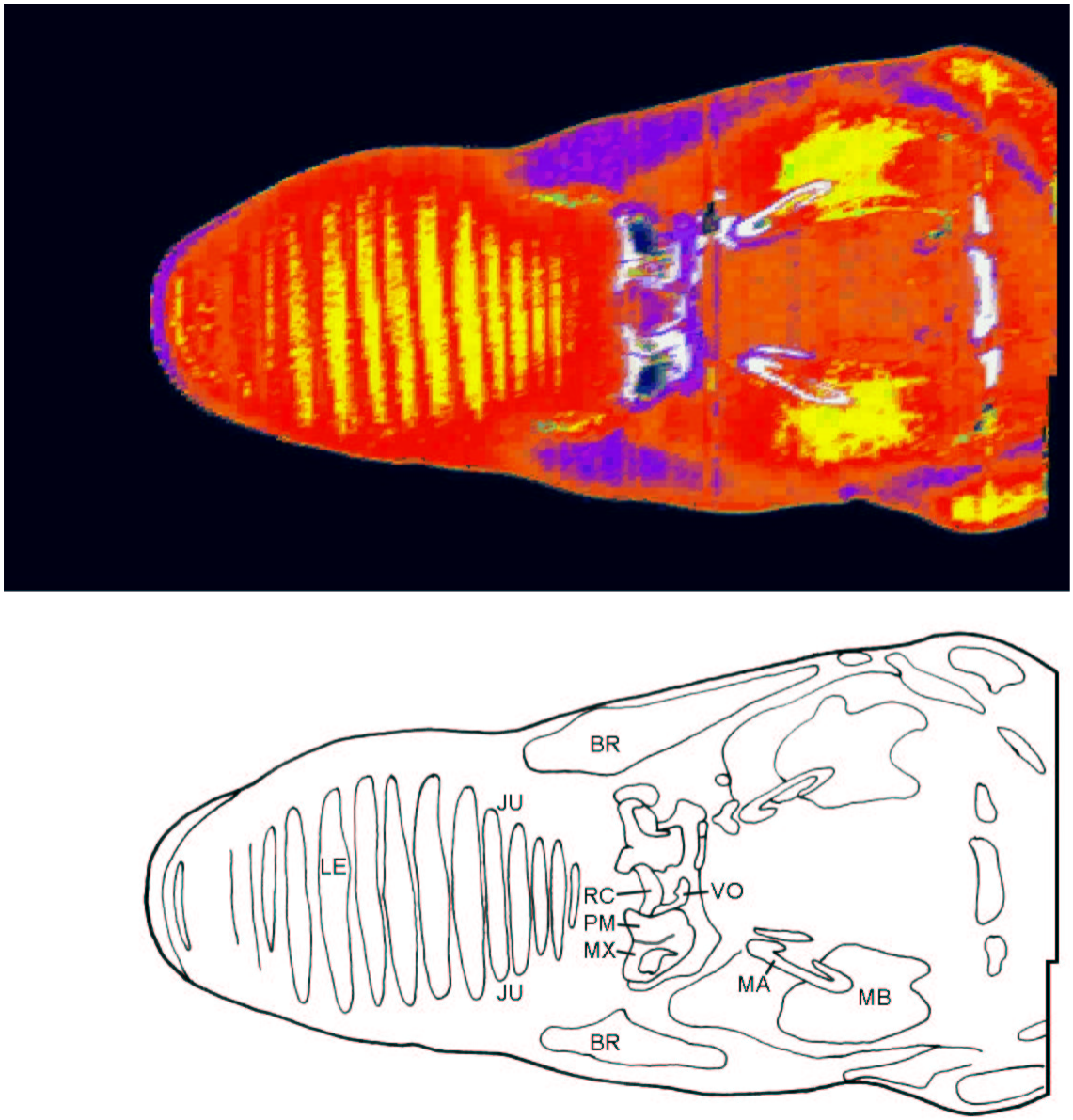


Figure 35: Reconstructed lowermost horizontal scan of a neonate sperm whale (*Physeter macrocephalus*) head showing the lenticular structure of the junk, the base of the rostrum, the rami of the mandibles with the mandibular fat bodies, the tongue and the hyoid apparatus. For plane orientation and scale see Fig. 31. Modified after Cranford, Huggenberger and Oelschläger (in prep). BR-bridle, JU-junk, LE-fatty lenses in junk, MA-mandible, MB-mandibular fat body, MX-maxilla, PM-premaxilla, RC-rostral cartilage (cartilaginous rostrum), VO-vomer.

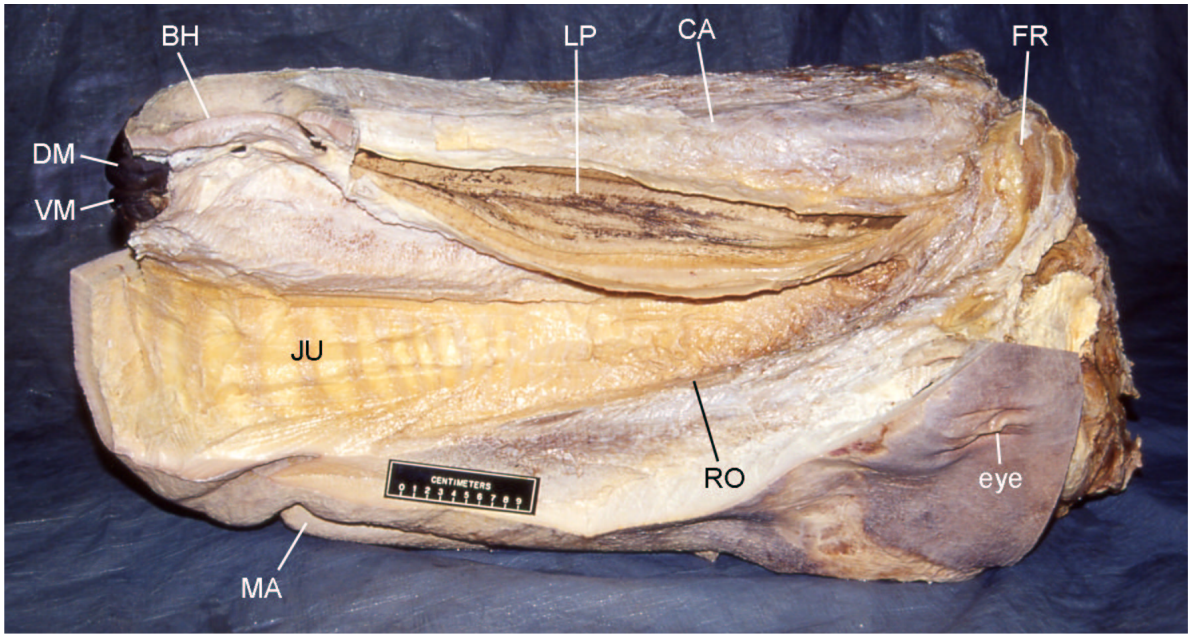


Figure 36: Left lateral dissection of a neonate sperm whale (*Physeter macrocephalus*) head ("Odie"). The left nasal passage is opened and its muscle is removed. Note that the black epithelium of the left nasal tract is detached. BH-blowhole, CA-case of spermaceti organ, DM-dorsal monkey lip, FR-frontal, JU-junk, LP-left nasal passage, MA-mandible, RO-rostrum, VM-ventral monkey lip.

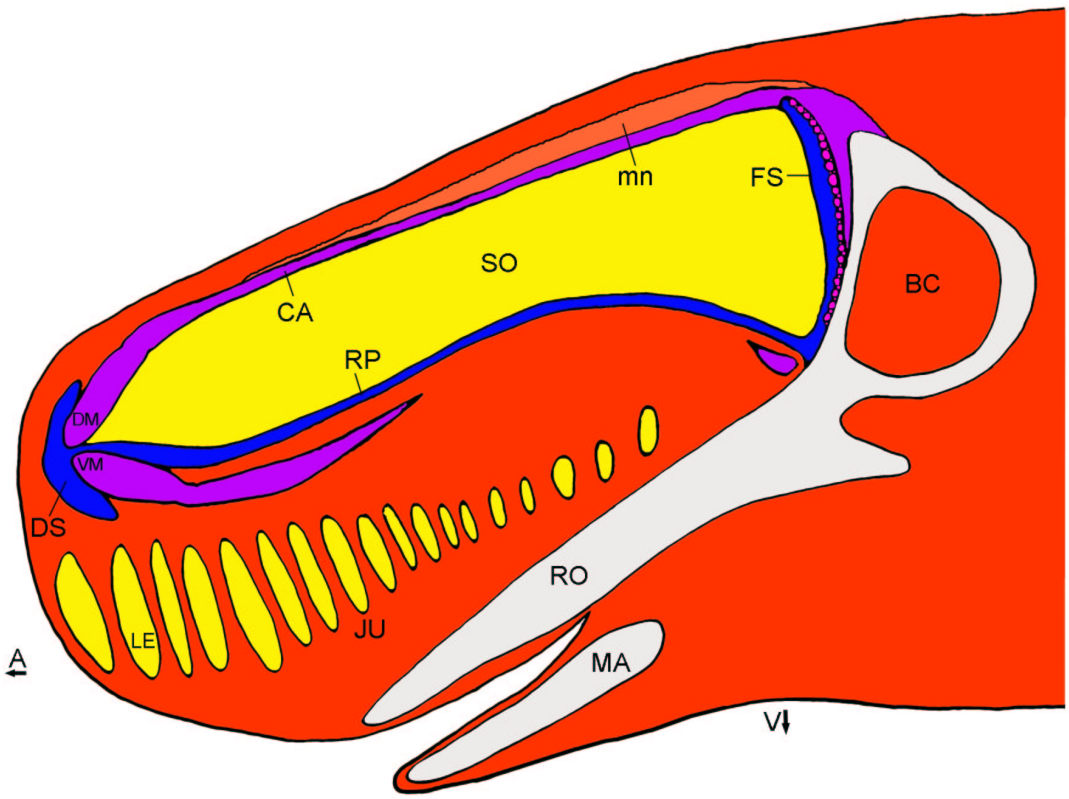


Figure 37: Schematic mediosagittal section of a neonate sperm whale (*Physeter macrocephalus*) head (modified from Cranford 1999). A-anterior, BC-brain cavity, CA-case of spermaceti organ, DM-dorsal monkey lip, DS-distal sac, FS-frontal sac, JU-junk, LE-fatty lenses in junk, MA-mandible, mn-maxillonasolabialis muscle, RO-rostrum, RP-right nasal passage, SO-spermaceti organ, V-ventral, VM-ventral monkey lip.

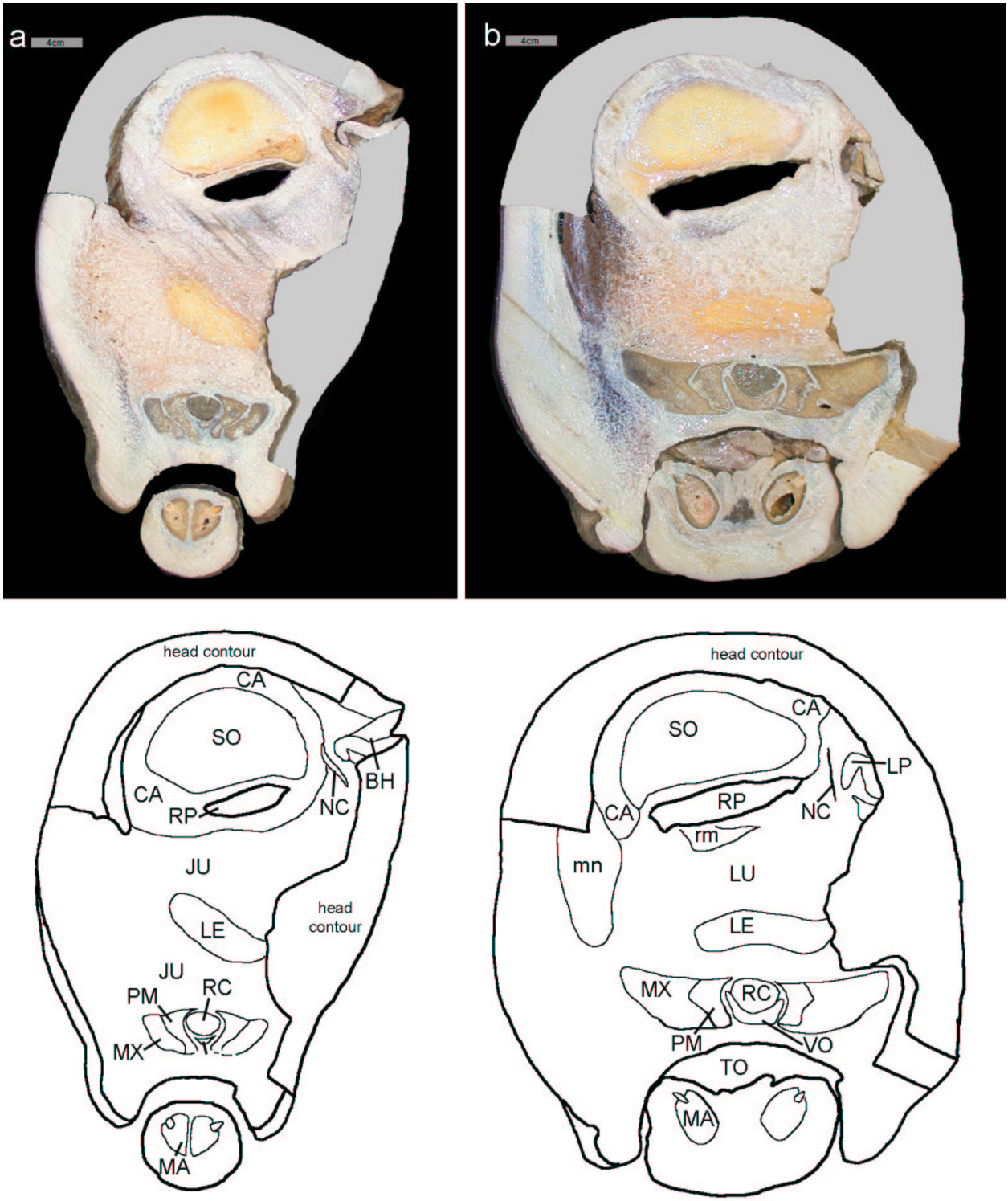


Figure 38: Continued next page

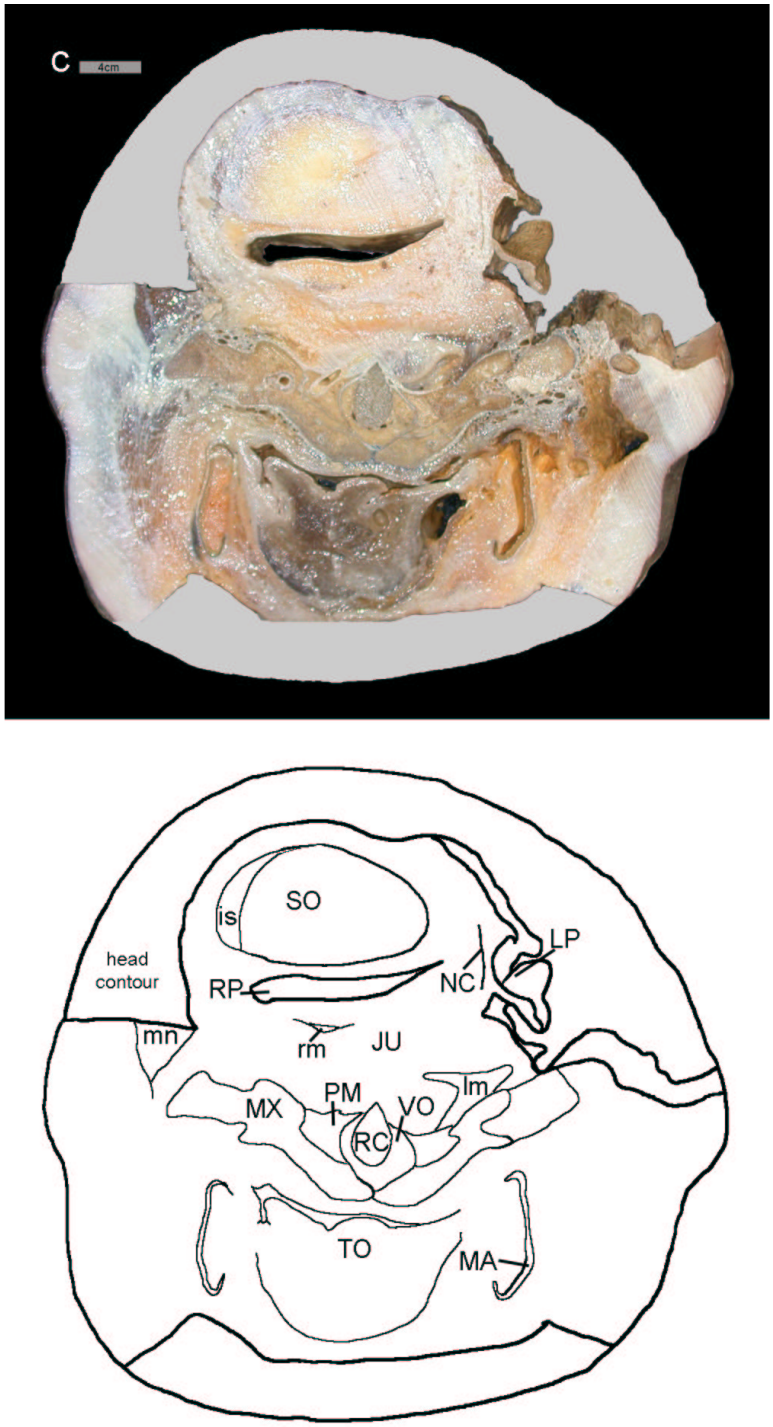


Figure 38: Transverse cryo-sections of the head of a neonate sperm whale in frontal view from anterior (a) to posterior (c) showing the position of the nasal roof cartilage. Position of planes see Fig. 3, note that the superficial layers of the nasal complex were dissected so that the head contour is added artificially. BH-blowhole, CA-case of spermaceti organ, is-intrinsic muscle of spermaceti organ, JU-junk, LE-fatty lenses in junk, lm-left nasal passage muscle, LP-left nasal passage, MA-mandible, mn-maxillonasolabialis muscle, MX-maxilla, NC-nasal roof cartilage, PM-premaxilla, RC-rostral cartilage (cartilaginous rostrum), rm-right nasal passage muscle, RP-right nasal passage, SO-spermaceti organ, TO-tongue, VO-vomer.

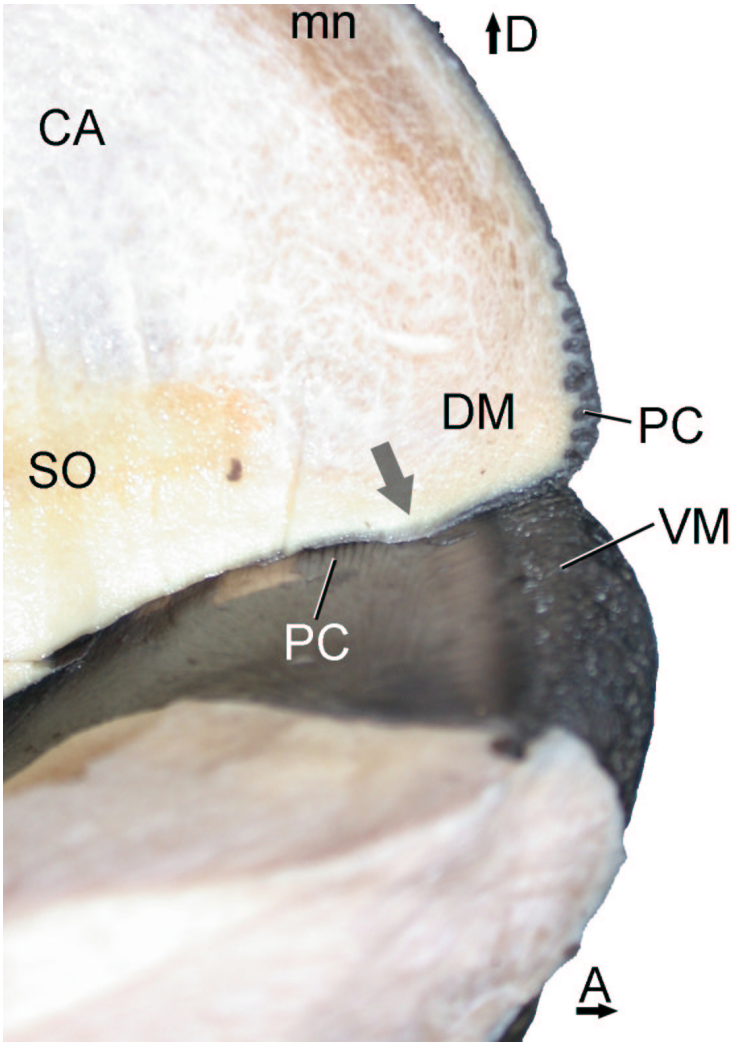


Figure 39: Lateral view of the monkey lips of a neonate sperm whale ("Odie"; *Physeter macrocephalus*). The dorsal lip is removed up to its mediosagittal plane so that the connection of the spermaceti fat and the connective tissue is visible. The arrow indicates the mortise of the mortise-tenon complex of the lips. Note that the whitish band parallel to the mortise-tenon folds is darkened due to the fixation of the specimen. A-anterior, CA-case of spermaceti organ, D-dorsal, DM-dorsal monkey lip, mn-maxillonasolabialis muscle, PC-plicae of monkey lips, SO-spermaceti organ, VM-ventral monkey lip.

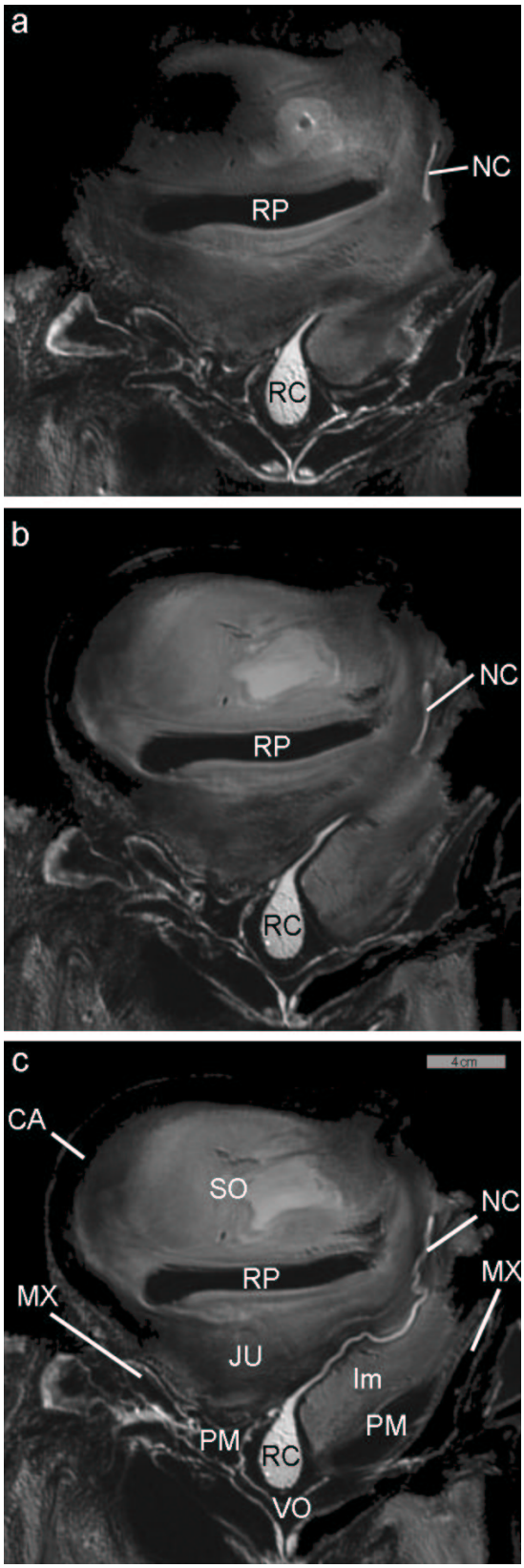


Figure 40: Transverse MRI scan of the head of a neonate sperm whale ("Odie"; *Physeter macrocephalus*) in frontal view (a) to posterior (c) showing the ramification of the nasal roof cartilage (NC) and the cartilaginous rostrum (RC). Position of planes see Fig. 3, note that the superficial layers of the nasal complex were dissected. CA-case of spermaceti organ, JU-junk, lm-left nasal passage muscle, MX-maxilla, NC-nasal roof cartilage, PM-premaxilla, RC-rostral cartilage (cartilaginous rostrum), RP-right nasal passage, SO-spermaceti organ, VO-vomer.

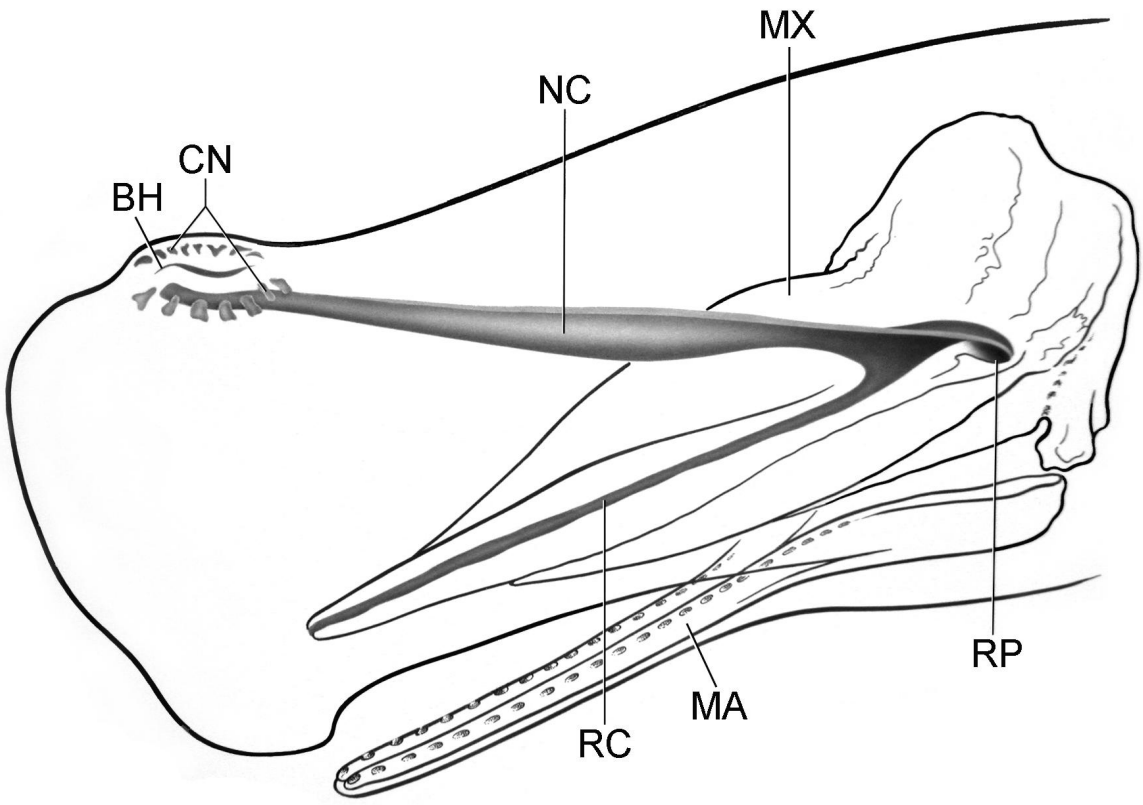


Figure 41: Schematic outline drawing (left dorsolateral view) of a sperm whale head showing the position of the nasal roof cartilage (NC) and the cartilaginous rostrum (RC). Modified after Klima 1990. BH-blowhole, CN-nostril cartilages, MA-mandible, MX-maxilla, NC-nasal roof cartilage, RC-rostral cartilage (cartilaginous rostrum), RP-right nasal passage.

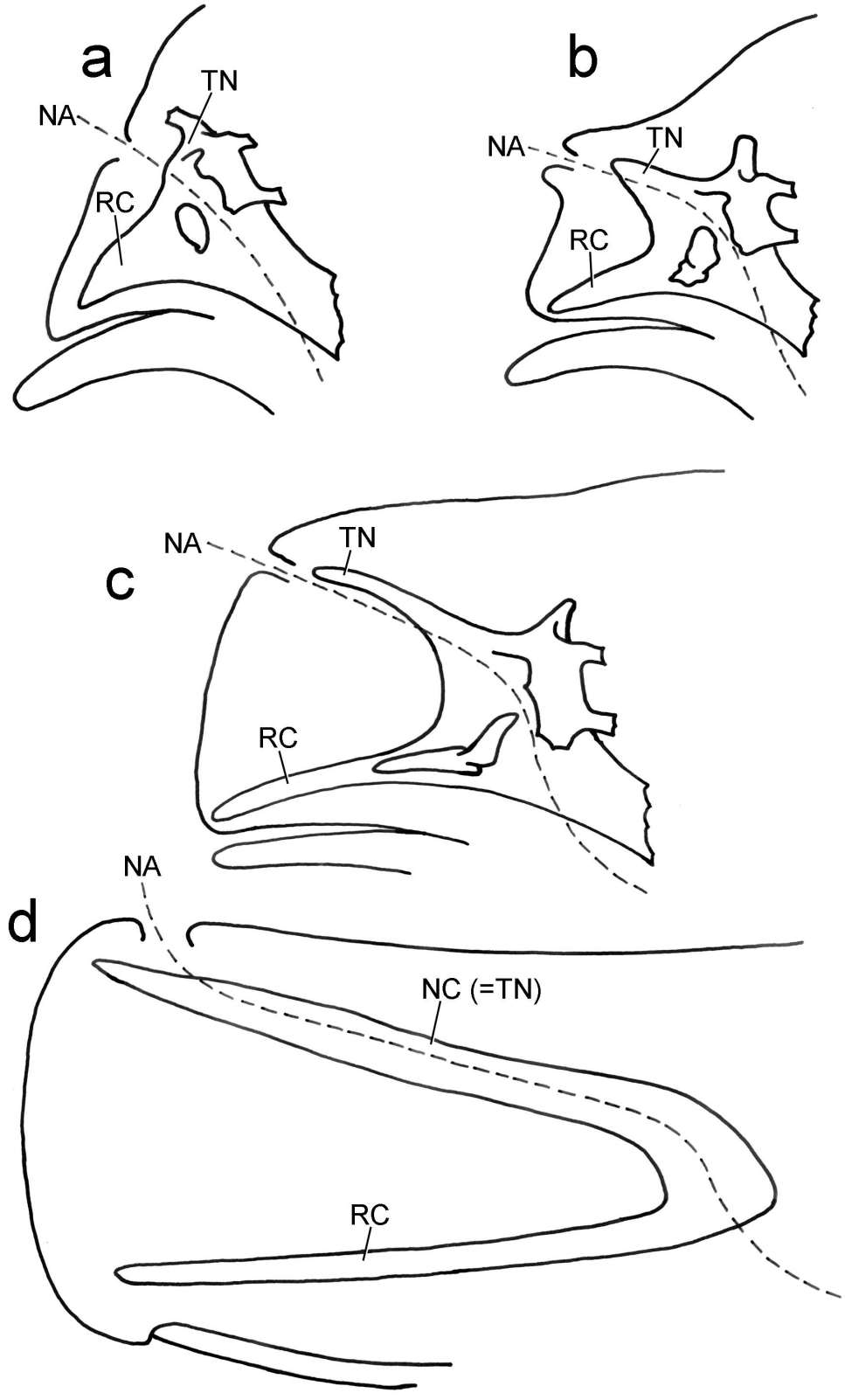


Figure 42: Schematic representation of developmental changes of the cartilaginous structures of the embryonic nasal skull in the sperm whale. The schemes show a sequence of four stages of 40 mm (a), 90 mm (b) 170 mm (c) and 340 cm (d) total length. (a, b, c modified from Behrmann and Klima 1985). NA-nasal passage, NC-nasal roof cartilage, RC-rostral cartilage (cartilaginous rostrum), TN-tectum nasi.

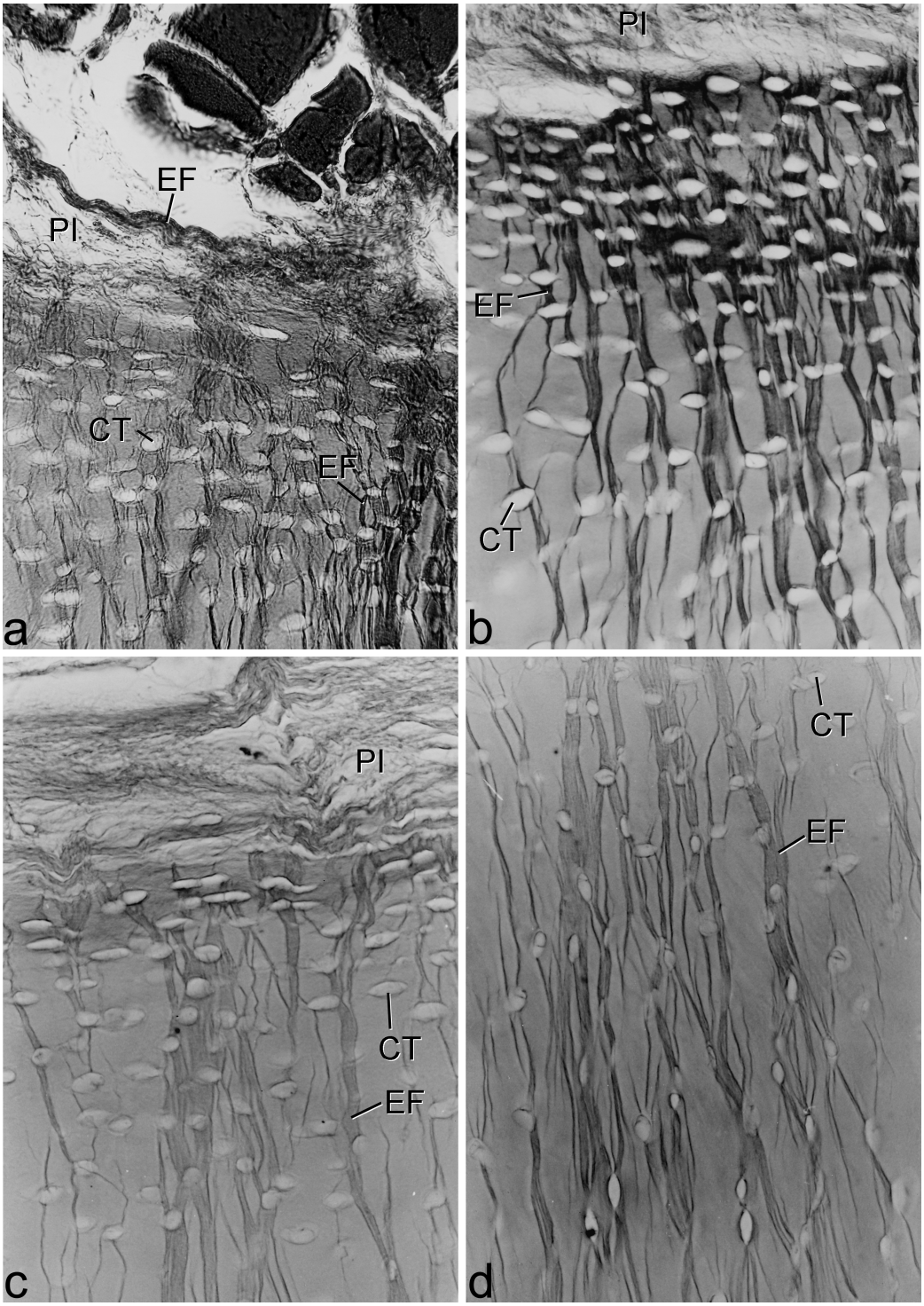


Figure 43: Hyaline cartilaginous tissue of the cartilaginous rostrum of the neonate sperm whale. a) arrangement of cartilage cells and their territories within the extracellular substance in overall view. b) detail of (a). c) blood supply in the form of a lacuna. d) blood supply in the form of a vessel including its wall structures. Stained with AZAN, approximate scale 1:180 (a, c, d) and 1:400 (b). CT-territory of cartilage cell, LB-blood lacuna, VB-blood vessel.

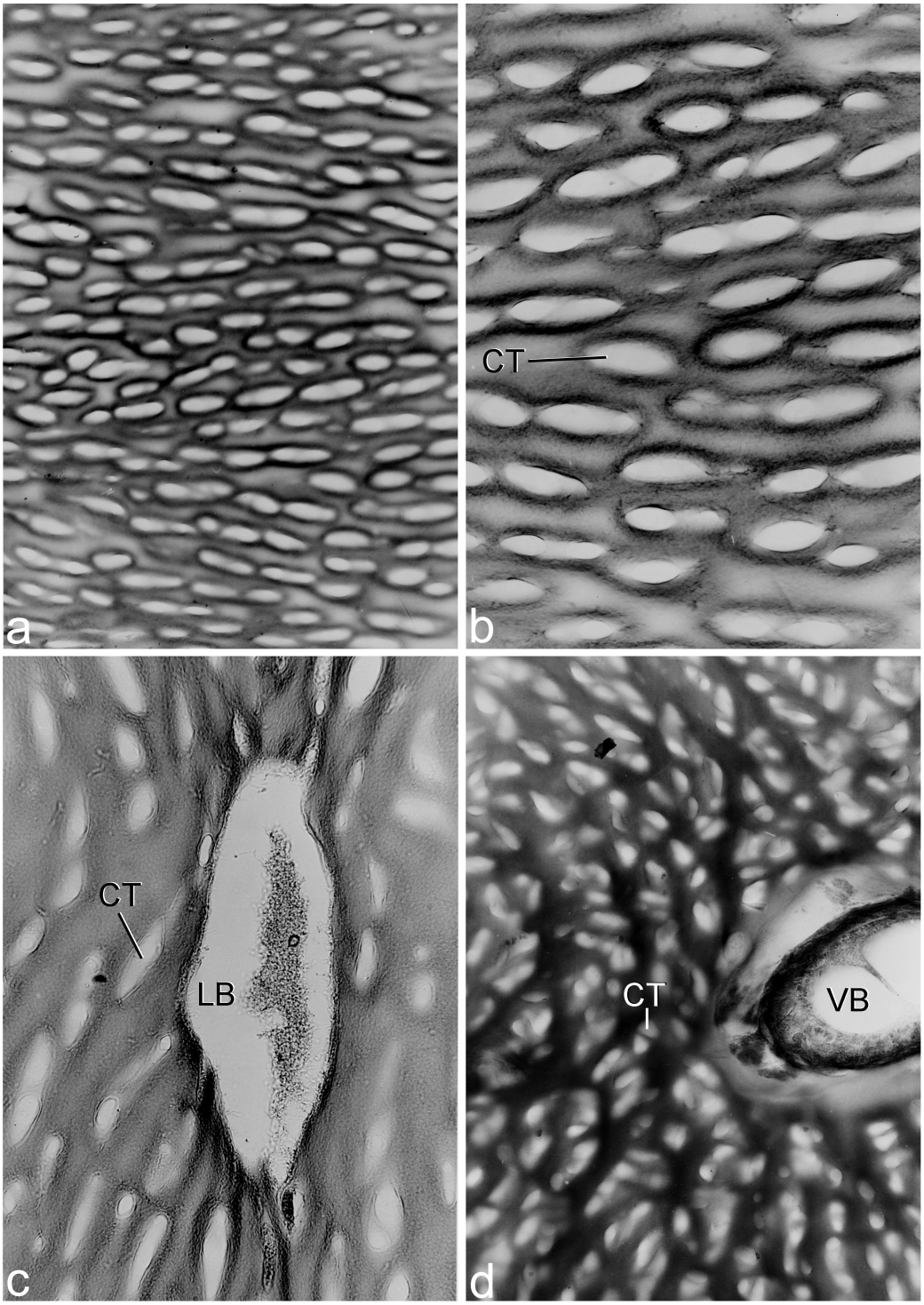


Figure 44: Elastic cartilaginous tissue of the nasal roof cartilage in the neonate sperm whale. a) perichondrium and periphery of cartilage. b) arrangement, proliferation, and ramification of elastic fibers in the periphery of the cartilage. c) penetration of the elastic fibers from the periphery to the center. d) parallel and straight elastic fibers in the center of the cartilage. Stained with AZAN (a, b) and resorcin (c, d), approximate scale 1:180. CT-territory of cartilage cell, EF-elastic fibers, PI-perichondrium.

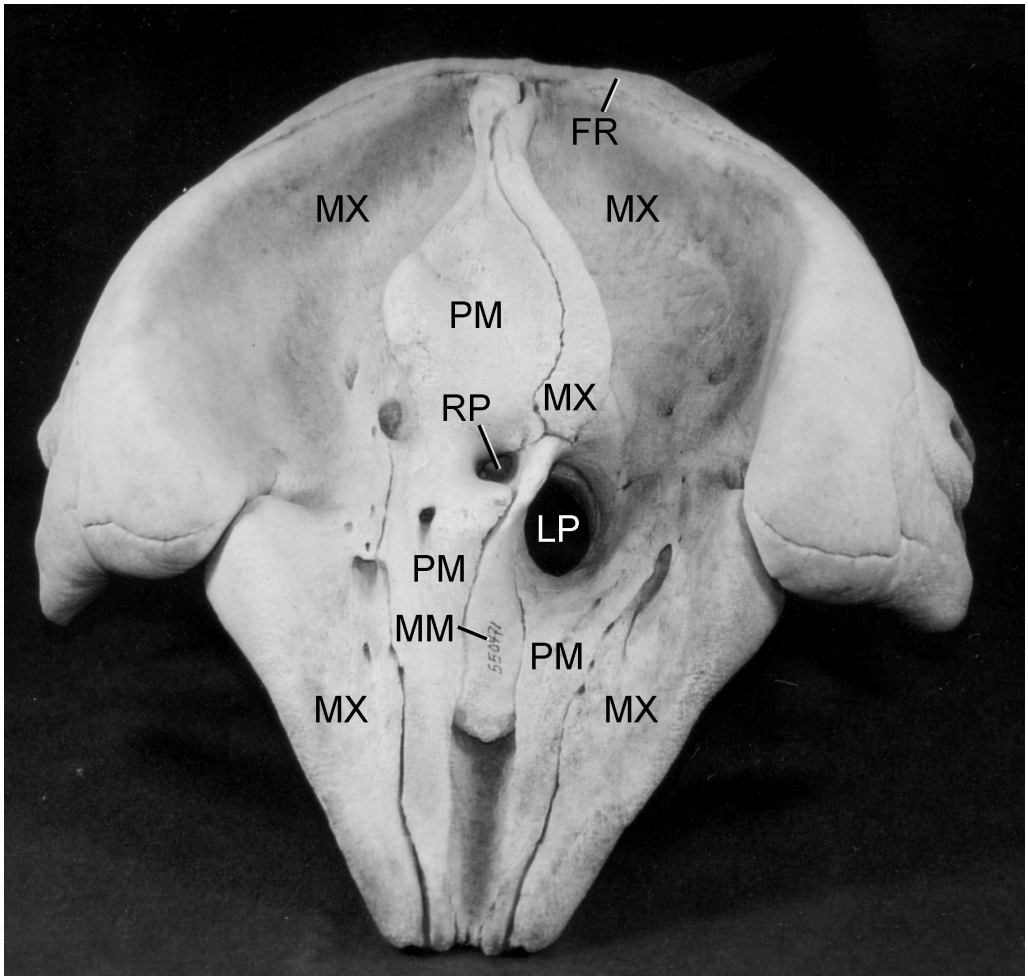


Figure 45: Frontal-dorsal view of an adult dwarf sperm whale (*Kogia sima*) skull showing its main components. The view is directly in the axis of the bony nasal passages Note the high degree of asymmetry. FR-frontal, LP-left nasal passage, MM-mesethmoid, MX-maxilla, PM-premaxilla, RP-right nasal passage. (Courteously: National Museum of Natural History, Smithsonian Institution, Washington, D.C., USA)

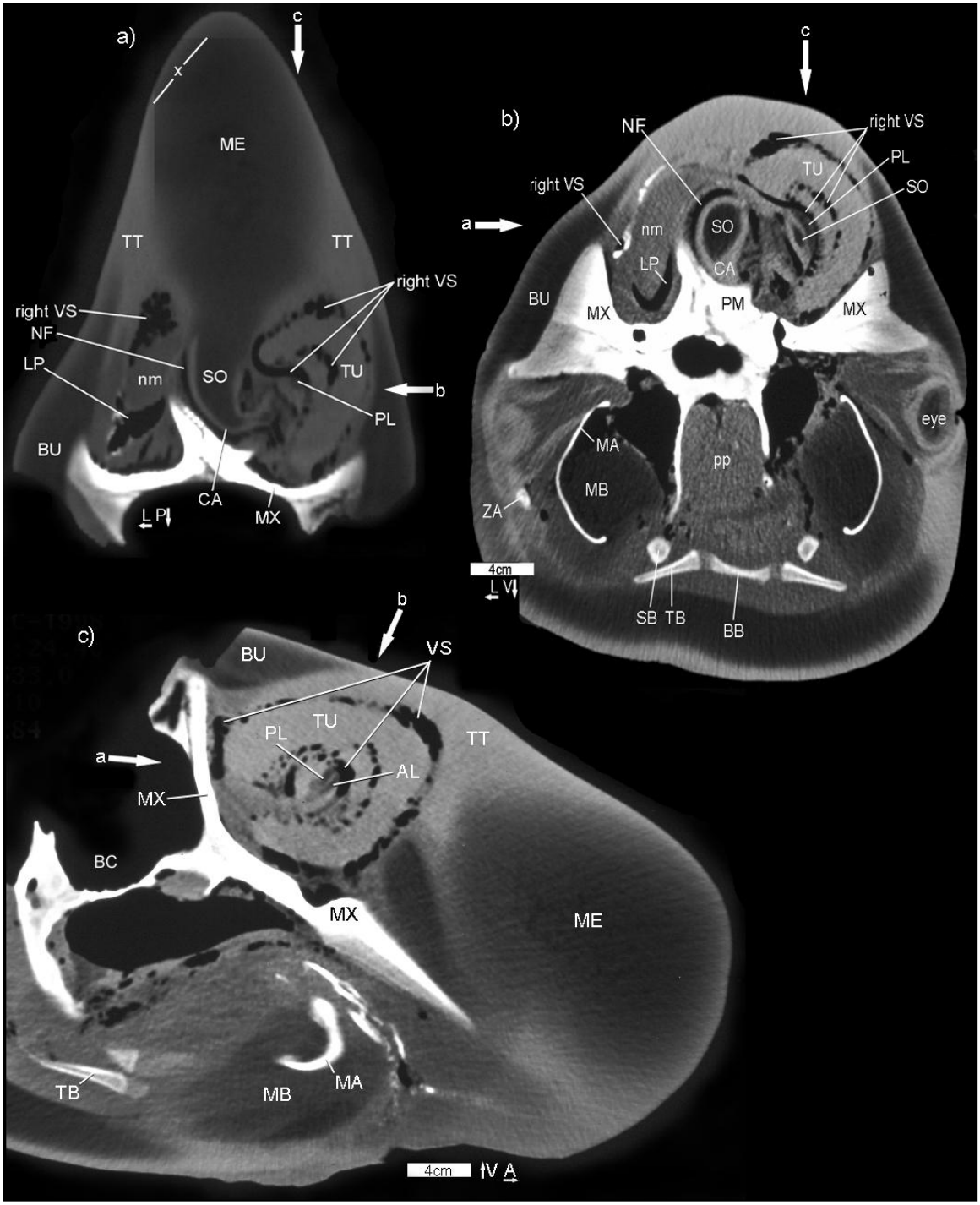


Figure 46: CT scans of a dwarf sperm whale (*Kogia breviceps*) head showing the structures of the nasal complex. a) horizontal plane, b) transverse plane, c) parasagittal plane. Plane orientation are indicated by arrows. A-anterior, AL-anterior right monkey lip, BB-basihyal bone, BC-brain cavity, BU-blubber, CA-case of spermaceti organ, L-left, LP-left nasal passage, MA-mandible, MB-mandibular fat body, ME-melon, MX-maxilla, NF-right nasofrontal sac, nm-nasal plug muscle, P-posterior, PL-posterior right monkey lip, PM-premaxilla, pp-palatopharyngeus muscle, SB-stylohyal bone, SO-spermaceti organ, TB-thyrohyal bone, TT-connective tissue theca, TU-torus, V-ventral, VS-vestibular sac, ZA-zygmatic arch. (Courteously: Dr. Darlene Ketten, Department of Biology, Woods Hole Oceanographic Institution, Woods Hole *and* Massachusetts Ear and Eye Infirmary [MEEI], Havard University, Boston, MA, USA; The scanning was supported by the U.S. Office of Naval Research)

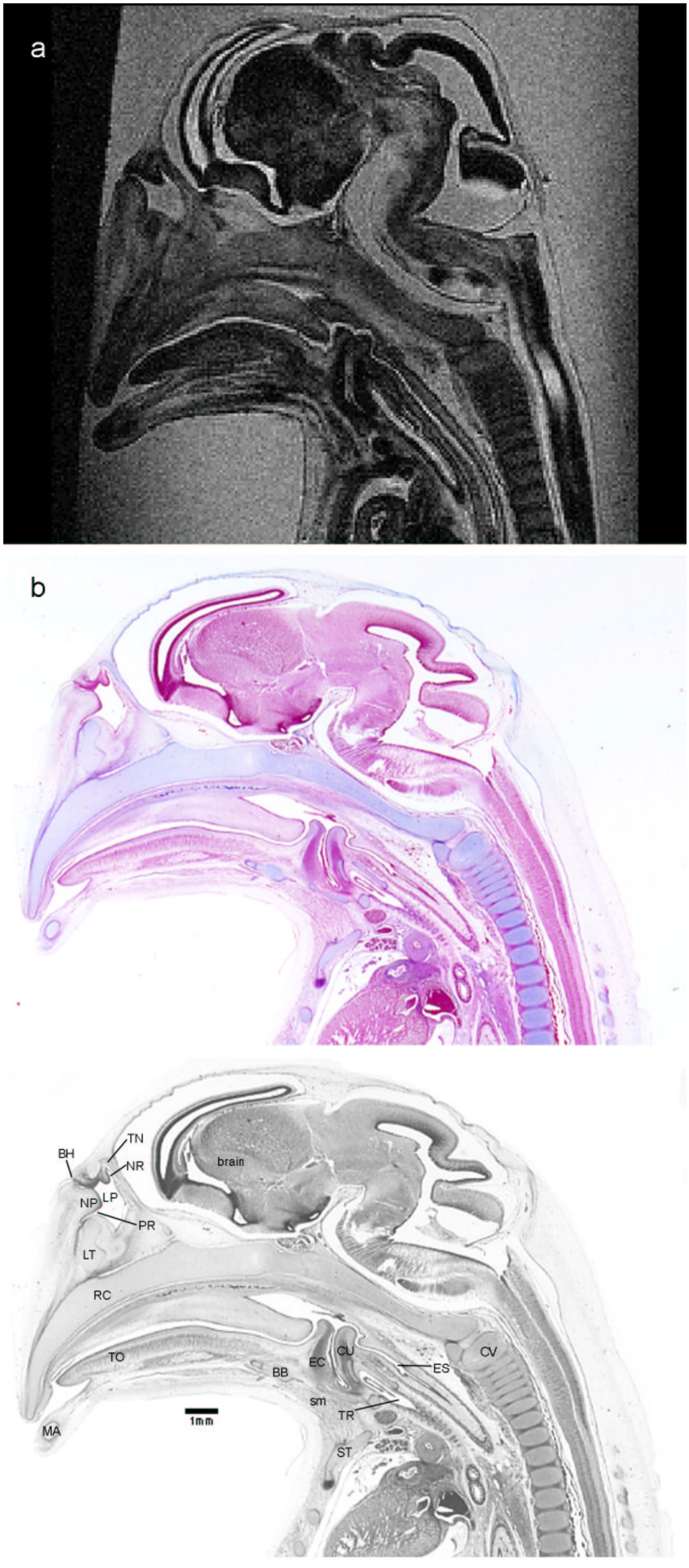


Figure 47: Parasagittal sections of the head of common dolphin (*Delphinus delphis*) fetuses showing the nasal complex and the laryngeal region. a) MRM scan (CRL-38mm; modified after Haddad et al. in prep.), b) histological section stained with AZAN (CRL-40.5mm). BB-basihyal bone, BH-blowhole, CU-cuneiform cartilage, CV-cervical vertebrae, EC-epiglottid cartilage, ES-esophagus, LP-left nasal passage, LT-lamina transversalis anterior, MA-mandible, NP-nasal plug, NR-nasofrontal sac rudiment, PR-premaxillary sac rudiment, RC-rostral cartilage (cartilaginous rostrum), sm-sternohyoid muscle, ST-sternum, TN-tectum nasi, TO-tongue, TR-trachea.

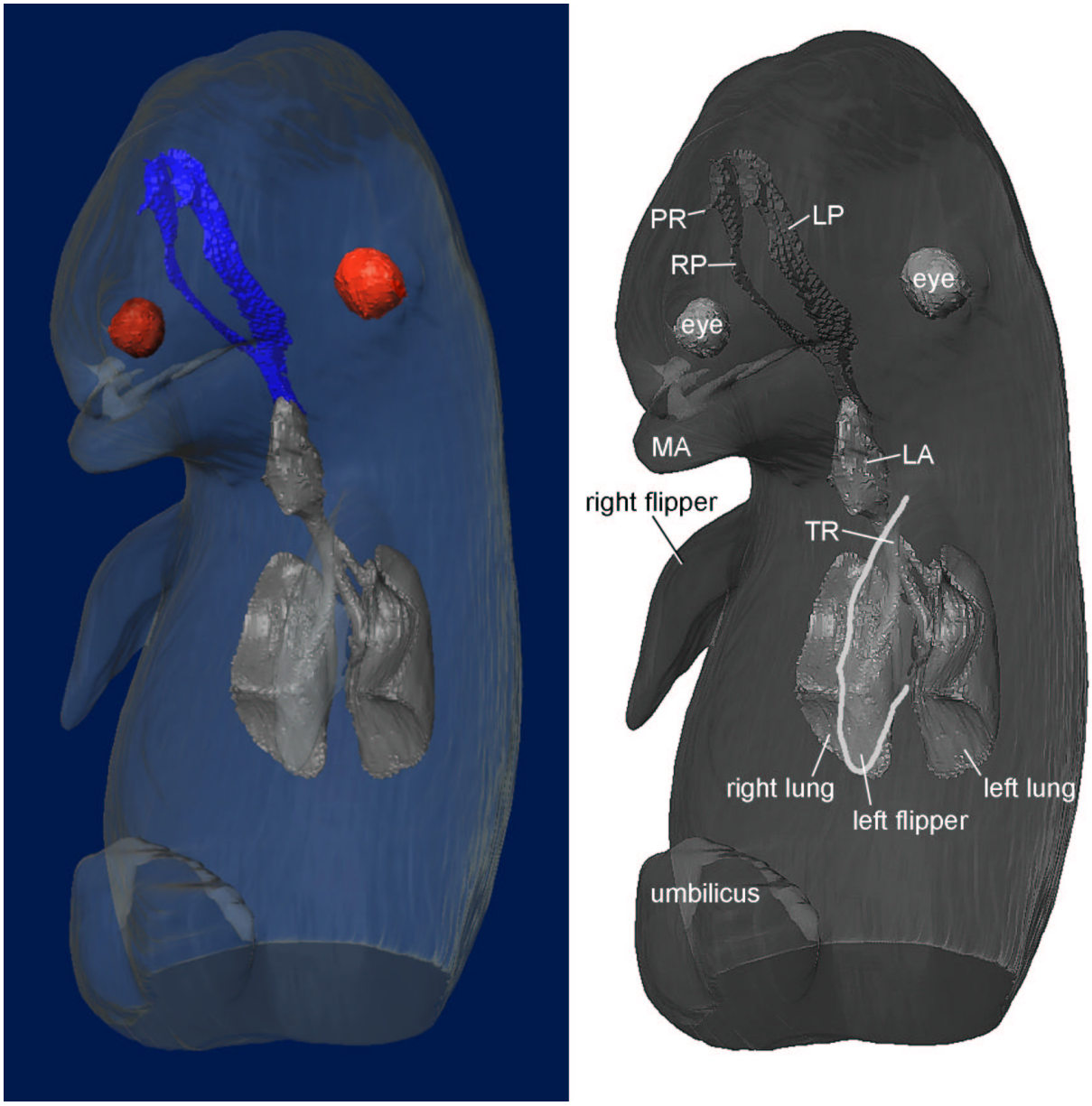


Figure 48: 3-D reconstruction of a common dolphin (*Delphinus delphis*) fetus (CRL-38mm) showing the position of the respiratory tract and the lung. LA-larynx, LP-left nasal passage, MA-mandible, PR-premaxillary sac rudiment, RP-right nasal passage, TR-trachea.

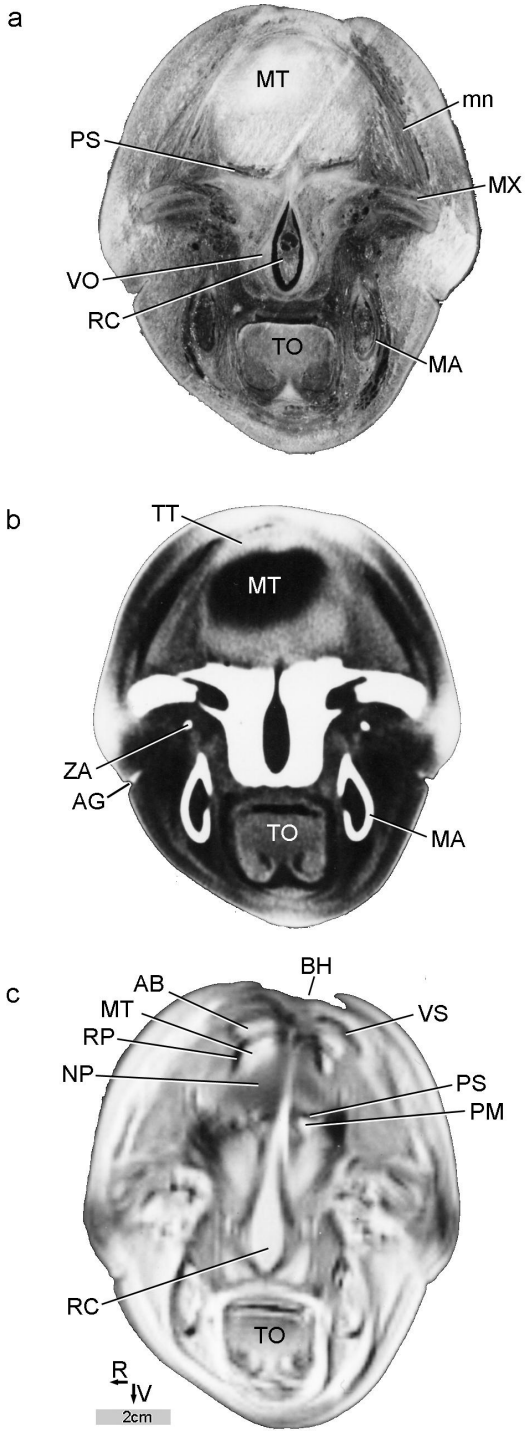


Figure 49: Transverse sections in frontal view of a perinatal spotted dolphin (*Stenella attenuata*) through the melon and rostral to the bony nasal passages, plane orientation see Fig. 4. a) cryo-section, b) CT scan, c) MRI scan (slightly more caudal to a and b but rostral to Fig. 50). Modified after Rauschamnn et al. (in prep.). AB-anterior dorsal bursa, AG-angle of gape, BH-blowhole, MA-mandible, mn-maxillonasolabialis muscle, MT-melon terminus, MX-maxilla, NP-nasal plug, PM-premaxilla, PS-premaxillary sac, R-right, RC-rostral cartilage (cartilaginous rostrum), RP-right nasal passage, TO-tongue, TT-connective tissue theca, V-ventral, VO-vomer, VS-vestibular sac, ZA-zygmatic arch.

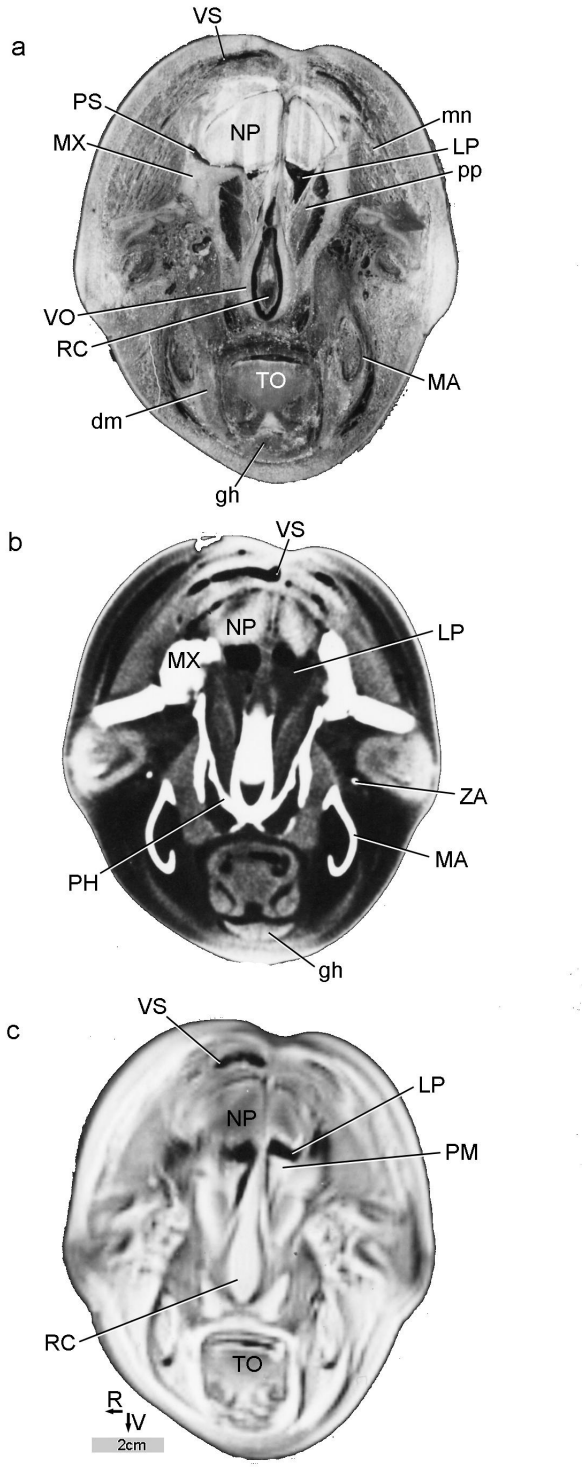


Figure 50: Transverse sections of a perinatal spotted dolphin (*Stenella attenuata*) in frontal view through the nasal passages, for orientation see Fig. 4. a) cryo-section, b) CT scan, c) MRI scan. Modified after Rauschamnn et al. (in prep.). dm-digastric muscle, gh-geniohyoid muscle, LP-left nasal passage, MA-mandible, mn-maxillonasolabialis muscle, MX-maxilla, NP-nasal plug, PM-premaxilla, PH-pterygoid hamulus, pp-palatopharyngeus muscle, PS-premaxillary sac, R-right, RC-rostral cartilage (cartilaginous rostrum), TO-tongue, V-ventral, VO-vomer, VS-vestibular sac, ZA-zygmatic arch.

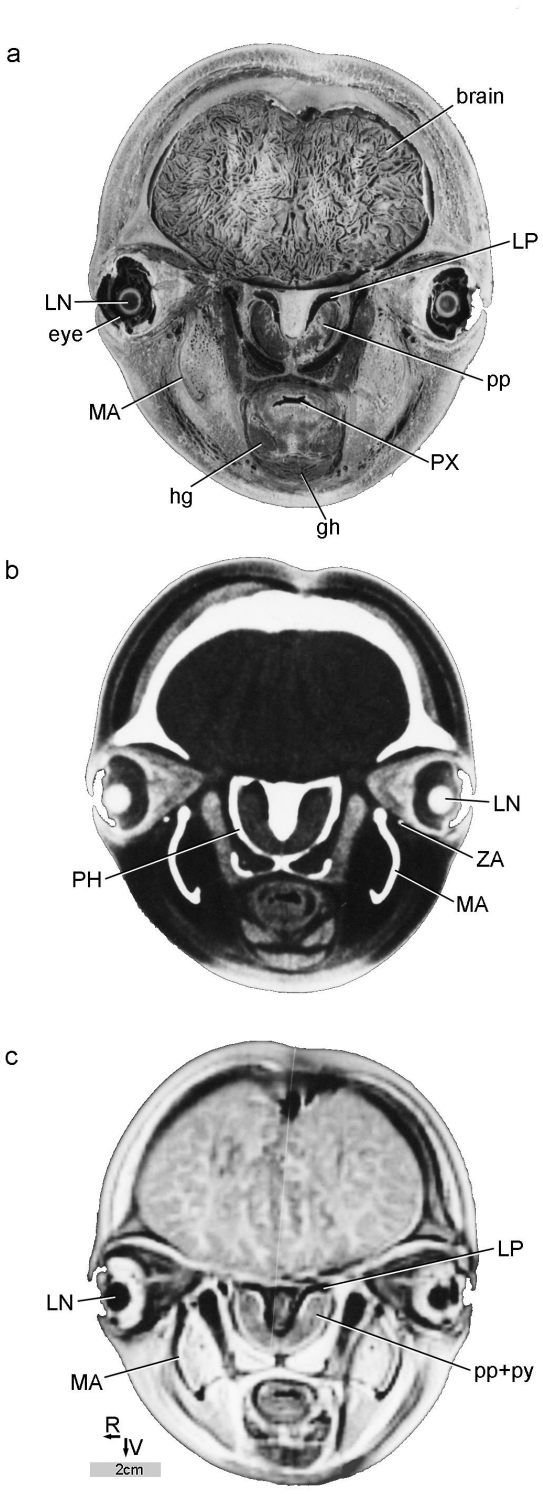


Figure 51: Transverse sections of a perinatal spotted dolphin (*Stenella attenuata*) in frontal view rostral to the larynx, for orientation see Fig. 4. a) cryo-section, b) CT scan, c) MRI scan. Modified after Rauschamnn et al. (in prep.). gh-geniohyoid muscle, hg-hyoglossus muscle, LN-lens, LP-left nasal passage, MA-mandible, PH-pterygoid hamulus, pp-palatopharyngeus muscle, py-pterygopharyngeus muscle, PX-pharynx, R-right, V-ventral, ZA-zygmatic arch.

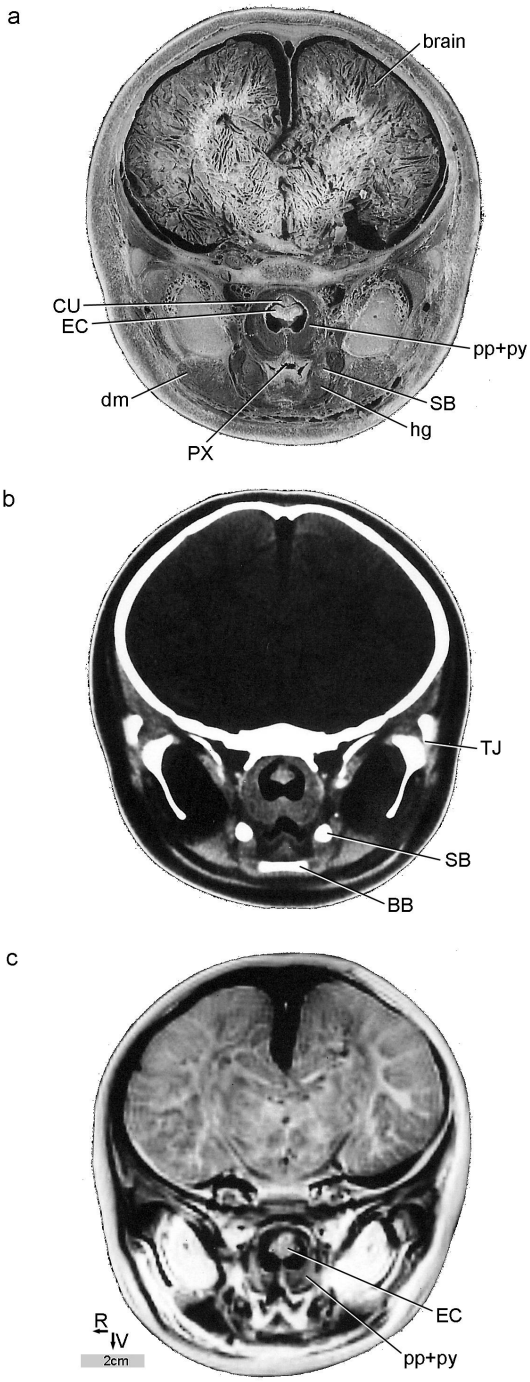


Figure 52: Transverse sections of a perinatal spotted dolphin (*Stenella attenuata*) in frontal view at the rostral tip of the larynx, for orientation see Fig. 4. a) cryo-section (brain tissue with many artifacts caused by the freezing of the specimen before sawing), b) CT scan, c) MRI scan. BB-basihyal bone, CU-cuneiform cartilage, dm-digastric muscle, EC-epiglottid cartilage, hg-hyoglossus muscle, pp-palatopharyngeus muscle, py-pterygopharyngeus muscle, PX-pharynx, R-right, SB-stylohyal bone, TJ-tympanomandibular joint, V-ventral.

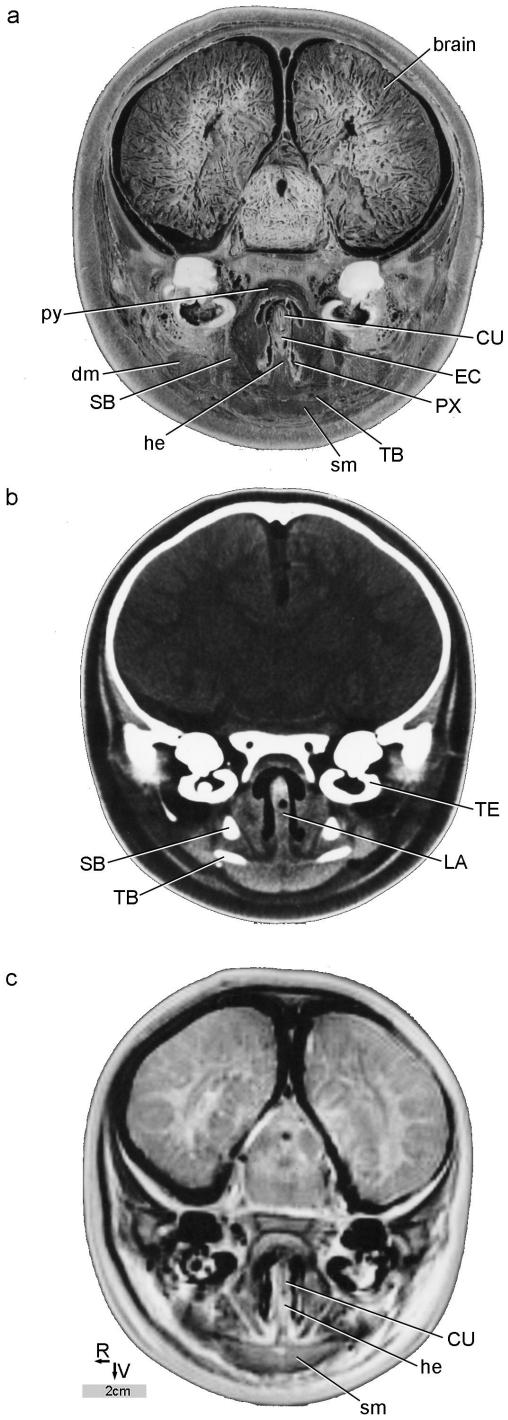


Figure 53: Transverse sections of a perinatal spotted dolphin (*Stenella attenuata*) in frontal view through the epiglottic spout of the larynx, for orientation see Fig. 4. a) cryo-section (brain tissue with many artifacts caused by the freezing of the specimen before sawing), b) CT scan, c) MRI scan. Modified after Rauschamnn et al. (in prep.). CU-cuneiform cartilage, EC-epiglottid cartilage, dm-digastric muscle, he-hyoepiglottic muscle, LA- larynx, py-pterygopharyngeus muscle, PX-pharynx, R-right, SB-stylohyal bone, sm-sternohyoid muscle, TB-thyrohyal bone, TE-tympanoperiotic bone, V-ventral.

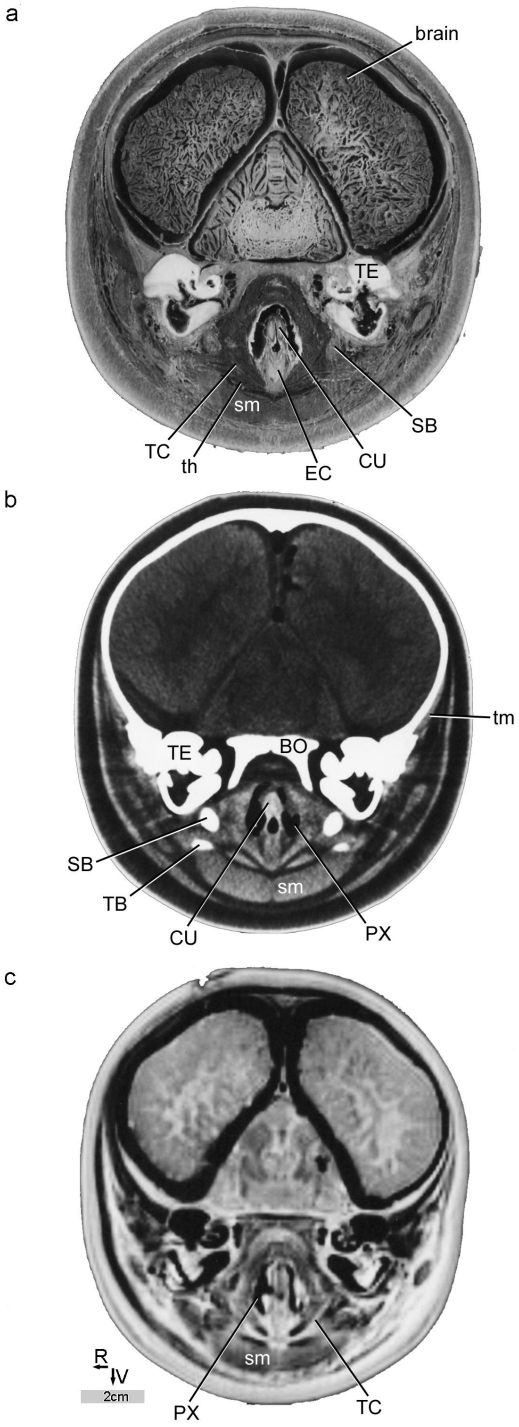


Figure 54: Transverse sections of a perinatal spotted dolphin (*Stenella attenuata*) in frontal view through the larynx caudal to Fig. 53, for orientation see Fig. 4. a) cryo-section (brain tissue with many artifacts caused by the freezing of the specimen before sawing), b) CT scan, c) MRI scan (slightly more caudal to a and b). Modified after Rauschamnn et al. (in prep.). BO-basioccipital, CU-cuneiform cartilage, EC-epiglottid cartilage, PX-pharynx, R-right, SB-stylohyal bone, sm-sternohyoid muscle, TB-thyrohyal bone, TC-thyroid cartilage, TE-tympanoperiotic bone, th-thyrohyoid muscle, tm-temporalis muscle, V-ventral.

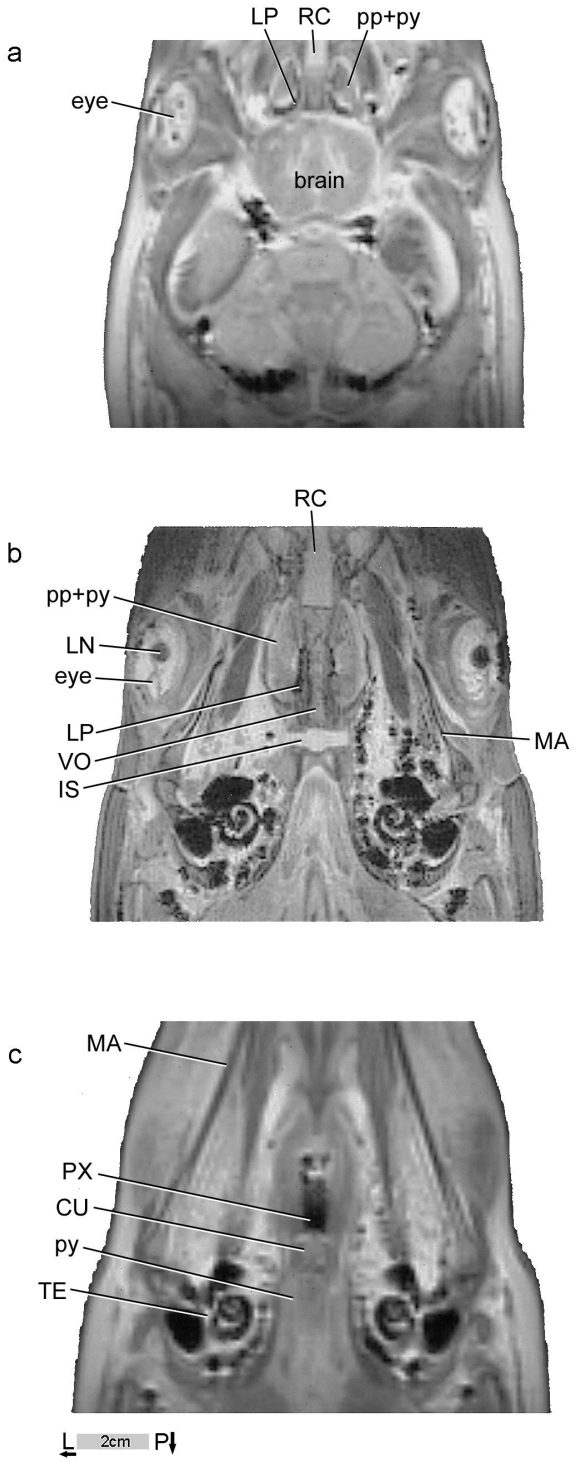


Figure 55: Horizontal MRI scans of a perinatal spotted dolphin (*Stenella attenuata*) from dorsal (a) to ventral (c) at level of the choanae, for orientation see Fig. 4. Note that the slice thickness is larger in (b) than in (a) and (c). Modified after Rauschamnn et al. (in prep.). CU-cuneiform cartilage, IS-intersphenoid synchrondosis, L-left, LN-lens, LP-left nasal passage, MA-mandible, P-posterior, pp-palatopharyngeus muscle, py-pterygopharyngeus muscle, PX-pharynx, RC-rostral cartilage (cartilaginous rostrum), TE-tympanoperiotic bone, VO-vomer.

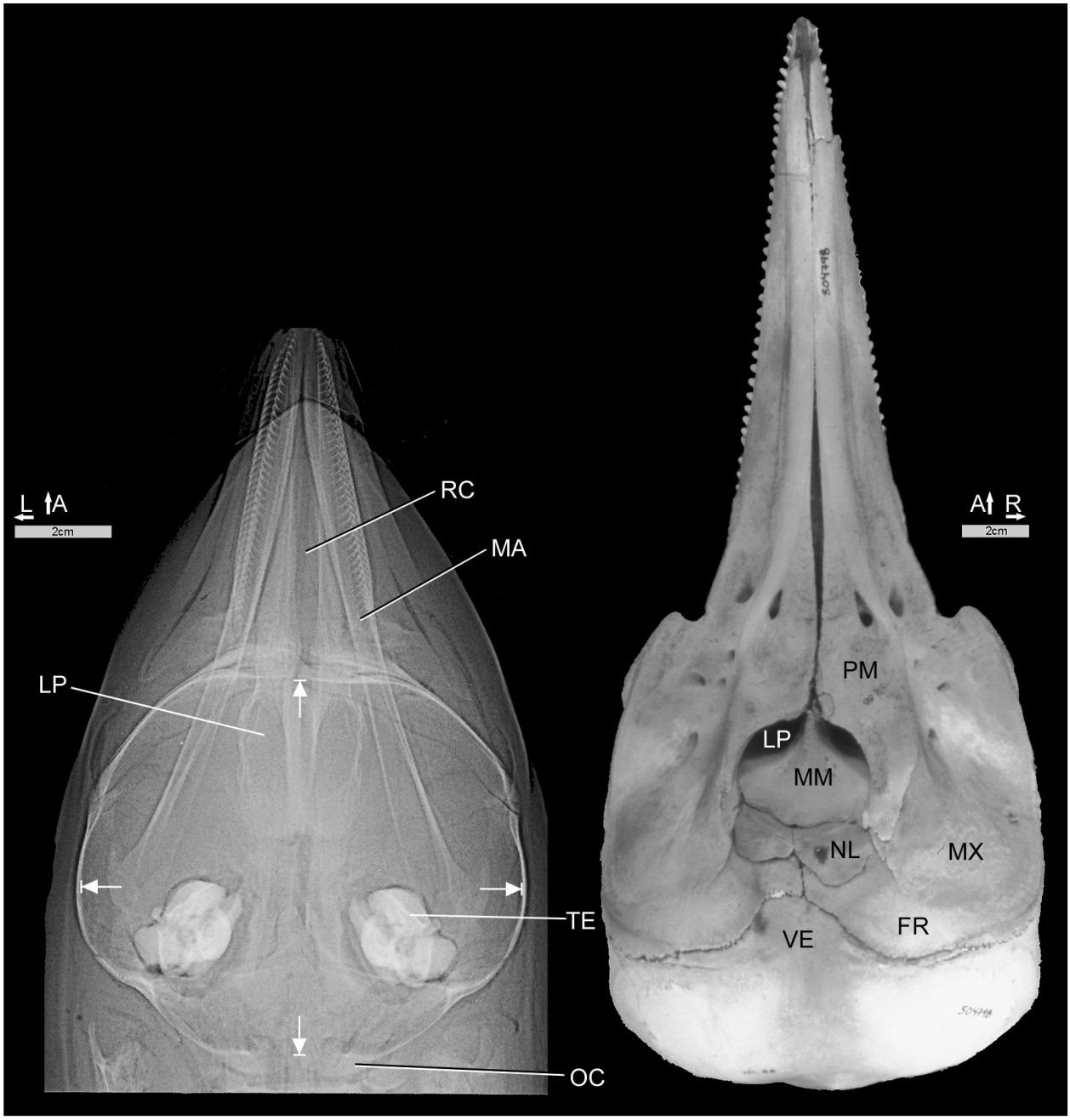


Figure 56: Left: x-ray photograph of a perinatal spotted dolphin (*Stenella attenuata*) skull in horizontal orientation. The arrows mark the cranial vault. Modified after Rauschamnn et al. (in prep.). Right: dorsal view of a subadult spotted dolphin skull (total length of animal: 145 cm). A-anterior, FR-frontal, L-left, LP-left nasal passage, MA-mandible, MM-mesethmoid, MX-maxilla, NL-nasal, OC-occipital condyle, PM-premaxilla, R-right, RC-rostral cartilage (cartilaginous rostrum), TE-tympanoperiotic bone, VE-vertex of skull.

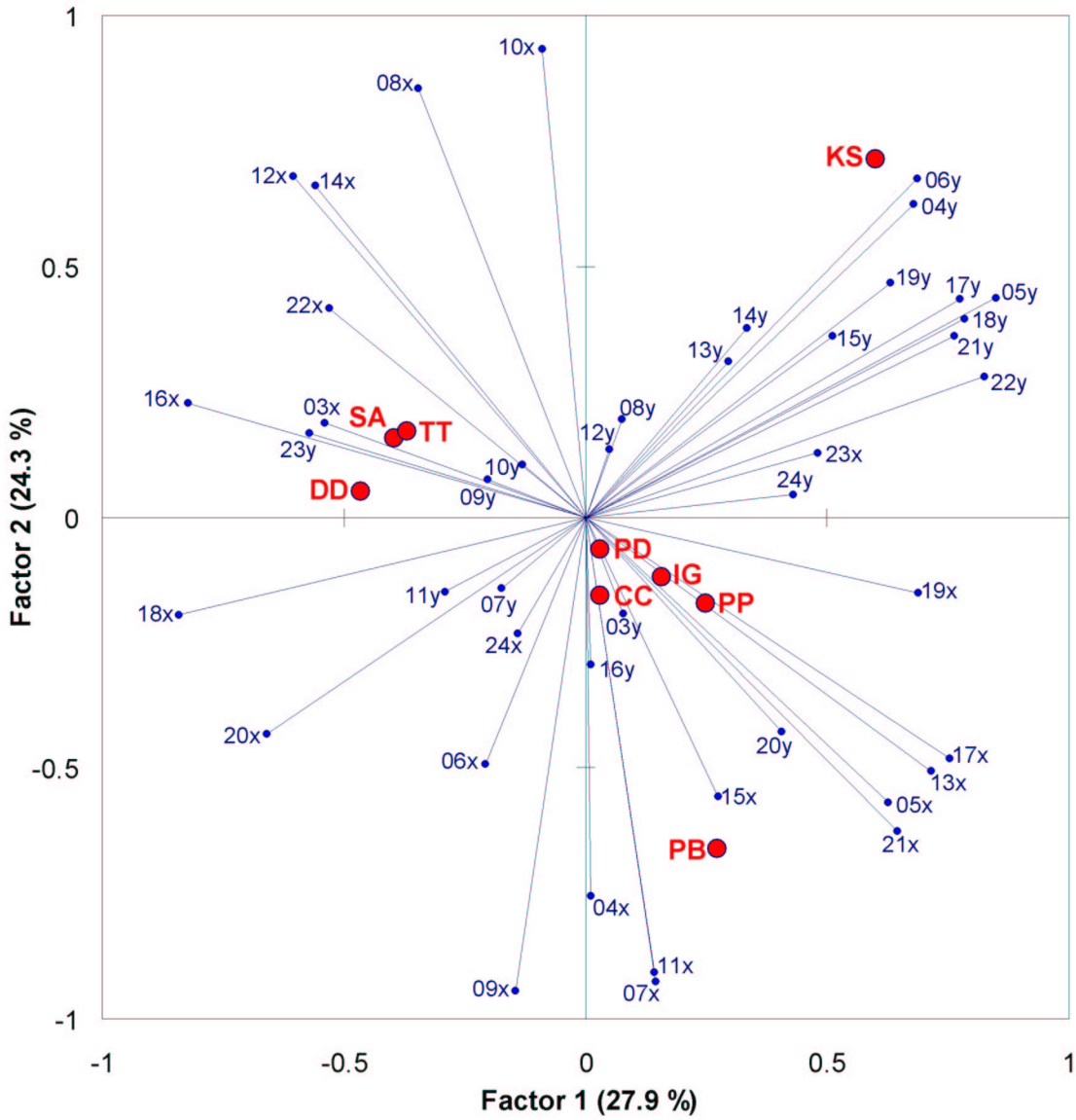


Figure 57: Graphical representation of first and second factors of the principle component analysis (PCA) of active variables (x and y values of landmark positions) and passive variables (species). For interpretation see Box 1 in chapter 5.3. *Cephalorhynchus commersonii* (CC), *Delphinus delphis* (DD), *Inia geoffrensis* (IG), *Kogia sima* (KS), *Phocoenoides dalli* (PD), *Phocoena phocoena* (PP), *Pontoporia blainvillei* (PB), *Stenella attenuata* (SA), *Tursiops truncatus* (TT)

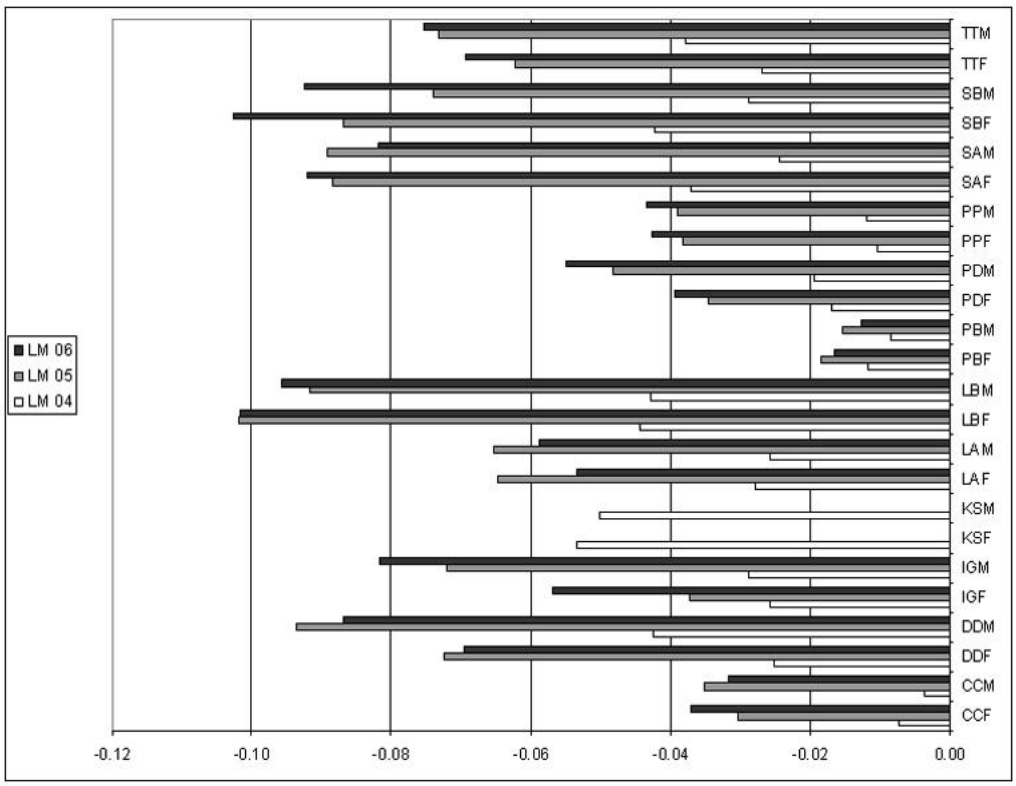


Figure 58: Distance of landmarks (LM) 4, 5, and 6 to the axis of the skull perpendicular to the skull axis, negative values mean a left position in relation to the skull axis, explanations see text. CCF - Cephalorhynchus commersonii female, CCM - Cephalorhynchus commersonii male, DDF - Delphinus delphis female, DDM - Delphinus delphis male, IGF - Inia geoffrensis female, IGM - Inia geoffrensis male, KSF - Kogia sima female, KSM - Kogia sima male, LAF - Lagenorhynchus acutus female, LAM - Lagenorhynchus acutus male, LBF - Lissodelphis borealis female, LBM - Lissodelphis borealis male, PBF - Pontoporia blainvillei female, PBM - Pontoporia blainvillei male, PDF - Phocoenoides dalli female, PDM - Phocoenoides dalli male, PPF - Phocoena phocoena female, PPM - Phocoena phocoena male, SAF - Stenella attenuata female, SAM - Stenella attenuata male, SBF - Steno bredanensis female, SBM - Steno bredanensis male, TTF - Tursiops truncatus female, TTM - Tursiops truncatus male.

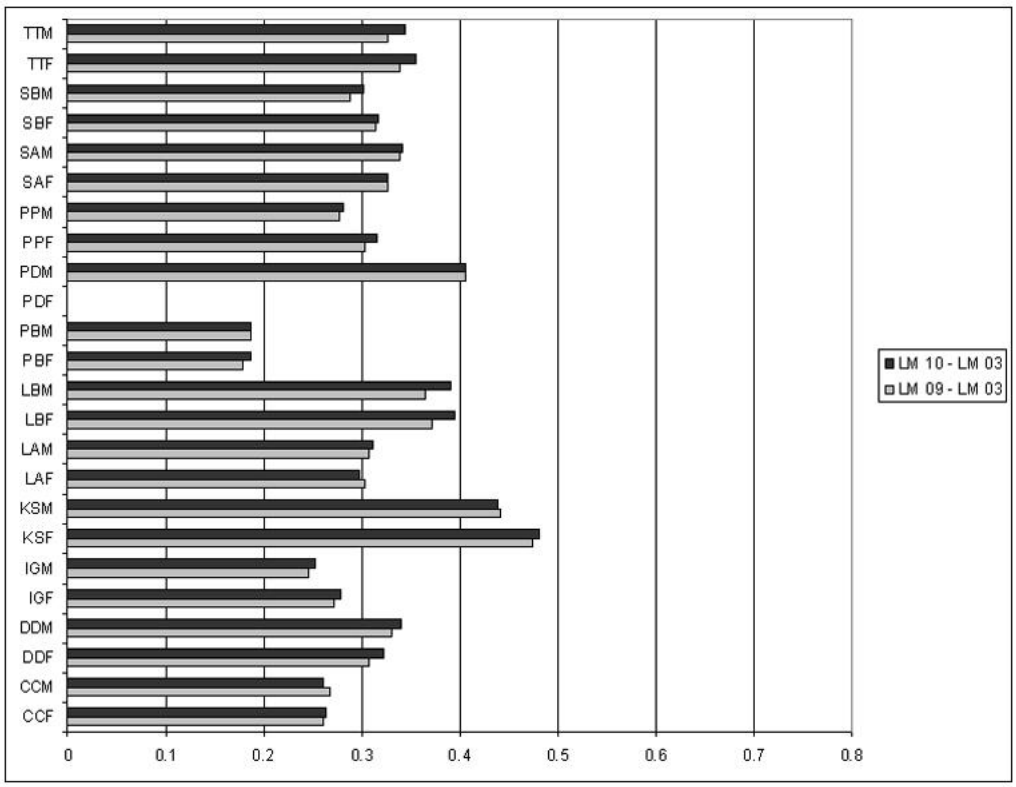


Figure 59: Rostrum width at its base to the facial skull on each side as judged by the distance of LM 9 - LM 3 and LM 10 - LM 3 perpendicular to the (artificial) skull axis (Table 3, Fig. 5, explanations see text). CCF - Cephalorhynchus commersonii female, CCM - Cephalorhynchus commersonii male, DDF - Delphinus delphis female, DDM - Delphinus delphis male, IGF - Inia geoffrensis female, IGM - Inia geoffrensis male, KSF - Kogia sima female, KSM - Kogia sima male, LAF - Lagenorhynchus acutus female, LAM - Lagenorhynchus acutus male, LBF - Lissodelphis borealis female, LBM - Lissodelphis borealis male, PBF - Pontoporia blainvillei female, PBM - Pontoporia blainvillei male, PDF - Phocoenoides dalli female, PDM - Phocoenoides dalli male, PPF - Phocoena phocoena female, PPM - Phocoena phocoena male, SAF - Stenella attenuata female, SAM - Stenella attenuata male, SBF - Steno bredanensis female, SBM - Steno bredanensis male, TTF - Tursiops truncatus female, TTM - Tursiops truncatus male.

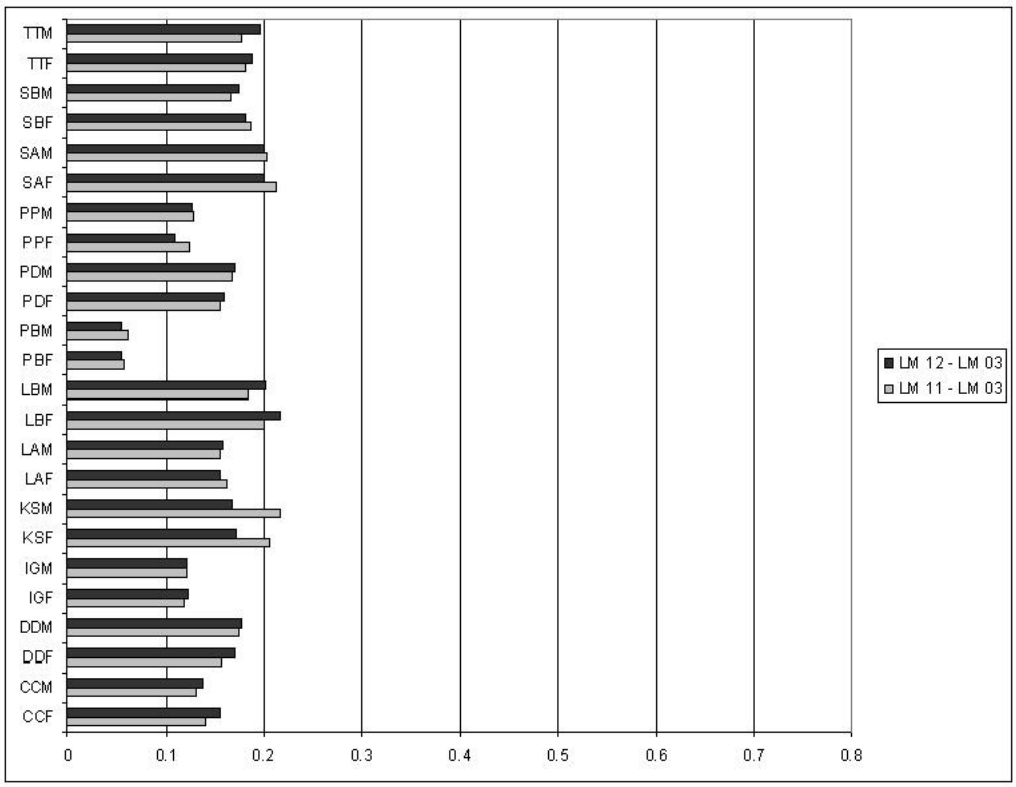


Figure 60: Width of the premaxillary bones at the border to the rostrum as judged by the distance of LM 11 - LM 3 and LM 12 - LM 3 perpendicular to the (artificial) skull axis (Table 3, Fig. 5, explanations see text). CCF - Cephalorhynchus commersonii female, CCM - Cephalorhynchus commersonii male, DDF - Delphinus delphis female, DDM - Delphinus delphis male, IGF - Inia geoffrensis female, IGM - Inia geoffrensis male, KSF - Kogia sima female, KSM - Kogia sima male, LAF - Lagenorhynchus acutus female, LAM - Lagenorhynchus acutus male, LBF - Lissodelphis borealis female, LBM - Lissodelphis borealis male, PBF - Pontoporia blainvillei female, PBM - Pontoporia blainvillei male, PDF - Phocoenoides dalli female, PDM - Phocoenoides dalli male, PPF - Phocoena phocoena female, PPM - Phocoena phocoena male, SAF - Stenella attenuata female, SAM - Stenella attenuata male, SBF - Steno bredanensis female, SBM - Steno bredanensis male, TTF - Tursiops truncatus female, TTM - Tursiops truncatus male.

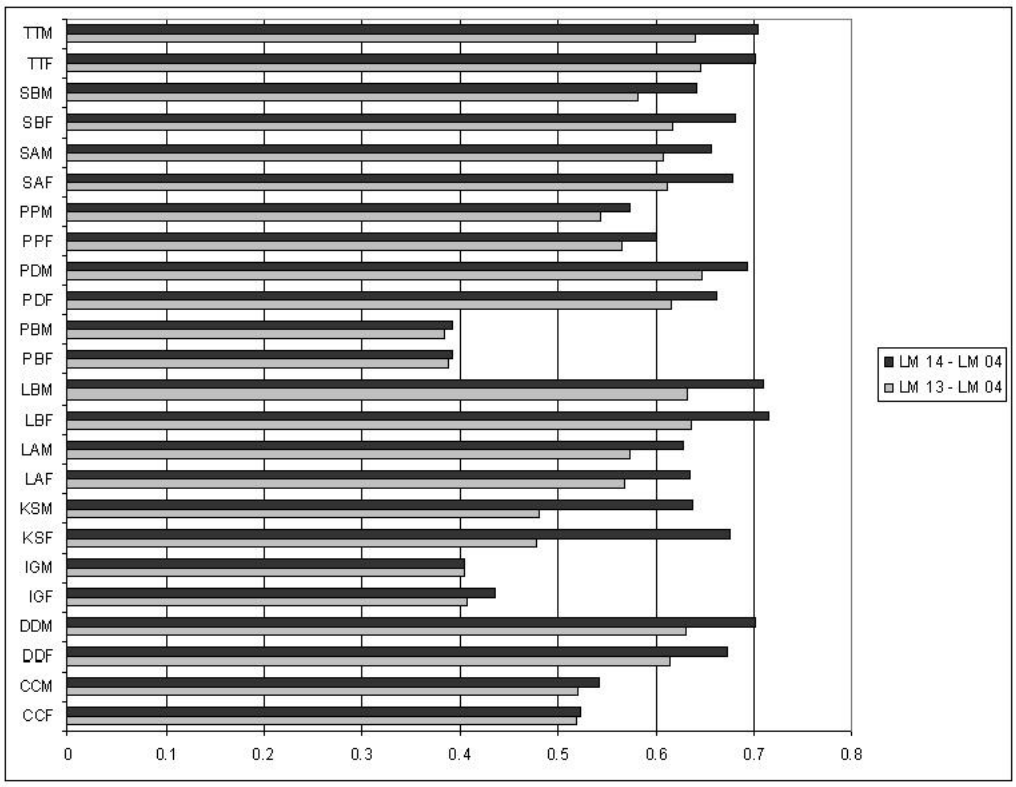


Figure 61: Width of the facial skull on each side as judged by the distance of LM 13 - LM 4 and LM 14 - LM 4 perpendicular to the (artificial) skull axis (Table 3, Fig. 5, explanations see text). CCF - Cephalorhynchus commersonii female, CCM - Cephalorhynchus commersonii male, DDF - Delphinus delphis female, DDM - Delphinus delphis male, IGF - Inia geoffrensis female, IGM - Inia geoffrensis male, KSF - Kogia sima female, KSM - Kogia sima male, LAF - Lagenorhynchus acutus female, LAM - Lagenorhynchus acutus male, LBF - Lissodelphis borealis female, LBM - Lissodelphis borealis male, PBF - Pontoporia blainvillei female, PBM - Pontoporia blainvillei male, PDF - Phocoenoides dalli female, PDM - Phocoenoides dalli male, PPF - Phocoena phocoena female, PPM - Phocoena phocoena male, SAF - Stenella attenuata female, SAM - Stenella attenuata male, SBF - Steno bredanensis female, SBM - Steno bredanensis male, TTF - Tursiops truncatus female, TTM - Tursiops truncatus male.

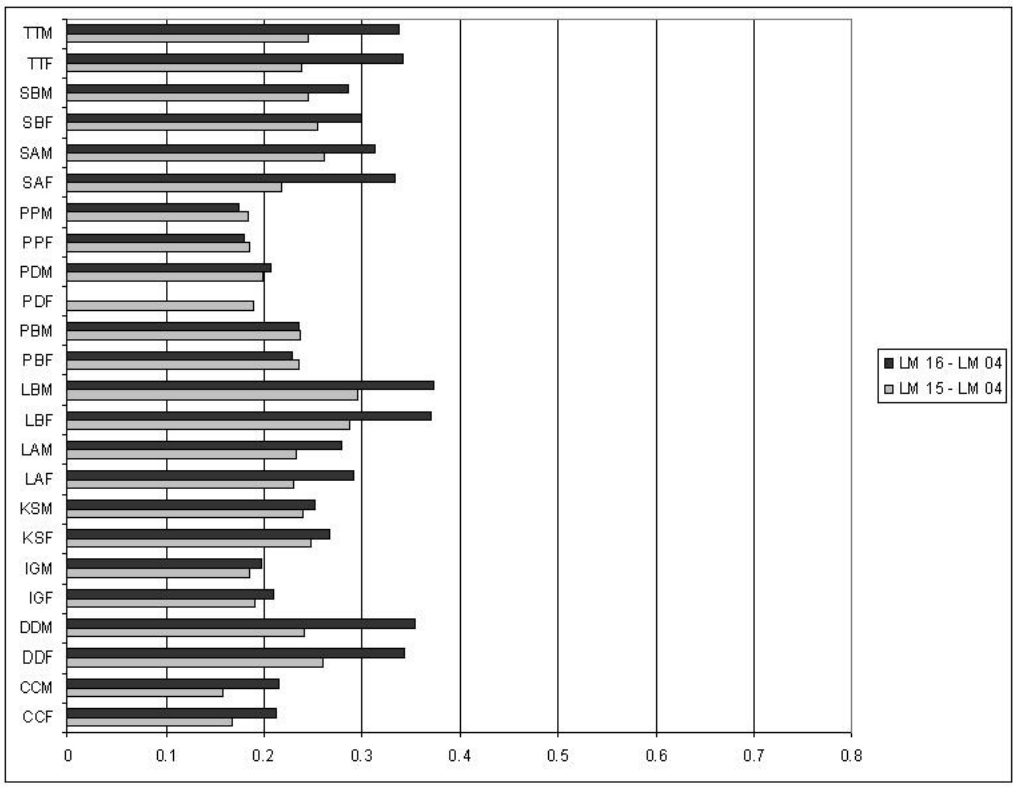


Figure 62: Maximal width of the premaxillary bones as judged by the distance of LM 15 - LM 4 and LM 16 - LM 4 perpendicular to the (artificial) skull axis (Table 3, Fig. 5, explanations see text). CCF - Cephalorhynchus commersonii female, CCM - Cephalorhynchus commersonii male, DDF - Delphinus delphis female, DDM - Delphinus delphis male, IGF - Inia geoffrensis female, IGM - Inia geoffrensis male, KSF - Kogia sima female, KSM - Kogia sima male, LAF - Lagenorhynchus acutus female, LAM - Lagenorhynchus acutus male, LBF - Lissodelphis borealis female, LBM - Lissodelphis borealis male, PBF - Pontoporia blainvillei female, PBM - Pontoporia blainvillei male, PDF - Phocoenoides dalli female, PDM - Phocoenoides dalli male, PPF - Phocoena phocoena female, PPM - Phocoena phocoena male, SAF - Stenella attenuata female, SAM - Stenella attenuata male, SBF - Steno bredanensis female, SBM - Steno bredanensis male, TTF - Tursiops truncatus female, TTM - Tursiops truncatus male.

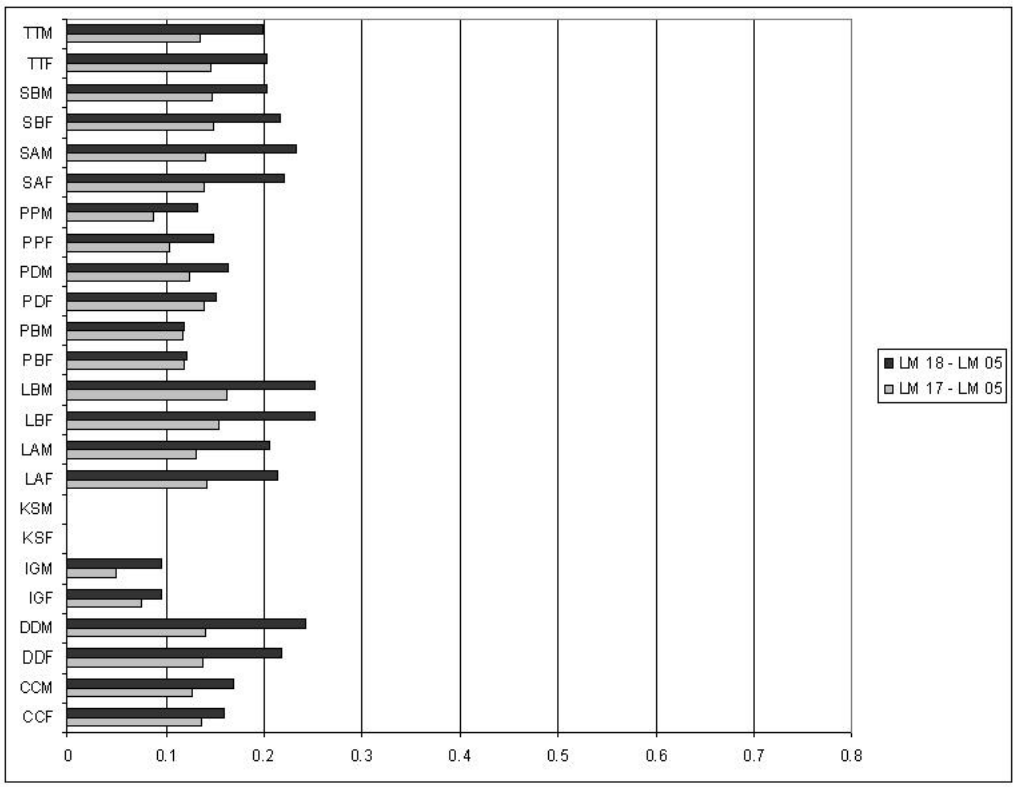


Figure 63: Width of the bony nares as judged by the distance of LM 17 - LM 5 and LM 18 - LM 5 perpendicular to the (artificial) skull axis (Table 3, Fig. 5, explanations see text). CCF - Cephalorhynchus commersonii female, CCM - Cephalorhynchus commersonii male, DDF - Delphinus delphis female, DDM - Delphinus delphis male, IGF - Inia geoffrensis female, IGM - Inia geoffrensis male, KSF - Kogia sima female, KSM - Kogia sima male, LAF - Lagenorhynchus acutus female, LAM - Lagenorhynchus acutus male, LBF - Lissodelphis borealis female, LBM - Lissodelphis borealis male, PBF - Pontoporia blainvillei female, PBM - Pontoporia blainvillei male, PDF - Phocoenoides dalli female, PDM - Phocoenoides dalli male, PPF - Phocoena phocoena female, PPM - Phocoena phocoena male, SAF - Stenella attenuata female, SAM - Stenella attenuata male, SBF - Steno bredanensis female, SBM - Steno bredanensis male, TTF - Tursiops truncatus female, TTM - Tursiops truncatus male.

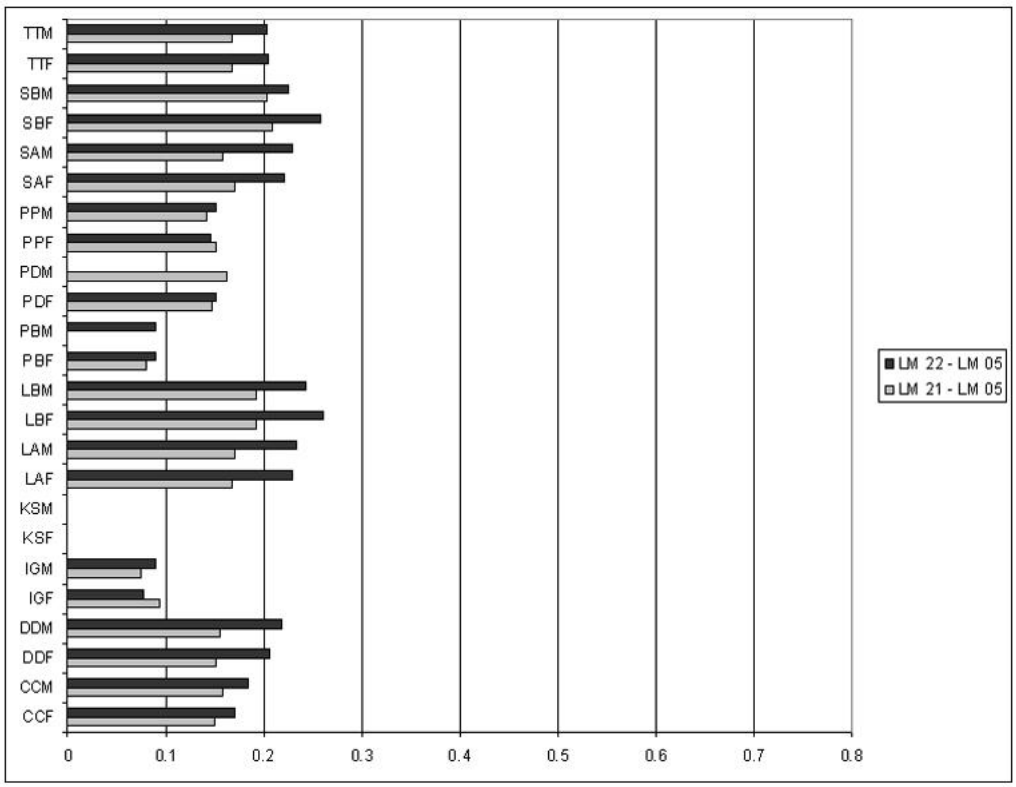


Figure 64: Width of the nasal bones as judged by the distance of LM 21 - LM 5 and LM 22 - LM 5 perpendicular to the (artificial) skull axis (Table 3, Fig. 5, explanations see text). CCF - Cephalorhynchus commersonii female, CCM - Cephalorhynchus commersonii male, DDF - Delphinus delphis female, DDM - Delphinus delphis male, IGF - Inia geoffrensis female, IGM - Inia geoffrensis male, KSF - Kogia sima female, KSM - Kogia sima male, LAF - Lagenorhynchus acutus female, LAM - Lagenorhynchus acutus male, LBF - Lissodelphis borealis female, LBM - Lissodelphis borealis male, PBF - Pontoporia blainvillei female, PBM - Pontoporia blainvillei male, PDF - Phocoenoides dalli female, PDM - Phocoenoides dalli male, PPF - Phocoena phocoena female, PPM - Phocoena phocoena male, SAF - Stenella attenuata female, SAM - Stenella attenuata male, SBF - Steno bredanensis female, SBM - Steno bredanensis male, TTF - Tursiops truncatus female, TTM - Tursiops truncatus male.

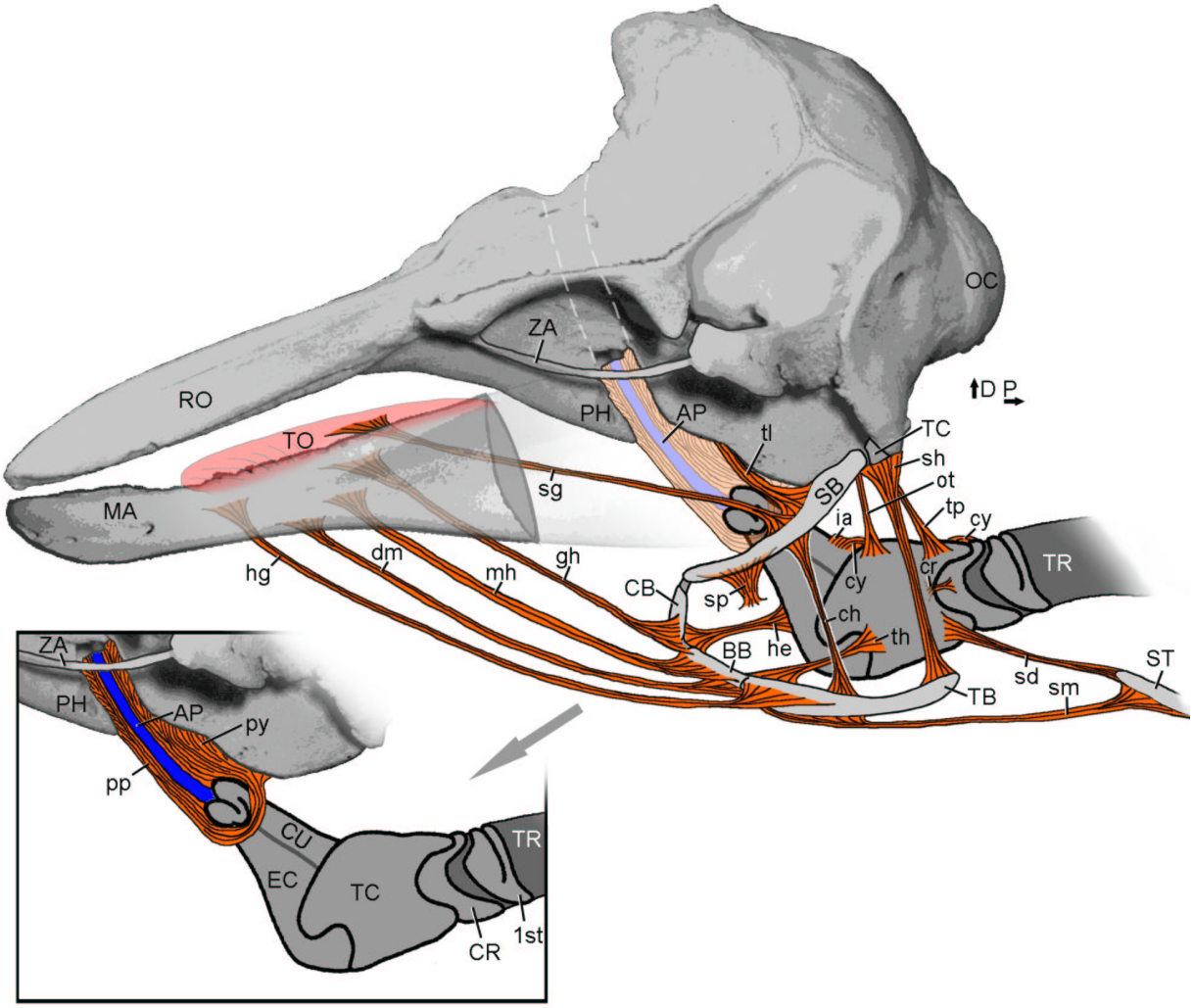


Figure 65: Schematic lateral view of the hyoid apparatus and the larynx as well as their associated musculature in the harbor porpoise (*Phocoena phocoena*). Note that the hyoid region is artificially dorsoventrally elongated to show the whole laryngeal region. The free end of the stylopharyngeus muscle (sp) inserts onto the pharynx. The hyoid muscle is not shown. 1st -first tracheal cartilage, AP-air passage, BB-basihyal bone, CB-ceratohyal bone, ch-ceratohyoid muscle, CR-cricoid cartilage, cr-cricothyroid muscle, CU-cuneiform cartilage, cy-cricoarytenoid muscle, D-dorsal, dm-digastric muscle, EC-epiglottic cartilage, gh-geniohyoid muscle, he-hyoepiglottic muscle, hg-hyoglossus muscle, ia-interarytenoid muscle, MA-mandible, mh-mylohyoid muscle, ot-occipitothyroid muscle, P-posterior, PH-pterygoid hamulus, pp-palatopharyngeus muscle, py-pterygopharyngeus muscle, RO-rostrum, SB-stylohyal bone, sd-sternothyroid muscle, sg-styloglossus muscle, sh-stylohyoid muscle, sm-sternohyoid muscle, sp-stylopharyngeus muscle (pharyngeal attachment not shown), ST-sternum, TB-thyrohyal bone, TC-tympanohyal cartilage, th-thyrohyoid muscle, tl-thyropalatine muscle, TO-tongue, tp-thyropharyngeus muscle, TR-trachea, ZA-zygmatic arch.

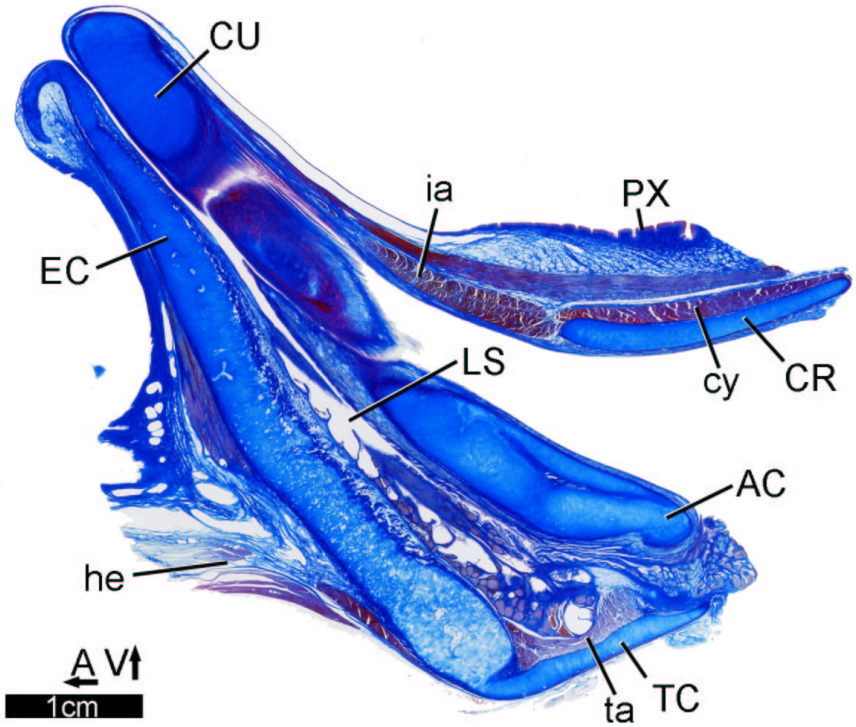


Figure 66: Mediosagittal microscopic section of the larynx of *Neophocaena phocaenoides* stained with AZAN kindly donated by G. Pilleri. A-anterior, AC-arytenoid cartilage, CR-cricoid cartilage, CU-cuneiform cartilage, cy-cricoarytenoid muscle, EC-epiglottid cartilage, he-hyoepiglottic muscle, ia-interarytenoid muscle, LS-laryngeal air sacculi, PX-pharynx, ta-thyroarytenoid muscle, TC-thyroid cartilage, V-ventral.

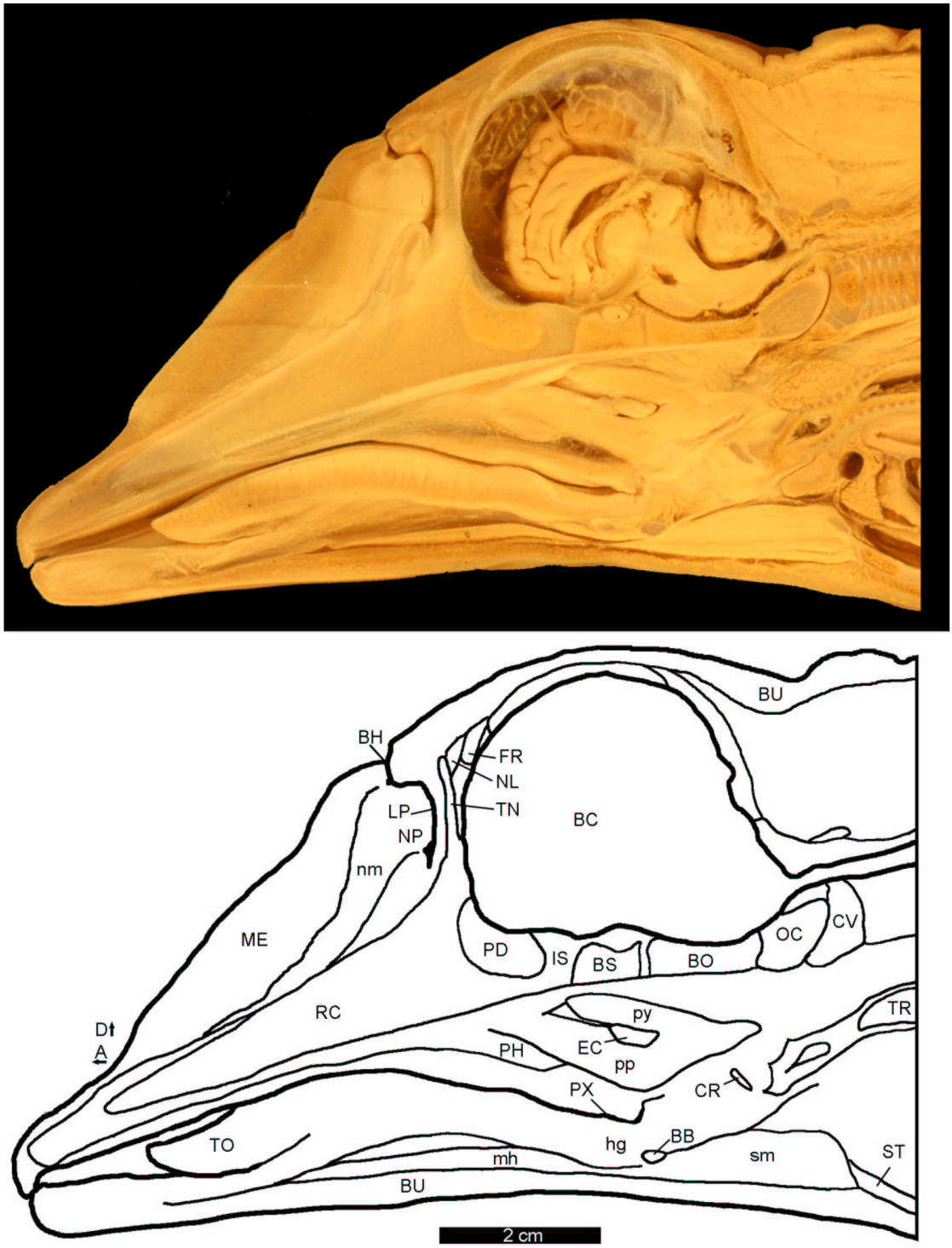


Figure 67: Nearly mediosagittal cryo-section of a late fetal head of a common dolphn (*Delphinus delphis*) showing anatomical structures of the nasal complex and the skull as well as the gular region. A-anterior, BB-basihyal bone, BC-brain cavity, BH-blowhole, BO-basioccipital, BS-basisphenoid, BU-blubber, CR-cricoid cartilage, CV-cervical vertebrae, D-dorsal, EC-epiglottid cartilage, FR-frontal, hg-hyoglossus muscle, IS-intersphenoid synchrondosis, LP-left nasal passage, ME-melon, mh-mylohyoid muscle, NL-nasal, nm-nasal plug muscle, NP-nasal plug, OC-occipital condyle, PD-presphenoid, PH-pterygoid hamulus, pp-palatopharyngeus muscle, PX-pharynx, py-pterygopharyngeus muscle, RC-rostral cartilage (cartilaginous rostrum), sm-sternohyoid muscle, ST-sternum, TN-tectum nasi, TO-tongue, TR-trachea.

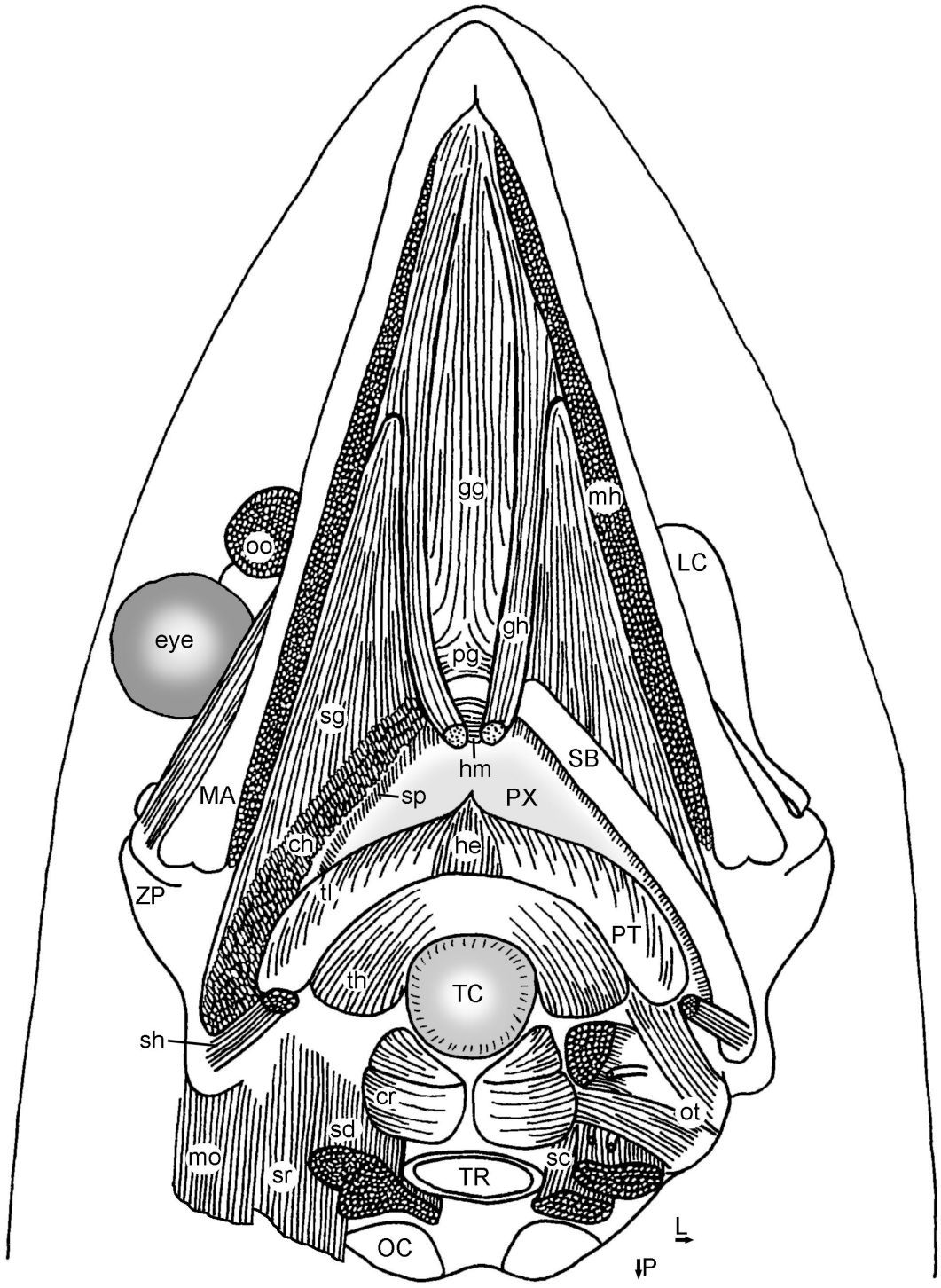


Figure 68: Ventral semi-schematic drawing of the gular musculature in the harbor porpoise (*Phocoena phocoena*). Note that the sphincter colli, the digastric, the hyoglossus, and the sternohyoid muscles are removed. ch-ceratohyoid muscle, cr-cricothyroid muscle, gg-genioglossus muscle, gh-geniohyoid muscle, he-hyoepiglottic muscle, hm-hyoid muscle, L-left, LC-lacrimal, MA-mandible, mh-mylohyoid muscle, mo-mastohumeralis muscle, OC-occipital condyle, oo-orbicularis oris muscle, ot-occipitothyroid muscle, P-posterior, pg-palatoglossus muscle, PT-dorsal periost of thyrohyal bone, PX-pharynx, SB-stylohyal bone, sc-scalenus muscle, sd-sternothyroid muscle, sg-styloglossus muscle, sh-stylohyoid muscle, sp-stylopharyngeus muscle, sr-sternomastoid muscle, TC-thyroid cartilage, th-thyrohyoid muscle, tl-thyropalatine muscle, TR-trachea, ZP-zygmatic process.

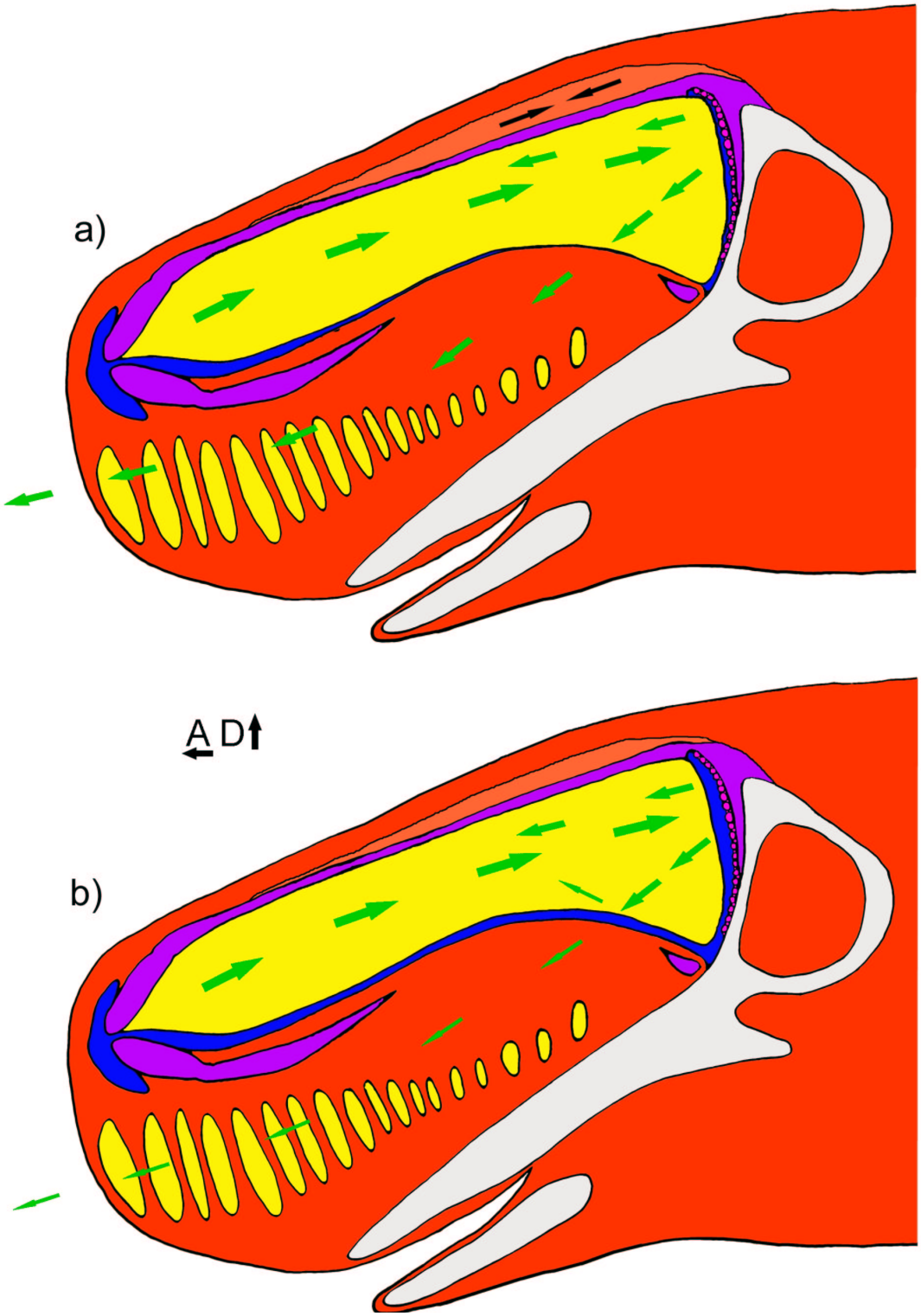


Figure 69: Schematic reconstruction of a sperm whale (*Physeter macrocephalus*) head showing the proposed mechanism to switch between the modes of the generation of echolocation clicks (a) and of coda clicks (b). Anatomical structures are explained in Fig. 37. The green arrows indicate the proposed way of sound through the nasal complex and the black arrows represent muscle tension. Further explanations see text. A-anterior, D-dorsal.

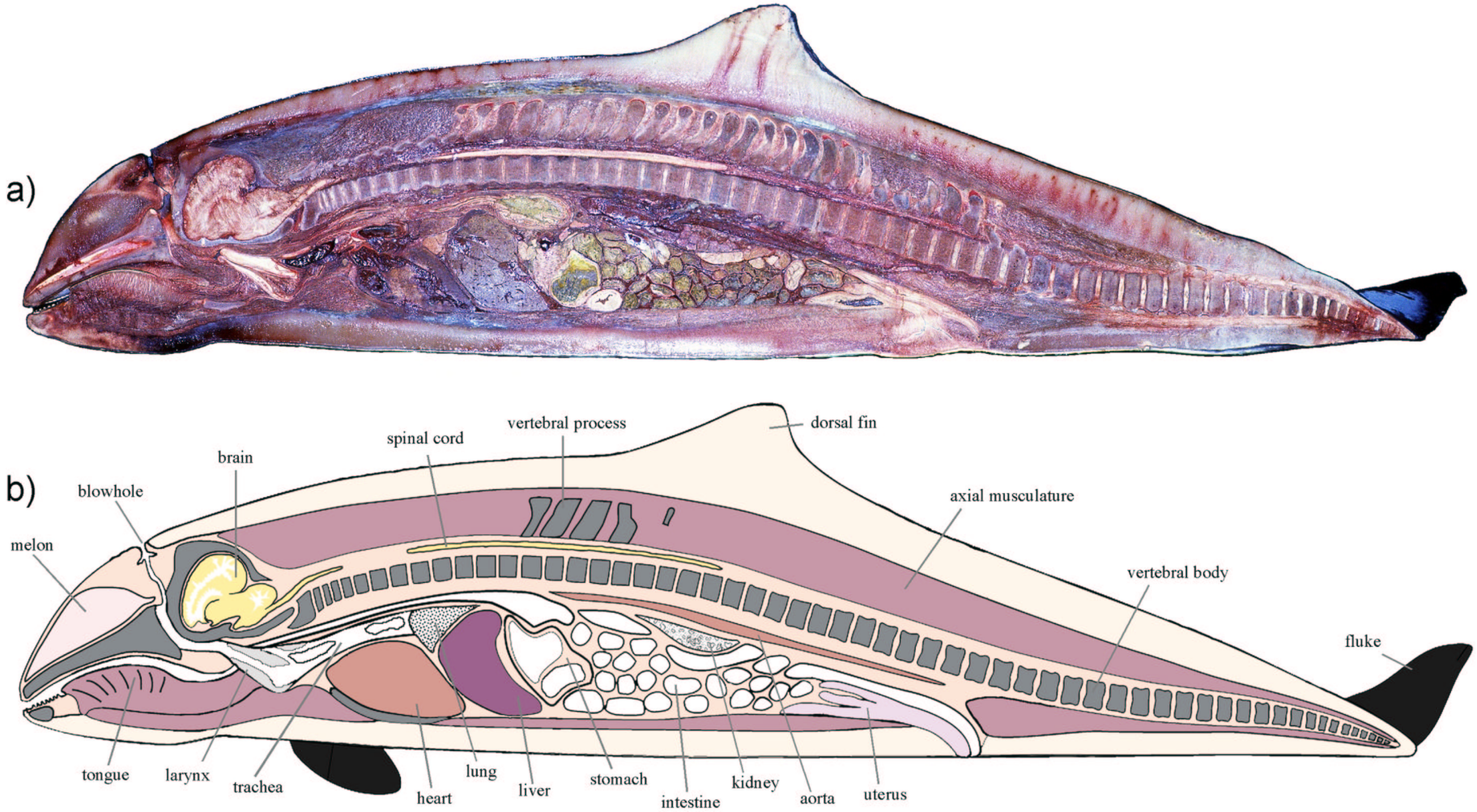


Figure 70: a) mediosagittal cryosection through a harbor porpoise, b) mediosagittal schematic reconstruction of a harbor porpoise showing the topographical relationship of organs (Courteously: H. Schäfer, Forschungsinstitut und Naturmuseum Senckenberg, Frankfurt a.M., Germany).

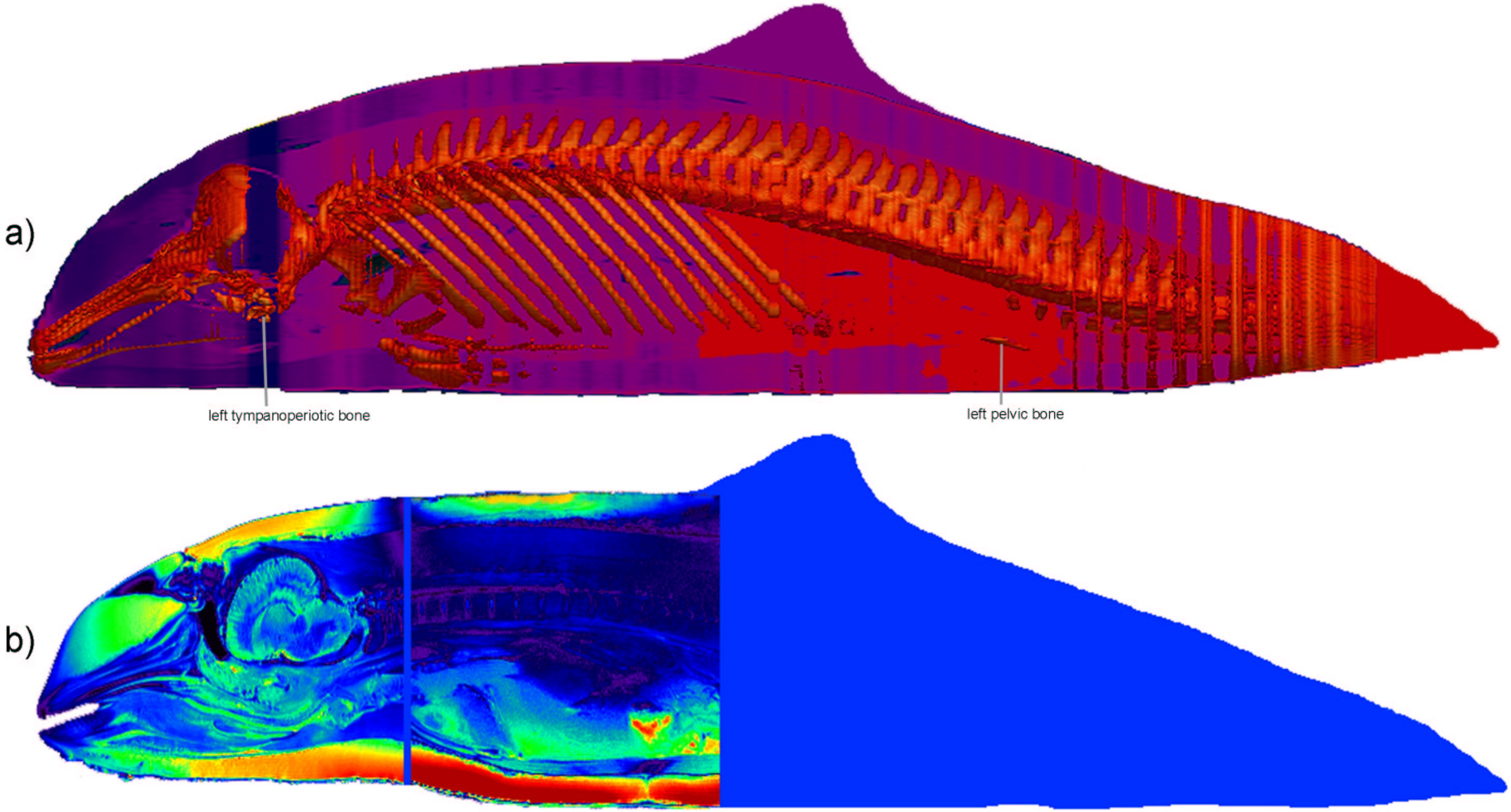


Figure 71: a) 3-d reconstruction based on computed tomography scans of a harbor porpoise showing the mediosagittal plane and the skeleton of the left body part. The bulla tympanica and pelvic bones are high lighted, b) color-mapped sagittal magnet resonance image of the harbor porpoise head and thorax region.

# Curriculum vitae

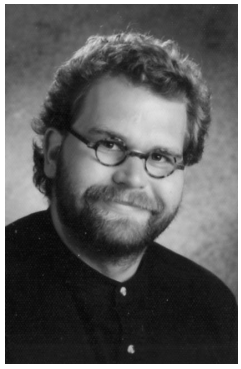

**Stefan Huggenberger**
Diplombiologe
Brünhildestr. 75
14542 Werder

Geburtsdatum: 05.11.1969
Geburtsort: Dormagen (Nordrhein-Westfalen)
Nationalität: Deutsch
Familienstand: ledig

| | |
|---|---|
| 23.05.1989 | Abitur am Norbert-Gymnasium Knechtsteden in Dormagen |
| 07.1989 - 09.1990 | Zivildienst |
| Winter 1990 | Immatrikulation im Fach Diplomchemie an der Universität zu Köln |
| Winter 1991 | Immatrikulation im Fach Diplombiologie an der Universität zu Köln |
| 04.10.1993 | Vordiplom im Fach Biologie an der Universität zu Köln |
| 13.01.1997 - 15.11.1997 | Diplomarbeit mit dem Titel „Schweinswale (*Phocoena phocoena* L.) der deutschen Nord- und Ostsee – Untersuchung zur geographischen Variation und zum Schadstoffproblem" als Kooperation der Universität zu Köln mit dem Deutschen Meeresmuseum in Stralsund |
| 02.12.1997 | Diplom im Fach Biologie an der Universität zu Köln in den Fächern Zoologie, Entwicklungsbiologie und Geologie/Paläontologie mit der Note sehr gut |
| Sommer 1998 | Organisation und Durchführung des europäischen Projekts „Konzept für Ostseeschweinswale mit politischer Lobby- und Öffentlichkeitsarbeit" zur Untersuchung der Populationsstruktur der Schweinswale in der Nord- und Ostsee |
| 03.11.1998 | Annahme als Doktorand im Fachbereich Biologie an der Johann Wolfgang Goethe-Universität Frankfurt am Main. Betreuer: Prof. Dr. Dr. h.c. C. Winter (Zoologisches Institut, Frankfurt a.M.) und Prof. Dr. H.A. Oelschläger (Dr. Senckenbergische Anatomie, Frankfurt a.M.) |
| Sommersemester 1999–Winter 2001 | Lehre im physikalischen Praktikum für Mediziner am Institut für Biophysik der J.W. Goethe-Universität Frankfurt am Main inklusive des Seminars „Schall und Ultraschall" |
| Mai und Juni 2001 und April 2002 | Mehrwöchige Forschungsaufenthalte im National Museum of Natural History der Smithsonian Institution, Washington, D.C. und im Hubbs Sea-World Research Institute, San Diego, CA., USA, gefördert durch den Deutschen Akademischen Austauschdienst (DAAD) |
| 01.03.2001 - 31.05.2003 | Stipendiat der Hessischen Landesgraduiertenförderung an der Johann Wolfgang Goethe-Universität Frankfurt am Main für das oben genannte Dissertationsprojekt |
| seit Oktober 2003 | Wissenschaftlicher Mitarbeiter am Institut für Biochemie und Biologie, Lehrstuhl Allgemeine Zoologie, der Universität Potsdam |

Werder, den 1. Oktober 2003